

## N O T I C E

THIS DOCUMENT HAS BEEN REPRODUCED FROM  
MICROFICHE. ALTHOUGH IT IS RECOGNIZED THAT  
CERTAIN PORTIONS ARE ILLEGIBLE, IT IS BEING RELEASED  
IN THE INTEREST OF MAKING AVAILABLE AS MUCH  
INFORMATION AS POSSIBLE

(NASA-CR-161836) UAH/NASA WORKSHOP ON THE  
USES OF A TETHERED SATELLITE SYSTEM (Alabama  
Univ. in Huntsville.) 235 p HC A11/MF A01  
CSCI 08G

N81-29479  
THRU  
N81-29493  
Unclass  
27166

G3/42

UAH/NASA WORKSHOP ON  
THE USES OF A TETHERED SATELLITE SYSTEM

THE SUMMARY PAPERS FROM  
THE UNIVERSITY OF ALABAMA IN HUNTSVILLE/NASA  
WORKSHOP CONDUCTED ON MAY 2-3, 1978  
HILTON HOTEL, HUNTSVILLE, ALABAMA

Edited by  
S. T. Wu  
School of Science and Engineering  
The University of Alabama in Huntsville  
Huntsville, Alabama 35807



## PREFACE

A tether line to connect two objects in space is not a particularly new concept. Tether experiments were actually conducted during the Gemini flights, but a comprehensive historical review is certainly not the intent of this Preface.

However, two specific documents are pertinent background for discussions of very long tether systems. The first, published in 1966, is "Satellite Elongation into a True 'Sky-Hook'" by Isaacs, Vine, Bradner, and Bachus [1]. This paper explored the ambitious proposition that a line might be lowered from a geosynchronous spacecraft over the equator to the stationary point beneath it on the Earth. While such a remarkable project was seemingly beyond the reach of current technology, the concept of a not-quite-so-long tether stabilized by gravity-gradient forces emerged as a serious possibility. It is interesting that this early paper nevertheless embraces the most far-reaching endeavor that is mentioned in these Proceedings.

The second document, published in 1974, "Shuttle-Borne 'Skyhook': A New Tool for Low-Orbital-Altitude Research," by Colombo, Gaposchkin, Grossi, and Weiffenback [2], advocated a tether system of a 100-kilometer or more extension as an auxiliary capability for the Space Shuttle. This application of the concept arose within the context of the Atmosphere, Magnetosphere, and Plasmas in Space (AMPS) study. The envisioned tethered satellite would carry instruments above or below the Space Shuttle for investigations of atmospheric, magnetospheric, and space plasma phenomena. This report, and sequels by the same authors, stimulated renewed interest in tether systems.

After 1974, other individuals suggested many additional uses for such a system. Also the technological and engineering aspects of the system were examined in a preliminary way [3,4]. Subsequently, the Marshall Space Flight Center of the National Aeronautics and Space Administration funded two ongoing design studies by aerospace industries. Hence, NASA officials recognized the timely value of a broad review and critical discussion of potential tether uses. The insight conveyed by a survey of uses can be of great value to those responsible for the implementation of

an actual system. Conversely, a knowledge of the preliminary design features of a tether system can help experimenters refine their suggested utilization. The University of Alabama in Huntsville (UAH) agreed to execute an information exchange satisfying all these objectives.

The UAH accomplished this through a Tethered Satellite System (TSS) Workshop. The results are reported for the benefit of all in these Workshop Proceedings. As the date for the Workshop became imminent, a more pressing objective arose in the need at NASA Headquarters for an immediate commentary on the value of a tether system. As a proposed hardware project, the tether system is currently in competition with other projects for limited resources. To satisfy this immediate requirement, officials at NASA Headquarters had the opportunity for participation in the concluding Workshop session via a telecon link.

Finally, I wish to express appreciation to Dr. S. T. Wu and to The University of Alabama in Huntsville for organizing and hosting the Workshop. The spirited discussions of the scientific and engineering aspects of the tether concept and the resulting documentation of them are a credit to this forward-looking institution.

Charles A. Lundquist  
NASA/Marshall Space Flight Center

- [1] Isaacs, J. D., Vine, A. C., Bradner, H., and Bachus, G. E., "Satellite-Elongation into a True 'Sky-Hook'," Science, Vol. 151, p. 682, February 11, 1966.
- [2] Colombo, G., Gaposchkin, E. M., Gross, M. D., and Weiffenback, G. C., "Shuttle-Borne 'Skyhook': A New Tool for Low-Orbital-Altitude Research," Smithsonian Institution Astrophysical Observatory, Cambridge, MA, 1974.
- [3] Baker, W. P., Dunkin, J. A., Galaboff, Z. J., Johnston, K. D., Kissel, R. R., Rheinfurth, M. H., and Siebel, M. P. L., "Tether Subsatellite Study," NASA Technical Memorandum TM X-73314, March 1976.
- [4] "Shuttle/Tethered Satellite System Conceptual Design Study," NASA Technical Memorandum TM X-73356, Preliminary Design Office, George C. Marshall Space Flight Center, AL, December 1976.

## TABLE OF CONTENTS

	<u>Page</u>
PREFACE	i
PURPOSE AND OBJECTIVES	vi
I. GEOLOGICAL APPLICATIONS	1
<b>SUMMARY</b>	1
by Robert Regan Phoenix Corporation	
Geomagnetic Field Mapping from a Satellite: Spatial Power Spectra of the Geomagnetic Field at Various Satellite Altitudes Relative to Natural Noise Sources and Instrument Noise	5
by M. G. McLeod and P. J. Coleman, Jr. University of California at Los Angeles	
Gravity Gradient Determination With Tethered Systems	33
by P. M. Kalaghan and G. Colombo Smithsonian Institution	
The Reduction and Analysis of Satellite Magnetometer Data	59
by Robert D. Regan Phoenix Corporation	
II. ATMOSPHERIC APPLICATIONS	92
<b>SUMMARY</b>	92
by George Carignan University of Michigan	
The Need for Measurements in the Lower Atmosphere	96
by C. A. Reber NASA/Goddard Space Flight Center	
The Interaction of a Tethered Satellite With the Atmosphere and the Resultant Environment	106
by J. H. deLeeuw University of Toronto and D. R. Taeusch University of Michigan	

	<u>Page</u>
The In Situ Measurement of Reactive Neutral Constituents in the Thermosphere by Atomic and Molecular Resonance Fluorescence by J. G. Anderson University of Michigan	111
Mass Spectrometric Measurements in the Lower Thermosphere by A. O. C. Nier University of Minnesota	120
Atmospheric Electrification by H. W. Kasemir NOAA/ERL	130
Chemical Releases by D. S. Evans NOAA/ERL and J. P. Heppner NASA/Goddard Space Flight Center	134
Aerodynamic Effects by G. R. Kerr The University of Alabama in Huntsville	151
Letter by R. E. Smith NASA/Marshall Space Flight Center	156
III. ELECTRODYNAMICS AND PLASMA STUDIES	159
SUMMARY by David L. Reasoner NASA/Marshall Space Flight Center	159
The Electrodynamic Tether by P. Roger Williamson, P. M. Banks, and K. Oyama Utah State University	163
Interactions of a Tethered Satellite System with the Ionosphere Mario D. Grossi and Giuseppe Colombo Harvard-Smithsonian Center for Astrophysics	176
The Tethered Subsatellite as a Tool for Large Body Plasma Flow Interaction Studies by Noble N. Stone NASA/Marshall Space Flight Center and Uri Samir University of Michigan	182

	<u>Page</u>
IV. ENGINEERING AND OPERATIONAL APPLICATIONS	195
<b>SUMMARY</b>	195
by M. P. L. Siebel	
NASA/Marshall Space Flight Center	
APPENDIX A	A-1
Agenda	
APPENDIX B	A-4
TSS Workshop Participants	
APPENDIX C	A-8
Tethered Satellite System	
by Charles C. Rupp and Jay H. Laue	
NASA/Marshall Space Flight Center	

## PURPOSE AND OBJECTIVES

Recently, Laue and Rupp (see Appendix C) reported on the engineering design of a Tethered Satellite System (TSS). This report shows that such an idea does indeed appear technologically possible, thus giving the opportunity for scientists to perform scientific investigations not previously attainable.

Upon the request and support from NASA, The University of Alabama in Huntsville has assumed the responsibility for reviewing the scientific and technical interest in the use of such a system. To this end we invited interested scientists from universities, government agencies and private industries to a two-day Workshop in Huntsville, Alabama for the purpose of becoming acquainted with Tethered Satellite System and discussing the uses of the TSS for various scientific investigations and technical applications.

The discussions were centered generally in four areas, as follows:

1. Geological Applications
2. Atmospheric Applications
3. Electrodynamics and Plasma Studies
4. Technology Applications

A detailed account of the presentations and discussions are included in the following chapters. *In particular, I wish to draw the reader's attention to the summary discussions beginning each of the four chapters.*

As the coordinator of this review effort, I would like to acknowledge those scientists whose cooperations made this activity so useful and successful. In particular, I would like to thank Dr. George Carignan, Dr. Robert Regan, Dr. David Reasoner, and Dr. Matt Siebel who served as discussion coordinators for the four areas and helped in carrying out this review effort and William Snoddy who served as our principal contact with the NASA Tethered Satellite System study activity. Also, the encouragement from Dean J. Hoomani of The University of Alabama in Huntsville is greatly appreciated, as is the support of Carol Holladay who served so well as secretary and typist throughout this activity.

S. T. Wu  
The University of Alabama in Huntsville

# I. GEOLOGICAL APPLICATIONS

## SUMMARY

Robert Regan  
Phoenix Corporation

### GEOLOGICAL APPLICATION

The tethered subsatellite, a totally new concept in spaceborne platforms, could effectively be utilized in studying the Earth's magnetic and gravity field to a degree not previously possible. The ability to selectively sample these fields over the entire globe at a variety of low altitudes combined with the capability of obtaining simultaneous measurement over a finite length interval, i.e., a gradiometer, provides increased resolution in the study of the anomalous planetary fields associated with geological structure. The capability of routinely obtaining long period measurements offers a much needed solution to the problem of monitoring the global temporal variations of the Earth's magnetic field. Thus, tethered subsatellite measurements would effectively complement many on-going NASA programs, such as Magsat and draw the same (or more) enthusiastic support from a wide variety of users.

In order to fully realize the potential role that such a system could fulfill, it is necessary to first outline the requirements for measurements of the Earth's gravity and magnetic fields and then detail some of these aspects by presenting the particular papers presented at the workshop.

#### Magnetic Field

Although many earth-orbiting satellites have measured magnetic fields to study the magnetosphere, very few of these satellites provide data of any practical value to solid earth studies. This is unfortunate in that near-earth satellite magnetic field data have been shown to have a unique and valuable role in this area. For example, over the past few years, there has been increasing interest in the studies of the broad-scale magnetic anomalies that appear in regional compilations of aeromagnetic data. These long wavelength anomalies, undoubtedly reflecting significant crustal structure, are so far proving enigmatic in their interpretation. One major problem is in their adequate definition. Satellite data are of considerable value both in defining such anomalies, and especially when combined with more

conventional data in their interpretation. Also, geomagnetic field models, spherical harmonic representations of the main geomagnetic field, are becoming of increased importance in exploration geophysics, as well as other areas. However, the limitations, primarily imposed by the poor spatial and temporal distribution of presently available data, affect all field model applications. These limitations can be greatly reduced by the use of satellite measurements, which provide global coverage in only a few weeks, as well as measurements of the field's temporal behavior. These and other considerations underscore the utility of satellite derived measurements of the earth's magnetic field.

The planned Magsat mission will adequately provide the data necessary for use in improving the geomagnetic field models for epoch 1980 and in studying long wavelength anomalies from an altitude of 300 km. However, there is still a need for continued monitoring of the geomagnetic field and for anomaly studies at lower altitudes.

As previously noted, one of the major impediments to obtaining accurate field models is the lack of global measurements obtained over a relatively short time interval. The ability of satellite measurements to meet this requirement is invaluable and should not be ignored after Magsat. Repeat observations at 5-10 year intervals with vector magnetometers are essential for monitoring the global field and for input to accurate field models.

One only has to consider the magnetic anomalies detected by POGO satellites, those anticipated from Magsat, and the few regional compilations of aeromagnetic data that exist to realize that for satellite magnetic anomaly studies "the lower the better."

The tether system could be utilized to obtain magnetic measurements at a minimum altitude between 100 and 120 km. At this satellite altitude, a magnetometer system could investigate magnetic anomaly features having dimensions substantially smaller than those studied by Magsat. The gain in spatial linear resolution should be approximately proportional to the ratio of the Magsat altitude to the tethered satellite altitude.

The successful resolution of such smaller anomalies is also facilitated by another capability of the tether concept. Separation of external current-induced fields can be greatly aided if measurements at several altitudes relative to the currents are obtained. Such measurements can be made (1) sequentially by operating the tethered satellite at different tether extensions, or (2) simultaneously by several instrumentation pods spaced on the tether line. Preliminary studies indicate the latter option is

particularly promising. The magnetometer instrumentation for such missions would be an outgrowth of previous satellite developments.

Plans for early utilization of the tether capability would envision adjusting the flight plan of a Shuttle mission to achieve favorable passes over geological areas of magnetic interest identified by a satellite such as Magsat or by other comparable means. These selected areas would then be studied in the increased detail offered by the tethered instrumentation. A more comprehensive, yet detailed, magnetic map of the earth would result from eventually operating the tethered magnetometer system over the extended times needed to obtain closely spaced global coverage. The Power Module planned to extend the Space Shuttle flight duration could provide the vehicle to meet this requirement.

#### Gravity Field

The terrestrial gravity field like the magnetic field is a naturally occurring planetary potential field. It differs from the magnetic field in that it is usually considered unidirectional because only the vertical component of the field is utilized. In addition, for all practical purposes, there is no temporal variation. It is similar to the magnetic field in that studies of the planetary field are utilized to determine gross internal structure of the Earth and the anomalous field reflects subsurface density and structural differences.

The measurement of the anomalous gravity field is more tedious and involved than with magnetics because of the effects of topography, need for precise elevation and latitude information, and the delicacy of the instruments. To date there has been no airborne nor absolute instrument of sufficient accuracy for anomalous field measurements developed. This has seriously inhibited the acquisition of data over logistically inaccessible areas. However in recent years, the analysis of satellite trajectories have permitted the production of regional gravity anomaly maps and definition of the undulations of the geoid (effectively equivalent to a geomagnetic field model) of acceptable accuracy. The problem however has been that the resolution is limited by the satellite altitude and the ability of accurately modeling its path.

The shuttle borne tethered subsatellite could be utilized in several ways to measure accurately both the anomalous and planetary components of the gravity field. The subsatellite trajectory could be determined to

detect such variation or more accurately, a gradiometer subsatellite could be utilized on the tether, or released from the tether, to directly monitor the gravity changes. This is perhaps a more attractive system in that it offers more definition of the anomalous component.

Thus for both gravity and magnetic field studies of academic and practical application, the tethered subsatellite provides an optimal platform. This summary has only highlighted the various aspects of the applications. The individual papers presented at the workshop provide more detailed information.

GEOMAGNETIC FIELD MAPPING FROM A SATELLITE:  
SPATIAL POWER SPECTRA OF THE GEOMAGNETIC FIELD AT  
VARIOUS SATELLITE ALTITUDES RELATIVE TO NATURAL  
NOISE SOURCES AND INSTRUMENT NOISE

M. G. McLeod and P. J. Coleman, Jr.  
Institute of Geophysics and Planetary Physics  
University of California at Los Angeles

Institute of Geophysics and Planetary Physics Publication #1810

April, 1978

Summary :

A plot of the vertical geomagnetic field component great circle power spectra is shown in Figure 1 as it would be observed at various satellite altitudes. These spectra were calculated from equations derived in the report by McLeod and Coleman (1977b). The core (or main) geomagnetic field is the dominant contributor to the power spectra for harmonics  $n < 15$  (0.003 HZ) while the crustal geomagnetic field is dominant above this frequency.

Figure 1 also shows a typical fluxgate magnetometer noise level as determined by measurements made at UCLA and given in the report by McLeod (1976).

Also shown on Figure 1 are two curves giving the natural noise level at the earth's surface, one curve for the auroral zone and one for lower latitudes. Because of the scale size of the magnetosphere and ionosphere, it is believed that these noise levels would also apply approximately at the satellite altitudes shown in Figure 1, i.e. below 500 km altitude. However, it is possible that ionospheric irregularities (turbulence) might increase the noise seen by the magnetometer above the values shown. The data for these curves was obtained from the reports by Campbell (1976) and Wertz and Campbell (1976). It may be observed that the natural noise is greater than the instrument noise over the entire frequency range for which useful measurements of the geomagnetic field may be made. The natural noise may be an order of magnitude less than shown by the curves on very "quiet" days (i.e. days when the index of geomagnetic activity,  $A_p$  is unusually low) while the natural noise may be an order of magnitude greater than shown by the curves on very "disturbed" days. Since  $A_p$  varies with the solar cycle, the natural noise level will vary with the solar cycle. The noise also varies to a lesser extent with time of day and season of year.

Since the natural noise (averaged for auroral zone and low latitudes) is greater than the crustal geomagnetic field at very low frequencies, it is desirable to remove these frequencies (say through the second harmonic which is 0.0004 HZ) from the data before further processing. Such a procedure was used with the POGO

data described in the report by Mayhew (1977). (Actually, a quadratic best fit was removed from data for portions of an orbit, which is equivalent to filtering low frequencies from the data.) Because low frequencies would be removed from the data, the greater long term stability obtainable from alkali vapor scalar magnetometers compared to fluxgate magnetometers is not needed, and a triaxial fluxgate magnetometer is, therefore, a suitable instrument for mapping the crustal geomagnetic field. (It can be used as a scalar magnetometer.)

It may be observed in Figure 1 that the natural noise power spectrum for low latitudes is equal to the crustal field power spectrum for 100 km satellite altitude at 0.1 HZ, while the auroral zone natural noise power spectrum equals the crustal field power spectrum for 100 km satellite altitude at 0.06 HZ. It is shown in the report by McLeod and Coleman (1977a) that the spatial resolution in km obtainable (for impulses) on a magnetic field map is given by  $2.2/(\pi f_M)$ , where  $f_M$  is the maximum useful frequency in cycles /km in the data (i.e. 0.14HZ  $\div$  8 km/sec for low latitudes and 0.06HZ  $\div$  8 km/sec for auroral zone). Thus the spatial resolution obtainable at low latitudes for a 100 km altitude satellite is 56 km, while at the auroral zone the obtainable spatial resolution is 93 km. At the higher satellite altitude of 300 km the obtainable spatial resolution is 224 km at low latitudes and 509 km at the auroral zone. At 500 km satellite altitude the obtainable spatial resolution is 467 km at low latitudes while maps cannot be made at all for the auroral zone unless the data is selected for "quiet" days. This discussion of spatial resolution is subject to the assumption that other sources of error, such as satellite positional errors, can be kept lower than the natural noise.

For the lower satellite altitudes, greater spatial resolution can be obtained than at higher altitudes. Furthermore, since the crustal geomagnetic field power spectrum is larger at lower altitudes, the relative error due to the natural noise is less than for higher altitudes.

## Introduction

This report presents some of the results of a study conducted at UCLA for George C. Marshall Space Flight Center concerning the use of a tethered earth satellite for mapping the crustal geomagnetic field. Such maps are useful as a guide to exploration strategy for minerals and petroleum, and serve to increase our understanding of the earth's crust.

The concept of a tethered earth satellite for low orbital altitude research has been described by Colombo et al (1974), while some of the considerations involving the use of such a satellite for geomagnetic field measurements have been described in the report by Lundquist et al (1977). This latter report described the concept of a Power Module that could be deployed from the Space Shuttle and used as an anchor to tether a subsatellite containing a magnetometer for the extended times needed to obtain closely spaced global coverage.

There are two important advantages in the use of a tethered satellite for mapping the crustal geomagnetic field, as opposed to using a free satellite for this purpose. First, because of the lower altitude of the measurements possible with a tethered satellite, greater spatial resolution of the magnetic field can be achieved. Second, the crustal geomagnetic field is larger at lower altitudes, so that natural noise sources contribute a smaller percentage error to the measurements.

Although aeromagnetic mapping allows still greater spatial resolution than is achievable with satellites and the crustal fields are larger at aircraft altitudes, these advantages are partly negated by the slower aircraft speeds. For a given path projected on the earth's surface, the "noise" due to external field variations will be larger in the case of aircraft since there is more time for the external field to vary.

Furthermore, much more closely spaced tracks are needed in the case of aircraft if aliasing of the data is to be avoided. Thus the time required to

obtain global coverage from an airplane is much longer than in the case of a satellite. The political problems in overflying foreign countries with aircraft are not negligible and it would probably prove to be impossible to obtain permission to overfly some foreign countries. Finally navigation and position determination is more difficult for aircraft than for satellites.

In this report, power spectra for the geomagnetic field at various satellite altitudes are presented together with power spectra of the natural magnetospheric and ionospheric noise and a power spectrum of instrumental noise for a typical fluxgate magnetometer. These power spectra are shown in Figure 1. The source of these data is described. The implications of these data relative to desirable instrument frequency response, stability and resolution specification as well as the implications relative to desirable spacecraft position and orientation accuracy specifications and desirable environmental (temperature, magnetic noise) specifications are discussed. Implications of these power spectra relative to choice of a suitable magnetometer and relative to desirable methods of data processing are considered. Finally, implications for desirable orbit and mission duration are discussed.

#### Great Circle Power Spectra of the Geomagnetic Field:

These power spectral are based on the theory and equations given in the report by McLeod and Coleman (1977b). If the radial component of the magnetic field along a great circle track of radius  $r$  centered at the earth's center is decomposed into a Fourier series whose fundamental frequency is the reciprocal of the track length and if the mean squared value of the radial magnetic field component for a frequency which is a multiple  $m$  of the fundamental frequency is then averaged for all great circle tracks having the same radius  $r$  and center, then the result of this averaging is given by equation (23) of the referenced report. This equation is repeated below as equation (1):

$$(1) \langle B_r^2 \rangle_m = \sum_{n=m}^{\infty} \frac{(n+1) R_n}{2 n+1} \left(\frac{a}{r}\right)^{2n+4} [P_n^m(0)]^2$$

The parameter  $a$  is the earth's radius equal to 6371 km., and the coefficients

$[P_n^m(o)]^2$  are given by:

$$(2) [P_n^m(o)]^2 = \frac{2 (n+m)! (n-m)!}{\left[ \frac{(n-m)!}{2} \frac{(n+m)!}{2} \right]^2 2^{2n}}$$

for  $(n+m)$  even and  $m \neq 0$ ,  $1/2$  the above value for  $m = 0$ ; and  $[P_n^m(o)]^2 = 0$  for  $(n+m)$  odd. The quantity  $R_n$  is the spatial power spectral density defined by Lowes (1966):

$$(3) R_n = (n+1) \sum_{m=0}^n (g_n^m)^2 + (h_n^m)^2$$

The quantities  $g_n^m$  and  $h_n^m$  are the coefficients of a spherical harmonic expansion of the scalar potential of the geomagnetic field (Chapman and Bartels, 1940):

$$(4) V = a \sum_{n=1}^{\infty} \sum_{m=0}^n \left(\frac{a}{r}\right)^{n+1} P_n^m(\cos\theta) [g_n^m \cos m\lambda + h_n^m \sin m\lambda]$$

where the functions  $P_n^m(\cos\theta)$  are the seminormalized associated Legendre functions used in geomagnetism.

Peddie and Fabiano (1976) have given the values of  $g_n^m$  and  $h_n^m$  for the geomagnetic field for  $n \leq 12$ . From these values, the values of  $R_n$  for  $n \leq 12$  can be calculated using equation (3). The values are:

$n$	$R_n$	$n$	$R_n$
1	$1.879 \times 10^9$	7	$1.275 \times 10^5$
2	$5.864 \times 10^7$	8	$1.769 \times 10^4$
(5) 3	$3.447 \times 10^7$	9	$1.273 \times 10^4$
4	$1.066 \times 10^7$	10	$3.103 \times 10^3$
5	$1.974 \times 10^6$	11	$1.382 \times 10^3$
6	$5.239 \times 10^5$	12	$6.834 \times 10^2$

where the units for  $R_n$  are  $\gamma^2$ . (One  $\gamma = 1nT$ ).

It is shown in the report by McLeod and Coleman (1977b) that the values of  $R_n$  are given approximately by:

$$(6) R_n = R_n^M + R_n^C$$

where:

$$(7) R_n^C = (2n+1) [(1-\exp(-n/290))/(n/290)] (0.260)$$

$$(8) R_n^M = \frac{2n+1}{n+2} (6.79 \times 10^8) (.284)^n$$

and the units are  $\text{gamma}^2$ .

Equation (7) gives the spatial power spectrum due to the crustal geomagnetic field while equation (8) gives the spatial power spectrum due to the main (or core) geomagnetic field. These equations were derived using data given by Alldredge et al (1963) and Peddie and Fabiano (1976) together with a simple plausible mathematical model for the core and crustal fields.

The preceding equations were programmed on a minicomputer in Hewlett Packard Fortran to calculate the values of  $\langle B_r^2 \rangle_m$ , using equation (5) for values of  $R_n$  for  $n \leq 12$ , and using equations (6) (7) and (8) for values of  $R_n$  for  $n \geq 13$ . The program is given as Appendix A.

The orbital frequency (in HZ) for a satellite in circular orbit is given by:

$$(9) f_o = 1.975 \times 10^{-4} \left(\frac{a}{r}\right)^{3/2}$$

The discrete spectrum given by equation (1) was approximated by a continuous spectrum by means of the formula:

$$(10) P_z(mf_o) = \frac{\langle B_r^2 \rangle_m}{f_o}$$

The continuous spectra are plotted in Figure 1 for altitudes of 6,100,300 and 500 km. The altitude of 6 km is, of course, not practical for a satellite. It represents the altitude above the earth's crust of the aircraft used to obtain the data given by Alldredge et al (1963), since the aircraft was at an average altitude of 3 km and we allow 3 km for the ocean depth. The calculated discrete spectrum for this altitude agreed well with the data given by Alldredge et al (1963).

#### Natural Noise Sources:

The power spectral densities for the natural noise sources at the earth's surface are shown in Figure 1 for both the auroral zone region and lower latitudes. These curves are based on data given by Campbell (1976) and Wertz and Campbell (1976). Many references to other workers in this area are given by these authors.

The natural noise is due to time variations in electric currents flowing above the earth's surface, viz, electric currents flowing in the ionosphere, magnetopause, a ring current due to charged particles trapped by the geomagnetic field, and field aligned currents connecting the ionosphere with the earth's tail region. The latter currents are associated with aurora, their path through the ionosphere is called the auroral electrojet which produces the largest amount of natural noise on the nightside of the earth in the auroral zone. There is also an equatorial electrojet due to motion of charged particles through the earth's magnetic field caused by atmospheric heating. The equatorial electrojet produces the largest amount of natural noise on the dayside of the earth near the equator.

These current systems do not rotate with the earth but are most nearly time stationary in a nearly inertial reference frame with one axis along the sun-earth line, a second axis perpendicular to the first and in the plane formed by the sun-earth vector and earth's spin axis, and a third axis perpendicular to the first two axes. However, the currents are time varying even in this frame due to influence of the geomagnetic axis moving in this frame and due also to varying pressure on the geomagnetic field because of varying solar wind pressure and solar disturbances. The natural noise shown in Figure 1 was measured on the earth which is moving with respect to the current systems, while an earth satellite would also be moving with respect to the current systems but at a different speed. Therefore, the noise observed by the satellite would not agree exactly with the noise shown in the figure, however, we expect that it would agree approximately at the higher frequencies shown in the figure. Moreover, the satellite is not at the earth's surface but may be in the ionosphere. Because of the scale size of the ionosphere, we expect that the noise observed at the satellite would not be changed much on this account. However, we have not found any quantitative data on possible fine scale structure (turbulence) in the ionospheric currents, and it is possible that such irregularities might increase the natural noise levels at the satellite above the values shown.

According to Campbell (1976), the natural noise spectrum in the period range five minutes to four hours has a maximum amplitude in the auroral zone, a minimum amplitude in the mid to low latitude region,  $20^{\circ} - 40^{\circ}$ , and a minor maximum amplitude at the equator. The slope of the function  $\log$  [power spectral density] vs.  $\log$  [frequency] is about two for this frequency range. According to Wertz and Campbell (1976), the spectrum for the period range 0.3 to 300 seconds shows similar behavior but greater slope. From these two references we get for the slope:

Freq.	Slope
.0001 to .03 HZ	2
.65 HZ	3.5

If we assume the slope can be fit by an equation of the form:

$$(11) \quad \frac{d \ln [P_z(f)]}{d \ln [f]} = 2 + 2.25f$$

where  $P_z(f)$  is the power spectral density of the vertical component of magnetic field, we get by integration of (11):

$$(12) \quad P_z(f) = A / [f^2 \exp (2.25f)]$$

where A is a constant of integration.

From Table 6 of the paper by Campbell (1976) the average power spectral densities of the H-component of geomagnetic field at a ten minute period for College, Alaska and San Juan, Puerto Rico are given by:

Station	Power Spectral Density
College, Alaska	$1.6 \times 10^4 \text{ gamma}^2/\text{HZ}$
San Juan, Puerto Rico	$5.3 \times 10^1 \text{ gamma}^2/\text{HZ}$

These data were obtained in 1965 during the middle portion of the solar cycle. Vertical magnetic field component power spectral density is about 25% of the H-component power spectral density, thus we get for the constant of integration A in equation (12):

Station	A
College, Alaska	$1.11 \times 10^{-2} \gamma^2 \text{ HZ}$
San Juan, Puerto Rico	$3.68 \times 10^{-5} \gamma^2 \text{ HZ}$

Plots of equation (12) with these values of A are shown in Figure 1 as natural noise spectra. From Campbell (1976), the spectra are about an order of magnitude less on very "quiet" days (16 Dec 1965) and about an order of magnitude greater on very "disturbed" days (16 June 1965). The spectra also vary to a lesser extent with time of day and season of year.

In addition to this noise, we should consider also the noise due to the motion of the satellite relative to the current systems. At 100 km satellite altitude, the amplitude of each of the low frequency harmonics in great circle power spectra of the crustal geomagnetic field vertical component is about 2 gamma rms. The amplitude is less at higher altitudes. The rms variation due to (non-time varying) external current systems is on the order of 10 gamma rms according to Olson (1975), distributed mainly in the first few harmonics. Thus the first few harmonics of the noise will be larger than the signal that is being measured.

#### Fluxgate Magnetometer Noise:

The power spectral density of the noise for a "typical" fluxgate magnetometer is shown in Figure 1. The data is based on measurements made at UCLA using sensors of the type produced by the Naval Ordnance Laboratories. The results of the measurements are given in the report by McLeod (1976), they are:

White noise :  $10^{-4}$  gamma<sup>2</sup>/HZ

1/f noise : 10 milligamma rms/decade

so that the power spectral density of the noise is:

$$(13) P_n(f) = [1 + 0.43/f] \times 10^{-4} \text{ gamma}^2/\text{HZ}$$

The measurements were made on an analog magnetometer similar to that described in the referenced report, but with increased sensitivity. The sensors were shielded by mu-metal from geomagnetic variations. It was determined that the noise was due to the sensor and not the electronics portion of the instrument. The measurements were made with an A/D converter and minicomputer. It was found that the noise depends upon the sensor drive current and waveform shape. It would be possible to reduce the noise by using larger sensors; however, since the instrument noise shown

is below the natural noise for the entire frequency range of interest there would be little benefit in reducing instrument noise below the level shown in Figure 1.

### Discussion

The data shown in Figure 1 have a number of implications relative to crustal geomagnetic field mapping from a low altitude earth satellite. These data are fundamental to intelligent mission planning and setting of specifications for the spacecraft and instrumentation. Although the data are actually applicable to mapping of the geomagnetic field by measurement of the vertical field component, they also apply approximately to mapping the geomagnetic field by measurement of the scalar field. The discrepancies in the latter case would be largest near the geomagnetic equator.

In processing the data from a magnetometer aboard an earth satellite one should remove those frequencies from the data for which the noise exceeds the signal from the geomagnetic field. For a 100 km satellite altitude the noise will exceed the signal for frequencies greater than 0.1HZ at low latitudes and for frequencies greater than 0.06 HZ in the auroral zone. It is shown in the report by McLeod and Coleman (1977a) that the spatial resolution (in km) obtainable on a magnetic field map is given by  $2.2/(f_M)$  where  $f_M$  is the maximum useful frequency (in cycles/km) in the data. If the frequencies in HZ given above are converted to frequencies in cycles/km by dividing by the satellite speed of 8 km/sec, then one finds from the above formula that the maximum spatial resolution obtainable at 100 km satellite altitude is 56 km for low latitudes and 93 km for the auroral zone. In a similar fashion we find that for 300 km altitude the maximum obtainable spatial resolution is 224 km at low latitudes and 509 km at the auroral zone, while for 500 km altitude it is 467 km at low latitudes and maps cannot be made at all for the auroral zone unless the data is selected for "quiet" days. These spatial resolutions are obtainable only if other sources of error than the natural noise, such as noise due to satellite positional errors, can be kept lower than the natural noise.

The data of Figure 1 plus the discussion of natural noise given earlier show that a fluxgate magnetometer is suitable for a mission to map the crustal geomagnetic field. It can be used as a scalar magnetometer and maps produced for measurements of the scalar field. Measurement of the scalar field instead of vector field removes the necessity for measuring or accurately controlling satellite orientation, although slightly better maps could be made from measurement of the vertical component of the geomagnetic field. An alkali vapor type scalar magnetometer is not needed, even though long term drift is less for such a magnetometer. This is because the natural noise for the first few harmonics is larger than the crustal geomagnetic field so that it is desirable to filter out the low frequencies from the data, thus long term drift of the magnetometer is not important. The magnetometer frequency response should be greater than 0.1 HZ, a response of 1.0 HZ is recommended so that the noise might be measured for frequencies between 0.1 HZ and 1.0 HZ. For this corner frequency, a sampling rate of 2 samples/sec is required to avoid aliasing the data. The magnetometer should have a dynamic range great enough to measure the largest fields that will be encountered. A range of  $\pm 64,000$  gamma is adequate for this purpose. Digitization noise is given by  $D^2/12$  where D is the digital window width in gamma. For a 100 km altitude satellite the digitization noise should be less than  $3.16 \times 10^{-3}$  gamma<sup>2</sup>/HZ, and for 1.0 HZ corner frequency this implies that D should be less than 0.195 gamma. For 128,000 gamma dynamic range this requires a 20 bit digitization level. Finally, the magnetometer noise should be less than the natural noise for low latitudes for the frequency range 0.0005 Hz (midway between the second and third harmonic of the orbital frequency) to 0.1 HZ. The digital fluxgate magnetometer described in the reports by McLeod (1976) and McLeod and Means (1977) can be built to meet all of these requirements, with a linearity in the A/D converter commensurate with the 20 bit digitization level.

The data presented in this report has implications for the data processing of magnetic field measurements from a low altitude earth satellite. Some of these implications have already been discussed. The first step in such a processing

procedure should be to remove most of the main (or core) geomagnetic field from the measurements. This can be done by subtracting an  $n = 15$  spherical harmonic analysis of the geomagnetic field from the data. The next step should be filtering of the resulting data to remove low frequencies (below 0.0005 HZ) and high frequencies (above 0.1 HZ for low latitudes and above 0.06 HZ for the auroral zone for a 100 km altitude satellite. This requires a time-varying filter.) A spherical harmonic analysis of the resulting data can then be done using techniques such as those described by Mayhew (1977) which have been used on data from the POGO satellite. (Mayhew also removed low frequencies from that data by subtracting a quadratic fit to the data for portions of an orbit.) Those terms in the resulting harmonic analysis corresponding to  $n \leq 15$  model of the field can be discarded. This discussion of data processing has been somewhat sketchy and is intended only to illustrate basic principles rather than details of the computer programming.

The data presented in this report is also useful for mission planning. A polar orbit in the dawn-dusk plane seems to be optimum for mapping the global crustal geomagnetic field, since such an orbit tends to avoid both the equatorial and auroral electrojets. The orbits should be separated by 40 km at the equator for a 100 km altitude satellite ( $8 \text{ km/sec} \div 0.1 \text{ HZ}$ )/2, so that 500 orbits are required to obtain global coverage. This requires making measurements for one month if all the data is useful. At 2 samples/sec, 5,000,000 data points would be obtained for each magnetometer axis. These data points can then be filtered and decimated to yield 500,000 data points. Although one month is sufficient to obtain data for making a global map, it would be desirable to obtain sufficient data to make at least three independent maps, which requires at least three months.

Finally, the data presented in this report can be used to set specifications on the possible sources of error in crustal geomagnetic field mapping from a low

altitude satellite. Basically, each of these error sources should have a power spectrum below the low latitude natural noise for the frequency range of interest, if the resulting map is not to be seriously degraded from what is potentially achievable. For a 100 km altitude satellite, the frequency range of interest extends from 0.0005 HZ to 0.1 HZ. The units for the error must be converted to magnetic field units. For the positional error, the conversion factor is 10 gamma/km for horizontal errors in position and 30 gamma/km for vertical errors. The temperature coefficient of the electronics portion of the magnetometer described in the report by McLeod (1976) is 0.062 gamma/°C. Magnetic sources aboard the satellite should have a power spectrum below the low latitude natural noise when measured at the magnetometer. If vector measurements are desired, the orientation error conversion factor is 62,000 gamma/radian which is equivalent to 0.3 gamma/arc second.

References:

1. Allredge, L. R., G. D. Van Voorhis, and T. M. Davis, "A Magnetic Profile around the World", J. Geophys. Res., vol. 68, pp. 3679-3692, 1963.
2. Campbell, W. H., "An Analysis of the Spectra of Geomagnetic Variations having Periods from Five Minutes to Four Hours", J. Geophys. Res., vol. 81, no. 7, pp. 1369-1390, March 1, 1976.
3. Chapman, S., and J. Bartels, "Geomagnetism", Oxford University Press, Oxford, 1940.
4. Colombo, G., E. M. Gaposchkin, M. D. Grossi and C. C. Weiffenbach, "Shuttle-Borne 'Skyhook': A New Tool for Low-Orbital Altitude Research", Smithsonian Institution Astrophysical Observatory, Cambridge, Mass., Sept., 1974.
5. Lundquist, C. L., M. P. L. Siebel, P. J. Coleman Jr., and M. G. McLeod, "Tethered Satellites for Magnetic Field Measurements", Marshall Space Flight Center Space Sciences Laboratory Preprint Series No. 77-108, (Summary of a Presentation for the Proceedings of the Workshop on the Application of Space Techniques to Geodynamics, Boulder, Colorado, July 18-23, 1977.)
6. Lowes, F. J., "Mean Square Values on Sphere of Spherical Harmonic Vector Fields," J. Geophys. Res., vol. 71, p. 2179, 1966.
7. Mayhew, M. A., "A Method of Inversion of Satellite Magnetic Anomaly Data," Goddard Space Flight Center Report No. X-922-77-260, Oct., 1977. (To be published in J. Geophys. Res.)
8. McLeod, M. G., "Interim Report on a Proposed Triaxial Digital Fluxgate Magnetometer for NASA Applications Explorer Mission -- A Design Study", U.C.L.A., IGPP Publ. No. 1643, Oct., 1976.
9. McLeod, M. G. and J. D. Means, "A Proposed Triaxial Digital Fluxgate Magnetometer for NASA Applications Explorer Mission--Results of Test of Critical Elements," U.C.L.A., IGPP Publ. No. 1698, April, 1977.

10. McLeod, M. G. and P. J. Coleman, Jr., "Geomagnetic Field Mapping from a Low Altitude Earth Satellite", U.C.L.A., IGPP Publ. No. 1742, July, 1977.
11. McLeod, M. G. and P. J. Coleman, Jr., "Spatial Power Spectrum of the Crustal Geomagnetic Field", U.C.L.A., IGPP Publ. No. 1778, Dec., 1977.
12. Olson, W. P., "The Contribution of External Current Systems to the Near Earth Magnetic Field", EOS Trans. A.G.U., vol. 56, no. 8, Aug., 1975.
13. Peddie, N. W., and E. B. Fabiano, "A Model of the Geomagnetic Field for 1975", J. Geophys. Res., vol. 81, pp. 2539-2542, 1976.
14. Wertz, R. and W. H. Campbell, "Integrated Power Spectra of Geomagnetic Field Variations with Periods of Three Tenths of Three Hundred Seconds", J. Geophys. Res., vol. 81, no. 28, pp. 5131-5140, Oct. 1, 1976.

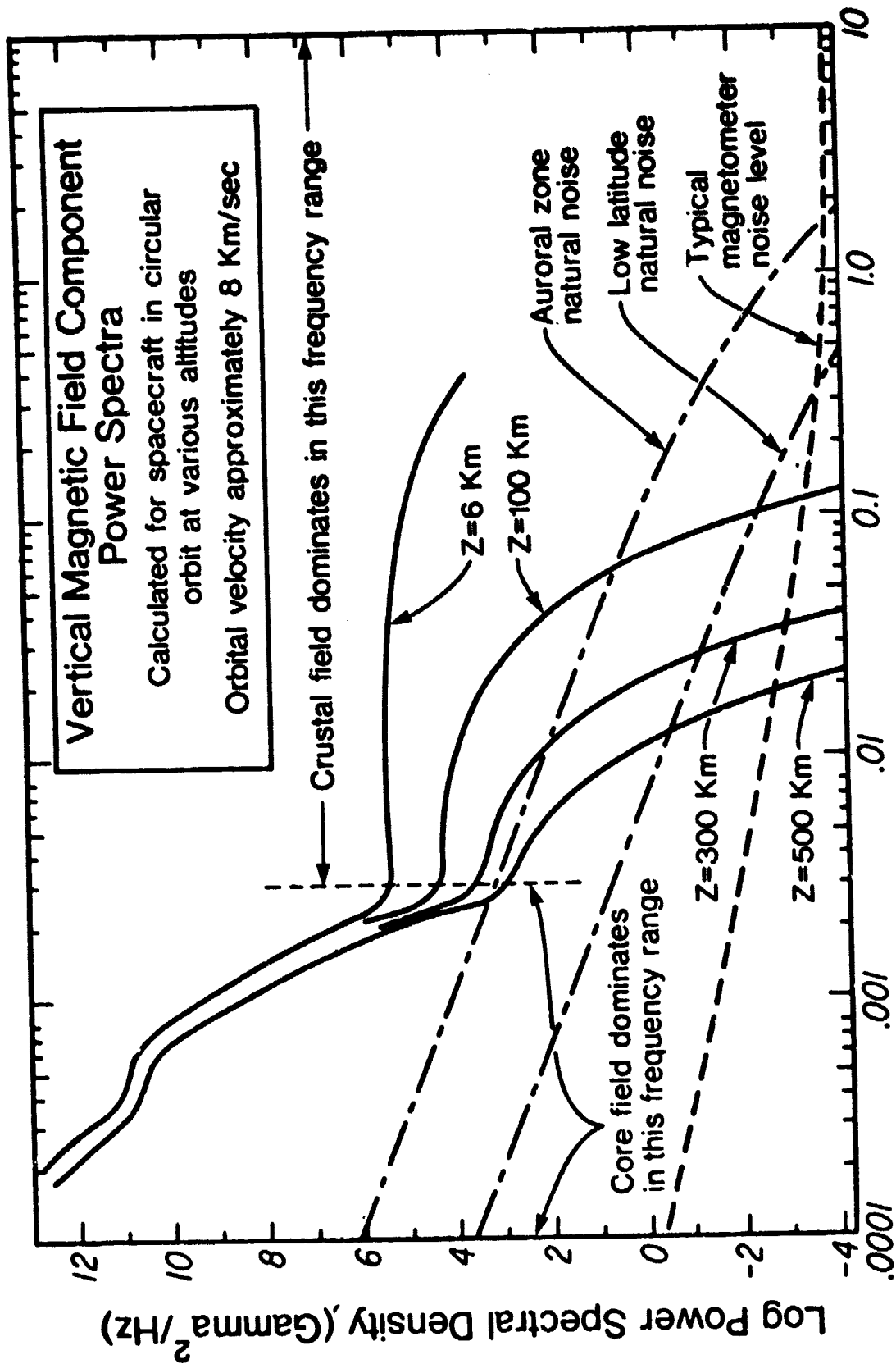


Figure 1

## Appendix A

### Program for Computing Geomagnetic Power Spectra:

The program "POW" listed on the following pages was used to compute great circle power spectra of the vertical component of the geomagnetic field according to equations (1) through (8) of this report. The program is written in Hewlett-Packard Fortran. The only data that need be entered in the program are the satellite altitudes. They are entered on line 6 of the program in km, the program as shown computes spectra for altitudes of 6, 100, 200, 300 and 500 km.

Following the program the computed values of  $\langle B_r^2 \rangle_m$  are tabulated in Table 1. The first column of the table is the harmonic number  $m$ , the next column is  $\langle B_r^2 \rangle_m$  for an altitude of 6 km, while the next four columns are  $\langle B_r^2 \rangle_m$  for altitudes of 100, 200, 300, and 500 km. Units for  $\langle B_r^2 \rangle_m$  are  $\text{gamma}^2$ .

The program is easily modified to compute  $\langle B_{11}^2 \rangle_m$  or  $\langle B_{\perp}^2 \rangle_m$  according to the equations given in the report by McLeod and Coleman (1977b), where  $\langle B_{11}^2 \rangle_m$  is the great circle power spectrum for the component of magnetic field along the great circle track and  $\langle B_{\perp}^2 \rangle_m$  is the great circle power spectrum for the component of magnetic field perpendicular to the great circle track and the radial direction.

To compute  $\langle B_{11}^2 \rangle_m$ , it is only necessary to change line 20 of the program from

$$F1 = (N + 1.) * R / (2 * N + 1.)$$

to

$$F1 = M * R * M / ((2 * N + 1.) * (N + 1.))$$

Values of  $\langle B_{11}^2 \rangle_m$  computed using this modification of the program are given in Table 2.

To compute  $\langle B_{\perp}^2 \rangle_m$ , somewhat more extensive changes in the program are necessary. Line 20 of the program must be changed to

$$F 1 = R / ((2 * N + 1.) * (N + 1.))$$

Also, the equation

$$M 1 = M + 1$$

must be inserted between lines 16 and 17 of the program, line 17 should be changed to

```
DO 100 N = M1, MM, 2
```

and line 19 should be changed to

```
CALL DPSQ (N, M, P)
```

Values of  $\langle B_{1}^2 \rangle_m$  computed using this modification of the program are given in Table 3.

Program "POW"

```

0001 FTN4,L
0002 PROGRAM POW
0003 DOUBLE PRECISION G
0004 CC READ(1,*) M,Z
0005 DIMENSION F(5),Z(5)
0006 DATA Z/6.,100.,200.,300.,500./
0007 ISM=0
0008 ISSM=20
0009 IIM=1
0010 G=0.0D0
0011 3 DO 1 IM=ISM,ISSM,IIM
0012 M=IM
0013 DO 2 I=1,5
0014 G=0.0D0
0015 MM=500+M
0016 IF(I.EQ.1) MM=4000
0017 DO 100 N=M,MM,2
0018 CALL SPEC (N,R)
0019 CALL PSQ (N,M,P)
0020 F1=(N+1.)*R/(2*N+1.)
0021 F2 = 6371./(6371.+ Z(I))
0022 F3 = F2**(2*N + 4)
0023 100 G = F1*F3*P + G
0024 2 F(I) = SNGL(G)
0025 1 WRITE(8,1000)M,F
0026 1000 FORMAT(1X,I10,5E10.4)
0027 AA=5
0028 IF(ISSM.GE.500) AA=4
0029 IIM=AA*IIM
0030 ISM=ISSM+IIM
0031 ISSM=AA*ISSM
0032 IF(ISSM.GE.3000) GO TO 4
0033 GO TO 3
0034 CC READ(1,*)ICON
0035 CC IF(ICON.NE.0)GO TO 1
0036 4 STOP
0037 END
0038 C
0039 C
0040 SUBROUTINE FACT (N,FL)
0041 FL = 1
0042 DO 100 I=1,N
0043 100 FL=I*FL
0044 RETURN
0045 END
0046 C

```

Program "POW" (continued)

```

0047 C
0048 SUBROUTINE PSQ(N,M,P)
0049 L = MOD((N+M),2)
0050 IF(L.EQ.1) GO TO 100
0051 I = 2
0052 IF(M.EQ.0) I = 1
0053 K = N-M
0054 L = N+M
0055 IF(K.LT.0) GO TO 100
0056 IF(K.GE.20) GO TO 200
0057 IF(L.GE.20) GO TO 300
0058 K2=K/2
0059 L2=L/2
0060 CALL FACT(K,FK)
0061 CALL FACT(L,FL)
0062 CALL FACT(K2,FK2)
0063 CALL FACT(L2,FL2)
0064 B=(FK2*FL2)**2
0065 S2=2.**(2*N)
0066 P=(I*FL^FK)/(B*S2)
0067 RETURN
0068 100 P=0
0069 RETURN
0070 200 PI=3.14159
0071 B=K*FLOAT(L)
0072 C=SQRT(B)
0073 P=4.*(1-N/(2*B))/(PI*C)
0074 RETURN
0075 300 PI=3.14159
0076 K2=K/2
0077 CALL FACT(K,FK)
0078 CALL FACT(K2,FK2)
0079 A=FK/(FK2**2)
0080 C=2*PI*L
0081 D=SQRT(C)
0082 E=2.**(K-2)
0083 P=A*(1.-1./(4*L))/(D*E)
0084 RETURN
0085 END
0086 C
0087 C

```

Program "POW" (continued)

```

0088 C
0089 SUBROUTINE DPSQ(N,M,D)
0090 A=1
0091 IF(M.EQ.0) A=0.5
0092 M1=M+1
0093 CALL PSQ(N,M1,P)
0094 D=A*P*(N+M1)*(N-M)
0095 RETURN
0096 END
0097 C
0098 C
0099 C
0100 SUBROUTINE SPEC(N,R)
0101 IF (N.LE.12) GO TO 100
0102 IF(N.LE.22) GO TO 200
0103 A=N/290.
0104 F=(1.0-EXP(-A))/A
0105 R=(2*N+1)*0.260*F
0106 RETURN
0107 200 A=6.79E+8
0108 B=0.284**N
0109 C=0.260*(1-N/580.)
0110 D=(2*N+1.)
0111 E=(2*N+1.)/(N+2.)
0112 R=A*E*B+D*C
0113 RETURN
0114 100 IF(N.EQ.1) R=1.879E+9
0115 IF(N.EQ.0) R=0.0
0116 IF(N.EQ.2) R=5.864E+7
0117 IF(N.EQ.3) R=3.447E+7
0118 IF(N.EQ.4) R=1.066E+7
0119 IF(N.EQ.5) R=1.974E+6
0120 IF(N.EQ.6) R=5.239E+5
0121 IF(N.EQ.7) R=1.275E+5
0122 IF(N.EQ.8) R=1.769E+4
0123 IF(N.EQ.9) R=1.273E+4
0124 IF(N.EQ.10) R=3.103E+3
0125 IF(N.EQ.11) R=1.382E+3
0126 IF(N.EQ.12) R=6.834E+2
0127 RETURN
0128 END
0129 ENDS

```

TABLE 1

$\langle B_r^2 \rangle_m$  versus m for Various Altitudes

Altitude	6	100	200	300	500	kilometers
m	$\langle B_r^2 \rangle_m$					
0	.9581E+07	.8479E+07	.7461E+07	.6580E+07	.5151E+07	
1	.1253E+10	.1147E+10	.1046E+10	.9553E+09	.7996E+09	
2	.2808E+08	.2488E+08	.2192E+08	.1936E+08	.1518E+08	
3	.1250E+08	.1078E+08	.9236E+07	.7931E+07	.5889E+07	
4	.3273E+07	.2742E+07	.2278E+07	.1899E+07	.1329E+07	
5	.5393E+06	.4385E+06	.3532E+06	.2854E+06	.1882E+06	
6	.1276E+06	.1008E+06	.7881E+05	.6183E+05	.3847E+05	
7	.2945E+05	.2253E+05	.1705E+05	.1295E+05	.7577E+04	
8	.4000E+04	.2936E+04	.2147E+04	.1579E+04	.8668E+03	
9	.2613E+04	.1857E+04	.1320E+04	.9437E+03	.4902E+03	
10	.6684E+03	.4373E+03	.2998E+03	.2072E+03	.1009E+03	
11	.2939E+03	.1708E+03	.1132E+03	.7605E+02	.3506E+02	
12	.1628E+03	.7909E+02	.5034E+02	.3269E+02	.1417E+02	
13	.6548E+02	.1423E+02	.7950E+01	.4809E+01	.1892E+01	
14	.5417E+02	.6820E+01	.3209E+01	.1760E+01	.6096E+00	
15	.5104E+02	.4789E+01	.1934E+01	.9573E+00	.2869E+00	
16	.5016E+02	.4190E+01	.1554E+01	.7191E+00	.1931E+00	
17	.4989E+02	.3973E+01	.1408E+01	.6250E+00	.1556E+00	
18	.4979E+02	.3858E+01	.1324E+01	.5692E+00	.1331E+00	
19	.4974E+02	.3771E+01	.1258E+01	.5252E+00	.1158E+00	
20	.4970E+02	.3692E+01	.1199E+01	.4861E+00	.1012E+00	
25	.4951E+02	.3316E+01	.9380E+00	.3297E+00	.5148E-01	
30	.4930E+02	.2962E+01	.7274E+00	.2211E+00	.2585E-01	
35	.4907E+02	.2632E+01	.5600E+00	.1471E+00	.1285E-01	
40	.4882E+02	.2330E+01	.4287E+00	.9716E-01	.6343E-02	
45	.4856E+02	.2056E+01	.3267E+00	.6385E-01	.3112E-02	
50	.4829E+02	.1808E+01	.2480E+00	.4179E-01	.1519E-02	
55	.4801E+02	.1587E+01	.1876E+00	.2725E-01	.7387E-03	
60	.4771E+02	.1390E+01	.1416E+00	.1771E-01	.3580E-03	
65	.4741E+02	.1215E+01	.1066E+00	.1148E-01	.1730E-03	
70	.4709E+02	.1060E+01	.8007E-01	.7427E-02	.8338E-04	
75	.4677E+02	.9240E+00	.6004E-01	.4795E-02	.4011E-04	
80	.4644E+02	.8042E+00	.4495E-01	.3090E-02	.1926E-04	
85	.4610E+02	.6991E+00	.3360E-01	.1988E-02	.9229E-05	
90	.4576E+02	.6070E+00	.2509E-01	.1277E-02	.4417E-05	
95	.4542E+02	.5266E+00	.1871E-01	.8197E-03	.2111E-05	

TABLE 1 (continued)

Altitude	6	100	200	300	500	kilometers
100	.4506E+02	.4564E+00	.1394E-01	.5254E-03	.1008E-05	
125	.4325E+02	.2208E+00	.3155E-02	.5607E-04	.2462E-07	
150	.4138E+02	.1054E+00	.7030E-03	.5883E-05	.5907E-09	
175	.3949E+02	.4977E-01	.1548E-03	.6098E-06	.1400E-10	
200	.3762E+02	.2334E-01	.3382E-04	.6267E-07	.3288E-12	
225	.3578E+02	.1088E-01	.7342E-05	.6397E-08	.7669E-14	
250	.3398E+02	.5049E-02	.1586E-05	.6497E-09	.1779E-15	
275	.3223E+02	.2335E-02	.3411E-06	.6572E-10	.4111E-17	
300	.3055E+02	.1076E-02	.7315E-07	.6626E-11	.9467E-19	
325	.2893E+02	.4951E-03	.1564E-07	.6662E-12	.2174E-20	
350	.2738E+02	.2273E-03	.3339E-08	.6683E-13	.4981E-22	
375	.2589E+02	.1041E-03	.7112E-09	.6692E-14	.1139E-23	
400	.2448E+02	.4766E-04	.1513E-09	.6691E-15	.2601E-25	
425	.2314E+02	.2178E-04	.3214E-10	.6680E-16	.5930E-27	
450	.2186E+02	.9946E-05	.6820E-11	.6663E-17	.1351E-28	
475	.2065E+02	.4538E-05	.1446E-11	.6639E-18	.3073E-30	
500	.1950E+02	.2069E-05	.3063E-12	.6610E-19	.6987E-32	
600	.1549E+02	.8890E-07	.6135E-15	.6459E-23	.0000E+00	
700	.1229E+02	.3801E-08	.1222E-17	.6276E-27	.0000E+00	
800	.9760E+01	.1622E-09	.2429E-20	.6083E-31	.0000E+00	
900	.7760E+01	.6917E-11	.4823E-23	.5885E-35	.0000E+00	
1000	.6179E+01	.2951E-12	.9583E-26	.0000E+00	.0000E+00	
1100	.4929E+01	.1261E-13	.1906E-28	.0000E+00	.0000E+00	
1200	.3939E+01	.5393E-15	.3796E-31	.0000E+00	.0000E+00	
1300	.3153E+01	.2310E-16	.7570E-34	.0000E+00	.0000E+00	
1400	.2528E+01	.9915E-18	.1415E-36	.0000E+00	.0000E+00	
1500	.2030E+01	.4262E-19	.0000E+00	.0000E+00	.0000E+00	
1600	.1633E+01	.1835E-20	.0000E+00	.0000E+00	.0000E+00	
1700	.1315E+01	.7909E-22	.0000E+00	.0000E+00	.0000E+00	
1800	.1060E+01	.3415E-23	.0000E+00	.0000E+00	.0000E+00	
1900	.8558E+00	.1476E-24	.0000E+00	.0000E+00	.0000E+00	
2000	.6914E+00	.6389E-26	.0000E+00	.0000E+00	.0000E+00	

TABLE 2

 $\langle B_{11}^2 \rangle_m$  versus m for Various Altitudes

Altitude	6	100	200	300	500 kilometers
m	$\langle B_{11}^2 \rangle_m$				
0	.0000E+00	.0000E+00	.0000E+00	.0000E+00	.0000E+00
1	.3119E+09	.2856E+09	.2605E+09	.2379E+09	.1992E+09
2	.1194E+08	.1060E+08	.9366E+07	.8289E+07	.6529E+07
3	.6934E+07	.5987E+07	.5132E+07	.4410E+07	.3279E+07
4	.2072E+07	.1737E+07	.1444E+07	.1204E+07	.8440E+06
5	.3694E+06	.3006E+06	.2423E+06	.1960E+06	.1294E+06
6	.9305E+05	.7358E+05	.5753E+05	.4516E+05	.2812E+05
7	.2211E+05	.1696E+05	.1285E+05	.9773E+04	.5726E+04
8	.3026E+04	.2250E+04	.1650E+04	.1216E+04	.6696E+03
9	.2045E+04	.1479E+04	.1053E+04	.7539E+03	.3723E+03
10	.4991E+03	.3495E+03	.2408E+03	.1669E+03	.8158E+02
11	.2055E+03	.1399E+03	.9366E+02	.6311E+02	.2918E+02
12	.9828E+02	.6479E+02	.4202E+02	.2746E+02	.1197E+02
13	.1616E+02	.9970E+01	.6165E+01	.3868E+01	.1567E+01
14	.6766E+01	.3769E+01	.2183E+01	.1300E+01	.4828E+00
15	.4303E+01	.2122E+01	.1135E+01	.6343E+00	.2126E+00
16	.3759E+01	.1697E+01	.8514E+00	.4509E+00	.1378E+00
17	.3747E+01	.1599E+01	.7663E+00	.3896E+00	.1105E+00
18	.3880E+01	.1585E+01	.7317E+00	.3593E+00	.9548E-01
19	.4052E+01	.1591E+01	.7094E+00	.3371E+00	.8417E-01
20	.4232E+01	.1600E+01	.6895E+00	.3172E+00	.7450E-01
25	.5116E+01	.1610E+01	.5871E+00	.2305E+00	.3996E-01
30	.5942E+01	.1564E+01	.4840E+00	.1624E+00	.2082E-01
35	.6712E+01	.1484E+01	.3903E+00	.1121E+00	.1064E-01
40	.7433E+01	.1384E+01	.3100E+00	.7625E-01	.5363E-02
45	.8108E+01	.1275E+01	.2433E+00	.5129E-01	.2676E-02
50	.8739E+01	.1163E+01	.1893E+00	.3421E-01	.1324E-02
55	.9331E+01	.1053E+01	.1462E+00	.2267E-01	.6514E-03
60	.9886E+01	.9469E+00	.1123E+00	.1494E-01	.3188E-03
65	.1040E+02	.8472E+00	.8586E-01	.9798E-02	.1553E-03
70	.1089E+02	.7547E+00	.6537E-01	.6403E-02	.7541E-04
75	.1135E+02	.6698E+00	.4960E-01	.4171E-02	.3650E-04
80	.1177E+02	.5925E+00	.3752E-01	.2709E-02	.1762E-04
85	.1217E+02	.5227E+00	.2831E-01	.1755E-02	.8487E-05
90	.1255E+02	.4599E+00	.2132E-01	.1135E-02	.4080E-05
95	.1289E+02	.4039E+00	.1602E-01	.7326E-03	.1958E-05

TABLE 2 (continued)

Altitude	6	100	200	300	500 kilometers
100	.1322E+02	.3539E+00	.1202E-01	.4720E-03	.9378E-06
125	.1454E+02	.1789E+00	.2795E-02	.5139E-04	.2323E-07
150	.1543E+02	.8799E-01	.6345E-03	.5466E-05	.5626E-09
175	.1599E+02	.4252E-01	.1417E-03	.5723E-06	.1342E-10
200	.1629E+02	.2029E-01	.3127E-04	.5926E-07	.3168E-12
225	.1638E+02	.9592E-02	.6843E-05	.6086E-08	.7420E-14
250	.1632E+02	.4503E-02	.1488E-05	.6211E-09	.1727E-15
275	.1613E+02	.2102E-02	.3218E-06	.6307E-10	.4002E-17
300	.1584E+02	.9769E-03	.6933E-07	.6379E-11	.9235E-19
325	.1549E+02	.4524E-03	.1489E-07	.6432E-12	.2125E-20
350	.1507E+02	.2089E-03	.3188E-08	.6469E-13	.4876E-22
375	.1462E+02	.9624E-04	.6811E-09	.6491E-14	.1117E-23
400	.1414E+02	.4424E-04	.1453E-09	.6502E-15	.2552E-25
425	.1365E+02	.2030E-04	.3093E-10	.6502E-16	.5826E-27
450	.1314E+02	.9305E-05	.6577E-11	.6495E-17	.1328E-28
475	.1262E+02	.4259E-05	.1397E-11	.6480E-18	.3025E-30
500	.1211E+02	.1948E-05	.2964E-12	.6460E-19	.6883E-32
600	.1014E+02	.8449E-07	.5969E-15	.6336E-23	.0000E+00
700	.8383E+01	.3638E-08	.1194E-17	.6173E-27	.0000E+00
800	.6875E+01	.1560E-09	.2379E-20	.5995E-31	.0000E+00
900	.5613E+01	.6681E-11	.4735E-23	.5808E-35	.0000E+00
1000	.4569E+01	.2860E-12	.9424E-26	.0000E+00	.0000E+00
1100	.3714E+01	.1225E-13	.1877E-28	.0000E+00	.0000E+00
1200	.3017E+01	.5253E-15	.3743E-31	.0000E+00	.0000E+00
1300	.2450E+01	.2255E-16	.7473E-34	.0000E+00	.0000E+00
1400	.1990E+01	.9693E-18	.1402E-36	.0000E+00	.0000E+00
1500	.1617E+01	.4172E-19	.0000E+00	.0000E+00	.0000E+00
1600	.1314E+01	.1798E-20	.0000E+00	.0000E+00	.0000E+00
1700	.1069E+01	.7762E-22	.0000E+00	.0000E+00	.0000E+00
1800	.8695E+00	.3355E-23	.0000E+00	.0000E+00	.0000E+00
1900	.7077E+00	.1451E-24	.0000E+00	.0000E+00	.0000E+00
2000	.5762E+00	.6287E-26	.0000E+00	.0000E+00	.0000E+00

ORIGINAL PAGE IS  
OF POOR QUALITY

Table 3

 $\langle B_{\perp}^2 \rangle_m$  versus  $m$  for Various Altitudes

Altitude m	6, $\langle B_{\perp}^2 \rangle_m$	100 $\langle B_{\perp}^2 \rangle_m$	200 $\langle B_{\perp}^2 \rangle_m$	300 $\langle B_{\perp}^2 \rangle_m$	500 $\langle B_{\perp}^2 \rangle_m$	kilometers
0	.3143E+09	.2877E+09	.2623E+09	.2394E+09	.2004E+09	
1	.1301E+08	.1150E+08	.1011E+08	.8907E+07	.6961E+07	
2	.4778E+07	.4117E+07	.3522E+07	.3022E+07	.2239E+07	
3	.1068E+07	.8939E+06	.7419E+06	.6175E+06	.4316E+06	
4	.1546E+06	.1255E+06	.1009E+06	.8136E+05	.5348E+05	
5	.3193E+05	.2517E+05	.1965E+05	.1539E+05	.9560E+04	
6	.6858E+04	.5204E+04	.3923E+04	.2972E+04	.1729E+04	
7	.9199E+03	.6463E+03	.4687E+03	.3424E+03	.1858E+03	
8	.5408E+03	.3582E+03	.2528E+03	.1799E+03	.9279E+02	
9	.1633E+03	.8369E+02	.5617E+02	.3841E+02	.1843E+02	
10	.8630E+02	.2959E+02	.1876E+02	.1238E+02	.5620E+01	
11	.6347E+02	.1378E+02	.8003E+01	.5025E+01	.2118E+01	
12	.4893E+02	.4150E+01	.1729E+01	.9097E+00	.3134E+00	
13	.4709E+02	.2986E+01	.9995E+00	.4475E+00	.1229E+00	
14	.4645E+02	.2616E+01	.7802E+00	.3147E+00	.7229E-01	
15	.4612E+02	.2448E+01	.6876E+00	.2618E+00	.5396E-01	
16	.4587E+02	.2334E+01	.6289E+00	.2301E+00	.4395E-01	
17	.4565E+02	.2236E+01	.5812E+00	.2055E+00	.3674E-01	
18	.4543E+02	.2146E+01	.5387E+00	.1843E+00	.3095E-01	
19	.4522E+02	.2060E+01	.4999E+00	.1656E+00	.2613E-01	
20	.4501E+02	.1978E+01	.4641E+00	.1488E+00	.2208E-01	
25	.4397E+02	.1619E+01	.3212E+00	.8781E-01	.9596E-02	
30	.4296E+02	.1329E+01	.2235E+00	.5215E-01	.4206E-02	
35	.4198E+02	.1094E+01	.1561E+00	.3114E-01	.1857E-02	
40	.4104E+02	.9019E+00	.1095E+00	.1868E-01	.8238E-03	
45	.4013E+02	.7452E+00	.7696E-01	.1124E-01	.3672E-03	
50	.3924E+02	.6166E+00	.5424E-01	.6785E-02	.1643E-03	
55	.3838E+02	.5110E+00	.3831E-01	.4166E-02	.7372E-04	
60	.3754E+02	.4240E+00	.2711E-01	.2491E-02	.3317E-04	
65	.3673E+02	.3522E+00	.1921E-01	.1514E-02	.1496E-04	
70	.3594E+02	.2929E+00	.1364E-01	.9215E-03	.6761E-05	
75	.3517E+02	.2438E+00	.9694E-02	.5619E-03	.3961E-05	
80	.3443E+02	.2031E+00	.6898E-02	.3431E-03	.1388E-05	
85	.3370E+02	.1693E+00	.4914E-02	.2097E-03	.6303E-06	
90	.3299E+02	.1412E+00	.3504E-02	.1234E-03	.2866E-06	
95	.3231E+02	.1179E+00	.2501E-02	.7864E-04	.1305E-06	

TABLE 3 (continued)

Altitude	6	100	200	300	500 kilometers
100	.3164E+02	.9848E-01	.1786E-02	.4823E-04	.5946E-07
125	.2854E+02	.4036E-01	.3357E-03	.4232E-05	.1184E-08
150	.2580E+02	.1672E-01	.6394E-04	.3771E-06	.2399E-10
175	.2338E+02	.6983E-02	.1230E-04	.3398E-07	.4920E-12
200	.2122E+02	.2936E-02	.2387E-05	.3089E-08	.1018E-13
225	.1930E+02	.1241E-02	.4659E-06	.2827E-09	.2124E-15
250	.1757E+02	.5267E-03	.9144E-07	.2602E-10	.4455E-17
275	.1603E+02	.2245E-03	.1803E-07	.2407E-11	.9394E-19
300	.1463E+02	.9599E-04	.3568E-08	.2235E-12	.1989E-20
325	.1338E+02	.4117E-04	.7086E-09	.2083E-13	.4229E-22
350	.1225E+02	.1771E-04	.1412E-09	.1948E-14	.9019E-24
375	.1122E+02	.7634E-05	.2819E-10	.1826E-15	.1929E-25
400	.1029E+02	.3299E-05	.5645E-11	.1717E-16	.4137E-27
425	.9450E+01	.1428E-05	.1133E-11	.1618E-17	.8893E-29
450	.8685E+01	.6194E-06	.2278E-12	.1527E-18	.1916E-30
475	.7988E+01	.2691E-06	.4588E-13	.1445E-19	.4134E-32
500	.7353E+01	.1171E-06	.9259E-14	.1369E-20	.8817E-34
600	.5321E+01	.4262E-08	.1559E-16	.1122E-24	.0000E+00
700	.3893E+01	.1581E-09	.2680E-19	.9388E-29	.0000E+00
800	.2875E+01	.5961E-11	.4685E-22	.7951E-33	.0000E+00
900	.2140E+01	.2278E-12	.8307E-25	.0000E+00	.0000E+00
1000	.1605E+01	.8806E-14	.1491E-27	.0000E+00	.0000E+00
1100	.1211E+01	.3439E-15	.2704E-30	.0000E+00	.0000E+00
1200	.9185E+00	.1355E-16	.4873E-33	.0000E+00	.0000E+00
1300	.7002E+00	.5382E-18	.0000E+00	.0000E+00	.0000E+00
1400	.5360E+00	.2153E-19	.0000E+00	.0000E+00	.0000E+00
1500	.4119E+00	.8664E-21	.0000E+00	.0000E+00	.0000E+00
1600	.3175E+00	.3507E-22	.0000E+00	.0000E+00	.0000E+00
1700	.2455E+00	.1427E-23	.0000E+00	.0000E+00	.0000E+00
1800	.1902E+00	.5832E-25	.0000E+00	.0000E+00	.0000E+00
1900	.1477E+00	.2393E-26	.0000E+00	.0000E+00	.0000E+00
2000	.1148E+00	.0860E-28	.0000E+00	.0000E+00	.0000E+00

GRAVITY GRADIENT DETERMINATION WITH  
TETHERED SYSTEMS

By

P. M. Kalaghan and G. Colombo

May 1978

Smithsonian Institution  
Astrophysical Observatory  
Cambridge, Massachusetts 02138

The Smithsonian Astrophysical Observatory  
and the Harvard College Observatory  
are members of the  
Center for Astrophysics

# GRAVITY GRADIENT DETERMINATION WITH TETHERED SYSTEMS

P. M. Kalaghan and G. Colombo

## I. Introduction

Determination of the characteristics of the Earth's gravity is of fundamental importance not only because of the need to comprehend and control the dynamical behavior of artificial satellites, but also because of the intimate relationship between the gravity field and the phenomenology comprising modern solid Earth dynamics investigations and ocean process studies (Kaula, 1970).

### 1.1 Solid Earth Studies

Evidence from studies of seismic wave propagation shows that the outer portion of the Earth consists of (1) a high-velocity zone, the lithosphere, which generally includes the crust and uppermost mantle, and is some 50 to 80 kilometers thick under the oceans and somewhat thicker under the continents; (2) a low-velocity zone, the asthenosphere, which is a layer of low effective strength on a geologic time scale and extends from the base of the lithosphere to a depth of several hundred kilometers; and (3) the lower remaining portion of the mantle, the mesosphere. The plate-tectonics concept is based on the observation that large blocks of the rigid lithosphere, thousands of kilometers in horizontal extent, appear to be moving ("floating" on the yielding asthenosphere) with respect to one another at average long-term rates of the order of 1 to 15 cm/yr (Isacks, et al., 1968). One manifestation of this plate motion is continental drift. Most large earthquakes, volcanic activity, mountain building, and tsunami generation, plus some terrestrial mineral resources, are located at the boundaries of the lithospheric plates. In fact, nearly all large-scale geological and geophysical phenomena occurring on the Earth's surface appear to be intimately related to this global pattern of plate motions.

However, no satisfactory theory of the mechanism(s) producing plate motion is available. It is very probable that both thermal convection and mass convection in the asthenosphere are involved. There is little question that knowledge of the density field, to a depth of 700 kilometers, would be of considerable importance in determining the basic mechanisms underlying plate motion. The structure of the Earth's gravity field provides one of the few available clues to the distribution of mass in the Earth.

Since the distribution of mass within the Earth uniquely determines the external gravity field, measurements of the latter contain information on the

density field. (It should be noted that the external field does not define the unique internal mass distribution). As a rough rule of thumb, a density feature within the Earth will produce a lateral variation in the external gravity field whose scale is comparable to the depth of the anomaly. Thus, the density field within the upper mantle at depths of the order of 100 to 700 kilometers will generally be reflected in horizontal variations of the gravity field with wavelengths of 100 to 700 kilometers. This suggests that measurements of intermediate-wavelength (100- to 1000-kilometer) features in the gravity field will be fundamental to advancing our understanding of plate tectonics processes.

## 1.2 Ocean Process Studies

The intermediate-wavelength structure of the Earth's gravity field is also of interest for another reason. The surface of the ocean contains topographic signatures of current systems, eddies, storm surges, tsunamis, barometric loading, etc., all of which are of considerable practical importance. There is a great interest in developing methods for maintaining frequent surveillance of these phenomena over the world's ocean. (A technique now being used is the satellite-borne radar altimeter on Geos 3, launched by the National Aeronautics and Space Administration (NASA) in April 1975.) However, the mean-sea-level surface also contains the topographic imprint of the Earth's gravity field - i.e., the geoid. Geoid undulations must be isolated from oceanographic features in order to study ocean dynamics phenomena. All the oceanic features listed above have topographic structures with significant lateral components in the range 100 to 1000 kilometers. The estimated geoid accuracy needed for this purpose is 10 centimeters in geoid height. Once again an accurate determination of the gravity field is required in order to carry out the investigation.

## 2. Gravity Measurements

Gravity field values over the earth have been measured for scores of years, both absolutely and relative to designated base stations. Extensive gravity surveys have measured relative field strengths over some of the more populated continental areas for both academic and economic reasons.

Absolute gravity field measurements have been made to about one part in  $10^6$ , most commonly by means of pendulums or by timing the free fall of objects. Relative measurements are made routinely two orders of magnitude more accurately with a number of standard gravimeters. Relative measurements to about one part in  $10^{-9}$  to  $10^{-10}$  can now be made by station tidal gravimeters. All of these measurements are of the gravitational acceleration, or gravity field strength, which is equal to about  $980 \text{ cm/sec}^2$  at the surface of the earth. The gravity field is the vertical derivative of the potential, which is not measured directly. An acceleration of  $1.0 \text{ cm/sec}^2$  is called 1 gal.

Areal gravity variations exclusive of differences due to elevation or latitude differences among stations are referred to as gravity anomalies. These are commonly less than 1 gal. The roots of mountain ranges and down-

warped ocean trenches provide anomalies of a few hundred milligals. Ore deposits commonly have anomalies of tens of milligals or less.

A sensitive method of gravity measurement was used in very flat areas for prospecting purposes several decades ago. This was the measurement of horizontal gravity field gradients and determination of the differential curvature of equipotential surfaces through use of an Eötvös torsion balance or a similar device. (The unit of gravity field gradient in common use is the Eötvös unit; 1 EU is a gradient of  $10^{-9}$  gal/cm.)

More recently, the structure of the gravity field has been calculated via orbital dynamics from accurate tracking of artificial satellites. Since satellite orbits are uniquely determined by the forces acting on the satellite and since gravity is by far the dominant force, the gravitational force can be inferred from the observed orbits and an appropriate orbit theory. This orbital-dynamics approach has been used successfully to measure the large-scale structure of the gravity field with considerable accuracy. However, orbital dynamics is not sensitive to intermediate- or short-wavelength gravity-field features. Specifically, spherical-harmonic terms of degree higher than 20 do not significantly influence satellite orbits, and this method is restricted therefore to gravity features with horizontal wavelengths greater than 2000 kilometers.

A third method of satellite gravity determination is the measurement of gravity field gradients at orbital altitude. Gravity gradiometers offer an interesting alternative technique to surface gravitational measurements and satellite perturbation analysis. Gradiometers provide several advantages compared to surface gravity measurements; the most important is the speed with which the data can be taken. A gradiometer satellite in a polar orbit can achieve complete coverage of the earth in a period of days. The data taken can be of nearly uniform accuracy, thus eliminating the need for weighting to reflect varying significance levels.

The most significant advantage of a satellite-borne gradiometer when compared to more conventional satellite techniques is that the gradiometer accentuates high frequencies because it measures a derivative of acceleration. Perturbation analysis of satellite trajectories is based on position measurement, which is obtained by integrating the acceleration twice, thus it is relatively insensitive to high frequencies. Current doppler radar techniques measure a relative velocity, which is a single integral of acceleration and again is less sensitive to high frequencies than the gradiometer.

In order to develop gravity field measuring instrumentation capable of measuring fine structures of the gravity field, a series of engineering feasibility and design studies has been carried out under NASA and Air Force sponsorship for spacecraft using a gravity gradiometer instrument. Some of the studies were performed for lunar-orbit missions (Bell, 1970; Bell et al., 1971; Ganssle, 1967; Savet et al., 1967; Thompson et al., 1965; Thompson, 1966; Thompson, 1970). Other studies were performed for earth-orbit missions. Forward (1973) considered a rotating resonance torsional gravity gradiometer,

while Metzger employed a rotating MESA gradiometer and a rotating-resonance torsional gravity gradiometer. Recently, Trageser (1970, 1973, and 1975) and Trageser and Johnson (1974) developed a floated gravity-gradiometric system using three independent gradiometers, each with a 10-cm spherical float, equipped with gyroscopes.

All the above studies have indicated that present state of the art gradiometer sensitivity is no better than 1 e.u., even in the laboratory environment. There is a consensus of opinion that a major development program would be required to increase of some order of magnitude this sensitivity. Clearly, a fresh new start is desirable.

### 3. The Dumbbell Gradiometer

A significant advance in the state of the art of gravity gradiometry is now possible through the utilization of Tethered Satellite Systems (Colombo et al., 1974). Recent analyses have indicated the feasibility of employing an orbiting system of two tethered masses as a sensitive gradiometer. This configuration has been named the "Dumbbell Gradiometer" (Colombo et al., 1976). Two particular forms are possible: the Dumbbell Free Flyer and the Shuttle-based Dumbbell.

#### 3.1 The Dumbbell Free Flyer

Figure 1 depicts a "Dumbbell" Free Flyer, the proposed sensor of gravity gradients from orbital heights. The system (Colombo et al., 1976) is implemented by terminating a tether in space with two end masses. The gravity gradient keeps the system aligned along the local vertical. Lengths considered thus far during the in-house study range from one kilometer to 20 kilometers, end masses considered range from 100 to 1000 kilograms.

When the orbiting Dumbbell system passes through a gravity field each end mass experiences a force proportional to the gravity field at its location. The differential force between the end masses then creates a tension in the tether. The tension in the tether is proportional to the difference in gravity force acting on the two end masses. Thus the tension is a measure of the mean gravity gradient existing in the space between the end masses.

##### 3.1.1 System response.

In quantitative terms, the tension,  $T$ , measured in the Dumbbell tether is related to the average gradient in the vertical acceleration  $\ddot{z}$ , as follows.

$$T = M \cdot L \left( \frac{\partial \ddot{z}}{\partial z} \right)_L$$

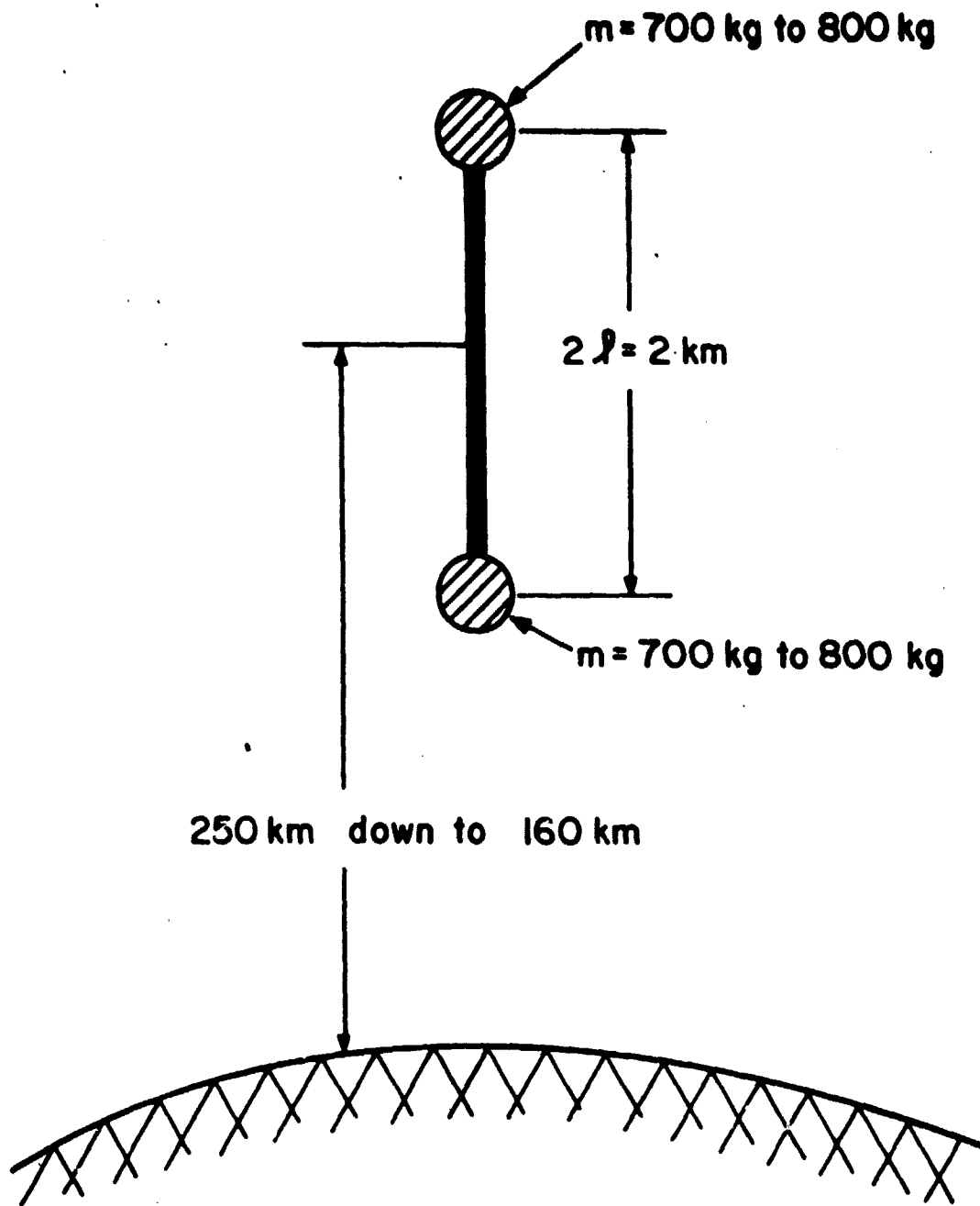


Fig. 1. - The Dumbbell configuration.

where

$M$  = the Dumbbell end mass,

$L$  = the Dumbbell length,

$\left(\frac{\partial \ddot{z}}{\partial z}\right)_L$  = the average value over length  $L$ .

For a simple  $r^{-2}$  gravity field model of the Earth, the tension can be expressed as

$$T = M \cdot L \cdot \frac{3GM_E}{(R_E + h)^3}$$

where

$G$  = the gravitational constant,

$M_E$  = the mass of the Earth,

$R_E$  = the mean radius of the Earth,

$h$  = the height of the Dumbbell center of mass above the surface of the Earth.

If Dumbbell traverses a gravity anomaly caused by a surface mass inhomogeneity,  $\Delta M$ , the differential tension becomes

$$\Delta T = M \cdot L \cdot \frac{3G\Delta M}{h^3}$$

Finally, the relative differential tension can be written

$$\frac{\Delta T}{T} = \left(\frac{\Delta M}{M_E}\right) \left(\frac{R_E + h}{h}\right)^3$$

From these expressions it can be seen that the Dumbbell tension is proportional to the product  $M \cdot L$  for the system. The relative differential tension however is proportional only to the mass contrast ( $\Delta M/M$ ) and the distance factor and is independent of  $M$  and  $L$ .

In quantitative terms, the vertical gradient at an altitude of 200 km above the Earth is approximately 3000 EU while the perturbation in this value caused by a 100 mgal surface anomaly, extending over a 120 by 120 km square amounts to only 0.4 EU. Similarly for a Dumbbell system with a 2 km length, 1000 kg end masses at 200 km altitude, the normal gravity gradient would produce a tension of 800,000 dynes while the variation caused by passage over the 100 mgal anomaly would be 100 dynes.

### 3.1.2 System Mechanization

A sample set of system parameters is given below:

tether length	2 km
terminating masses	700 kg to 800 kg each
life	approximately 20-30 days
orbital height	250 km down to 160 km in 30 day lifetime
measurement sensitivity with 5-second integration time(*)	$1.2 \times 10^{-2}$ e.u.
measurement resolution	3 parts in $10^6$ (minimum detectable signal 1 dyne)
area/mass ratio	0.015 to 0.02
tether material	Kevlar

A possible system mechanization of the Dumbbell Free Flyer has been worked out by Colombo *et al.*, 1976. Consider the most relevant subsystem: the device that measures the tether's tension, the fundamental observable for the experiment.

Figure 2 is a schematic representation of this measurement device; it consists of a twin-pulley bogey that is cantilever-mounted to the terminating mass. The tether wire is led over the pulleys, as shown in the figure, so that a tension  $T$  in the wire creates a bending moment  $TL$  in the left-hand portion of the beam, where strain gauges are located. The quantity  $L$  here represents the offset the bogey produces in the tether.

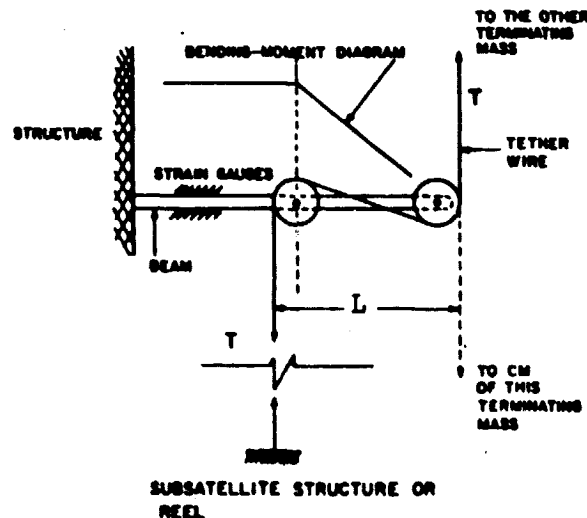


Figure 2. Proposed device for measuring the tension on the wire.

(\*) Assuming only the noise of the electronic amplifiers of the sensor.

The beam is designed to survive 10 kgw load and is capable (with a 5-second integration time) of an absolute sensitivity of  $10^{-5}$  kgw (10 dyne tension change in an environment consisting both of an unsteady tension component ( $10^{-3}$  kgw) and a steady component (1 kgw). Measurement resolution is 1 part in  $10^{+5}$  (Colombo et al., 1976). An advanced version of the device (with improved electronics) can provide a measurement resolution of 1 part in  $10^6$  with threshold sensitivity of 10 dynes, or 1 part in  $10^5$  with a threshold sensitivity of 1 dyne. The substantial dynamic range involved does not appear to present serious difficulties to the designers of the device.

In addition to the tether tension (at both ends), the following observables must be monitored and recorded:

a. Position of the two terminating masses as obtained by tracking them from ground. This will provide accurate range data and crude angular data on the orbiting system.

b. Relative angular position of the mass that is in the higher orbit with respect to the one in the lower orbit by means of the star tracker and the optical beacon described in Colombo et al., 1976.

c. Length of the tether (parameter of the system).

### 3.1.3 Supporting Studies

In the Appendices of this report we have summarized analyses of the expected system performance by (1) constructing models of the gravity anomalies and (2) computing the related signal strength, i.e., the tether tension, and (3) performing an initial appraisal of the expected system noise level, above and beyond the noise of the electronic amplifiers of the tension detection and measurement system. In all cases, no fundamental technical difficulties have been discovered.

In addition to this preliminary analysis, we have also examined the problems involved in the data inversion. Although we do expect them to be difficult we do not think they will be insurmountable. In fact, we were able to develop a simple data analysis approach that allowed inference of the presence of several 100 mgal anomalies places along the ground track of the system.

### 3.2 A Shuttle-Based Dumbbell Experiment

As indicated in the previous section, the ultimate configuration of Dumbbell is a Free Flyer: This will minimize system noise and will make it possible to approach the level of sensitivity corresponding to the low internal noise of the instrument's amplifiers. However, preliminary experimentation with Dumbbell can also be carried out on the forthcoming Shuttle flight on which NASA is planning to install a long tether connected to a subsatellite. On a Shuttle flight, Dumbbell will find a more noisy environment, with consequent substantial decrease of measurement sensitivity. The low cost of the experiment would amply compensate for this disadvantage, however.

Using simulation software developed at SAO under contract NASA 8-32199 we have calculated the expected perturbations introduced into the tether's tension by gravity anomalies with a Shuttle-based Dumbbell system. We have assumed that Shuttle/subsatellite system is stabilized, after full deployment, about a reference circular-orbit configuration at a height of 400 km. We have assumed system with  $10^5$  kg on the upper end, to represent the Shuttle Orbiter and 500 kg on the lower end to represent the subsatellite. The tether length employed in this case was 20 km. The model of the anomaly adopted was an array of 3 masses  $\times$  3 masses in a surface grid with dimensions 100 km  $\times$  100 km. An estimate of the absolute value of the tension and of its percentage variation above a gravity anomaly is given in Table 1.

Table 1. Wire tension and changes as a function of gravity-anomaly intensity.

Time counted from arbitrary epoch (sec)	$A_g = 0$		$A_g = 100 \text{ mgal}$		$A_g = 500 \text{ mgal}$	
	Tension (dynes)	Tension (dynes)	$\Delta$ Tension Tension	Tension (dynes)	$\Delta$ Tension Tension	
110.6	836512	836511	$-0.12 \times 10^{-5}$	836507	$-0.06 \times 10^{-4}$	
121.0	836601	836601	0.00	836600	$-0.01 \times 10^{-4}$	
131.3	836690	836693	$0.36 \times 10^{-5}$	836707	$0.20 \times 10^{-4}$	
141.7	836778	836794	$1.91 \times 10^{-5}$	836856	$0.93 \times 10^{-4}$	
150.3	836851	836888	$4.42 \times 10^{-5}$	837034	$2.19 \times 10^{-4}$	
160.7*	836940	837001	$7.29 \times 10^{-5}$	837249	$3.69 \times 10^{-4}$	
171.1	837027	837080	$6.33 \times 10^{-5}$	837293	$3.18 \times 10^{-4}$	
181.4	837114	837137	$2.75 \times 10^{-5}$	837228	$1.36 \times 10^{-4}$	
190.1	837186	837193	$0.84 \times 10^{-5}$	837220	$0.41 \times 10^{-4}$	
200.5	837272	837272	0.00	837272	0.00	

\*Passage over center of 100-km  $\times$  100-km anomaly.

Assuming that the internal noise of the amplifiers of the tension-measuring device (Colombo et al., 1976) is approximately  $1 \times 10^{-5}$  (fractional change in tether tension), it can be seen that the signal produced by the 100 milligal anomaly (see Table 1) is  $7.29 \times 10^{-5}$  or eight times the minimum detectable signal of the amplifiers.

It is certainly recognized that the perturbations introduced by the Shuttle and its environment (air drag, thrusting, vibrations, motion of the crew, etc.) represent a substantial increase in system noise. An approach to remove or at least mitigate the influence of the Shuttle-generated noise is under investigation. One possible method would be the use on-board the Shuttle of a sensitive accelerometer (the Mesa Cactus variety, characterized by a sensitivity of  $10^{-8}$  to  $10^{-9}$  g) in order to measure the component of the acceleration noise induced by the Shuttle along the direction of the tether.

#### 4. Conclusion

A more detailed investigation of the Earth's gravity field is needed for application to modern solid earth and oceanic investigations. The use of gravity gradiometers presents a powerful technique to measure the intermediate wavelength components of the gravity field. One particularly innovative configuration of a gradiometer involves a tethered pair of masses orbiting the earth and stabilized by the vertical gravity gradient of the earth. A measurement of the tension in such a system, called the DUMBELL system, would allow the determination of the vertical gradient of the anomalous component of the Earth's gravity field. Preliminary analysis of the dynamics, mechanization, expected signal levels and noise environment have all indicated that the Dumbbell system is feasible.

## 5. References

- Bell, C. C., "Lunar Orbiter Selenodesy Feasibility Demonstration," Final Report, NASA Contract NAS 8-24788, January 1970.
- Bell, C. C., Forward, R. L., and Williams, H. P., "Simulated Terrain Mapping with the Rotating Gravity Gradiometer," in Advances in Dynamic Gravimetry, ed. by W. T. Kattner, Instr. Soc. Amer., Pittsburg, pp. 115-128, 1971.
- Colombo, G., Gaposchkin, E. M., Grossi, M. D., and Weiffenbach, G. C., "Shuttle-Borne 'Skyhook': A New Tool for Low-Orbital-Altitude Research," Smithsonian Astrophys. Obs. Reports in Geoastronomy No. 1, September 1974.
- Colombo, G., Arnold, D. A., Binsack, J. H., Gay, R. H., Grossi, M. D., Lautman, D. A., and Orringer, O., "Dumbbell Gravity-Gradient Sensor: A New Application of Orbiting Long Tethers," Smithsonian Astrophys. Obs. Reports in Geoastronomy No. 2, June 1976.
- Forward, "A Review of Artificial Satellite Gravity Gradiometer Techniques for Geodesy," presented at the First International Symposium on the Use of Artificial Satellites for Geodesy and Geophysics, Athens, May 1973; also in Hughes Aircraft Company Res. Rep. No. 469, 1973.
- Ganssle, E. R., "Gravity Gradiometry Mission Feasibility Study," Final Report, NASA Contract NAS 8-21182, 1967.
- Isacks, B., Oliver, J., and Sykes, L. R., "Seismology and the New Global Tectonics, Journal Geophysical Research, vol. 73, pp. 5855-5899, 1968.
- Kaula, W. M., editor, "The Terrestrial Environment: Solid-Earth and Ocean Physics," Report of a Study at Williamstown, Massachusetts, NASA CR-1579, 1970.
- Savet, P. H., et al., "Gravity Gradiometry," Final Report, NASA Contract NAS 8-21130, December 1967.
- Thompson, L. G. D., Bock, R. O., and Savet, P. H., "Gravity Gradient Sensors and Their Applications for Manned Orbital Spacecraft," presented at the Third Goddard Memorial Symposium, American Astronomical Society, Washington, D. C., March 1965.
- Thompson, L. G. D., "Gravity Gradient Instruments Study," Final Report, NASA Contract NASW-1328, August 1966. .

Thompson, L. G. D., "Gravity Gradient Preliminary Investigation," Final Report, NASA Contract NAS 9-9200, January 1970.

Trageser, M. B., "A Gradiometer System for Gravity Anomaly Surveying," presented at the Invitational Symposium on Dynamic Gravimetry, Fort Worth, Texas, March 1970; also MIT/CSDL Report R-588, June 1970.

Trageser, M. B., "Gravity Gradiometer Status Report," MIT/CSDL Report C-3935, June 1973.

Trageser, M. B., "Feasibility Model Gravity Gradiometer Test Results," Presented at the American Institute of Aeronautics and Astronautics Guidance and Control Conference, Boston, August 1975; also MIT/CSDL Report P-179, July 1975.

Trageser, M. B., and Johnson, D. O., "Preliminary Gravity Gradiometer System Study," Final Report, JPL Contract 954309, June 1976.

## APPENDIX I

### Analysis of Expected Signal Level

The signature of a gravity anomaly can be represented by the field produced by a grid of point masses on the surface of the earth. The vertical component of the acceleration and the vertical derivative of the acceleration are computed along a track passing over the anomaly. The vertical derivative is the signal that would be measured by a Dumbbell gravity gradiometer. The acceleration  $\ddot{r}$  produced by a point anomaly M is

$$\ddot{r} = -GM\vec{r}^{-3}$$

where  $r$  is the vector from the anomaly to the gradiometer and  $r = |\vec{r}|$ . The vertical component  $\ddot{z}$  of the acceleration is

$$\ddot{z} = -GMzr^{-3}$$

The vertical derivative of  $\ddot{z}$  is

$$\frac{\partial \ddot{z}}{\partial z} = GM(3z^2r^{-5} - r^{-3})$$

In the case where the satellite is directly overhead, this reduces to

$$\frac{\partial \ddot{z}}{\partial z} = 2GMr^{-3}$$

If an area has a gravity anomaly  $\Delta g$  ( $\text{cm}/\text{sec}^2$ ) this can be represented by a surface layer of density  $\sigma$  ( $\text{g}/\text{cm}^2$ ) using the formula

$$G\sigma = \frac{\Delta g}{2\pi}$$

Multiplying  $\sigma$  by an area  $A$  gives a quantity with units of  $GM$ . In the cases considered here, the total mass of the anomaly has been set equal to the integrated surface density of a 100 milligal anomaly ( $.100 \text{ cm}/\text{sec}^2$ ) over a 120 by 120 km area. This gives a value for  $GM$  of

$$\begin{aligned} GM &= G\sigma dA = \frac{\Delta g}{2\pi} dA \\ &= \frac{.100}{2\pi} (120 \times 10^5 \text{ cm})^2 \\ &= 2.29 \times 10^{12} \text{ cm}^3 \text{ sec}^{-2} \end{aligned}$$

The anomaly has been represented in three ways to study the effect of how the mass causing the anomaly is distributed. In the first case, the anomaly is represented by one point mass located on the surface. In the second case, the anomaly is represented by a  $7 \times 7$  grid containing 49 points spaced 20 km apart, thereby covering a  $120 \times 120$  km area. Each point contains one 49th of the total mass. In the third case the spacing between points is 40 km so that a  $240 \times 240$  km area is covered. Keeping the total mass constant, case three is equivalent to a 25 milligal anomaly over a  $240 \times 240$  km area.

Figures AI-1 through AI-4 show the vertical component of the acceleration and the vertical derivative of the acceleration which is the quantity measured by the Dumbbell gravity gradiometer. The four figures are for satellite altitudes of 120, 200, 220, and 300 km, with the anomaly located on the surface of the earth. The acceleration, which is negative, is plotted down from the zero line and is given in milligals ( $10^{-3}$  cm/sec<sup>2</sup>). The derivative of the acceleration, which is mostly positive, is plotted up from the zero line in eötvös units ( $10^{-9}$ /sec<sup>2</sup>). The horizontal scale is distance along the orbital path with the origin directly over the center of the anomaly. The three curves for each quantity correspond to a lumped mass, a  $120 \times 120$  km, and a  $240 \times 240$  km distribution of mass. The lumped mass always gives the most peaked curve and the  $240 \times 240$  the flattest curve.

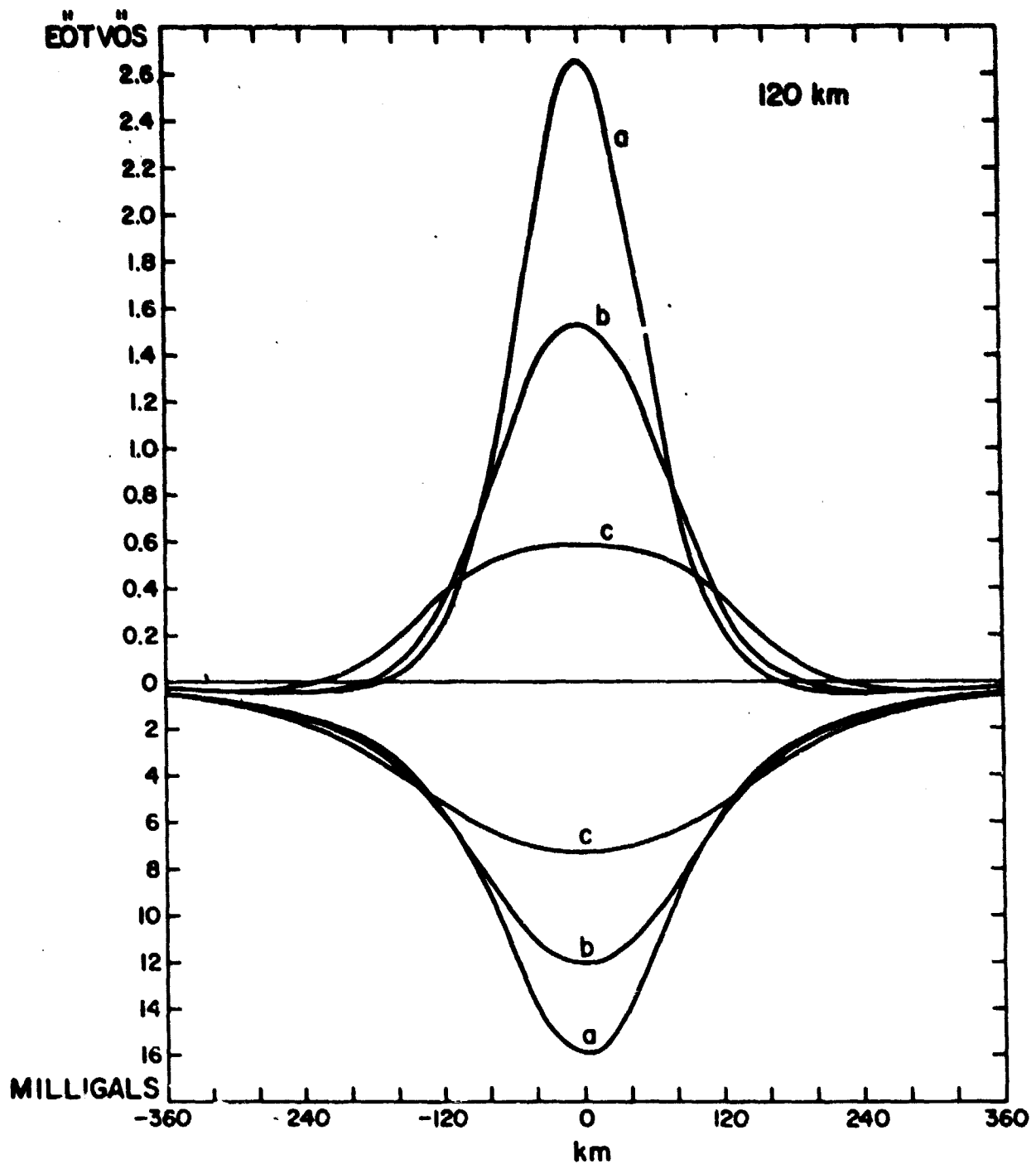


Fig. AI-1. -- Vertical acceleration and vertical derivative of the acceleration along the orbital path due to: a) a point mass; b) a  $120 \times 120$  km; and c) a  $240 \times 240$  km distribution of mass. In all cases the total mass equals the integrated mass of a 100 milligal anomaly over a  $120 \times 120$  km area (satellite altitude 120 km).

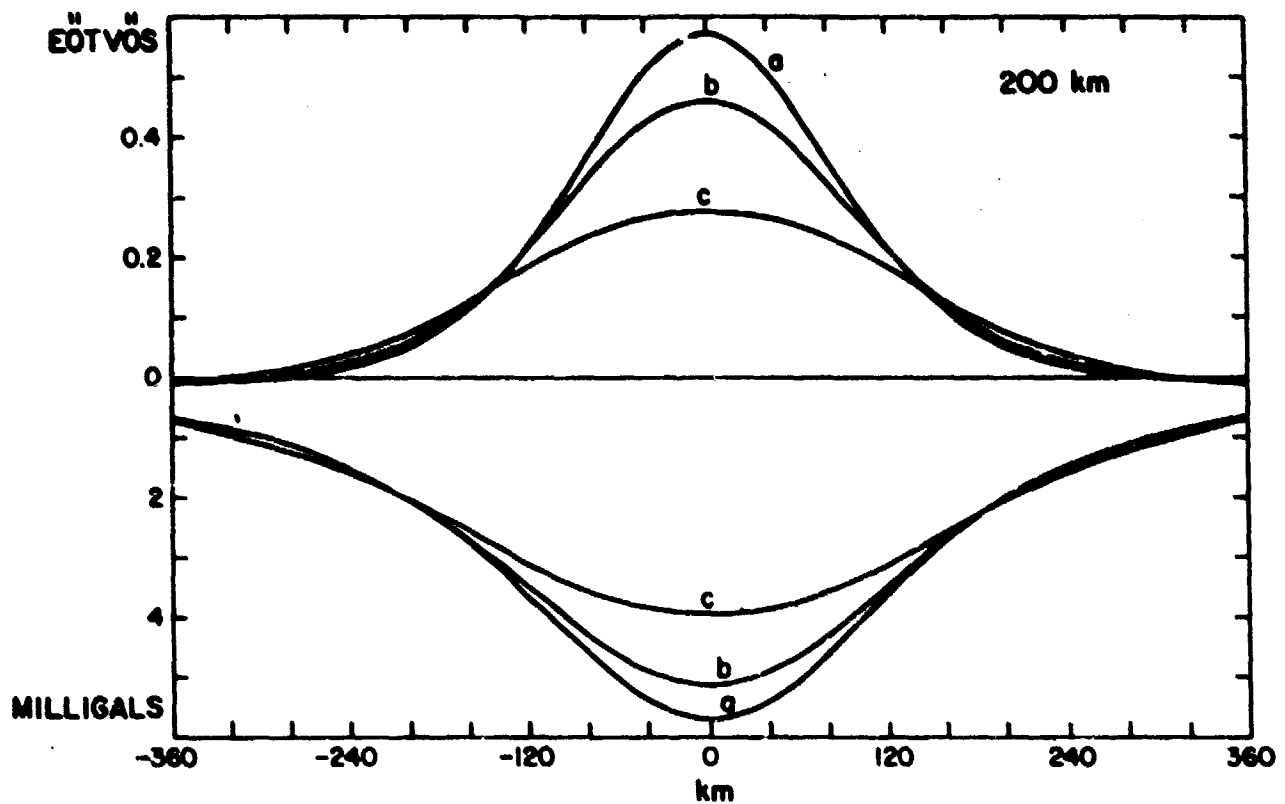


Fig. AI-2. — Vertical acceleration and vertical derivative of the acceleration along the orbital path due to: a) a point mass; b) a  $120 \times 120$  km; and c) a  $240 \times 240$  km distribution of mass. In all cases the total mass equals the integrated mass of a 100 milligal anomaly over a  $120 \times 120$  km area (satellite altitude 200 km).

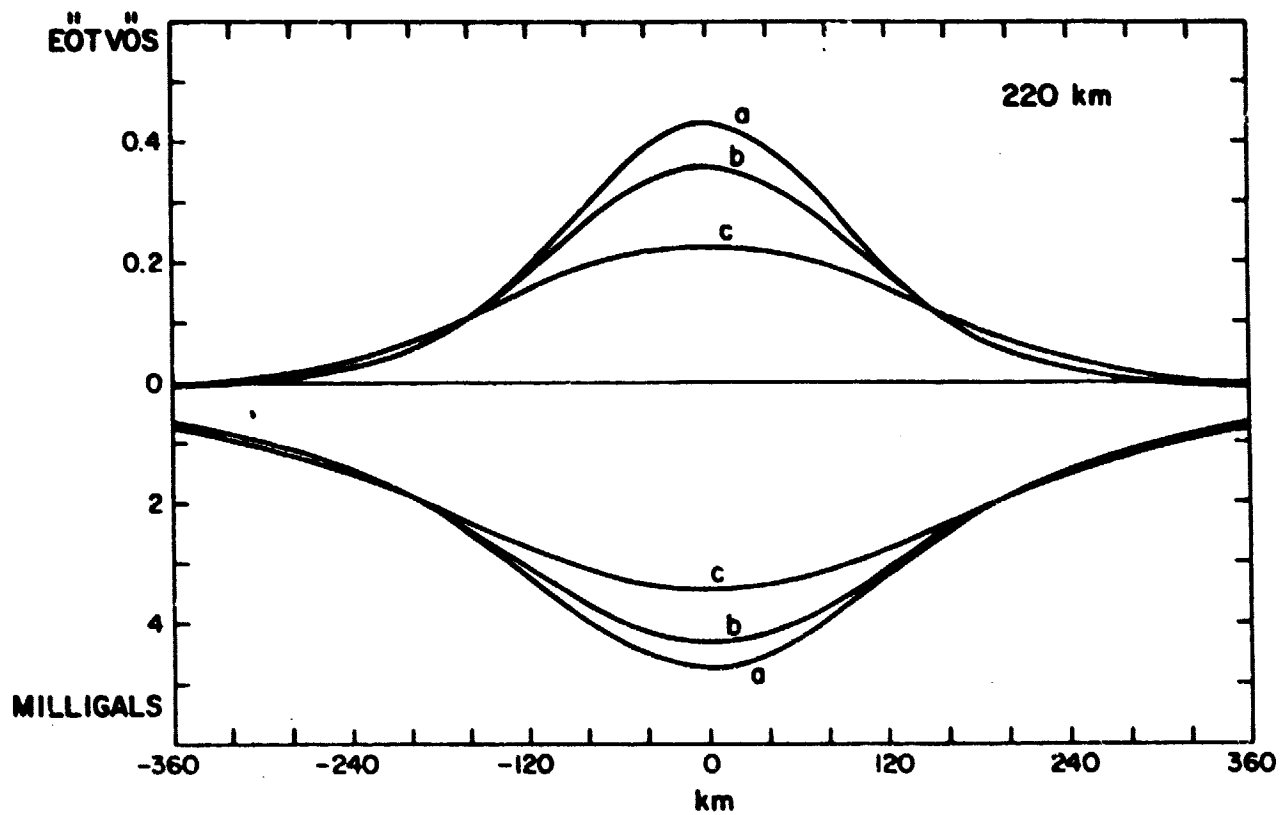


Fig. AI-3. - Vertical acceleration and vertical derivative of the acceleration along the orbital path due to: a) a point mass; b) a  $120 \times 120$  km; and c) a  $240 \times 240$  km distribution of mass. In all cases the total mass equals the integrated mass of a 100 milligal anomaly over a  $120 \times 120$  km area (satellite altitude 220 km).

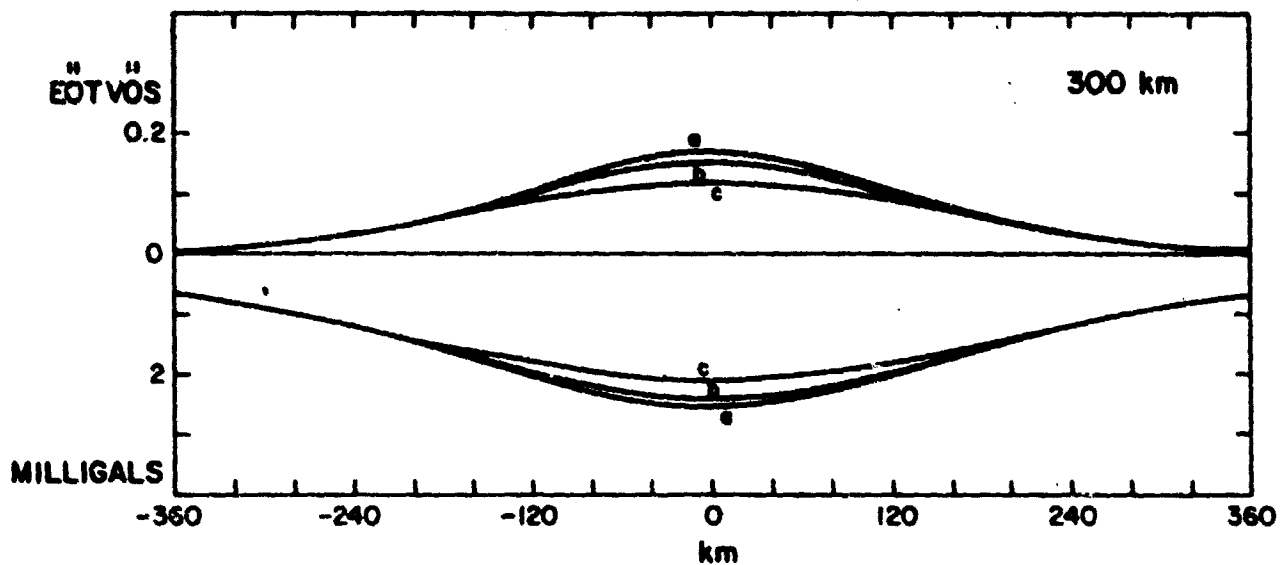


Fig. AI-4. — Vertical acceleration and vertical derivative of the acceleration along the orbital path due to: a) a point mass; b) a  $120 \times 120$  km; and c) a  $240 \times 250$  km distribution of mass. In all cases the total mass equals the integrated mass of a 100 milligal anomaly over a  $120 \times 120$  km area (satellite altitude 300 km).

## APPENDIX II

### Initial Evaluation of System Noise

We have performed preliminary calculations of system noise by assuming the presence of density irregularities in the atmosphere at Dumbbell heights. These irregularities might, in fact, be the most relevant single source of system noise.

The long-tether Dynamical Simulation Program existing at SAO was employed to examine the sensitivity of the tether tension to atmospheric global variations. The configuration considered was that with end mass of  $10^{+3}$  kg linked by a 2 km tether, orbiting at an altitude of 220 km. The tether was assumed to be made of KEVLAR with a 1 mm diameter. The gravity anomaly was modelled as a rectangular surface layer with a side dimension of 100 km and with a surface density sufficient to create an anomaly at the 100 mgal level. The atmospheric density model employed was that of Jacchia. In addition to the basic model, a noise component in the density was also included. The noise component  $\Delta\rho$  was assumed to be of the form:

$$\Delta\rho = \left( A \sin \frac{2\pi t}{P} \right) \rho$$

where  $\rho$  = density computed from Jacchia's model  
A = amplitude of the noise component  
P = fundamental period of the noise component  
t = time

Taking A = 1% and P = 15 sec the tension was calculated for the Dumbbell system for an orbital arc of 10 minute duration and passing directly over the 100 mgal anomaly. An additional run was made without the anomaly and with A set to zero.

A particularly simple measure of the effects of both the anomaly and the atmosphere density variation can be obtained by subtracting the calculated tension obtained in the second run from those obtained in the first run. The resulting tension difference values are defined as the "differential tension". Figure AII-1 depicts a gravity anomaly signature when there is an anomaly in the presence of the atmospheric density noise previously given and for the case when there is no atmospheric noise. From this figure, it can be seen that the tension follows the density variation very closely. The physical mechanism of coupling is the drag heating effect which supplies an input thermal flux directly proportional to the local density. In the case shown the anomaly signature is clearly discernible above the atmospheric effects and suggest that anomalies as small as 10-20 mgal are discernible. It is anticipated that close investigation of possible system parameter tradeoffs will yield a configuration which would actually minimize the system sensitivity to density fluctuations and would thereby allow both smaller anomalous regions to be detected and/or larger density variations to be tolerated.

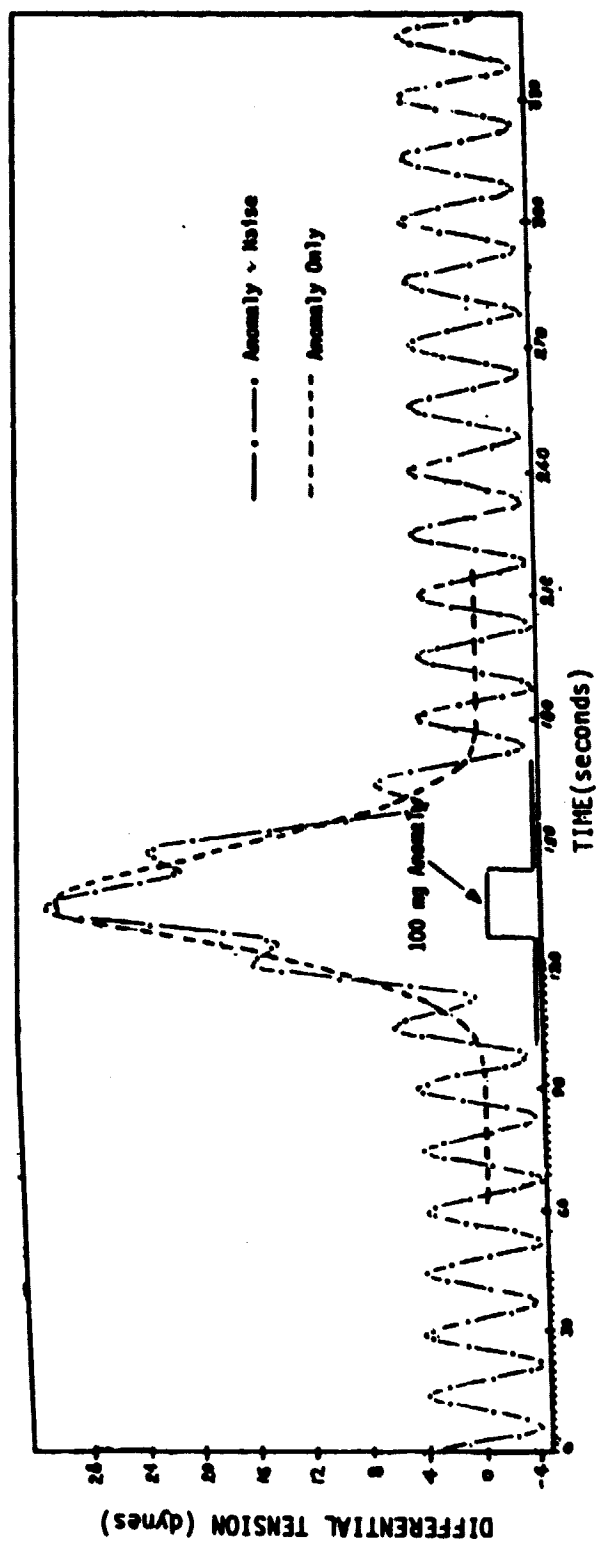


Fig. AII-1. - Gravity anomaly signature in the presence of atmospheric noise interference.

### APPENDIX III

#### Parametric Analysis and System Performance Optimization

Figure AIII-1 illustrates the relationships between the basic system parameters: sensitivity, lifetime, Dumbbell height, weight and length.

It can be shown that by specifying the sensitivity (minimum detectable gradient in eötvös units and minimum detectable tension change in dyne), one specifies the product  $m \times l$  (terminating mass  $\times$  length) of Dumbbell. We remind that:

$$\text{sensitivity (eu)} = \frac{\text{sensitivity (dyne)} \cdot 10^9}{m \times l}$$

Curves A, B and C in Figure AIII-1 are traced for  $m \times l$  products of  $2.13 \cdot 10^{10}$  cgs,  $7.24 \cdot 10^{10}$  cgs, and  $2.4 \cdot 10^{11}$  cgs respectively.

Curves D, E, and F make it possible then to determine the  $A/m$  ratio (to be read on the scale of the vertical axis on the right side of the Figure) for  $m \times l$  products corresponding respectively to curves A, B, and C (D corresponds to A, E to B and F to C).

Finally, Curve G, makes it possible to determine the lifetime of the system, with days in orbit read on the scale of the horizontal axis at the top of the figure (right side).

Let's give an example of how the graph in Figure AIII-1 can be used. Let's suppose that we want to achieve a sensitivity of  $1.2 \cdot 10^{-2}$  e.u., with a tension measurement sensitivity of 1 dyne, representing 3 parts in  $10^6$  of the total tension. Curve B is therefore the one to be used. If now we adopt a tether length  $l = 1$  Km, curve B shows that each end mass must be 740 Kg.

To find now the  $A/m$  ratio that characterizes the system, we must use curve E (to be employed every time that curve B is used). By entering in it with  $l = 1$  Km, we read on the scale at the right side  $A/m = 0.02$ .

Finally, in order to determine the lifetime of the system, we must use curve G, entering in it with  $A/m = 0.02$ . On the horizontal scale at the top of the Figure we read: 19 days.

This example should be sufficient to demonstrate the usefulness of the Figure in performing trade-off studies, and in selecting (in first approximation) an optimal set of parameters, when there is a specific constraint in one or more of them.

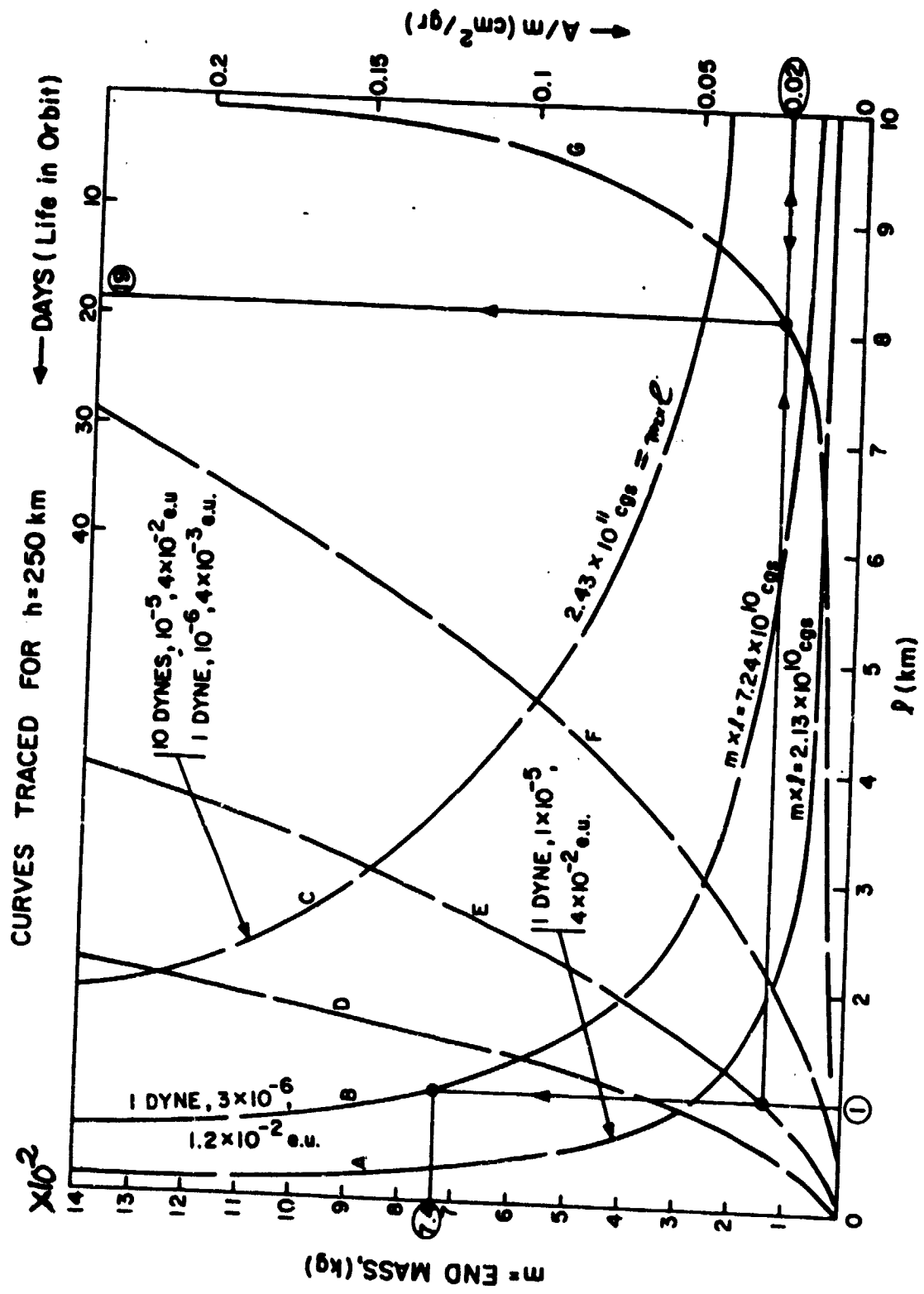


Fig. AIII-1. - Parametric representation of basic system characteristics.

## APPENDIX IV

### Existing Software Package for Tethered Satellite System

Under contract NAS 8-32199, Smithsonian Astrophysical Observatory has developed a complex software package for the simulation of the dynamical and thermal behavior of a Tethered Satellite System. The approach embodied in this simulation has been to discretize the tether into a set of  $N$  point elements each with the physical characteristics (mass, area, conductivity, etc.) of a finite length tether segment. These point elements are employed as the centers of application of the externally applied forces and the internal tether tension, as well as the centers of accumulation of the heating and cooling thermal fluxes. A system of coupled differential equations have been derived which represent both the dynamical and thermal variation of each element. The dynamical evolution of the system is obtained by numerically integrating these equations. The cartesian coordinates of each element are tabulated as a function of time and the displacement, tension, and temperature of each element is graphically displayed. The graphical displays of the dynamical variables are presented as projections of the coordinates onto an orbital reference system defined by the motion of one particular element selected by the user. (Most often the reference system is chosen to be that of the end-element representing the Shuttle; the resulting graphics display the time variation of the In-Plane, Out-of Plane and Radial components of the remaining point elements relative to the Shuttle.)

The unique features of this simulation system are its generality, the extensive force model employed, and the inclusion of thermal effects. In particular, the dynamical forces include (1) a terrestrial gravity field expansion composed of spherical harmonics to degree and order 20, (2) a full earth gravity anomaly model represented by a surface layer density distribution of arbitrary complexity (3) solar and lunar gravitational forces (4) atmospheric drag forces with realistic density models (5) solar radiation pressure (6) earthshine radiation pressure and (7) tidal forces. The Tether mechanical force model includes: (1) a linear stress strain relationship modified by the thermal expansion characteristics of the tether material and (2) a visco-elastic damping force and (3) an arbitrary control law capability for deployment retrieval and station keeping modes of operation. The present thermal model includes heating from solar radiation, earthshine radiation, and atmospheric drag and cooling by radiation.

Up to 20 elements may be employed in the current software configuration. There are no restrictions on the mechanical, thermal or bulk characteristics of any tether segment or on the initial conditions representing the eccentricity or orientation of the Shuttle orbit.

Figure AIV-1 illustrates the general configuration for the use of a 20 km tether linking the shuttle and subsatellite with the tether represented by 9 point elements. Figure AIV-2 is a sample of the graphical display of the "in-Plane" motion of each mass point other than the Shuttle for a period of approximately two orbits. The vertical scale is in cm and the horizontal scale is in seconds. Symbol "2" represents the subsatellite motion relative to the Shuttle. All displacements are reference to their value at  $t = 0.0$  so that the motion of all elements could be displayed on the same scale. In actual fact, each point is separated by 2.5 km = 250,000 cm from its nearest neighbors.

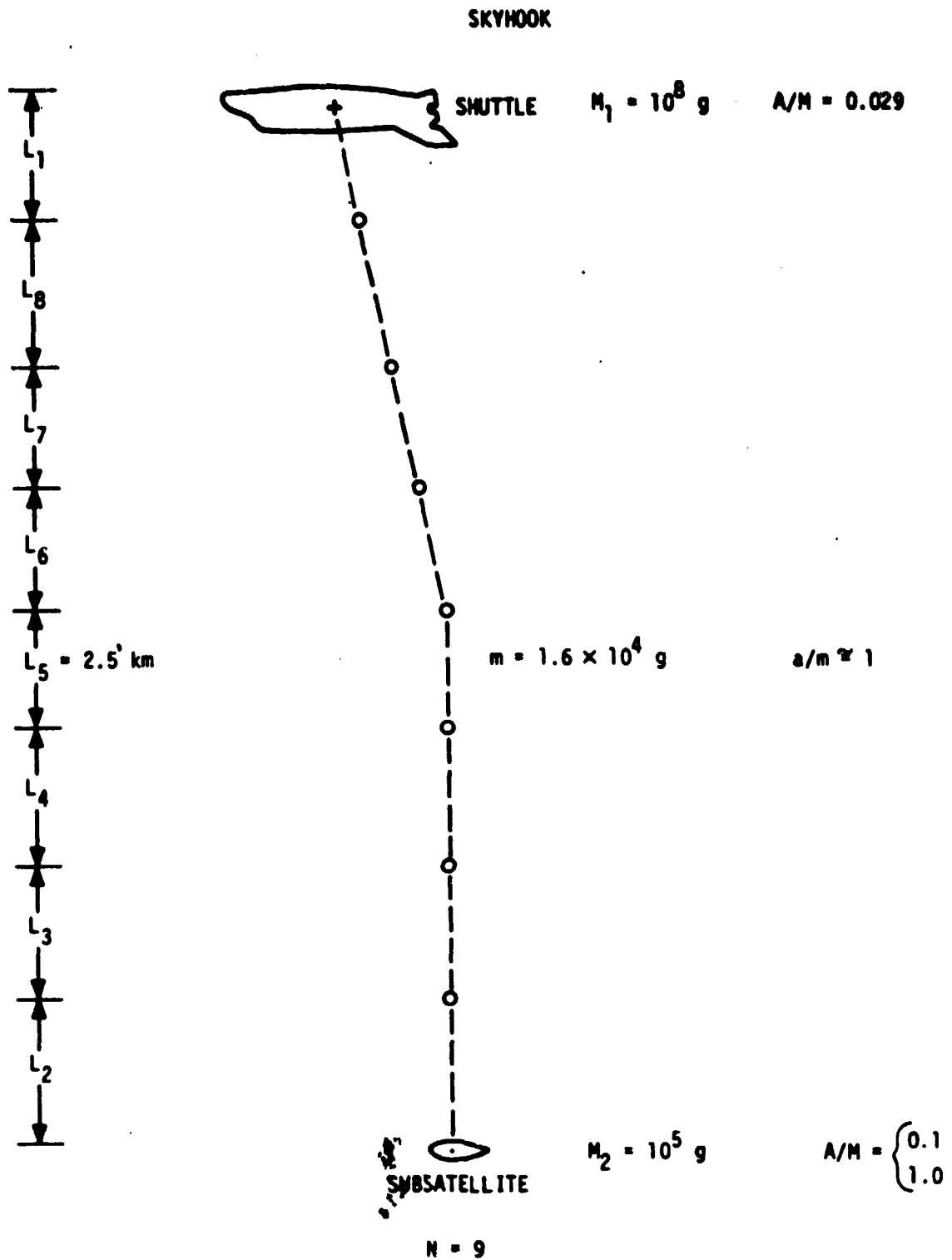


Fig. AIV-1. - Nine-mass-point representation of 20 km tether.

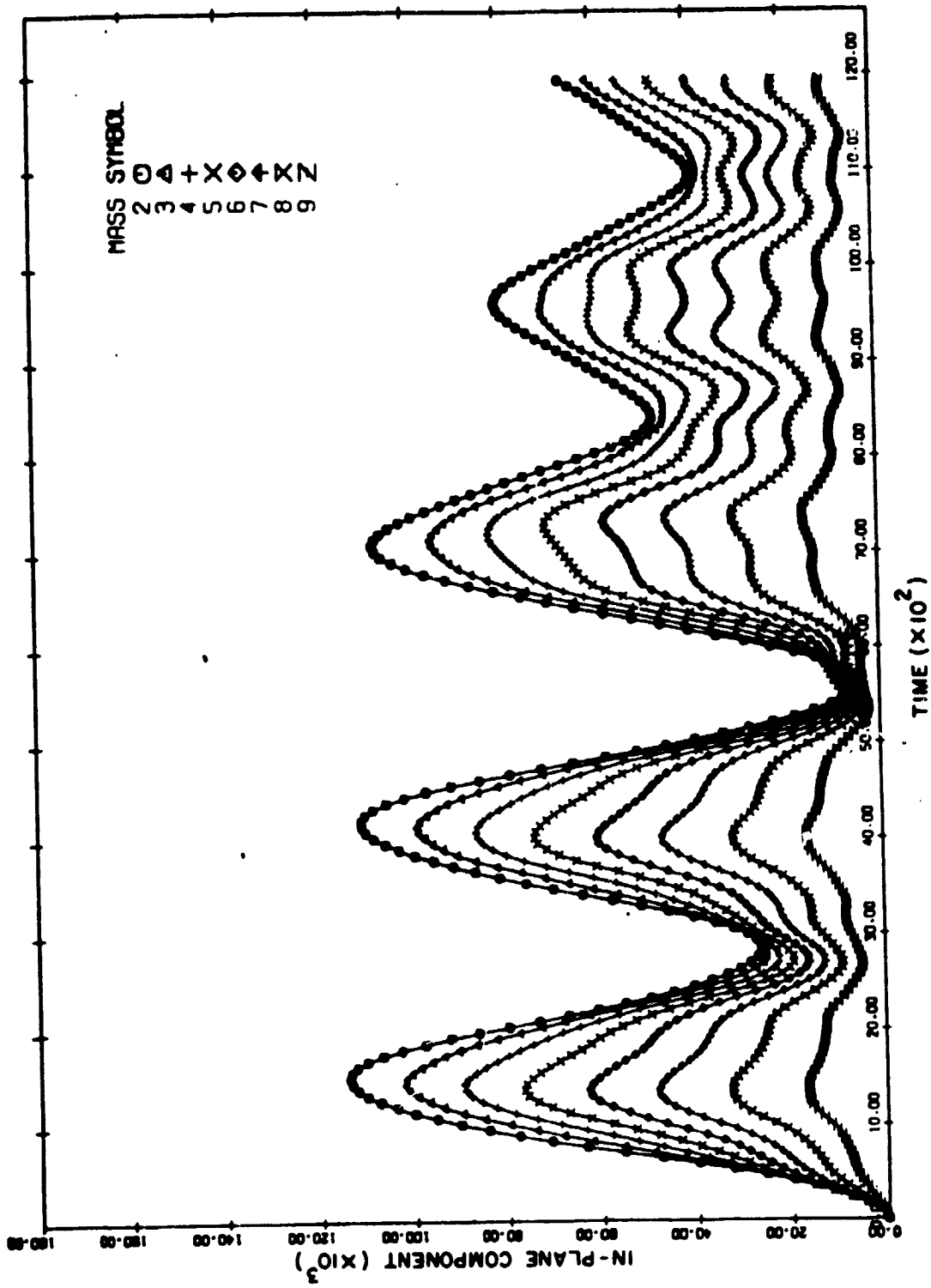


Fig. AIV-2. - Example of "in-plane" motion of each mass point of the configuration in Fig. AIV-1.

THE REDUCTION AND ANALYSIS OF  
SATELLITE MAGNETOMETER DATA +

by

Robert D. Regan \*

The Phoenix Corporation  
1600 Anderson Road  
McLean, Virginia 22101

- \* Work done while at the U.S. Geological Survey
- + Paper submitted to GEOPHYSICS

**Abstract**

Reduction and interpretation techniques for satellite magnetometer measurements differ significantly from the techniques routinely applied to conventional data. However, the resultant data can be useful in the studies of broad-scale magnetic anomalies. Although the unequal spacing, in three dimensions, of the satellite data and the variation in the direction and intensity of the main geomagnetic field pose some interpretation problems, these problems can be suitably handled by using modifications of several standard techniques. The variation in altitude of the satellite measurements can also be used to advantage in some analyses.

## Introduction

Over the past few years interest has been increasing in the studies of the broad-scale magnetic anomalies that appear in regional compilations of aeromagnetic data, and in the regional and global maps provided by satellite magnetometer measurements. These long-wavelength anomalies, suspected of representing significant crustal structure, are so far proving enigmatic in their interpretation. One major problem is their adequate definition. Certainly, satellite data can be of considerable value in defining such anomalies and invaluable, especially when utilized with airborne data, in their interpretation. However, the reduction and interpretation of satellite magnetometer data differ significantly from the standard techniques that are routinely applied to conventional measurements. Any researcher utilizing the satellite data should be aware of its characteristics. The purpose of this paper is to discuss the reduction of the data, to detail its morphology, and to present interpretational techniques that are applicable.

### Available Satellite Magnetometer Data

Although many earth-orbiting satellites have been used to study the magnetosphere, only data from several such satellites are of any value to solid-earth studies. The three Polar Orbiting Geophysical Observatory (POGO) satellites have presented the best data available to date. These satellites spanned the time interval between 1965 and 1971, and their alkali vapor magnetometers provided total field measurements every  $\frac{1}{2}$  second over the elliptical orbits of 400 to approximately 1,500 km. The polar orbit ensured a reasonable global coverage. The Russian satellite Kosmos-49, in orbit for only 11 days, provided total field measurements below its orbital inclination of  $50^{\circ}$  at an average altitude of 375 km.

Although none of these satellites was ideally suited for magnetic anomaly studies, the results obtained by Regan et al (1975) and Regan and Marsh (1978) demonstrated the utility of satellite magnetometer measurements to such studies and provided the basis for Magsat (Langel et al, 1977). This satellite, ideally designed for magnetic anomaly studies, is scheduled for launch in late 1979. In a low (-300 km) polar orbit, the satellite will provide scalar and vector magnetic measurements over the entire globe for a period of approximately 6 months.

## Data Reduction

Several factors affect the magnetic data obtained by satellite. The major problem is that the magnetic measurements are being made from a fast-moving spacecraft in a continually changing orbit. Compounding the problem is the question of tracking accuracy, i.e., determining the precise position of the satellite. Also problematical is the dynamic nature of the earth's magnetic field and the fact that measurements of geological anomalies are made at a distance quite removed from the source; consequently, the magnetic anomaly value has decreased significantly and closely approximates disturbances due to external fields. Also, with a moving vehicle, it is difficult to separate a spatial disturbance from a temporal one.

The measured field is a composite of the geomagnetic field (internal and external), its temporal variations (of considerably more importance in this case, because the instrument is closer to some external field sources, and the duration of the survey is much longer than standard surveys), the anomalous field, and variations due to measurement error, altitude error, etc. As in standard magnetic surveys, the first objective of the reduction is to define or extract the anomalous field.

The best way to illustrate how this is achieved and to outline the data-reduction problem is to detail how Regan et al (1975) reduced the POGO satellite measurements. Any reduction of satellite magnetometer data would probably follow a similar vein. The data reduction steps began after the satellite measurements had been collated into useable form. When actual satellite data are used, two digital tapes are received initially, one from the tracking stations and the other from the satellite containing the magnetic measurements and "housekeeping" information. Once the magnetic measurements were calibrated and reduced to intensity values (gammas), then the data sets were merged, using the common parameter of time. The final tape for further reduction contained the time of the measurement, the latitude, longitude, and altitude of

the spacecraft, and the measured value. The data-reduction process was accomplished by screening all available data according to suitable selection criteria.

First, the external field effects were minimized by screening the POGO data with the Kp index (planetary magnetic activity index), a logarithmic 3-hourly value ranging from 0 to 9<sup>+</sup> that indicates the state of disturbance of the geomagnetic field. Ideally, the data should be screened for Kp=0, the most quiet state. However, in the case of the POGO data, this did not result in a sufficiently dense data set (i.e., too many points were discarded). As a result, the allowable value of Kp was set at 2<sup>+</sup>, and satellite data were accepted during the times when Kp<sub>≤</sub>2<sup>+</sup>, but this allowed some magnetically disturbed data into the data set. Thus, a correction, primarily designed to correct for this DS variation (Sugiura and Heppner, 1968) was designed by Cain and Davis (1973; also Davis and Cain, 1973) and applied to the data. The DS effect was modeled by fitting data over each satellite half-orbit (i.e., pole to pole) with a first term of a zonal harmonic series. However, the correction proved to be unreliable in higher magnetic latitudes, and the data set was truncated at +50<sup>0</sup> geomagnetic latitude.

If the satellite traverses all local times, then local times between 0900 and 1500 hours, the period of maximum diurnal variation, should be excluded from the data. Such a correction was also applied to the POGO satellite data.

As a result of this data-screening process, we are left with a data set that has had the effect, or at least the major part of the effect, of the external field removed from it. Such a data set has been termed a "reduced" data set and is the basis for further analysis.

In essence, this is how, at present, satellite data is being corrected for external disturbances per se. Although the effects of such disturbances may be diminished in subsequent data-reduction techniques, it would be fruitful to conduct additional investigations in removing

these effects from the data.

An additional screening should be used if the satellite is in a highly elliptical orbit, for then the data collected near apogee are of little or no value because of the rapid decay of the anomalous signal. An altitude cutoff of 700 km was applied to the POGO data, which ranged from 400 to 1,500 km in altitude.

The next step is to isolate the anomalous field by removing the internal geomagnetic field. Assuming that the magnetic field is due to a primary source in the core and secondary sources in the crust, the mantle being a zone of no magnetization, then removal of the core field results in the desired anomalous crustal field.

Removal of the core field is, in essence, a regional/residual separation and is best accomplished by using a geomagnetic field model to represent the core field. The field model, a spherical harmonic series of four variables ( $\phi$ , latitude;  $\theta$ , longitude;  $r$ , altitude or geocentric distance; and  $\tau$ , time) is fit to the data set, using a least squares technique. In such an approach, the most difficult value to estimate is the maximum degree of the series. However, spectral studies suggest that a harmonic series of degree and order 13 adequately represents the core field. Thus, such a series was fit to the reduced POGO data. The resulting function was then evaluated at each measurement point and subtracted, leaving anomalous values, termed  $\Delta F$  values. Ideally, these  $\Delta F$  values represent the anomalous crustal field. However, the characteristics of these data must be examined in detail before further reduction can be attempted.

## Morphology of the Data Set

During the 6 years of data collection, the POGO satellites provided approximately 200 million magnetic field measurements. The reduced data set resulting from the data screening process contains only 800,000 measurements, or about 0.2 percent of the total. The measurements are distributed in altitude from satellite perigee of approximately 400 km to the cutoff altitude of 700 km; the average altitude is 525 km. Figure 1 is a histogram showing the number of measurements vs. satellite altitude. Reasonable spatial coverage is attained with these data, as there is an average of 21 points per  $1^{\circ}$  latitude-longitude area. However, the data set is composed of unequally spaced measurements in three dimensions. The data consist usually of segments of orbits almost randomly located and often have significant variations in altitude between adjacent samples. The various features of the data can best be examined in detail by looking at one particular area of the global data set.

For the past few years, we have been working on a major magnetic anomaly located over central Africa. This feature, termed the Bangui anomaly (Regan et al, 1973), was the first to be noted in satellite data (Cain and Sweeney, 1973); it has attracted our interest because it is an isolated feature over a stable continental interior. Also, the anomaly is associated with an area of fairly complex regional and local geology containing several economic mineral deposits. Figure 2 shows the area of satellite data. The satellite tracks in this area contained in the reduced data set are shown on Figure 3A, and the altitude distribution, on Figure 3B. The severe altitude variations are quite apparent. In one place between longitude  $23^{\circ}$  and  $25^{\circ}$ , there is a difference of approximately 110km.

One crude method of representing the data, and one that was used in the calculation of the global magnetic-anomaly map (Regan et al, 1975) is to construct  $1^{\circ}$  latitude-longitude averages of the anomalous

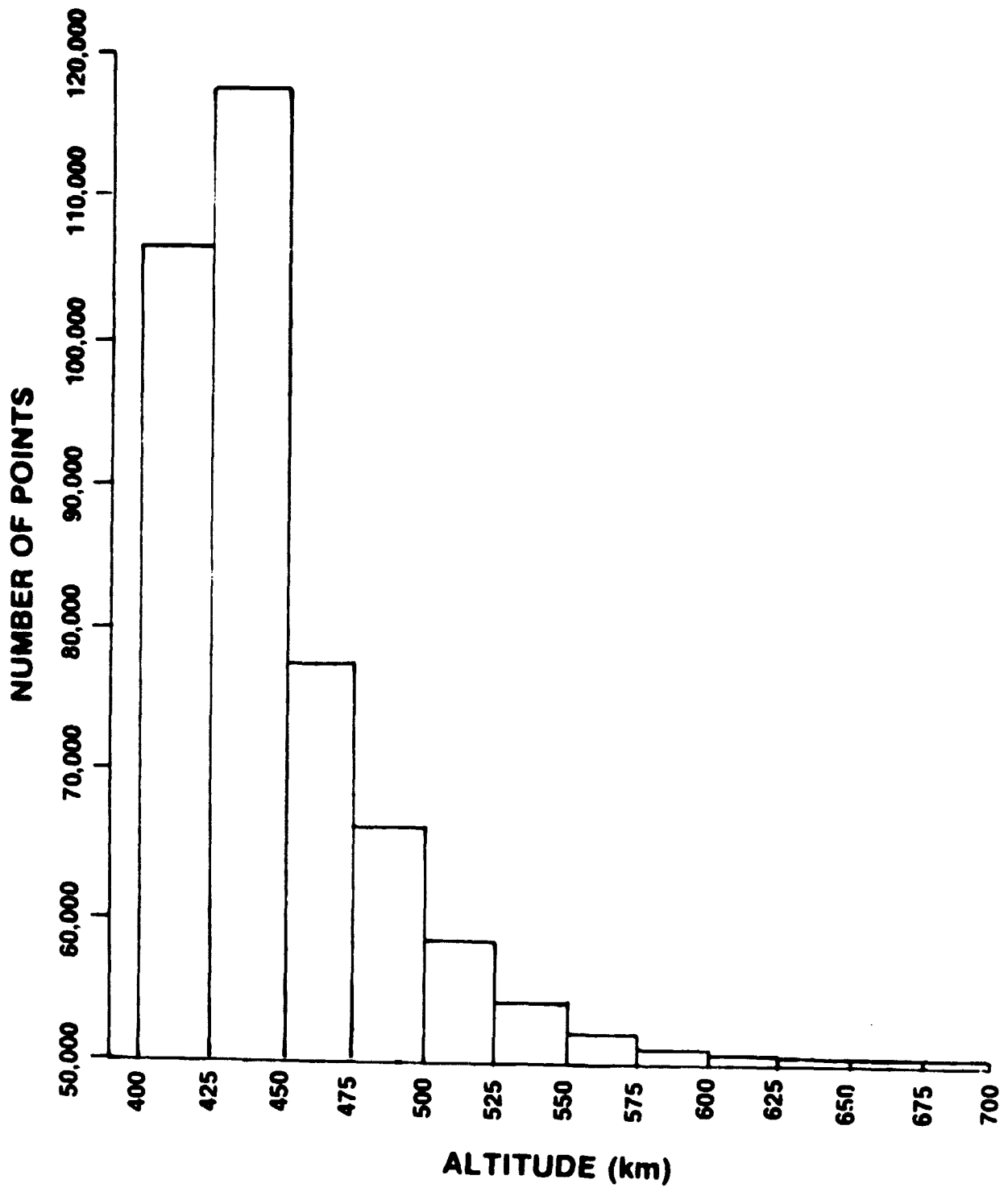


Figure 1 - Histogram of number of POGO satellite magnetometer measurements in the reduced data set as a function of altitude.

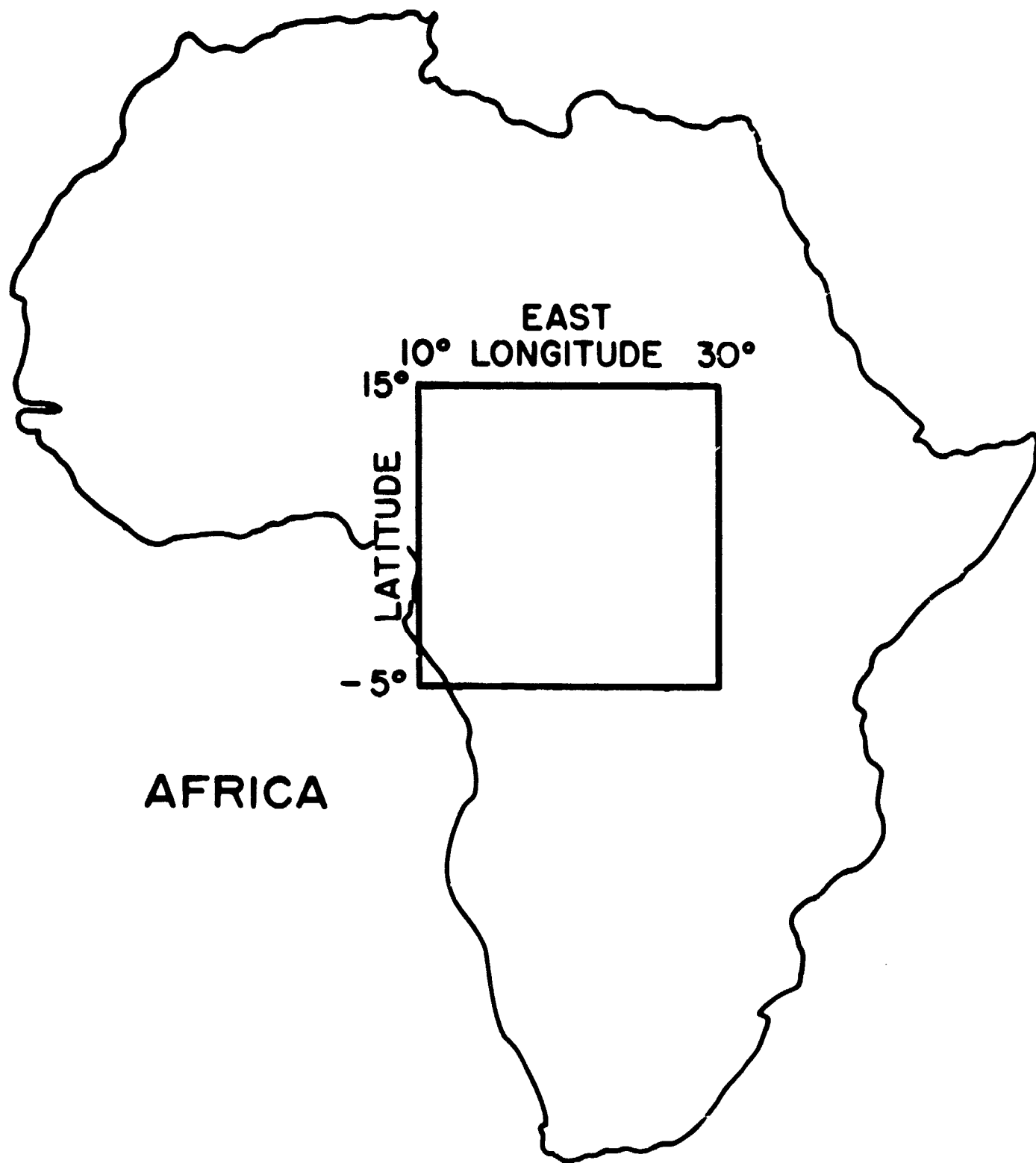


Figure 2 - Location map of study area.

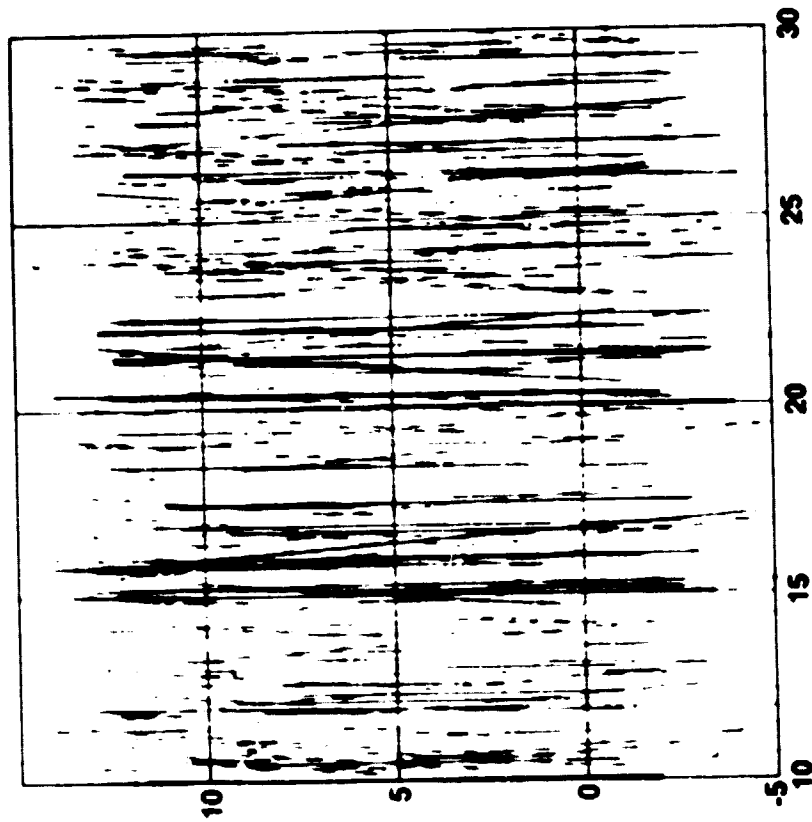


Figure 3A - Satellite ground tracks

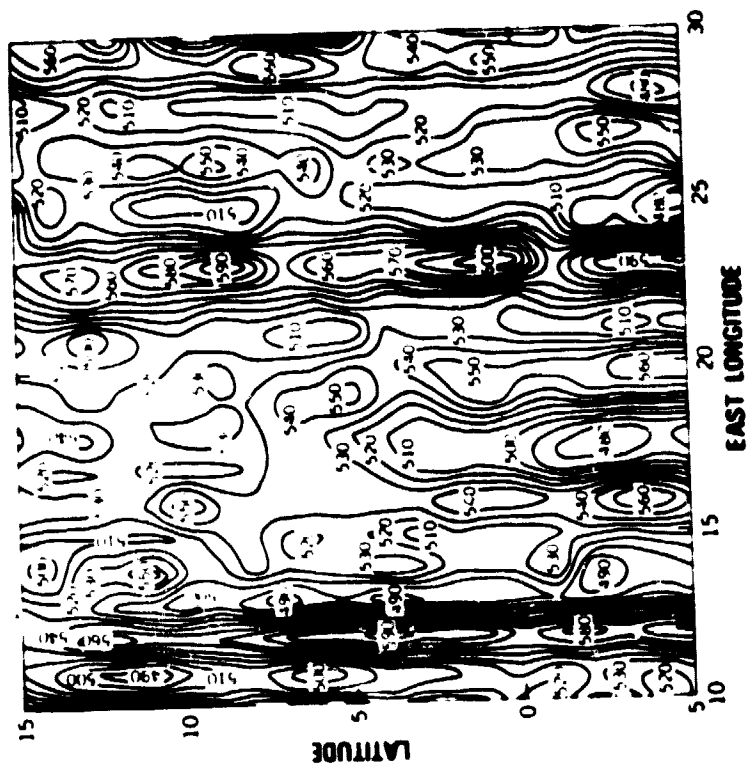
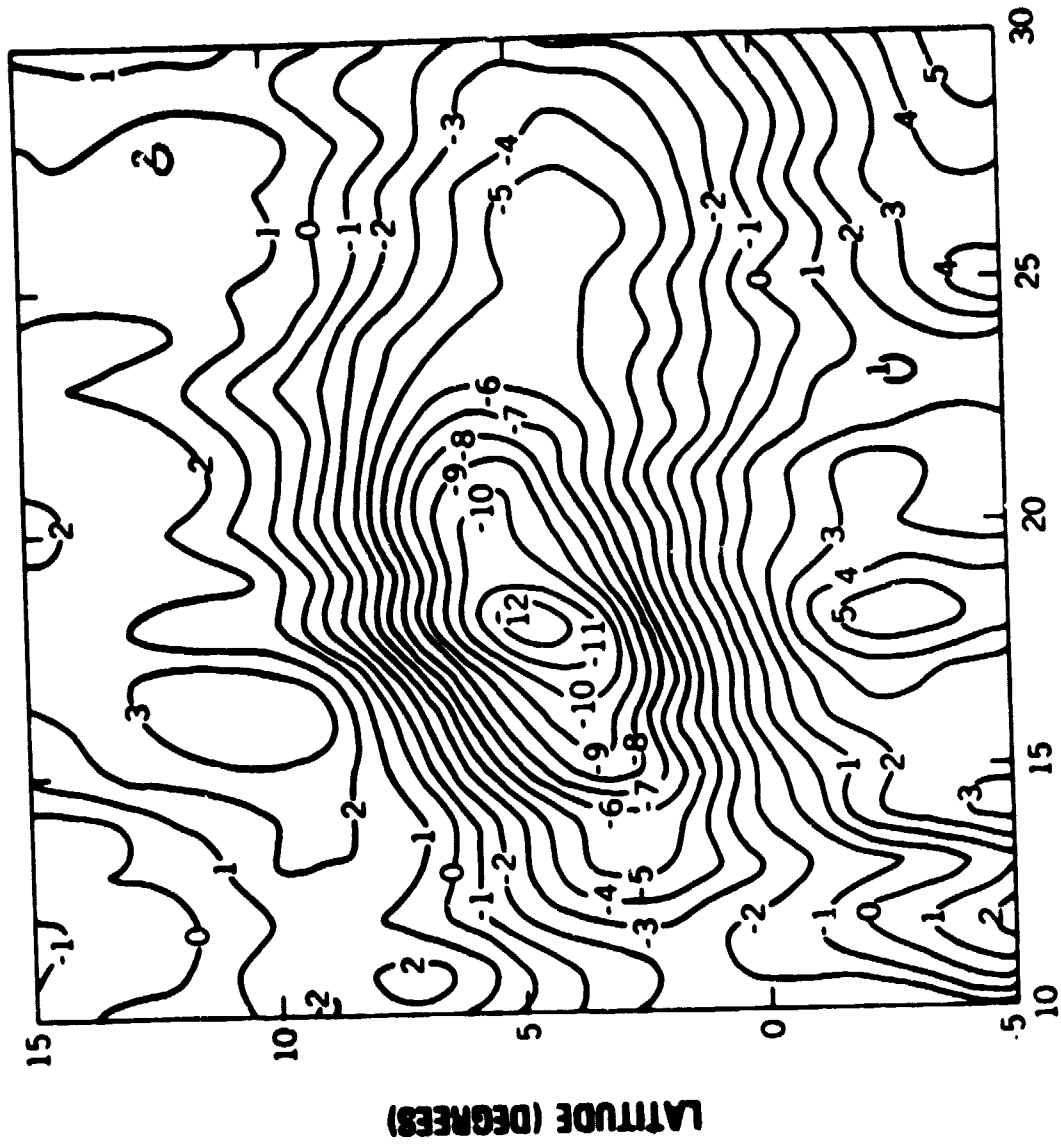


Figure 3B - Satellite altitudes;  
contour interval = 10 km.

field. This construction simply entails the calculation of the arithmetic mean of all the  $\Delta F$  within a  $1^\circ \times 1^\circ$  prismatic area, the bottom of which is determined by satellite perigee, and the top, by the satellite apogee or altitude screen used in constructing a data set. All altitude information is lost in such a representation, and this method has been used only as a first representation of the data set.

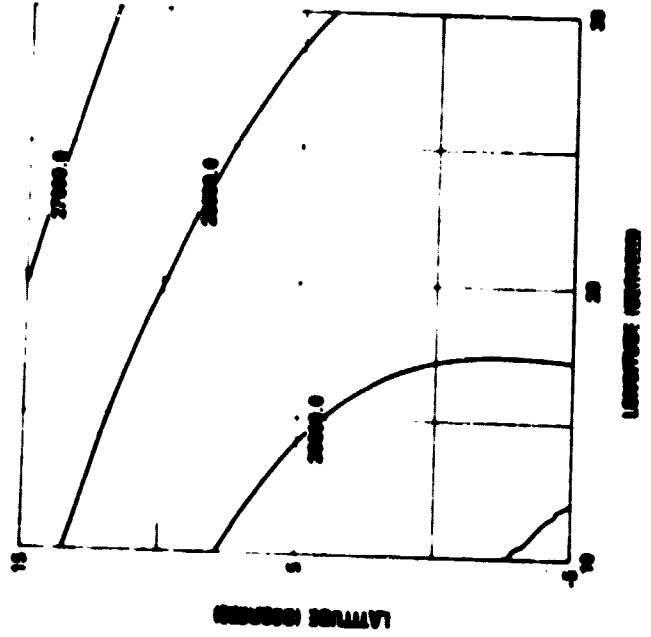
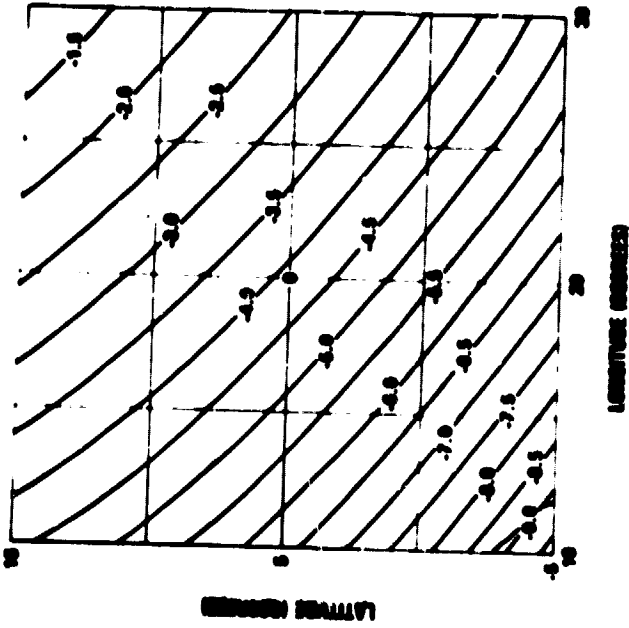
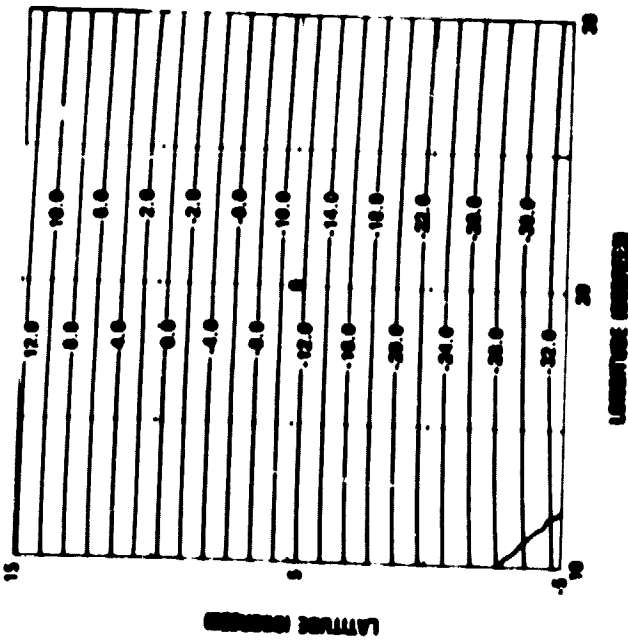
Figure 4 shows the  $1^\circ$  average map over our test area. The Bangui anomaly is quite apparent, a 12-gamma low extending approximately east-west. However, for this area near the geomagnetic equator, a "low" represents a positive increase in magnetization. Some subtle striping is also evident along the approximate satellite trajectory; it is attributed to altitude variation. If Figure 4 is compared with Figure 3B, an almost perfect correlation is apparent between the altitude variations and the striping in the data. To overcome this, the data should be reduced to a common altitude, a major step in reducing the satellite data for further analysis.

Another problem, making further analysis more difficult, is the variation of inducing-field intensity and direction. Even over an area such as that covered by the Bangui anomaly, this variation can be considerable. Figure 5 shows the variation over this area in the main field, inclination, declination, and total intensity at satellite altitudes, calculated from the POGO (8/71) geomagnetic field model. The effect would be even greater in surveys spanning greater variations in latitude.



**LONGITUDE (DEGREES)**

Figure 4- 1° averaged satellite magnetic-anomaly map over the study area. Contour interval is 1 gamma.



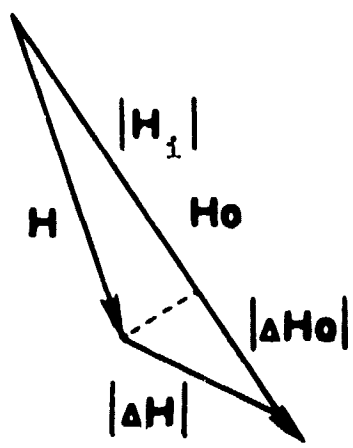
## Data Analysis

One problem in further analysis is that present satellite data are composed of total field measurements, and the total field under these conditions (i.e., varying directions) does not satisfy LaPlace's equation (Bhattacharyya, pers. comm). Thus, the many standard reduction techniques that are routinely used are not applicable. Consider the fact that total field magnetometers only measure the magnitude of the total field without sensing its direction. Usually, it is assumed that the anomalous vector is in the direction of the main field, that this direction is constant, and we operate on a scalar quantity. However, in a changing field, we cannot separate an anomalous change in the induced field from one that is due to a change in field direction. We must consider the vector nature of the field; Figure 6 is a diagrammatic representation. Here, the total field measurement is seen to be the magnitude of the resultant vector constructed from the inducing and anomalous field.  $H_i$  would be that part of the total field measurement subtracted via a field model, and the resulting  $\Delta H_o$  is  $\Delta F$  or the anomalous value. It can be seen that  $\Delta F$  is the projection of the  $\Delta H$  vector on  $H_o$ , and because we are measuring magnitude only, we cannot resolve a variation in anomalous vector magnitude from one of direction. In reality, over broad areas, both effects are present, and proper analysis requires that we consider them.

### Reduction to a Common Surface

To adequately consider broad-scale magnetic-anomaly maps in the light of standard maps, the data must be reduced to a common altitude and inclination. Several techniques have been proposed for this.

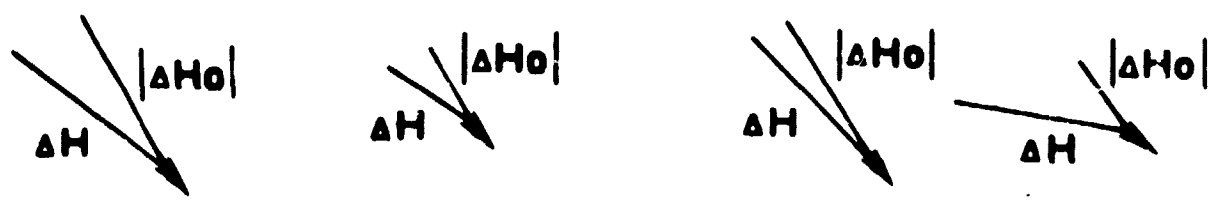
The equivalent source technique, as described by Bott (1967) and Dampney (1969), can be directly applied to the reduction of satellite magnetic measurements (Regan and Davis, 1975; Mayhew and Davis, 1976). In such a technique, the parameters of an arbitrarily chosen layer or



- H:** INDUCING FIELD
- $\Delta H$ :** ANOMALOUS FIELD
- $|H_o|$ :** TOTAL FIELD MEASUREMENT
- $|H_i|$ :** GEOMAGNETIC FIELD MODEL VALUE
- $|\Delta H_o|$ :**  $\Delta F$

**VARIATIONS IN  $\Delta F$  CAN BE OF TWO TYPES**

- A. VARIATION IN INTENSITY**
- B. VARIATION IN DIRECTION**



**IN REALITY  $\Delta F$  IS A COMBINATION OF BOTH**

Figure 6 - Schematic representation of the discrimination of anomalous values from total field intensity data.

volume of magnetized material are determined so that the values of the anomalous magnetic field calculated from such a source reproduce the observed values. Usually, the source parameters are determined in a least-square sense, using the observed data. Although the equivalent source may be positioned at any altitude relative to the measured or observed data, it was set at the surface of the earth in order to imitate the effects of the geological sources more realistically.

Henderson and Cordell (1971) published a technique for the reduction of potential field data obtained at differing altitudes to a common plane. Their technique uses a finite harmonic series representation of the three-dimensional data, combined with a least-squares approach for the solution of the coefficients. This technique has also been successfully used in the reduction of satellite magnetic data by Regan and Davis (1975).

Recently, Bhattacharyya (1977) proposed a technique specifically designed for the efficient reduction of satellite data to a common altitude and inclination. He adapted a procedure previously devised for the reduction of aeromagnetic data over regions of rugged terrain (Bhattacharyya and Chan, 1977). This technique uses an equivalent dipolar distribution of magnetization at the observation surface and utilizes the relationship between the observed values and the spatial gradient of magnetization of this layer to calculate the magnetic-field values at any point above the surface. The resultant data can then be continued downward to any desired surface.

We might briefly review the pros and cons of all these techniques and then compare the results with some test cases and actual data. Bhattacharyya's technique vigorously meets all the theoretical assumptions and allows for the calculation of the components, as well as the total field at any inclination and altitude. In addition, it is mathematically efficient. The only minor drawback is that the field is initially determined on a common surface at an altitude higher than that

of any measurement point. This then demands that downward continuation be used to bring the data to a lower altitude. This process can introduce errors. In particular, the very short wavelength anomalies in the data set can be amplified in any downward continuation because these anomalies are not due to any source in the earth, but rather to altitude discrepancies or other measurement noise, and their apparent source is near the satellite. To avoid this amplification, the data on the initial common surface must be filtered, which involves a choice of filter, cutoff wavelength, etc. However, filtering should not be a major source of error.

Basically, Bhattacharyya's technique can be considered comparable with an equivalent source technique, and any equivalent source technique, properly used, i.e., with full consideration of the vector field, should also work. The only major problem is the choice of source, location, and geometry. Certainly, Bhattacharyya's choice of a dipole at each measurement point is ideal in that it preserves the full nature of the data; however, Regan and Davis (1975) have had success with  $4^{\circ}$  grid. One disadvantage of these techniques is that they are not as computationally simple as Bhattacharyya's.

An advantage of using a source below the satellite is that the field can be determined at any point above the source (which is now much below the satellite), and no downward continuation is necessary. Also, a three-dimensional and/or a deep (with respect to the satellite) source imparts some degree of smoothing to the data that minimizes error due to altitude variation.

The limitations of the Henderson and Cordell technique is that it is based on the assumptions that  $\Delta^2 F=0$ , and that the data are in a rectangular coordinate system. Nevertheless, the technique is computationally simple, and by suitable choice of maximum degree, provides some natural filtering of the data. Also, the field can be calculated on any common spherical surface, although utilizing a surface far below the satellite altitudes is equivalent to downward continuation, and

errors can be introduced. The assumption of a rectangular coordinate system is not problematical and can be handled through a coordinate transformation. However, as we have mentioned,  $\nabla^2 F \neq 0$  for the satellite, and the effect of this on resultant calculations is unknown. However, this can be examined by comparison with other techniques.

Figure 7 shows the results of the application of the Henderson and Cordell technique to the actual satellite data over the test area. In the center are the actual satellite data, on the left the field determined at the satellite points using the Henderson and Cordell technique, and on the right, the field at 525 km, computed from the Henderson and Cordell technique. Although it looks quite good, it is hard to evaluate the results objectively. To do so, we next examined model data.

Figure 8 shows on the left-hand side the calculated field at 575 km generated from a simple mathematical model of the Bangui anomaly. The next maps in this figure are the result of applying the equivalent source ( $4^\circ$  prisms at surface), and the Henderson and Cordell techniques to a pseudosatellite set of  $\Delta F$  values generated by calculating the anomalous field due to the Bangui model at actual satellite positions, and then reducing the data to a common surface using these techniques. These can be compared with figure 6 of Bhattacharyya (1977), which was derived from actual satellite data.

In general, the results of the various techniques show much similarity. However, Bhattacharyya's technique is the most rigorously valid and computationally simple. In addition to permitting reduction of the data at common inclination and declination, it also permits calculation of the principal components.

#### Analysis of Reduced Data

Once the data have been reduced to a common surface, they are amenable to other types of analyses such as the use of an equivalent source technique to map variations in apparent crustal magnetization and Curie isotherm.

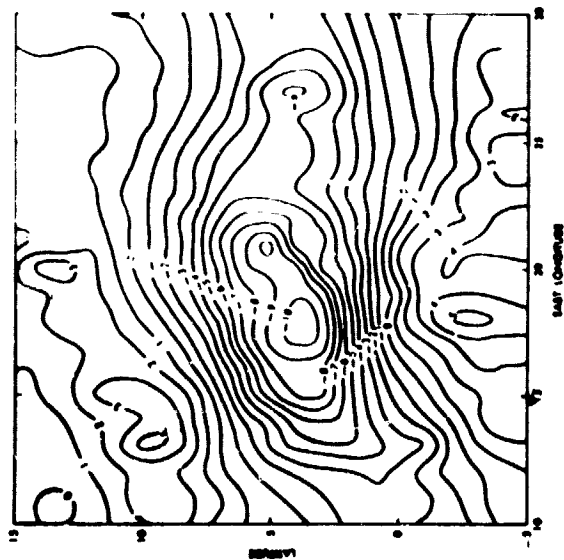
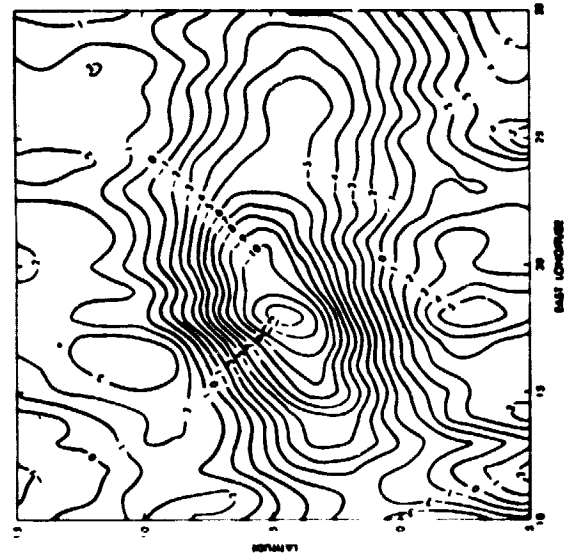
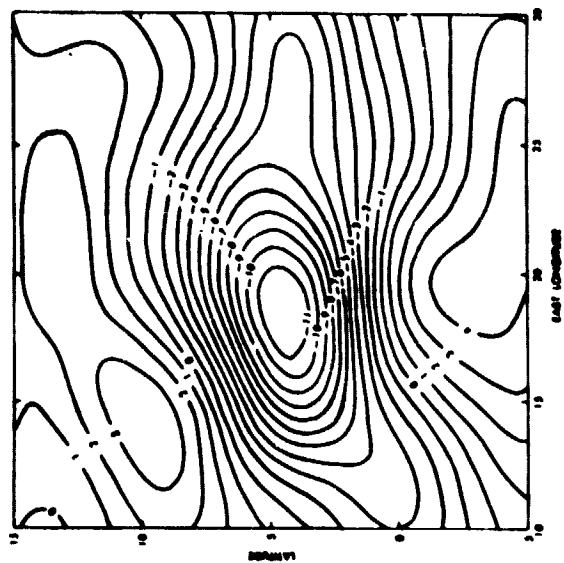


Figure 7 - Comparison of results of Henderson and Cordell technique. Contour interval = 1 gamma. (A) field determined at satellite points using Henderson and Cordell technique; (B) actual satellite data; (C) field computed at 525 km using Henderson and Cordell technique.

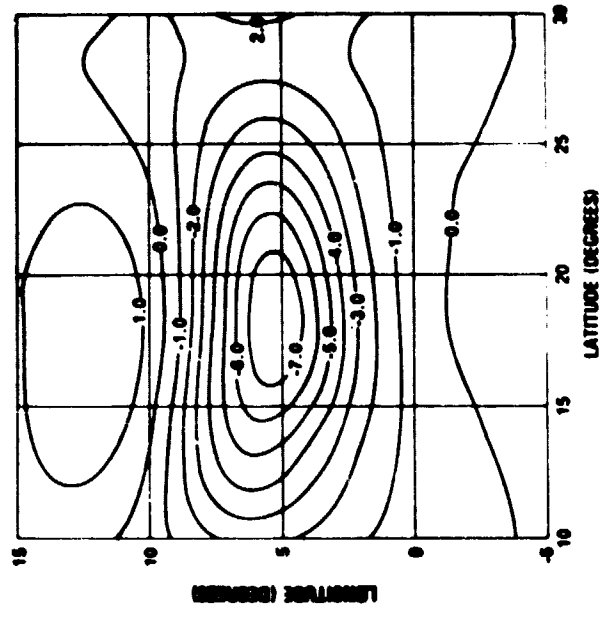
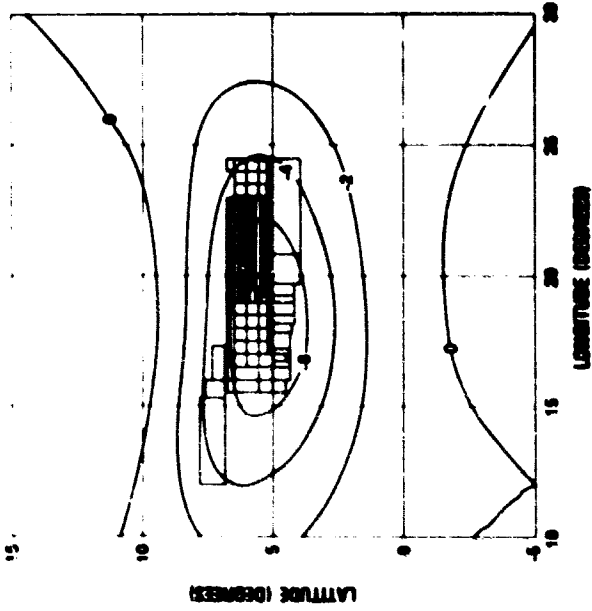
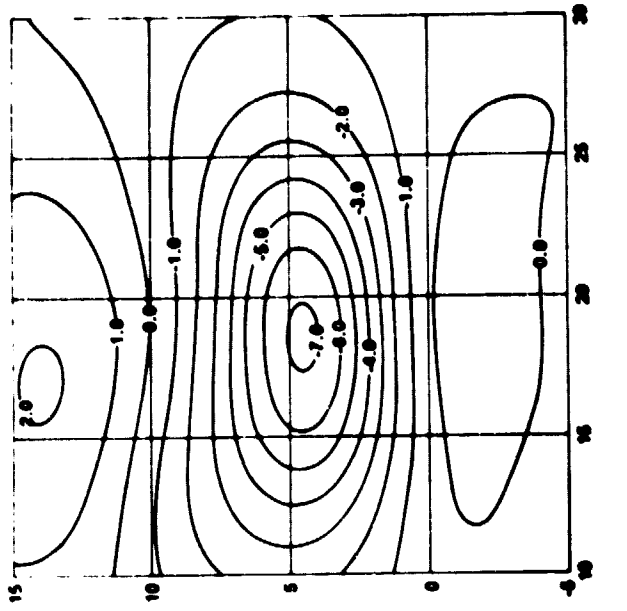


Figure 8 - Comparison of Henderson and Cordell and equivalent source techniques using pseudo-satellite data. (A) model field at 575 km. contour interval = 2 gamma; (B) calculated field at 575 km using equivalent source technique. contour interval = 1 gamma; (C) calculated field at 575 km using Henderson and Cordell technique. contour interval = 1 gamma.

Four-degree prisms were utilized once again, after the data had been reduced to a common altitude with the Henderson and Cordell technique, to represent the crust of the Earth. Their tops were set at the surface of the Earth, and the bottoms (for the purpose of susceptibility calculation) were at 20 km depth. Ideally, solid spherical rectangles should be used rather than rectangular prisms. However, the development of an analytical expression for the magnetic anomaly for this type of body has so far proven to be intractable. Although an expression for the magnetic anomaly of such a body under the constraint of constant inclination was developed in terms of spherical harmonics, it is not practical because of the high degree and resulting coefficients required to model a body of modest dimension. However, a severe error is probably not introduced over the test area by ignoring the curvature of the Earth.

By using the satellite data reduced to a common altitude of 525 km, the apparent susceptibility of the prismatic blocks was mapped by means of least squares. The vector nature of the field was fully incorporated into the calculation, and no difference was found in using the data before or after the correction for constant inclination has been applied, so long as the data were correctly treated.

The mapped susceptibility is shown in figure 9. This map shows susceptibility contrast relative to some mean or average crustal susceptibility, and it is related to the volume of the equivalent source prism. For example, if we decrease the depth of a prism (say to 10 km), then we would have to double the susceptibility.

The validity of this technique has been checked with model data, and the results can also be compared with the interpretation of the Bangui anomaly and with known tectonic data. For example, figure 9 also shows, along with the susceptibility model, a simplified tectonic map of this area. The susceptibility data clearly outline the zone of tectonic uplift between the two sedimentary basins. Also, the model for the Bangui anomaly indicates a positive magnetization contrast in this

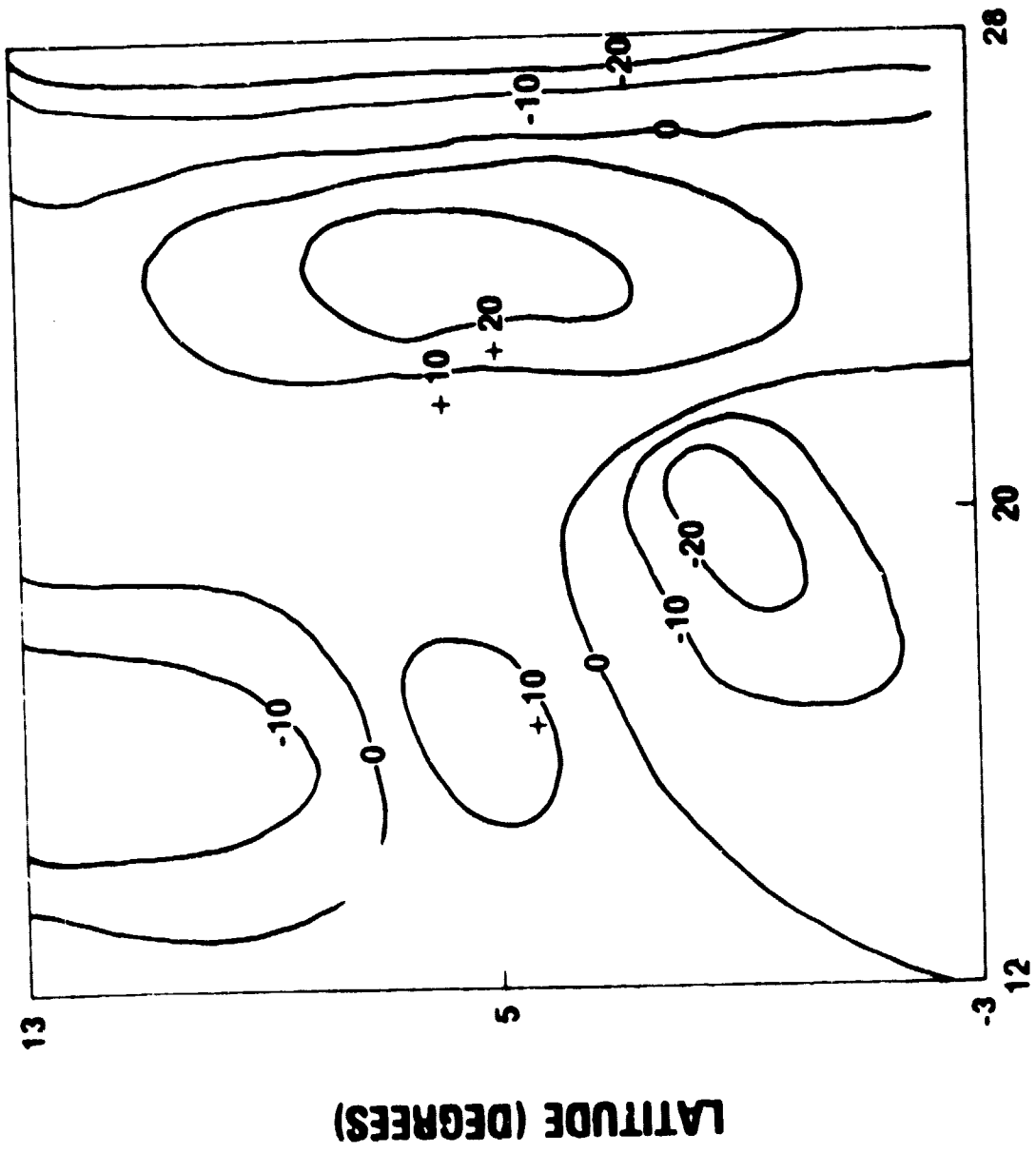


area due to an increase in susceptibility and volume. The only problem with the data so far has been that the 4° prismatic bodies are too coarse, and we are now working with a 2° prism equivalent source, which would also reduce the error resulting from ignoring the Earth's curvature.

In a similar manner, it is also possible to fix the susceptibility of the equivalent source model and to map the depth to the bottom. Classically, this parameter is the least sensitive to map, but we are helped in this situation in that the sources are relatively thin compared with satellite altitude, and the anomalies are greatly influenced by the bottom of the bodies. Utilizing the same source, but fixing the susceptibility at 0.01 cgs units and allowing the bottom to vary, the depth to the bottom was determined (fig. 10). Again, this contrast is relative to some average depth and is totally related to the magnetization, as is evidenced by the similarity between this figure and that for the susceptibility contrast. Again, this information agrees well with the model and tectonic data, and the technique shows some promise. If the bottom variations can be equated with variations in the Curie isotherm, then we may have a valuable tool for mapping the inflections of this surface.

The data in reduced form are also amenable to geologic interpretation, particularly when reduced to a common altitude because, in the indirect method of interpretation, i.e., working from models, it is possible to account for the variation in field direction by proper analysis. An example of this is the interpretation of the Bangui anomaly, the major anomaly in the study area. A thorough interpretation of this anomaly encompassing the consideration of all geological and geophysical data has been presented by Regan and Marsh (1978). In the present paper we recount the construction of the computer model using the satellite, aircraft, and surface magnetic data.

Because the causative body dimensions are approximately 700 km in the east-west direction, and 200 km in the north-south direction, no significant error is introduced if we once again neglect the



**LONGITUDE (DEGREES)**

Figure 10. Depth Contrast Over the Study Area Using the Equivalent Source Model. Contour Interval is 10 km.

curvature of the Earth over the dimension of this body and use sufficiently small prisms. Therefore, the equation for the magnetic anomaly of a rectangular three-dimensional prism was utilized. The variation in the direction of the inducing field was introduced and the curvature error minimized by dividing the prism into small segments and determining the magnetic field value at the center of each component prism by means of a geomagnetic field model. In a similar manner, the magnetic field at each measurement point was determined. It was assumed that only induced magnetization was present, and the direction cosines of the induced magnetic moment of each component prism were determined. The direction cosines were also calculated at each measurement point. For each measurement point, the attraction of individual component prisms was computed and summed.

By using a trial and error approach in the first approximation, the satellite data were fit. Then the model was adjusted to fit both the airborne and surface measurements. The 1° averaged magnetic anomaly map at satellite measurement points resulting from the final model is shown in figure 11; and the quality of the result should be examined by comparison with figure 4.

#### Analysis of Unreduced Data

Although we have stressed the reduction of satellite data to a common altitude and inclination for direct analysis, considerable information in the altitude variations should not be discarded, for, in essence, the various satellite passes afford us a multilevel survey over any particular area.

These data can probably best be used in a statistical or probabilistic approach toward interpretation. They can also be examined to determine the depth of the source of the anomalies, because the question exists whether satellite magnetic anomalies are crustal or not. In an attempt to answer that question, a fairly simple analysis was performed on the satellite data over the study area.



Figure 12 shows several satellite passes at different altitudes over the Bangui anomaly. By utilizing these and other arbitrarily chosen passes, the maximum amplitude of 33 passes was selected and combined with the maximum amplitude of the two Project MAGNET aeromagnetic profiles in this area. By using the fact that the anomalies decay in a power law fashion away from the source and that there is some inverse relationship between the anomalous values at several altitudes, the following equation was solved for both K and N by least squares:

$$\left( \frac{K+R_1}{K+R_2} \right)^N = \frac{\Delta F_2}{\Delta F_1}$$

where

$R_1$  is the altitude of the measurement  $\Delta F_1$

The solution yielded a K of 78 km, which would be the depth, and an N of 2.13. It should also be mentioned that, although ground data were not used in the solution, the equation with these parameters accurately predicts the measured anomalous value at ground level, as shown in figure 13.

In order to examine a crustal source, say depth of 50 km, and a core source, depth of 2900 km, these values of K were substituted into the equation, and the resultant exponential term was determined. A plot of the resulting predicted values is also shown in figure 13. This plot indicates quite strongly that the anomalous values are due to crustal or lithospheric sources.

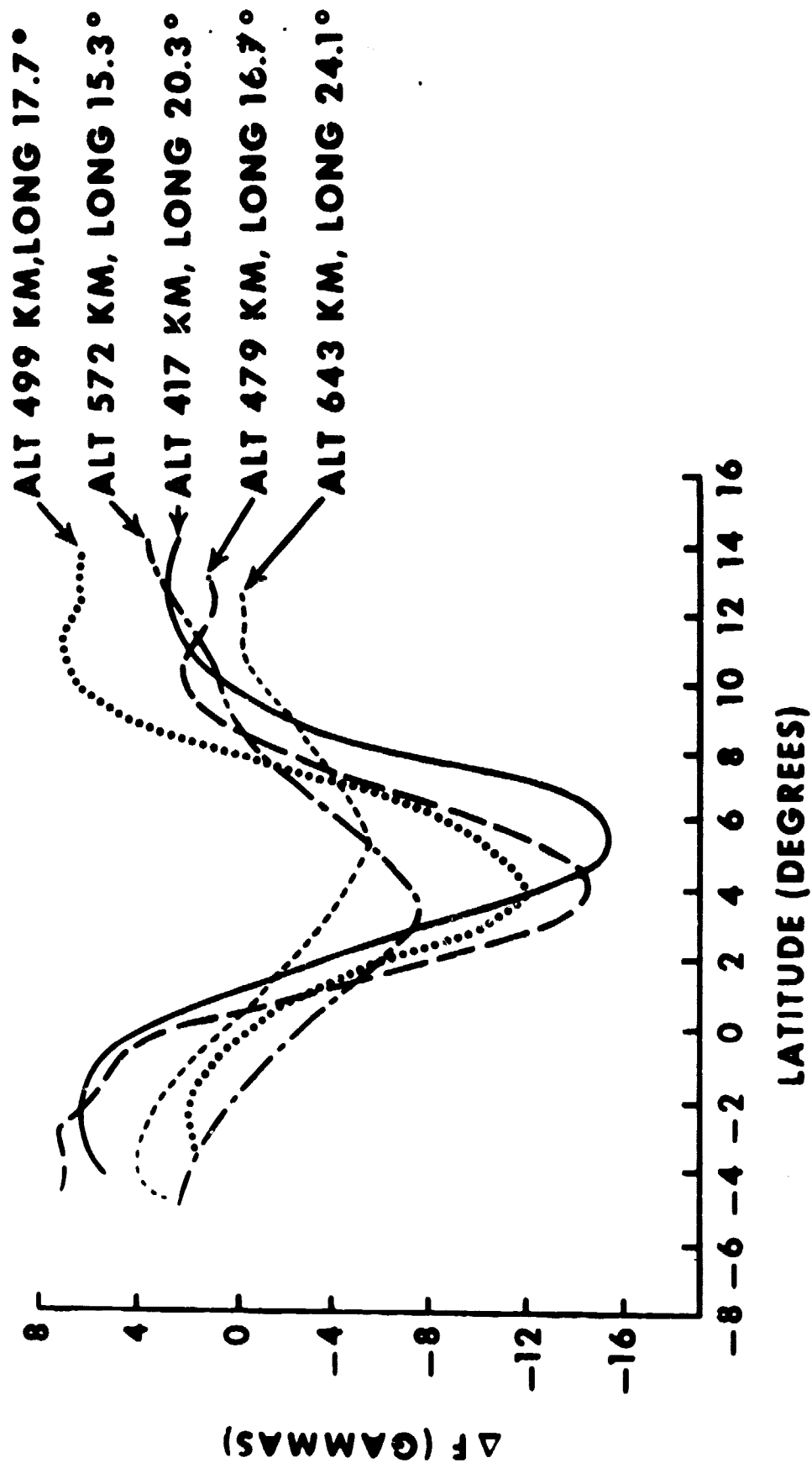


Figure 12 - Barqvi anomaly as detected during five satellite passes.

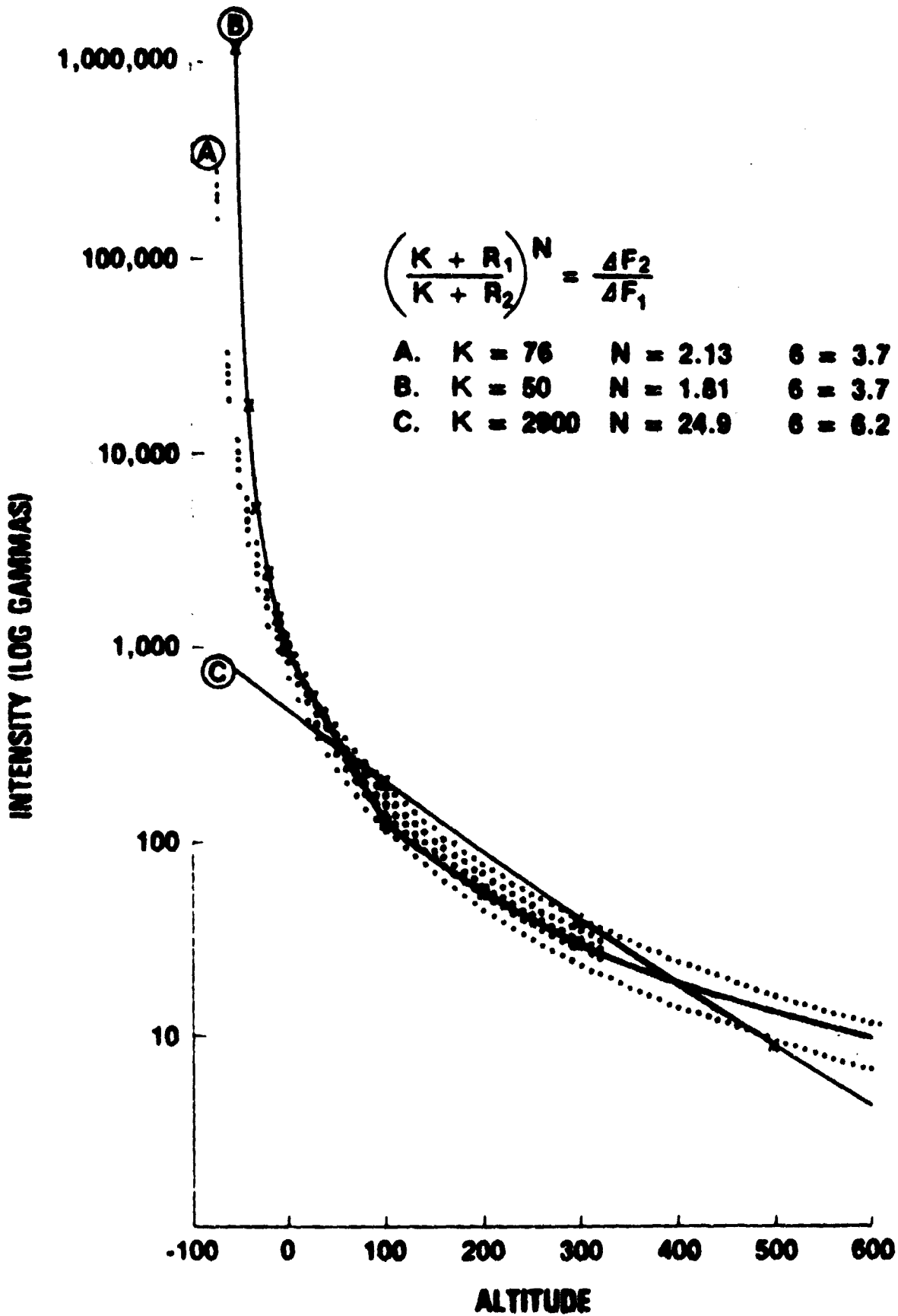


Figure 13 - (A) Fit is exponential decay function to satellite and aeromagnetic data and its extrapolation; (B) theoretical curve for a source at 50 km (C) theoretical curve for a source at 2900 km

C-2

### Summary

In summary, we have reviewed some of the pitfalls and some of the advantages of satellite data. The necessity for accurate preliminary screening and the reduction to common altitude and inclination have been demonstrated, also, the consideration that must be paid to the vector nature of the background field. With the full realization of this constraint and with the data at a common surface, the routine analysis of these data is then quite straightforward.

### References Cited

- Bhattacharyya, B.K., 1977, Reduction and treatment of magnetic anomalies of crustal origin in satellite data: Jour. Geophys. Res., vol. 82, no. 23, p. 3379.
- Bhattacharyya, B. K., and Chan, K. C., 1977, Reduction of magnetic and gravity data on an arbitrary surface acquired in a region of high topographic relief: Geophysics, vol. 42, No. 7, p.1411
- Bott, M.H.P., 1967, Solution of the linear inverse problem in magnetic interpretation with application to oceanic magnetic anomalies: Roy. Soc. London Proc. Ser. A., vol. 194, p. 332.
- Cain, J.C., and Davis, W. M., 1973, Low latitude variations of the magnetic field, in Symposium on Low Level Satellite Surveys, p. 67-87: Intern. Assoc. Geomag. and Aeronomy, Paris, France.
- Cain, J. C., and Sweeney, R. 1973, The POGO Data: Jour. Atmos. and Terr. Physics, vol. 35, p. 1231.
- Dampney, C. N., 1969, The equivalent source technique: Geophysics, vol. 34, no. 1, p. 39.
- Davis, W. M., and Cain, J. C., 1973, Removal of DS from POGO satellite data (abst.): EOS(AGU Trans.) 54(4), p. 242
- Henderson, R. G., and Cordell, L., 1971, Reduction of unevenly spaced potential field data to a horizontal plane by means of finite harmonic series: Geophysics, vol. 36, no. 5, p. 856.
- Langel, R. A., Regan, R. D., and Murphy, J. P., 1977, MAGSAT: A satellite for measuring near-earth magnetic fields: NASA Rept. x-922-77-199.
- Mayhew, M. A., and Davis, W. M., 1976, Magnetic anomalies at satellite elevations over the United States and adjacent areas: EOS, (AGU Trans.) vol. 57, no. 12, p. 908.

- Regan, R. D., Davis, W. M., and Cain, J. C., 1973, The Bangui magnetic anomaly abst: EOS, (AGU Trans.) vol. 54, no. 4, p. 256.
- Regan, R. D., Cain, J. C., and Davis, W. M., 1975, A global magnetic anomaly map: Jour. Geophys. Res., vol. 80, no. 5, p. 794.
- Regan, R. D., and Davis, W. M., 1975, Reduction of satellite magnetometer data for geological studies abst.: EOS (AGU Trans.) vol. 56, no. 6, p. 356.
- Regan, R. D., and Marsh, B. D., 1978, The Bangui anomaly: Its geological origin: Jour. Geophys. Res. (in press)
- Sugiura, M., and Heppner, J. P., 1968, The earth's magnetic field, in Introduction to Space Science, 2nd ed., edited by W.N. Hess and G. D. Medd: Gordon and Breach, New York, p. 5-92.

OM 17  
TO  
P 96

## II. ATMOSPHERIC APPLICATIONS

### SUMMARY

George Carignan  
University of Michigan

#### THE APPLICATION OF THE TETHERED SATELLITE TO PROBLEMS OF ATMOSPHERIC SCIENCE

The tethered satellite has broad appeal to a wide segment of the atmospheric science community. Its appeal is based, for the most part, on the accessibility it provides to the lower reaches of the thermosphere and possibly the mesosphere. This region of the atmosphere which heretofore has been accessible only by sounding rockets is relatively poorly understood and it is a region of great importance. Between the altitudes of about 30 and 120 km the atmosphere ceases to be mixed by turbulence and winds and molecular diffusion begins to predominate. Constituents thus separate according to their atomic weight and, additionally, molecular oxygen is dissociated and atomic oxygen becomes an important constituent. Hydrogen and nitrogen are also dissociated and a rich, complex photochemistry unfolds. The prospect of studying this part of the atmosphere with satellite borne instruments is exciting and the Tethered Satellite System promises to provide this capability.

In a Workshop sponsored by the NASA Marshall Space Flight Center and the University of Alabama at Huntsville, formal presentations were made which explored the utility of a tethered satellite for atmospheric measurements. These presentations, almost without exception, were strong statements of advocacy for the development of such a system and this general sentiment was reinforced by audience reaction. The written versions of these formal presentations together with some written comments from other participants in the workshop are assembled here to provide a record of the proceedings.

Some of the difficulties involved in making measurements from a low altitude satellite were presented and discussed. Most of the proposed measurements can be made from the tethered satellite using existing instruments down to 120 km and there would be a substantial scientific return from such measurements. The interaction of the satellite with the atmosphere below about 120 km modifies the local environment. Mass spectrometers would undoubtedly require further development to operate in this regime and there would be difficulties in relating the measurements to the ambient environment. The resonance fluorescence measurements, on the other hand, are designed for use in a continuum and would be immediately applicable to lower altitudes.

The use of the tethered satellite for release of chemicals as tracers for measuring atmospheric dynamical properties and as sources of perturbations for investigating magnetosphere-ionosphere coupling mechanisms was presented and was received with enthusiasm. Several of the most pressing atmospheric science questions are studied by experiments involving chemical releases and the tethered satellite would be of great value in bringing operational flexibility to low altitude releases. Moreover, the chemical release techniques seem fully compatible with the tethered satellite and so could be applied immediately with very little development.

One attribute of the tethered satellite system which attracted great interest from several disciplines is the potential for simultaneous measurement at various altitudes along the tether. An important example of the value of this capability is the simultaneous observation of atmospheric composition at different altitudes to study the phase and amplitude characteristics of waves propagating through the medium. An observation of this kind would enable a major advancement in the understanding of gravity waves.

The tenor of the workshop was decidedly positive. The tethered satellite system would provide the capability to make several of the most needed measurements in atmospheric science.

Summarized briefly below are four major categories of scientific questions which are addressed in the subsequent individual presentations. Measurements which could be made from a tethered satellite to answer these questions are also summarized. The list of questions and associated measurements is not exhaustive but does summarize the most discussed topics.

1. Atmospheric Composition -

Questions: How does the composition of the atmosphere vary in the region 80-150 km? What is the height of the turbopause and how does it vary globally and temporally? What are the details of the photochemistry?

Measurements:

Mass Spectrometry  
Resonance Fluorescence

2. Atmospheric Dynamics -

Questions: What is the global pattern of circulation in the 80-150 km altitude range? What is the nature of wave propagation in this region and how is the wave energy dissipated? What are the mechanisms that couple the mesosphere and the thermosphere?

Measurements:

Chemical Releases  
Mass Spectrometry  
Lidar

3. Atmospheric Electricity -

Questions: How does the tropospheric electric field couple to the ionosphere?

Measurement:

Electric Fields along the Tether

4. Aerodynamics -

Question: What are the detailed physics of gas-surface interactions at 8 km/sec velocity?

Measurements:

Mass Spectrometers  
Drag  
Temperature  
Density

Contributions to the Proceedings

(Titles of Papers, Authors Names and Affiliation)

1. The Need for Measurements in the Lower Atmosphere  
Dr. C. A. Reber, NASA, Goddard Space Flight Center
2. The Interaction of a Tethered Satellite with the Atmosphere and the Resultant Environment  
Dr. J. H. deLeeuw, Institute for Aerospace Studies, University of Toronto  
Mr. D. R. Tausch, University of Michigan
3. Measurements of Reactive Species  
Dr. J. G. Anderson, University of Michigan
4. Mass Spectrometric Measurements  
Professor A. O. C. Nier, University of Minnesota
5. Atmospheric Electrification  
Dr. H. W. Kasemir, National Oceanic and Atmospheric Administration/  
Environmental Research Laboratory
6. Chemical Release  
Dr. D. S. Evans, National Oceanic and Atmospheric Administration  
Dr. J. P. Heppner, NASA, Goddard Space Flight Center
7. Aerodynamic Effects  
Dr. G. Karr, The University of Alabama in Huntsville
8. Letter  
Dr. R. E. Smith, NASA, Marshall Space Flight Center

**THE NEED FOR MEASUREMENTS IN THE LOWER ATMOSPHERE**

**May 1-2, 1978  
Huntsville, Alabama**

**C. A. Reber  
NASA/Goddard Space Flight Center**

### The Need for Measurements in the Lower Thermosphere

The lower thermosphere (roughly 80 km to 150 km altitude) is an atmospheric transition region of great scientific interest, but it is also a region heretofore largely unexplored due to the relative difficulty of making measurements in it. Rocket flights have produced some data, but in-situ satellite data are scarce due to the high drag encountered at the lower altitudes. The Atmospheric Explorer (AE) satellites obtained data (in their elliptic phases) routinely down to 150 km, and sampled for several months between 130 and 140 km. The highly desirable circular orbit data from AE did not extend below 200 km and there are essentially no satellite data at all below 130 km.

This region is characterized by a number of geophysical phenomena which possess intrinsic interest as well as which have important ramifications for other regions of the atmosphere. Among these are:

The mesopause, the very low temperature region around 85 km which marks the upper boundary of the mesosphere, and the lower thermosphere where the very large increase of temperature with altitude leads up to the highest temperature region of the atmosphere. (See Figure 1). The mesopause is thought to be cooled mainly by infrared radiation from carbon dioxide ( $\text{CO}_2$ ) and ozone ( $\text{O}_3$ ); it has the interesting and poorly understood property of being colder at high latitudes in the summer than it is in the winter. The lower thermosphere is heated primarily from above by absorption of extreme ultraviolet (EUV) solar irradiation and downward conduction of this energy. There is also some local energy input due to dissipation of upward propagating tidal and gravity waves. The vertical and global

temperature structure and energetics of this region are only poorly understood, although they are generally used for the lower boundary conditions in detailed models of the upper atmosphere.

The "turbopause", the upper boundary of the region of the atmosphere where turbulent processes maintain the mixing ratios constant for the major gas species. Above the "turbopause" the atmosphere tends toward a diffusive distribution in which the gases are distributed according to their individual mass-dependent scale heights. The "turbopause" is discussed mathematically in terms of the competition between the eddy diffusion coefficient and the molecular diffusion coefficients for the gas species. It is generally assumed to be a rather thick region with an effective altitude (defined by the intersection of the extrapolations of the mixed and diffusive altitude profiles) near 100 km. The exact nature and altitude of the turbopause have strong effects on the downward heat flux and also on the transport of constituent gas species in this region. The turbopause thus controls the number densities of many species in the upper thermosphere and exosphere, including atomic oxygen, hydrogen, helium and argon. Figure 2 shows the sensitivity of high altitude helium to the turbopause, parameterized by various values for the eddy diffusion coefficient. The seasonal and diurnal variation of helium is observed to be more than a factor of 40. A competing explanation for this large variation is thermospheric winds. Until we understand the morphology of the turbopause, however, the actual cause for these and other compositional variations will not be known.

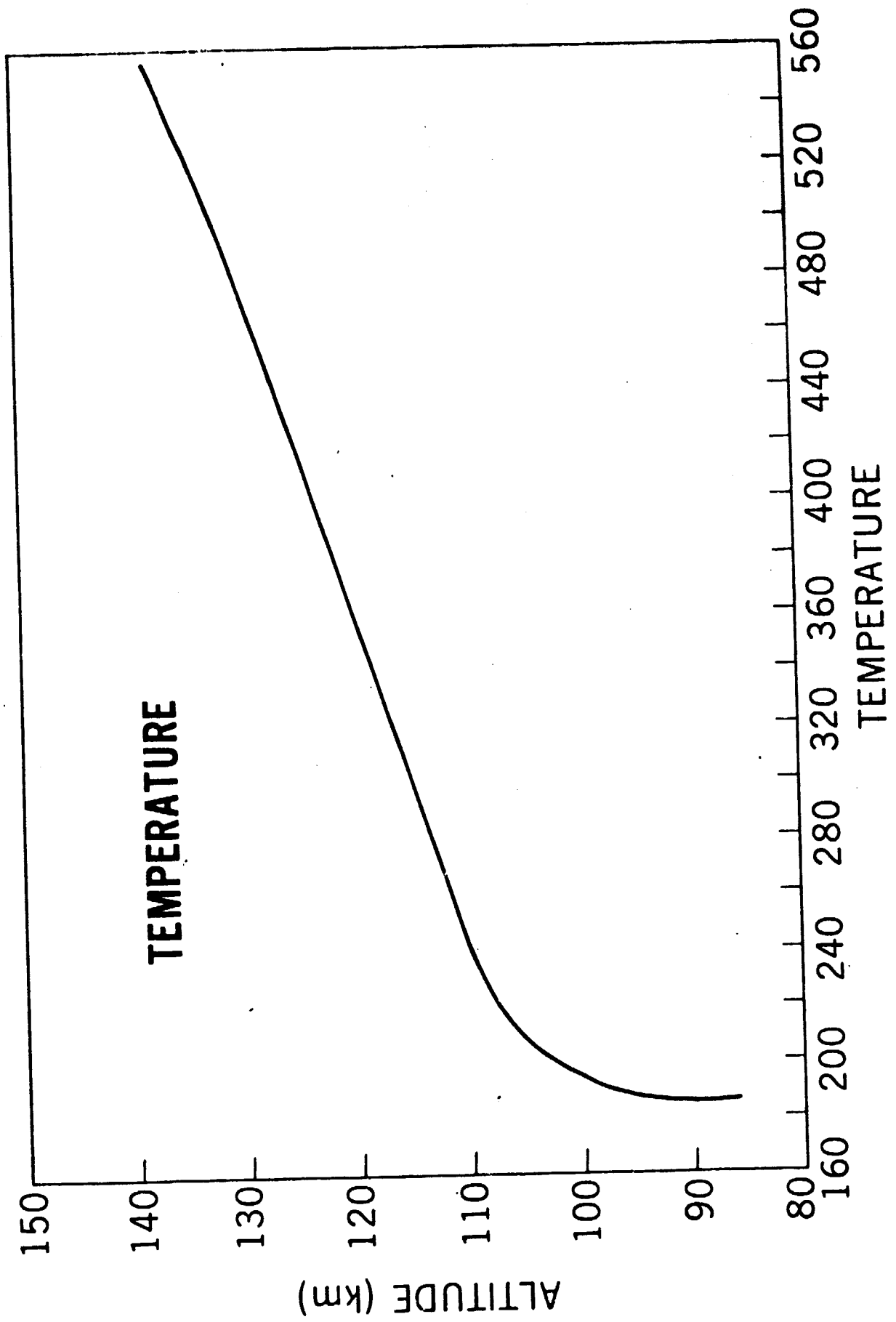
Dissipation of tidal wave and gravity wave energy in this region provides a significant, but poorly known energy source for the lower thermosphere. Ground-based incoherent scatter radar probing of the region between 100 km and 130 km indicates a semi-diurnal component of neutral gas temperature, indicative of an upward propagating tidal mode. Travelling ionospheric disturbances (TID's) have been assumed to be internal atmospheric gravity waves, propagating generally from high latitude regions toward the equator (but also related to local tropospheric weather activity). Satellite data have recently shown that the neutral species also partake in these wave modes, with species-dependent phases and amplitudes (Figure 3). Calculations show wave motion to be extremely important in the spread of energy and momentum deposited in the upper atmosphere, particularly that deposited at high latitudes during periods of magnetic activity. For meaningful calculations, however, one needs the altitude and geographic distribution of the propagation characteristics of these waves, and these are not yet available.

Magnetospheric energy inputs at high latitudes include energetic particle precipitation, joule heating, and direct coupling of momentum to the neutral gas from the ions driven by convecting magnetic field lines. This energy source is always present, but is highly enhanced during periods of geomagnetic activity when it may exceed the local energy input from the solar EUV. Significant particle inputs affect the atmosphere as low as the upper mesosphere, while the bulk of the joule heating is thought to take place near 150 km. The effect of this energy on thermospheric circulation is seen in Figure 4 (Roble) where

low (4a), moderate (4b), and high (4c) magnetic activity effects are illustrated. Figure 5, using data from the circular orbit phase of AE-C, shows the dramatic effects on atmospheric composition poleward of 40° caused by moderate magnetic activity. For the proper understanding of this phenomenon, data such as these are needed down to at least 125 km.

Summary of current problem areas

- What is the relative importance of the turbopause versus winds in determining the composition of the thermosphere?
- What is the mechanism of the coupling between the mesosphere and the thermosphere? How important is wave dissipation in this coupling? What is the effect of this coupling on minor species transport and the radiation balance of this region?
- Why is the high latitude summer mesopause colder than the winter mesopause?
- What is the morphology and variation of magnetospheric energy inputs at high latitudes? How much of this energy is transported to other regions of the atmosphere and how much is dissipated locally?
- What are the propagation characteristics of atmospheric gravity waves in the altitude region between 100 and 200 km?



$2.19 \times 10^6 \text{ cm}^{-3}$ . The calculated values are obtained by using the same computer program used in the dynamic-diffusion calculations, setting the wind equal to zero, and using  $1200^\circ$  for the exospheric temperature. It can be seen from Figure 3 that either of the two eddy diffusion profiles mentioned can produce satisfactory agreement with the high altitude data and one need only choose the appropriate constant value; either  $1.8 \times 10^6 \text{ cm}^2 \text{ sec}^{-1}$  for the constant profile or  $2.5 \times 10^6 \text{ cm}^2 \text{ sec}^{-1}$  for the Johnson and Gottlieb profile satisfy the data.

The shape of the vertical profile for helium is not affected by the eddy diffusion coefficient used in the calculation. This can be seen in Figure 4 where helium density profiles for various constant eddy diffusion coefficients are shown

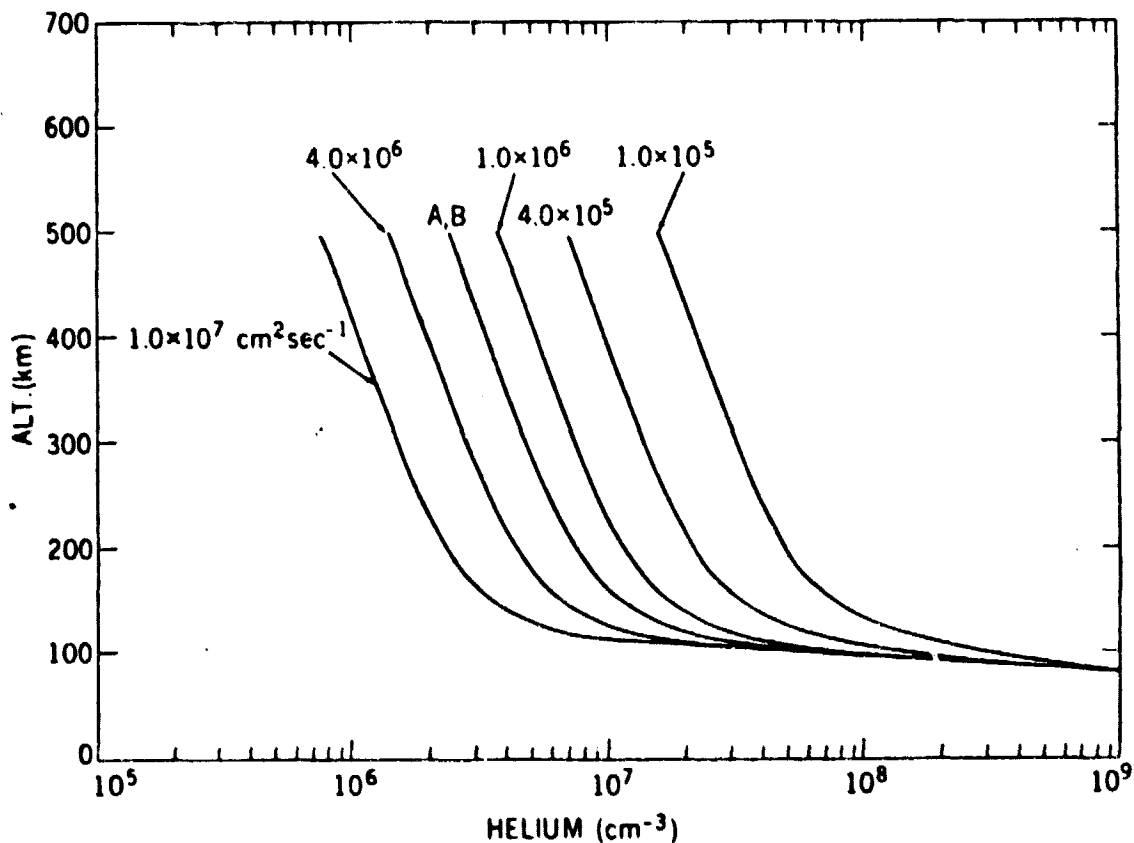
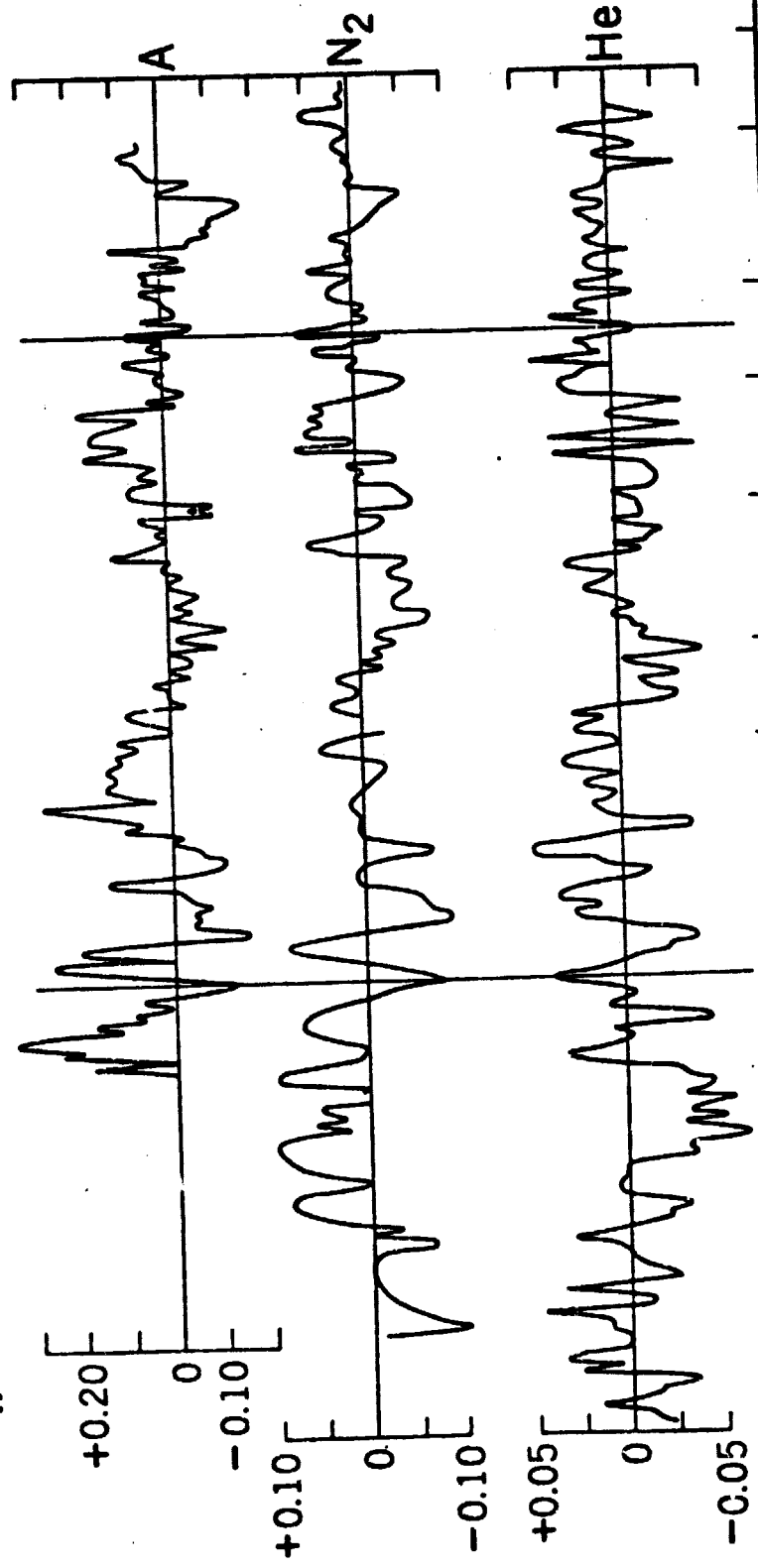


Figure 4. Helium density as a function of altitude for various constant values of the eddy diffusion coefficient and for the eddy diffusion coefficients of Figure 2 (marked A and B). The exospheric temperature,  $T_\infty$ , is  $1200^\circ$ .

$\frac{\Delta n}{n}$  7 FEB 1974 16:36 UT LONGITUDE -55°



# SOLSTICE

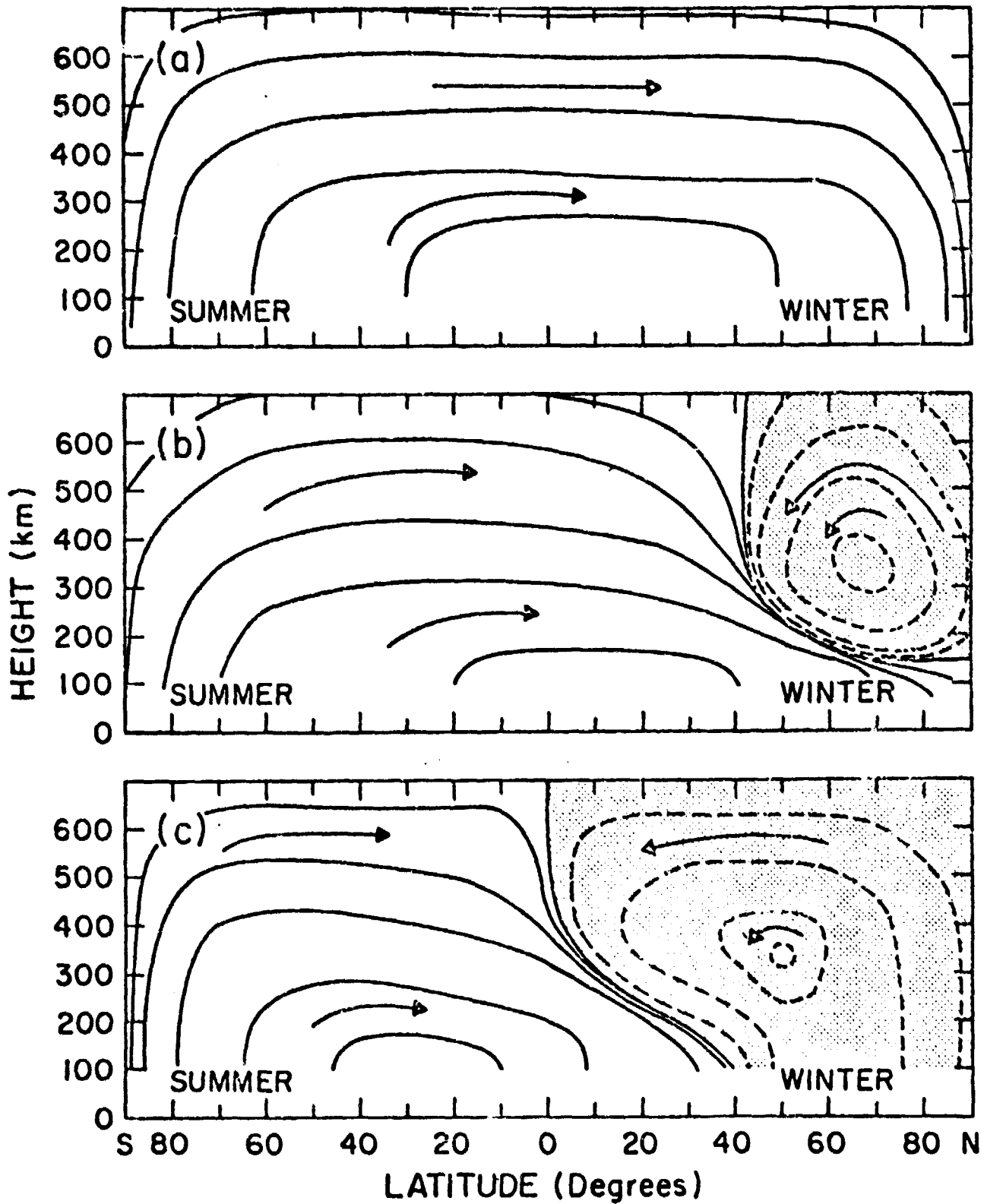
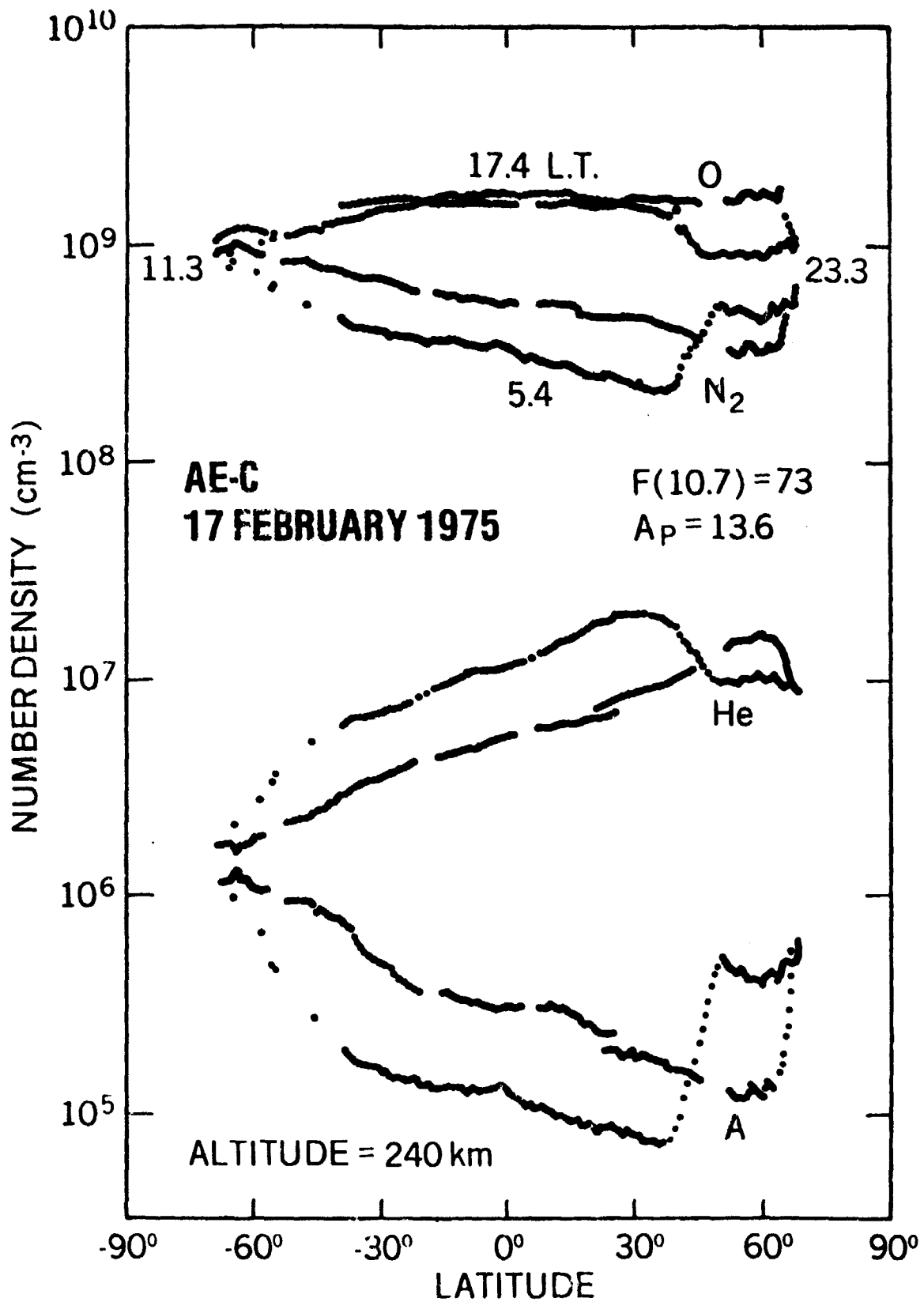


Fig. 12



23  
N81-29484

THE INTERACTION OF A TETHERED SATELLITE WITH THE  
ATMOSPHERE AND THE RESULTANT ENVIRONMENT

May 1-2, 1978  
Huntsville, Alabama

J. H. deLeeuw  
Institute for Aerospace Studies  
University of Toronto

D. R. Taeusch  
Space Physics Research Laboratory  
Department of Atmospheric and Oceanic Science  
University of Michigan  
Ann Arbor, Michigan 48109

## TETHERED SATELLITE

From the study material it appears that downward penetration to altitudes of about 100 km might just be possible. In this range equilibrium temperatures become high and will set a limit to sophisticated on-board instrumentation, but because the heating effect drops rapidly with increasing altitude, operation at a lower limit of 100 to 110 km should be possible.

At about 140 km the mean free paths are of similar magnitude as the satellite size and rapidly become considerably smaller than the satellite for lower altitudes. This means that the aerodynamic flow field is no longer 'free molecular' and conditions enter the so-called transition regime. Unlike the free molecular situation, which is determined by the properties of particle-surface interactions, and where calibration of instruments is attainable in space simulators with molecular beam apparatus, the flow field is now influenced by collisions; aerodynamic effects become progressively more important as the altitude diminishes from 140 km (near free molecular) to 100 km (near continuum conditions).

The aerodynamic effects produce changed conditions at the satellite of all properties of state including the composition of the gas. The difficulty is that theoretical predictions for complicated geometries in the transition regime are not available. Alternatively, calibration under proper scale conditions is possible, although onerous because in any aerodynamic test facility it is difficult to cover more than about half of the transition regime. Nearly free molecular conditions are particularly difficult (but not impossible) to simulate.

One approach to making measurements under these conditions is to use methods where the aerodynamic effects can be ignored. This is so when the measurements, although local, are made at a sufficient distance from the vehicle that ambient conditions prevail at the test station. Laser excitation or electron-beam excitation come to mind in this regard. In fact, UTIAS has developed electron-beam rocket instruments for measurements in this altitude range. The electron beam is a broadly exciting mechanism, which produces luminosity from all species in the ambient atmosphere. It has to be oriented to minimize aerodynamic effects in the beam region, but it will yield multi-channel data on individual species concentration, rotational temperature, and the excitation level of vibrational states of molecular nitrogen.

We are interested in the tethered satellite program along the following lines:

1. Participation in the calibration of apparatus like mass spectrometers under free molecular conditions.
2. Participation in the design and execution of relevant calibration experiments in the transition regime in our low density wind tunnels.
3. Potential access to the tethered satellite for beam instrumentation. This would involve aerodynamic design input on the satellite, both as to preferred shape for the experiments and aerodynamic control for up-stream pointing.
4. Participation in aerodynamic design for the purpose of stabilization, pointing, etc., required for other experiments.

THE TETHERED SATELLITE  
Neutral Atmospheric Studies

D. R. Tausch

As stated previously, the lower altitudes at which the tethered satellite would operate are in a region where the mean free path is on the order of or less than the satellite dimensions. For a satellite velocity of 7.5 km/sec, this means the flow about the vehicle is characterized by 1) weak shock waves, 2) transition between free molecular and compressible fluid flow, and 3) excitation and ionization flow fields caused by the specular reflection of the free stream molecules with subsequent collision processes, near the vehicle, between the reflected and free stream flows. These phenomena have not been well studied either by theory or by laboratory techniques.

Lest this sound negative and an insurmountable problem in aerodynamics, let me state that the tethered satellite would be an excellent tool to use to study these phenomena heretofore unobtainable in earth based laboratories.

Aside from this science for science sake type of study, much could be added to our knowledge of the neutral atmosphere by measurements in circular orbit in the 100 to 130 km region. At the present time, the variability in this altitude region is known to exist, but the amount of variability and the temporal and spatial relationships to the diurnal, seasonal and solar variations are completely unknown. The usual fixed boundary conditions of model atmospheres at 120 km altitude attest to this lack of knowledge.

Mass spectrometer and/or pressure sensor measurements at these altitudes are straight forward. One need only set up a flow system which will assure the proper pressure levels within a measuring chamber appropriate to the type of sensor used. The absolute value of the ambient conditions of interest may not be immediately obtainable due to the current lack of knowledge of the external flow relationships, but the relative variability would be determined.

In general, the tethered satellite experiment is an exciting concept. There are certainly problems to be solved, but they appear solvable. The knowledge to be gained from the previously unperformable experiments will be worth the effort required to solve these problems.

D6  
N81-29485

THE IN SITU MEASUREMENT  
OF REACTIVE NEUTRAL CONSTITUENTS IN  
THE THERMOSPHERE BY ATOMIC  
AND MOLECULAR RESONANCE FLUORESCENCE

2 May 1978  
Huntsville, Alabama

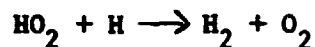
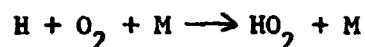
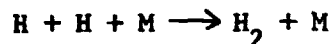
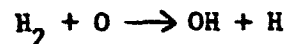
J. G. Anderson  
Space Physics Research Laboratory  
Department of Atmospheric and Oceanic Science  
University of Michigan  
Ann Arbor, Michigan 48109

## REACTIVE NEUTRAL SPECIES IN THE THERMOSPHERE

The Tethered Satellite System in combination with in situ atomic and molecular resonance fluorescence techniques can, for the first time properly treat the problem of simultaneously determining the absolute density of atomic and molecular species known to control the photochemical structure of the upper atmosphere. There are in particular two families of reactants which can be treated by these techniques.

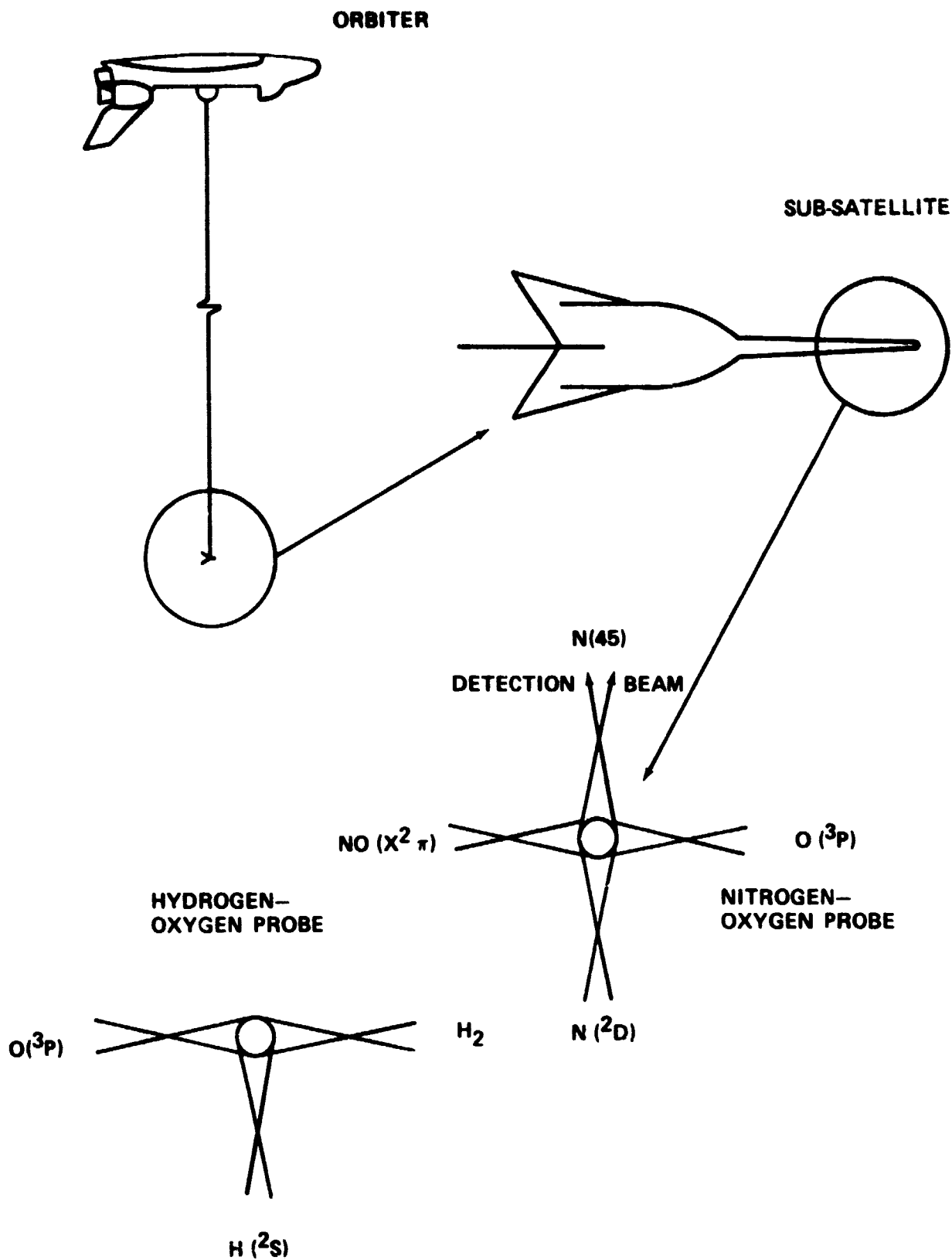
(A) The nitrogen oxygen family consisting of NO, N(<sup>4</sup>S), N(<sup>2</sup>D) and O(<sup>3</sup>P) which are chemically interrelated because the production and destruction of NO is controlled by N(<sup>2</sup>D) and N(<sup>4</sup>S) respectively. Atomic oxygen fills out the group since it is the major quenching agent for N(<sup>2</sup>D). Although these species have been examined by remote sensing techniques, their concentration has not been simultaneously measured within the same volume element.

(B) The escape of hydrogen from the earth is believed to be controlled by flux limiting factors in the lower thermosphere. It would be of significant value to test this theory by simultaneously observing H, H<sub>2</sub> and O(<sup>3</sup>P) on a global scale since the exchange between H and H<sub>2</sub> is primarily through the reaction sequence



Because considerable theoretical effort has been expended in this problem which is a central question in thermospheric aeronomy today, the TSS could make a major contribution.

A brief schematic description of the experiment is presented on the pages which follow.



IN SITU  
MOLECULAR RESONANCE FLUORESCENCE

$$S = \bar{F}_\sigma [X] \{ \Sigma T \eta \} L$$

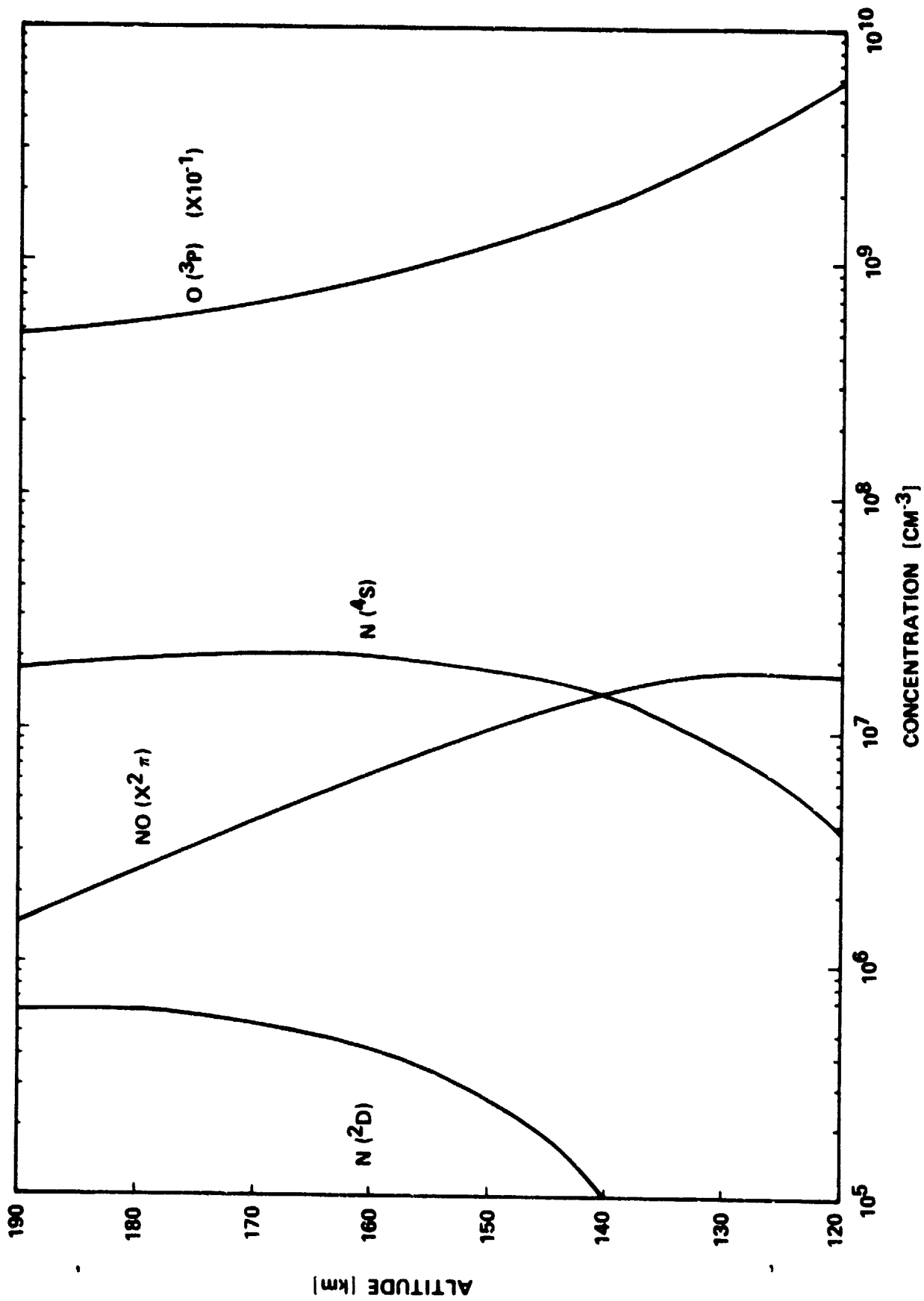
$$= C(\bar{F}) [X]$$

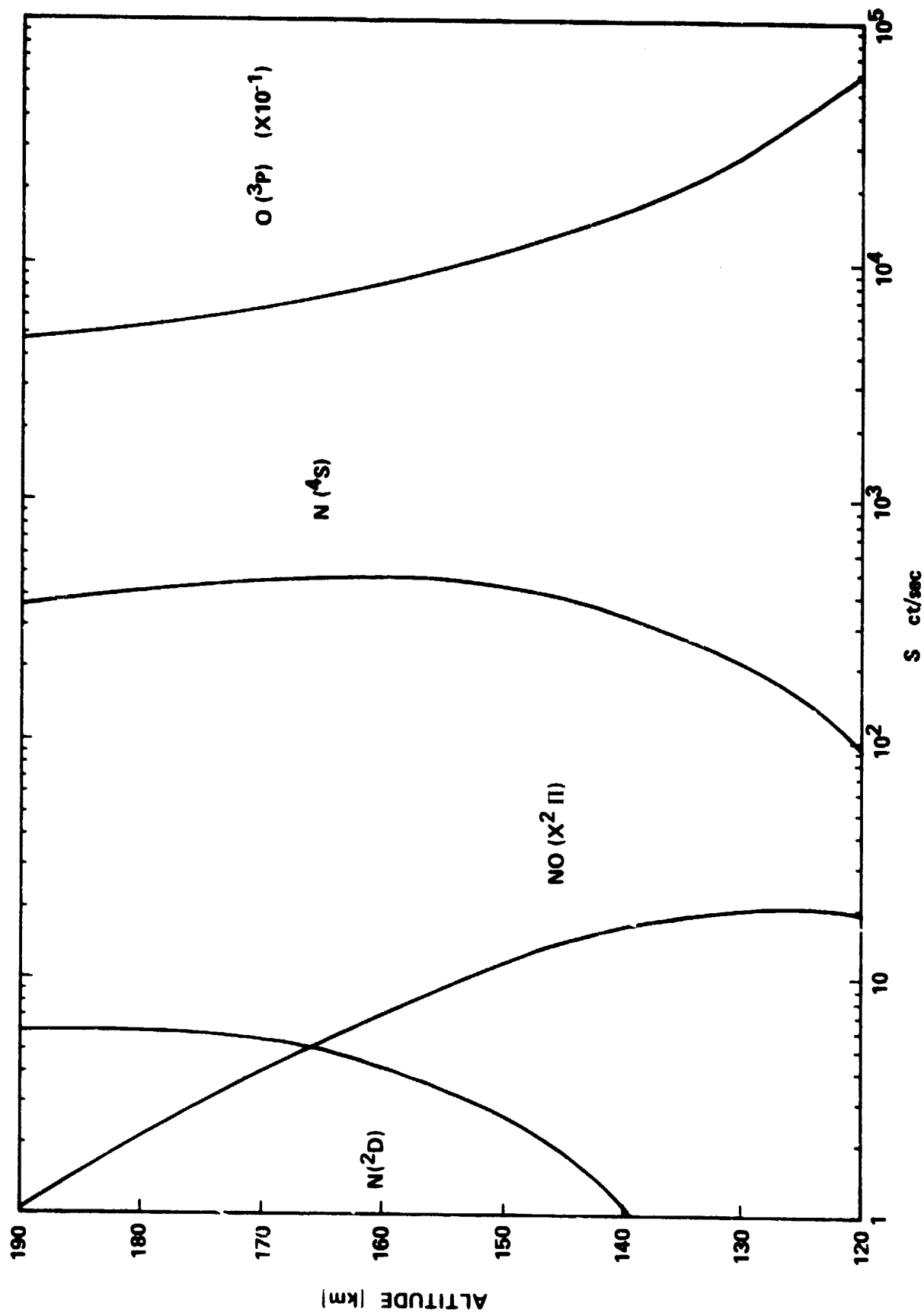
$$C(\bar{F}) = \sum_J \sum_V \sum_B F(J, V, B)_\sigma \frac{S(J, B)}{2J+1} \frac{A(V', V'') S(J'', B)}{\sum_{J''V''B} A(V', V'') S(J'', B)}$$

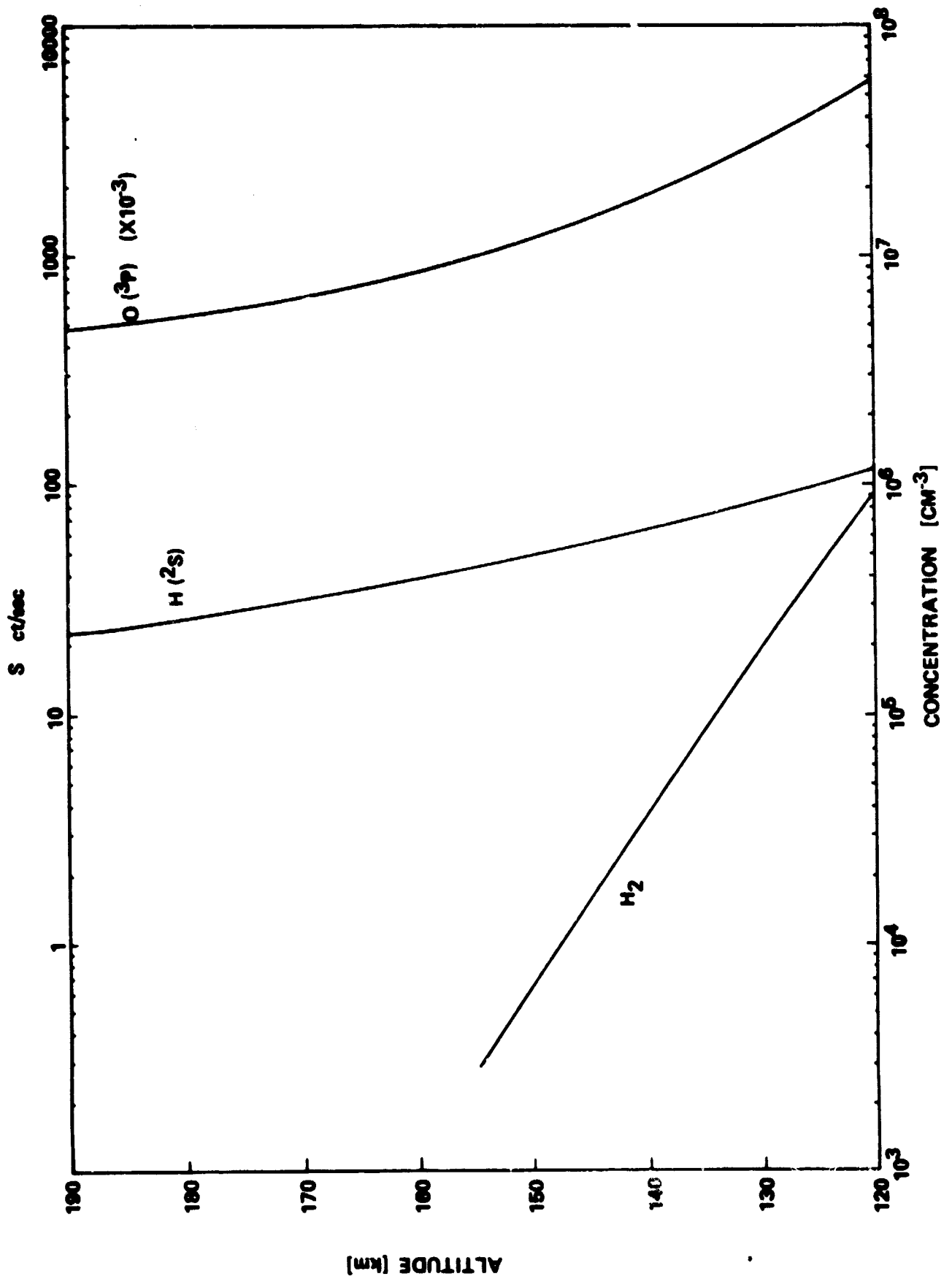
$$\text{NO}(X^2\pi) \quad C_{\text{NO}} = 1 \times 10^{-6} \text{ cm}^3 \text{ sec}^{-1}$$

$$\text{OH}(X^2\pi) \quad C_{\text{OH}} = 3 \times 10^{-6} \text{ cm}^3 \text{ sec}^{-1}$$

$$\text{H}_2(X^1\Sigma_u^+) \quad C_{\text{H}_2} = 10^{-4} - 10^{-5} \text{ cm}^3 \text{ sec}^{-1}$$







## APPROXIMATE REQUIREMENTS

- A. WEIGHT OF ELECTRONICS, OPTICS AND POWER SOURCE FOR  
A 4 EXPERIMENT PACKAGE  
35 KG
- B. WEIGHT OF COOLANT TO COLLAPSE SHOCK FRONT  
50-80 KG
- C. POWER CONSUMPTION DURING MEASUREMENT PHASE  
25 AMPS @ 28 VOLTS

MASS SPECTROMETRIC MEASUREMENTS  
IN THE LOWER THERMOSPHERE

May 1-2, 1978  
Huntsville, Alabama

A. O. C. Nier  
School of Physics and Astronomy  
Minneapolis, Minnesota 55455

## Mass Spectrometric Measurements in the Lower Thermosphere

Alfred O. Nier

School of Physics and Astronomy, University of Minnesota  
Minneapolis, Minnesota, 55455

Mass spectrometers have been carried on numerous rockets and satellites for the purpose of determining the composition of the neutral thermosphere. Most of the measurements have been made by satellite and cover the altitude range above 150 km. A few of the rocket measurements extend down to 120 km, there being practically no determinations below this altitude.

Figure 1 is a schematic drawing of the open source magnetic deflection type mass spectrometer (OSS) used on the Atmosphere Explorer-C, -D, and -E satellites [Nier et al., 1972] as well as on a number of rocket flights. It consists of an ion source (at the left), a combination of electric and magnetic fields for making a mass analysis, and a pair of collectors for measuring the analyzed ion current. The gas beam enters the ion source from the left, strikes the various electrodes and diffuses back out through the grid opening in the plate 1. Ions are produced by the electron beam, whose cross section is shown as a dot in the space between the two collimating magnets M. The ions produced are drawn out of the ionizing region, are accelerated and focused on slit  $S_1$ , after which they pass into the analyzing region. Mass spectra are swept by changing the ion acceleration and deflection voltages.

Quadrupole mass spectrometers have also been used extensively in space applications, differing mainly in the method of making the mass analyses. While each of the types of instruments may have advantages in particular

applications, the performance of the different instruments are roughly comparable and the discussion which follows could refer to either type instrument, or for that matter to other types as well.

When, in a laboratory calibration, air is introduced into an instrument such as the Atmosphere Explorer OSS type, a spectrum such as shown in Fig. 2 is obtained. Clearly seen are the principal atmospheric constituents,  $N_2$ ,  $O_2$  and Ar. Also seen are fragments at mass 14 and 16 corresponding in part to atomic nitrogen and oxygen ions, respectively, produced in the ionization process in the instrument ion source. The peaks at 20, 14.5, and part of the 14 and 16 peaks are due to doubly charged ions, also produced in the ionization process and following the same trajectories as do singly charged ions of half the mass. The isotopic molecules  $^{18}O^{16}O$ ,  $^{17}O^{16}O$ ,  $^{15}N^{14}N$  are clearly seen as is  $^{36}Ar$ .  $CO_2$  and  $H_2O$ , present as impurities, are also evident.

In practice, complete spectra such as shown in Fig. 2 are generally swept for diagnostic purposes. The more common procedure is to jump from peak to peak in what is called a peak-stepping mode, observing only peaks of interest. This enables one to obtain more readings of interest in the time available. The repetition rate typically varies from a fraction of a second to several seconds depending upon the number of peaks included in the mode chosen.

When a mass spectrometer is carried on a fast moving vehicle such as a rocket or satellite moving through the thermosphere, a number of problems arise which are not encountered in the laboratory. Above 120 km the ambient pressure <sup>is</sup> sufficiently low that the atmosphere can be admitted directly to the ion source, as shown in Fig. 1. If the instrument is carried on an earth satellite moving to the left, gas enters the source as a molecular beam of

8.5 km speed upon which is superimposed the Maxwellian speed distribution characteristic of the ambient temperature. The high beam speed produces a stagnation pressure in the ionizing region which is proportional to the square root of the molecular weight of the particles; for  $N_2$  this leads to a particle density which is approximately 65 times greater than it would be if the vehicle were not in motion. If the opening in plate 1 is a pinhole (in which case the instrument is said to have a closed source), the stagnation can be calculated exactly. If the opening is large, as in Fig. 1, the stagnation cannot be calculated and must be measured, using a high speed laboratory beam. For the instrument shown in Fig 1 this was done, using the high speed molecular beam facility at the institute for Aerospace Studies of the University of Toronto [Hayden et al., 1974]. It was found that the stagnation characteristic was very nearly the same as for a true "closed source" instrument. From a stagnation standpoint the two may thus be treated alike.

Because the gas entering the ion source is determined by the projected area of the aperture to the ion source, the signal falls off with the cosine of the angle of attack, except near  $90^\circ$  where it approaches that which would be observed for a stationary vehicle. Since the reading of the instrument depends upon the angle of attack, it is clear that the latter must be known if quantitative measurements are to be made. Either a despun vehicle, with the instrument looking forward, as a spinning vehicle with the normal to the aperture of the instrument passing through the forward direction may be employed, each having certain advantages.

While mass spectrometers similar to those discussed here have operated at altitudes as low as 100 km when carried on sounding rockets, the exposure to high pressure in such cases was for only very short intervals of time so

no harmful effects took place. The Atmosphere Explorer instruments operated only for short intervals at altitudes below 150 km and then only down to 129 km when the satellite was in the spinning mode. At 120 km the total particle density is approximately  $5 \times 10^{11}/\text{cm}^3$ . For this particle density the equilibrium pressure in the ion source would be approximately  $9 \times 10^{-4}$  torr, which is about the highest pressure at which a mass spectrometer ion source can be operated. A 7 mil tungsten wire filament has a life in air of about 26 hours at this pressure [Mauersberger and Olson, 1973]. The pressure in the mass analyzing region of the instrument is considerably less as this part of the instrument may be pumped with a combination ion sputter and titanium evaporation pump.

The quantitative measurement of atomic oxygen and nitrogen, thermospheric constituents which are highly reactive chemically, poses a different problem. Tausch et al. [1973] demonstrated that in satellite-borne mass spectrometers atomic oxygen is converted to the molecular form as a result of reactions in the instrument's surface and can be measured quantitatively as a result. The method is applicable at high altitudes where ambient molecular oxygen concentrations are low and ambiguity is avoided. Likewise, Mauersberger et al. [1975] showed that atomic nitrogen reacted with atomic oxygen on mass spectrometer surfaces to form NO, and could be measured as such. Again the method is specifically applicable at high altitudes where the amount of ambient NO is low.

One of the features of the open source geometry shown in Fig. 1 is that the instrument may be operated in what is called the "fly-through" mode. In this mode the electric fields normally employed for drawing ions out of the ionizing region are reduced to zero or made slightly repelling. As a result, incoming gas particles which hit instrument surfaces and lose their energy (as

most do) do not enter the ion accelerating region and hence are not measured. On the other hand, ambient particles which have not struck surfaces retain their 8.5 km/sec velocity relative to the vehicle as they pass through the ionizing electron beam. This velocity corresponds to approximately 1/3 electron volt of energy per a.m.u. of mass. Hence an incoming atomic oxygen atom has an energy of about 5 eV, an oxygen molecule 10 eV, etc. This initial energy enables ions formed from the incoming particles to enter the accelerating and analyzing region and be measured. The method made possible the unambiguous simultaneous determination of atomic and molecular oxygen [Nier et al., 1974]. As applied to date the method required that the satellite be in a spinning mode with the normal to the instrument passing through the "forward" direction.

With a closed source instrument, Spencer et al. [1976] and Hedin et al. [1976] used the instrument response as a function of angle of attack as a means for measuring atmospheric temperature and winds.

In summary, both open and closed source mass spectrometers carried on satellites have functioned routinely down to 150 km, providing quantitative values of  $N_2$ ,  $O_2$ , O, N, Ar and He concentration. There is every reason to believe these measurements could be extended down to 120 km with but minor changes in existing instruments, recognizing that the main limitation at present appears to be filament life. For closed source instruments there would not necessarily be a limitation as additional pumping could be employed in the ion source, thus reducing the pressure.

Below 120 km the pressure becomes so high that it does not appear that open-source instruments are practical. Closed source instruments with sufficiently small entry orifices and adequate pumps can operate at any pressure. Present day instruments modified by existing pumping systems could thus be employed even on tethered satellites which make excursions below the turbopause. While these could not, with present techniques, perform some of the interesting measurements being made by open source instruments in the more tenuous thermosphere, many useful measurements would still be possible. If a pair of tethered satellites separated by 10 kilometers could be deployed near the turbopause, extremely important concentration and temperature gradients could be made in this very interesting region of the atmosphere.

## REFERENCES

- Hayden, J. L., A. O. Nier, J. B. French, N. M. Reid, and R. J. Duckett, The Characteristics of an Open Source Mass Spectrometer Under Conditions Simulating Upper Atmosphere Flight, *Int. J. Mass Spectrom. and Ion Phys.* 15, 37-47, 1974.
- Hedin, A. E., N. W. Spencer, W. B. Hanson, and P. Bauer, Comparison of Neutral Temperature Inferred from Instruments on the AE-C Satellite, *Geophys. Lett.* 3, 469-471, 1976.
- Mauersberger, K., M. J. Engebretson, W. E. Potter, D. C. Kayser, and A. O. Nier, Atomic Measurements in the Upper Atmosphere, *Geophys. Res. Letters* 2, 337-340, 1975.
- Mauersberger, K., and D. H. Olson, Mass Spectrometer Ion Source Filament Lifetimes in the Presence of Oxygen, *Int. J. Mass Spectrom. and Ion Phys.* 11, 72-74, 1973.
- Nier, A. O., W. E. Potter, D. R. Hickman, and K. Mauersberger, The Open-Source Neutral-Mass Spectrometer on Atmosphere Explorer-C, -D, and -E, *Radio Science* 8, 271-276, 1973.
- Nier, A. O., W. E. Potter, D. C. Kayser, and R. G. Finstad, The Measurement of Chemically Reactive Atmospheric Constituents by Mass Spectrometers carried on High-Speed Spacecraft, *Geophys. Res. Letters* 1, 197-200, 1974.
- Spencer, N. W., R. F. Theis, L. E. Wharton, and G. R. Carignan, Local Vertical Motions and Kinetic Temperature from AE-C as Evidence for Aurora-Induced Gravity Waves, *Geophys. Res. Lett.* 3, 313-316, 1976.
- Taeusch, D. R., G. R. Carignan, and C. A. Reber, Neutral Composition Variation above 400 Kilometers during a Magnetic Storm, *J. Geophys. Res.* 76, 8318-8325, 1971.

COUNTING MULTIPLIERS

Low- High-  
Mass Mass

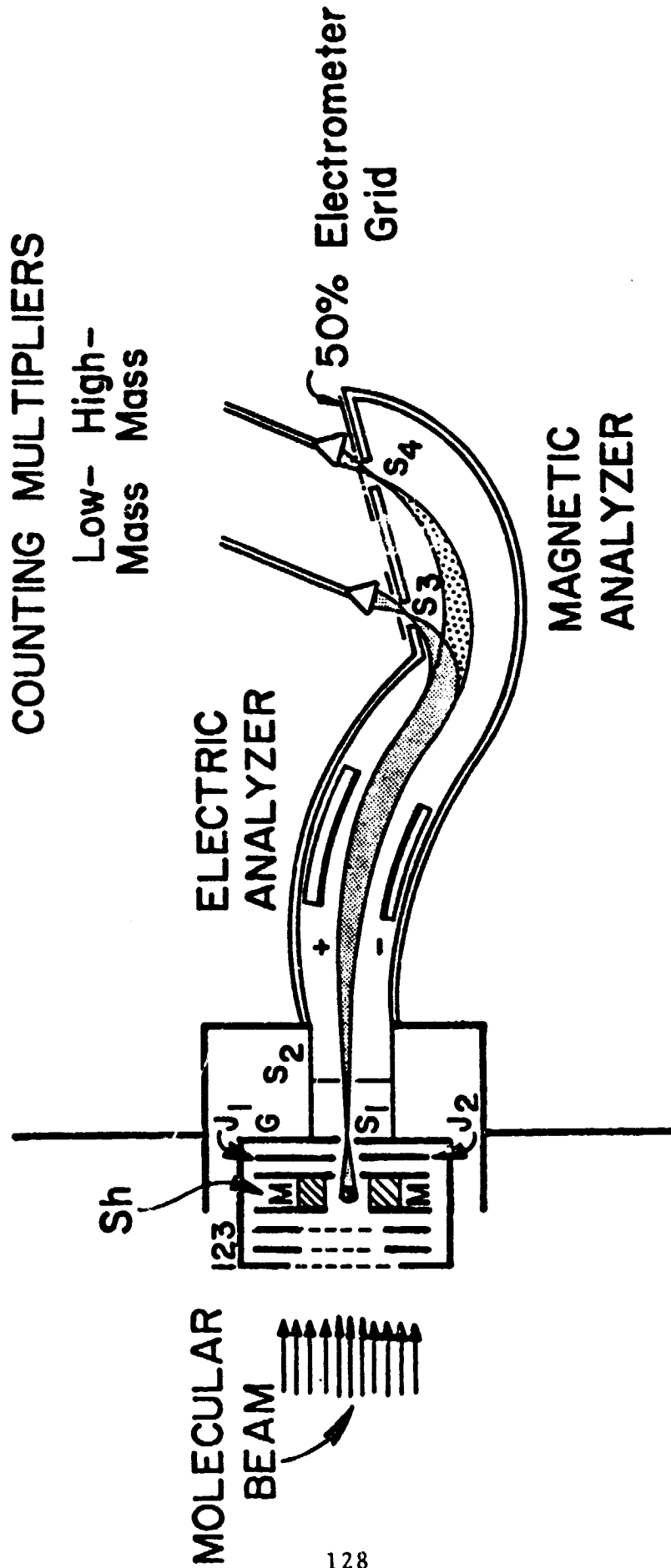
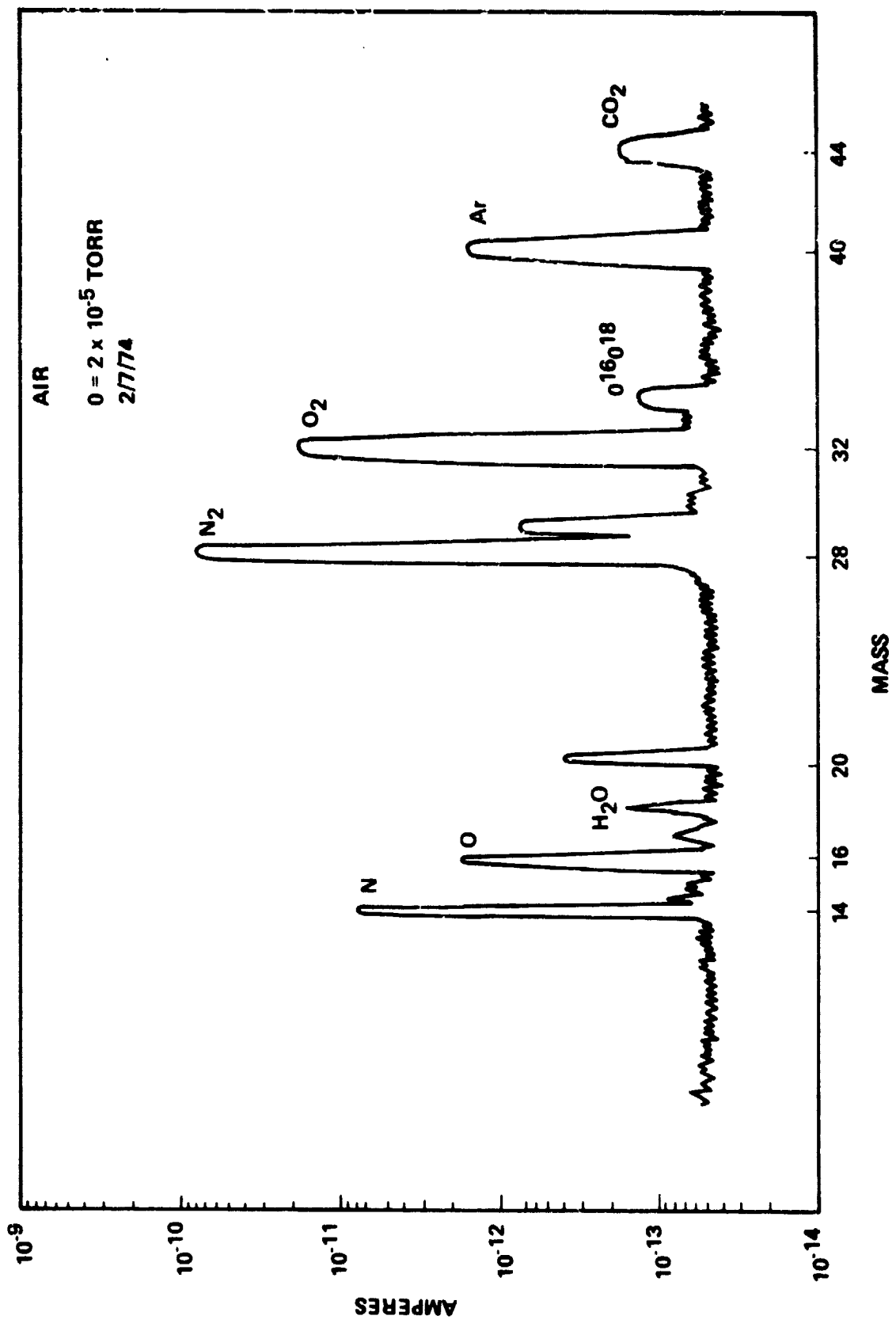


Fig. 1. Schematic Drawing of Atmosphere Explorer Open-Source Mass Spectrometer.



ATMOSPHERIC ELECTRIFICATION

May 1-2, 1978  
Huntsville, Alabama

H. W. Kasemir  
National Oceanic and Atmospheric Administration/ERL

COMMENTS BY HEINZ W. KASEMIR, NOAA/APCL, BOULDER, TO THE CONFERENCE OF NASA/MSFC IN HUNTSVILLE, ALABAMA, APRIL 10 AND 11, 1978.

Research areas of atmospheric electricity that could be explored from the shuttle or the tethered satellite: The generally accepted model of the atmospheric electric global circuit is that of a leaky spherical condenser (Israël, 1961) given in Fig. 1 (Mühleisen, 1968)

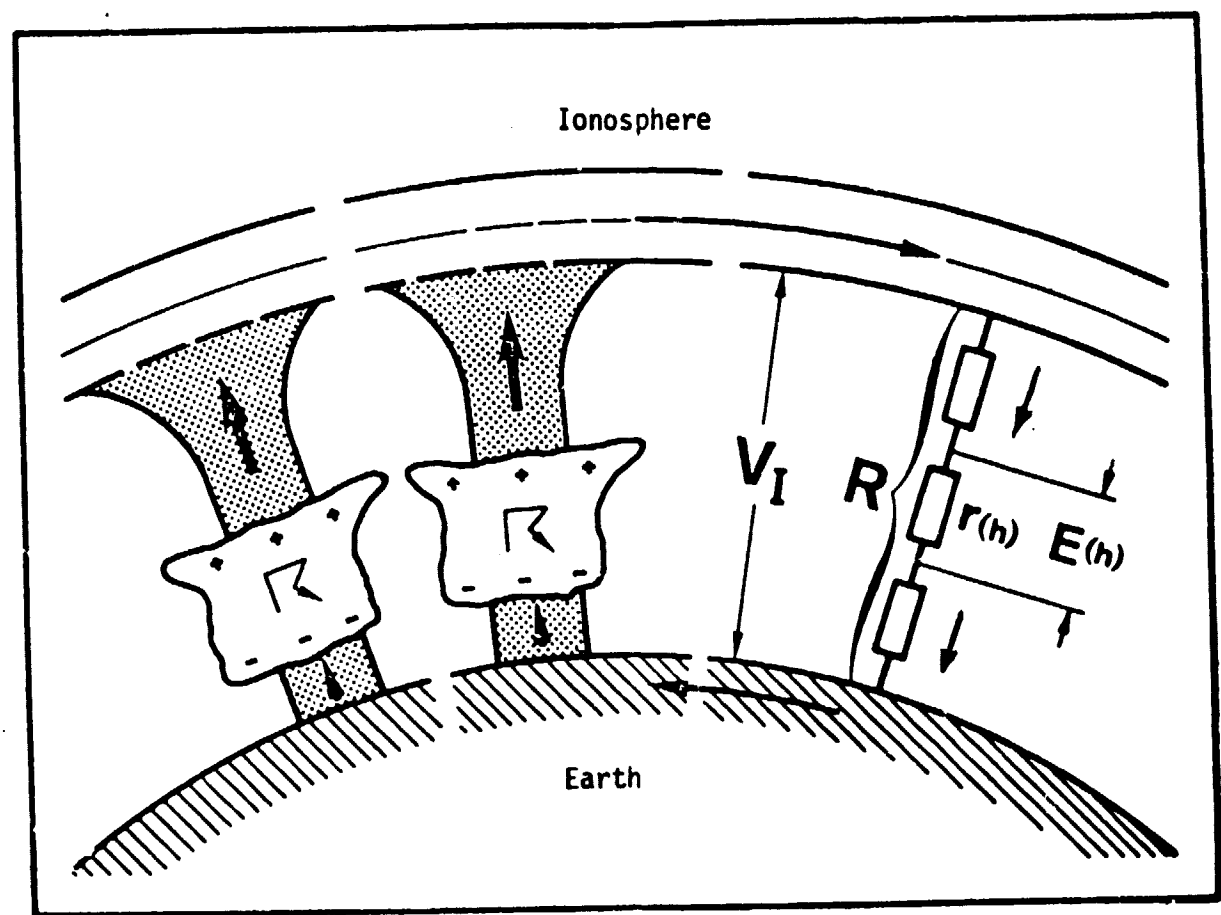


Fig. 1 Atmospheric electric global circuit. Current flow indicated by arrows.

The thunderstorms are assumed to be the generators of the atmospheric electric current flow. In the load circuit the current flows up from the positive charged top of the storm to the ionosphere, spreads out horizontally in the ionosphere around the globe, flows down to earth in the fair weather regions and returns through the earth to the negative charged base of the storm. Hereby, it is assumed that the ionosphere is

an equipotential layer with approximately infinite conductivity to insure horizontally homogeneous distribution of charge delivered by the thunderstorm.

The ionospheric part of the model is based on a physical misconception. To enforce a sideways spread of the charge or current--lets say at the lower boundary of the ionosphere--the ionosphere would have to be an extremely good insulator, not an extremely good conductor. Otherwise, the current will continue to flow radially outwards. It may even penetrate the ionosphere and enter interplanetary space. This has been repeatedly pointed out (Kasemir, 1971, Kasemir, 1977). The atmospheric electric current flow in the ionosphere is experimentally, as well as theoretically, an unexplored area of geophysics.

The shuttle and especially the tethered satellite would give the first opportunity to make in-situ measurements of the electric current of thunderstorms reaching the ionosphere, of the influence of the earth's magnetic field on the current flow and of a host of other related problems. Related problems are, for instance, the coupling of the electromagnetic field emitted by a lightning discharge to whistler mode propagation and monitoring the world lightning activity by ELF signals. (Schuman resonances).

The atmospheric electric current (air-earth current density) and the electric field (passive antenna) has been measured from a balloon up to 30 km altitude with a vertical dipole antenna of 20 or 50 m length suspended from the balloon (Kasemir, 1960). A lightweight low-power electrometer converts the input signal in the order of millivolts to frequency and modulates an ordinary meteorological radiosonde transmitter. The transmitted signal is then received and demodulated at the ground. This instrument and measuring principle may serve as a guideline for measuring the atmospheric electric field or current density in the ionosphere. Needless to say, conditions in the ionosphere are markedly different from those at 30 km altitude. It will be necessary to consider the tensor character of the conductivity, magnetically induced fields, the influence of other electro magnetic generators etc. However, very crude estimates of signal to noise ratio, measuring capabilities and so on indicate that measurements of thunderstorm currents reaching the ionosphere should be possible from a tethered satellite using the suspending wire as an antenna.

I would like to propose this briefly sketched research for in-depth assessment and consideration for conducting these measurements from the tethered satellite.

#### REFERENCES

Israël, H. "Atmosphärische Elektrizität II", Verlag Geest and Portig, Leipzig, 1961.

Fischer, H. J. and R. Mühleisen, "Das elektrische Feld in der freien Atmosphäre.", University Tübingen, Germany, 1968.

Kasemir, H. W., "The atmospheric electric ring current in the higher atmosphere", Pageoph 84, 76-88, 1971.

Kasemir, H. W., "Problems of the atmospheric electric circuit". Proceedings, International Conference on Atmospheric Electricity, 1977.

Kasemir, H. W. "A radiosonde for measuring the air-earth current density", USASRD Technical Report 2125, 1960.

Key problems of atmospheric electricity by TSS using tether as sensor:

- 1) Monitor world wide thunderstorm activity by measuring current injected into the lower ionosphere from each individual storm.
- 2) Prove or disprove that thunderstorms are the generators in the global atmospheric electric circuit.
- 3) Study of fair weather and thunderstorm currents in the ionosphere.

**CHEMICAL RELEASES**

**May 1-2, 1978  
Huntsville, Alabama**

**D. S. Evans  
National Oceanic and Atmospheric Administration/SEL**

**J. P. Heppner  
NASA/Goddard Space Flight Center**

COMMENTS CONCERNING THE VALUE OF PERFORMING  
CHEMICAL RELEASES FROM A TETHERED SATELLITE SYSTEM

During the past year or so a committee, sponsored by AMPS and under the chairmanship of J. Heppner, has been studying the use of chemicals released from orbiting satellites as a tool for understanding processes within the earth's magnetosphere, atmosphere and ionosphere. A large number of potential experiments were identified, ranging from introducing tracable material into the solar wind in order to study its transport to and within the magnetosphere, to injecting material into the outer magnetosphere to stimulate the precipitation of trapped charged particles, to the release of material at lower altitudes to create waves - both mechanical and electromagnetic. The work of this committee has led to the formal proposal for a Chemical Release Module, a facility class instrument to be carried into orbit by the shuttle.

Of interest so far as the tether satellite working group is concerned, is that between 1/3 and 1/2 of all the experiments suggested for the Chemical Release Module involved the release of materials at altitudes below 200 km and ranging down to 105 km. These requirements were recognized and the CRM is designed to have an orbit adjust capability so that its perigee could be made very low so that these experiments could be performed. It was recognized that such orbits are short lived and so it was anticipated that the low altitude releases would in general be made over a limited period of time at the end of the nominal 6 month lifetime of an individual CRM. This mode of operation introduces a certain degree of inflexibility. Most important, the decision to lower the CRM perigee to perform a low altitude release must be made hours, if not days, before the release itself. The decision is, in addition, more or less irrevokable. This means that it will be very difficult to perform releases under prespecified geophysical conditions (e.g., nearly or within an aurora). Indeed, some of the proposed low altitude experiments required that the final decision to perform the release be postponed to T - 1 min so as to insure that the proper geophysical conditions were present.

Thus the two great advantages of a tether system insofar as chemical releases are concerned are first, the ability to place a chemical release

canister at altitudes between 105 and 200 km without concern of orbit decay and second, re-introducing flexibility into the decision making leading to a release.

The objectives of chemical releases made below 200 km tend to group into two broad ranges. The first are releases made to "seed" the upper atmosphere and ionosphere with some readily identifiable material and then trace the motion of the chemical in time the purpose being to study naturally occurring transport processes. The second range of objectives covers perturbation experiments where the purpose is to significantly alter the natural situation and observe the reaction. It also turns out that as a general (but certainly not invariable) rule the "seeding" releases below 200 km have as their objectives the study of the dynamics of the upper neutral atmosphere, while the perturbation oriented releases are directed toward altering ionospheric parameters and perturbing the ionospheric current in order to infer things about other portions of the current system remote from the release point.

In all cases the two great virtues of the shuttle orbiter, its weight carrying ability and its velocity, are utilized to advantage in these experiments. For purposes of seeding, large amounts of material may be released at a modest rate with the orbital motion of the vehicle insuring that a vast area is seeded. The perturbation experiments generally involve the rapid release of large amounts of material depending upon the injection of energy and momentum into a small volume of space to produce the perturbation.

In the area of upper atmosphere dynamics, several problems have been identified which can be studied profitably with chemical releases. One such area is that of thermospheric winds. In the past such winds have been studied by using chemical releases from sounding rockets. These experiments have established the existence of neutral winds above 100 km and shown that they blow over a wide range in latitude from the arctic to the tropics. These winds in fact represent a major transport of mass and energy from one location to another at altitudes above 110 km or so. The sounding rocket experiments have also shown that the wind field has very significant gradients in the vertical direction as well as day-to-day variability.

One thing the sounding rocket technique is unable to study is the gradients in the wind field in the horizontal direction. Such measurements are fundamental to understanding the transport of neutral gas within the thermosphere. Moreover, horizontal gradients in the wind field are certain to exist because the major driving force, pressure gradients induced by energy input in the auroral zone, is itself highly structured in space. A 2-dimensional map of the wind field above 120 km could be obtained by releasing vapor trails of material that can be tracked optically from the ground. Candidate vapors could be Lithium or Sodium (because of their rather long ionization times and the fact that these atoms scatter solar photons) or vapors that undergo chemiluminescence such as tri-methyl-aluminum. The ejection of even modest amounts of material (10's of kg) can produce visible trails 1000's of km long which persist for many 10's of minutes, long enough for the neutral wind patterns to be measured over large areas.

A second area of interest involves atmospheric gravity waves. These large-scale internal atmospheric waves also involve significant transport of mass and energy within the thermosphere in the vertical direction as well as the horizontal. Thus far, such waves have been studied mainly through radar techniques where, at best, an array of ionosondes can study the behavior of "traveling ionospheric disturbances" which are believed associated with atmospheric gravity waves. Spatially periodic variations in neutral gas densities that have been observed on low altitude satellites have also been interpreted in terms of gravity waves.

It has been argued (not very forcibly by Colin Hines) that the presence of gravity waves in the thermosphere may influence the character of the middle atmosphere through the subtle process of altering the mesopause boundary conditions and modulating the flow of energy across that boundary.

The study of atmospheric gravity waves by means of chemical releases will proceed very similarly to the study of neutral winds (indeed a local measurement of neutral gas motion is not really sufficient to separate gravity waves and winds - if indeed the two physical concepts are mutually exclusive). For the study of gravity waves it would become important to observe the altitude variation in the release trail after it had come to

equilibrium with the ambient atmosphere and also vertical motions on the part of the release trail. In effect one is attempting to deposit a marker into the atmosphere, much as an oil slick on water, and inferring the motion of the supporting fluid by examining the motion of the marker.

In private conversations, Prof. A. Nier suggested still another potential use for materials release from a tether satellite. If the release gas is composed of a rare isotope ( $\text{He}^3$ ,  $\text{Ne}^{21}$ ,  $\text{A}^{38}$ , or  $\text{A}^{39}$ ), and tests made by sensitive mass spectrometers for the appearances of the isotope in other volumes of space, then inferences can be made concerning the transport of gases, particularly across horizontal boundaries such as the turbopause or tropopause. Prof. Nier cited, as an example of the feasibility of such experiments, the detection of  $\text{Ne}^{21}$  released from an installation in Idaho at stations far removed from the release site.

The common feature of these three sample experiments is that the release vapor is intended to act as a tracer the motion of which will expose the natural transport processes within the upper atmosphere. In contrast, the next sample experiment is designed to perturb the natural equilibrium of things and to observe the response.

One of the major problems in space physics concerns the nature of auroras, substorms, magnetospheric dynamics, and the 3-dimensional current system--all of which are undoubtedly manifestations of the same set of underlying processes. Perhaps the problem is formulated best in terms of the current system. It is known that a dissipative current (i.e.,  $\vec{J} \cdot \vec{E}$  locally greater than zero) flows in the auroral ionosphere. It is also known that dynamo mechanisms located near the earth such as neutral winds driving ionization normal to the magnetic field or atmospheric tides were totally incapable of explaining the origin of the dissipative current. The dynamo must be located within the outer magnetosphere remote from the earth's ionosphere and atmosphere.

While the nature of this dynamo is unknown (which is much of the problem) the currents that flow from the dynamo depend upon

- A. The nature of the dynamo.
- B. The nature of the electrical load which is the ionosphere.
- C. The nature of the charged particles which must be transported back and forth between the ionosphere and the dynamo so as to close the

current and keep the steady state divergence of the current everywhere zero.

While access to the dynamo region is difficult (one really doesn't know where it is), access to the ionospheric load portion of the circuit is straightforward through the use of the tether satellite. It would be very instructive to perturb this portion of the circuit in an effort to infer the properties of other portions of the circuit--much as one can infer the nature of a generator in a laboratory by studying its response to a varying electrical load.

Large gas releases into the ionosphere at 120-140 km from a high velocity tethered satellite represent a straightforward means of altering the electrical load presented by the ionosphere to the magnetospheric dynamo. There appear to be a variety of methods of doing this:

A. Releasing a gas which has a strong affinity for electrons, thus converted free electrons to negative ions and altering the local conductivities.

B. Releasing an alkali vapor which will quickly photoionize in sunlight, thus increasing the local electron-ion densities and the electrical conductivities.

C. Releasing a benign gas at high velocity and depending upon the following effects to produce the perturbation.

1. Heating of the ambient atmosphere because of the large injection of free energy which in turn raises local collision frequencies and thus conductivities.
2. The creation of a localized neutral wind giving the ionosphere in that volume a dynamo-like character and thus altering the electrical load.
3. The production of additional ionization by means of direct or indirect interactions between the fast release gas and the ambient neutral atmosphere and ionosphere.

No matter which method is used or what effect is dominant, it is certain that significant perturbations to the local ionosphere will occur. Observing the subsequent behavior of the current system will yield much insight into the dynamo and the ability of charged particles to provide currents between the dynamo and the load.

What I have tried to do is describe several sample experiments which could be profitably done using the shuttle/tether satellite system to release vapor into the upper atmosphere. In all cases the use of the shuttle/tether satellite provides two great advantages.

1. It allows the release canister to be placed in a stable "orbit" at altitudes below 200 km where many releases are proposed to be done.
2. It would allow the decision to make a release to be postponed to literally the last minute so that preselected geophysical conditions could be present at the time of release.

It might also be pointed out that the subsequent observational study of the releases--either their motion within the neutral atmosphere or their effect on currents--will largely be done from the ground beneath the releases or from rockets flown through the releases. The orbiter, because of its high velocity leading to a short observing time of the effects of the release, is in general a poor viewing platform.

## Thoughts About the CRM, Particularly as a Tool for Performing Large-Scale Perturbation Experiments

Broadly speaking, potential uses of the CRM divide themselves into two areas depending not upon techniques, but rather the underlying scientific motivation for performing the experiment. The first broad area is concerned with the "passive" study of naturally occurring physical processes within the near earth environment such as, for example, very high altitude wind patterns or plasma flow patterns within the magnetosphere. The second broad area concerns itself with artificially disrupting or perturbing the natural processes and observing how the neutral atmosphere-ionosphere-magnetosphere system reacts. Of course, at the very basic level there is the common scientific objective of understanding in a quantitative fashion the physics of the problems at hand.

It is of interest to note that the two primary virtues of the shuttle, its weight carrying ability and its high velocity in orbit, are used to advantage in pursuing both areas. In the case of studying the natural environment without external perturbations, large amounts of tracer material can be released within a large volume of space within a short time and, thus, allow the observation of the very large scale behavior of the system maintaining an adequate "signal to noise" so to speak. In the case of a perturbation experiment, the large masses of material that can be released combined with the very high release velocities allow very significant energy and momentum "injections" to be made within smaller, but selected volumes of space so as to perturb the natural behavior of the atmosphere-ionosphere-magnetosphere system.

Because this essay concerns itself primarily with the perturbation

aspects of material releases, it is instructive to point out the potential magnitude of such energy and momentum perturbations. With the maximum re-entry payload, the shuttle orbiter weighs some 80,000 kg. At orbital velocity at 300 km altitude, this body possesses some  $2.5 \times 10^{19}$  ergs of kinetic energy and about  $2.4 \times 10^{18}$  ergs of gravitational potential energy. For point of comparison, this amount of energy would support a major auroral display for about 1,000 sec. Furthermore, at times during the shuttle orbiter re-entry, the peak power dissipation may approach  $10^{17}$  ergs/sec which is equivalent to the total power of dissipation in a fairly intense global auroral display. Moreover, in the case of the shuttle re-entry, the energy is deposited into a localized volume of the upper atmosphere in contrast to the huge volumes associated with an auroral display.

While it may be possible to productively study the perturbations introduced into the upper atmosphere and ionosphere during a shuttle re-entry, it would be unduly restrictive in terms of magnitudes, time intervals, and spatial locations to depend solely upon re-entries. It is for this reason, among many others, that the chemical release facility possesses overwhelming advantages.

Technically, in order for released material to introduce a significant perturbation in either energy or momentum within a restricted volume must be in the form of a gas whose velocity can be quickly braked by an interaction with the ambient medium. At high altitudes ( $> \sim 300$  km) where collisional effects are negligible, this means that the gas must be ionized so that it is decelerated by an interaction with the geomagnetic field. At altitudes below  $\sim 200$  km, the released

gas will be rapidly decelerated through collisions with the ambient neutral atmosphere whether or not it is ionized. Should the released gas become ionized, either through direct collisional ionization or some more indirect process, the deceleration would be even more rapid.

In order to estimate the magnitude of the perturbation effects that may be expected from a gas release made at an altitude where the interaction is collisionally dominated, consider the following example: Argon gas is released at the rate of 10 kg/sec for 10 sec from a pressurized canister moving at 10 km/sec through the upper atmosphere between 110 km and 160 km. Table 1 shows some parameters of the unperturbed atmosphere over this altitude range.

The first question that may be asked concerns the volume of ambient atmosphere in which the release gas comes to rest. To first approximation, it is clear that the perturbed volume must approach a cylinder, the axis of which lays along the trajectory of the canister. It may also be argued that to first approximation the length of this cylinder corresponds closely to the path length over which gas was released. This argument is based upon the fact that the release gas should diffuse transverse to the canister trajectory about as fast as along it and thus in stopping move about as far transverse to the line of release as along it. This line of reasoning suggests that the length of the cylinder of perturbed atmosphere cannot be more than a few cylinder radii longer than the path length over which gas was released.

Thus the perturbed volume may be approximated by

$$V = \pi R^2 (L + 2R)$$

where  $L = 100$  km in this example and  $R$  remains an unknown. The unknown

may be removed by assuming that the release gas is "stopped" when the target gas (the ambient atmosphere) has been accelerated to 200 m/sec directed velocity, which is a fraction of the thermal speed of the unperturbed atmosphere. Conservation of momentum then requires that some 5,000 kg of ambient atmosphere be involved in stopping the total 100 kg of Argon that was released. From this, the appropriate volume of atmosphere as a function of altitude may be found and thus R calculated. Table 2 shows the results. It is clear that atmosphere over a considerable area is set into motion.

It is of interest to point out that the mass of 5,000 kg ambient atmosphere moving at 200 m/sec possesses a total kinetic energy of  $10^8$  J which is only 2% of the  $5 \times 10^9$  J of kinetic energy associated with the released gas. The remaining 98% is injected, as free energy, into the ambient atmosphere. This energy represents a very considerable energy perturbation as may be judged from Table 3 where the injected energy density is compared with the thermal energy density on the part of the ambient atmosphere prior to release. The manner in which this energy is dissipated can take many forms: heating of the ambient atmosphere, production of airglow and/or aurora through collisional excitation of the gas, or the creation of ionization which might occur through the "critical velocity" process. However, little theoretical analysis of this has been done and knowledge of how a high velocity gas release dissipates its energy may have to await the actual experiment.

There are many scientific studies for which such perturbations of the upper atmosphere would be a useful tool. A few among these are the study of upper atmosphere dynamics, the creation of gravity waves,

or even the point production of intrasonic waves in order to study their propagation characteristics. However, perhaps the most interesting experiment would be to use high velocity gas releases to perturb the high latitude current system which is driven largely by a magnetospheric dynamo mechanism.

In order to explore the possibilities of doing this, it is worthwhile to discuss some of the physics associated with the high latitude electrojet. For convenience, a Cartesian co-ordinate system with  $z$  being altitude along a presumed vertical geomagnetic field and  $x, y$  being the co-ordinates in the horizontal plane presumed normal to the magnetic field line is adopted for the following discussion. The magnetospheric dynamo communicates its influence to the ionosphere by means of magnetic field aligned currents and makes its influence felt by developing an electric field  $\vec{E}_m$  within the ionosphere. It is generally agreed that because of the high conductivity parallel to the magnetic field within the ionosphere ( $< 400$  km), this electric field is altitude independent in a co-ordinate system fixed to the earth. Thus  $\vec{E}_m$  may be assumed to depend only on the co-ordinates  $x$  and  $y$  but not  $z$

$$\vec{E}_m = \vec{E}_m(x, y). \quad (1)$$

However, the electric fields that determine the current flow in the ionosphere are those in the frame of reference stationary to the local medium which because of the influence of neutral winds transporting local ionization, need not be identical to the electric fields in the frame fixed to the earth. If there is a neutral wind field

$\vec{u}(x, y, z)$  then in order to compute current flow, an "effective electric field" must be defined.

$$\vec{E}_{\text{eff}}(x, y, z) = \vec{E}_m(x, y) + \vec{u}(x, y, z) \times \vec{B}. \quad (2)$$

This altitude dependent electric field may then be used to compute horizontal current intensities using the local Hall and Pedersen conductivities.

$$\vec{J}(x, y, z) = \sigma_p(x, y, z) [\vec{E}_m(x, y) + \vec{u}(x, y, z) \times \vec{B}] + \frac{\sigma_H(x, y, z)}{|\vec{B}|} [\vec{B} \times (\vec{E}_m(x, y) + \vec{u}(x, y, z) \times \vec{B})] \quad (3)$$

where  $\sigma_p$  and  $\sigma_H$  are the altitude dependent Pedersen and Hall conductivities, respectively.

The total horizontal current intensity may be obtained by integrating  $\vec{J}(x, y, z)$  over altitude -

$$\vec{J}_H = \int_0^{\infty} \vec{J}(x, y, z) dz \quad (4)$$

In the steady state, the current densities flowing along the field line are related to the details of the horizontal current system through the divergence equation

$$\frac{\partial J_z(x, y, z)}{\partial z} = -\frac{\partial J_x(x, y, z)}{\partial x} - \frac{\partial J_y(x, y, z)}{\partial y} \quad (5)$$

The net current density flowing along the field line between the ionosphere and magnetosphere is then

$$J_z(x, y) = \int_0^{\infty} \frac{\partial J_z(x, y, z)}{\partial z} dz \quad (6)$$

Within the auroral regions, the current  $J_z(x, y)$  is thought to be directly related to that process which accelerates electrons and produces aurora. It is important to note that in the course of perturbing the horizontal current system, the field aligned component is likely to be perturbed as well.

The reason for formally developing the equations which describe the ionospheric and field aligned current systems at high latitude is to expose those parameters which if perturbed would result in the change in the current system.

It is obvious that perturbing the two conductivities  $\sigma_H(x, y, z)$  and  $\sigma_p(x, y, z)$  will in turn change the current system. Because the classical expressions for conductivities are a direct function of local electron densities, it has often been proposed that chemical releases be designed to directly alter these densities. For example, a large scale Ba release made from the CRM, if done in sunlight, would greatly enhance the local electron densities. The same can be said for a high velocity neutral gas release should the "critical velocity" experiment work. It has also been proposed that a gas having a strong electron affinity be released so that negative ions are formed at the expense of free electrons. This will also impact local conductivities (particularly the Hall) and thus change the current system.

Still another, but more subtle, way of influencing the conductivities is to take advantage of the fact that the conductivities depend upon ion neutral collision frequencies and thus upon the local gas temperature. As described earlier, a high velocity neutral gas release injects a large amount of energy into the ambient upper atmosphere and, even if no

additional ionization is created, the local temperature increase in the ambient gas will change the local Hall and Pedersen conductivities as a result of increasing the collision frequencies.

Still a fourth method of perturbing the current system is through the dependence of the currents on the neutral wind fields  $\vec{u}(x, y, z)$ . This may be a particularly convenient way of affecting the currents within an auroral arc because the evidence is that the electric field of magnetospheric origin ( $\vec{E}_m(x, y)$ ) is of very low intensity in these regions.

As pointed out above, the release of a high velocity neutral gas cloud results in significant momentum injection into the neutral atmosphere. In fact, it was shown that volumes of neutral atmosphere 100 km long and  $\text{km}^2$  in cross section will be set in motion through collisions with the released gas. This represents the creation of a local neutral wind at altitudes where the conductivity is high enough that significant dynamo effects are expected. This leads to perturbations in the effective electric field  $\vec{E}(x, y, z)$  and thus the current system.

No matter what approach is used to perturb the current system, the general scenario is the same. The release must take place within the altitude range 110 km to 160 km where ion-neutral collision frequencies, and thus conductivities, are significant. The releases should occur at high latitudes where an electric field of magnetospheric origin is present and where particle precipitation produces a natural background of ionospheric conductivity. There would be great interest in performing the release along a trajectory which intersected an aurora.

This is one, among many, reasons for performing the release at night.

The amounts of release material would range from a minimum of 100 kg up to the maximum permitted by the CRM. There may be a desire to release material from several nearby containers simultaneously so as to increase the cross section of atmosphere that is perturbed.

The supporting observations would by and large have to be done from the ground, possibly together with sounding rockets. These observations would be in the main optical (to look for airglow or changes in aurora associated with the release), radar (to search for ionization perturbations and to detect neutral winds), and magnetic (to look for changes in the current system).

TABLE 1

Altitude	Number density/cm <sup>3</sup>	Mass density/gm/cm <sup>3</sup>	Thermal mean free path cm
110 km	$2.25 \times 10^{12}$	$1 \times 10^{-10}$	111
120	$5.5 \times 10^{11}$	$2.5 \times 10^{-11}$	455
140	$8.9 \times 10^{10}$	$4.4 \times 10^{-12}$	2800
160	$3.4 \times 10^{10}$	$1.4 \times 10^{-12}$	7300

TABLE 2

Altitude	Volume of atmosphere perturbed	Length of cylinder (km)	Radius (m)
110 km	$5 \times 10^{16}$ cm <sup>3</sup>	100.8	400 m
120 km	$2 \times 10^{17}$ cm <sup>3</sup>	101.6	800 m
140 km	$1.1 \times 10^{18}$ cm <sup>3</sup>	103.7	1840 m
160 km	$3.6 \times 10^{18}$ cm <sup>3</sup>	106.6	3280 m

TABLE 3

Altitude	Ambient Energy Density of ergs/cm <sup>2</sup>	Energy Density Introduced by Gas	Ratio
110 km	$1.2 \times 10^{-1}$	$9.8 \times 10^{-1}$	8.24
120 km	$4.04 \times 10^{-2}$	$2.45 \times 10^{-1}$	6.06
140 km	$1.28 \times 10^{-2}$	$4.45 \times 10^{-2}$	3.49
160 km	$6.3 \times 10^{-3}$	$1.36 \times 10^{-2}$	2.16

N81-29489

D10

**AERODYNAMIC EFFECTS**

May 1-2, 1978  
Huntsville, Alabama

G. R. Karr  
The University of Alabama in Huntsville

## Contribution to Workshop on Uses of a Tethered Satellite System

### Atmospheric Interaction with Tethered Satellites

Gerald R. Karr, Associate Research Professor of Mechanical Engineering,  
The University of Alabama in Huntsville, Huntsville, AL 35807

#### INTRODUCTION

The tethered satellite concept provides an ideal platform for the study of the interaction of the atmosphere with satellites of various shapes and surfaces under a wide range of flow conditions. From experiments which would measure the drag, lift, and torque acting on the tethered satellite, important information could be obtained which would have application to (1) satellite lifetime prediction, (2) determination of properties of the upper atmosphere, and (3) scientific information on the interaction of high speed molecules with surfaces (the gas surface interaction). These experiments using the tethered satellite concept are ones that have not been performed in the laboratory due to the extreme difficulty of duplicating the flow properties characteristic of that experienced by satellites in near earth orbit.

#### EXPERIMENTAL OBJECTIVES

The basic objective of the proposed aerodynamic studies using the tethered satellite concept is to obtain drag, lift, and torque data as a function of the following variables:

- (1) angle of attack with respect to flow
- (2) body shape (sphere, cone, cylinder, flat plate, etc.)
- (3) surface properties (composition, temperature, roughness, etc.)
- (4) flow properties (molecular composition, velocity, temperature, mean free path)

The tethered satellite concept is capable of providing a considerable range in the variables of interest in this proposed experiment. Tethered satellites of various external shapes could readily be oriented at various angles of attack and measurements made on the forces and torques acting on the satellite due to the interaction with the high speed flow. Surface material, temperature, and roughness could be controlled and adjusted over a wide range of values with relative ease. The capability of the tethered concept which has particular application and benefit to this experiment is the wide range of flow conditions which can be obtained.

Assuming that a one meter size tethered satellite can be flown at an altitude range of from 100 to 200 Km, the following range in flow properties would be experienced by the satellite as a function of altitude.

Altitude Km	Temperature oK	Pressure torr	Density Kg/m <sup>3</sup>	Molecular Weight	Mean Free Path m	Mean Random Molecular Velocity m/s
100	195	$2.4 \times 10^{-4}$	$5.60 \times 10^{-7}$	28.4	.142	382
150	635	$3.4 \times 10^{-6}$	$2.1 \times 10^{-9}$	24.10	33	747
200	855	$6.4 \times 10^{-7}$	$2.5 \times 10^{-10}$	21.30	240	922

The above table shows that the flow conditions vary over a wide range over the altitude capability of the tethered satellite. For example, the Knudsen number (mean free path/characteristic length) for a 1 meter size is seen to be of order  $10^2$  at the high altitude down to a  $10^{-1}$  at the low altitude. This capability would allow testing in free molecule flow at high altitudes and testing well into the transition flow region at low altitudes. Consider also the range in speed ratio (satellite velocity/mean random molecular velocity)

for a satellite attached to the shuttle which is at a velocity of 8000 m/s. The speed ratio is 10 at the high altitude and near 20 at the low altitude. The molecular composition is seen to vary in terms of average molecular weight by almost a factor of 1.5. The range in flow conditions that the tethered system can provide coupled with the capability to vary the satellite shape, angle of attack, and surface properties shows a tremendous potential for contribution to the science of rarefied gas dynamics.

#### POTENTIAL BENEFIT OF EXPERIMENTAL RESULTS

The information gained from the proposed experiment would have application to (1) satellite orbit prediction, (2) atmospheric density and wind determination, and (3) advancement of the science of rarefied gas dynamics.

The accurate prediction of the perturbation of satellite orbits has long been hampered by the lack of accurate information on the interaction of the satellite with the upper atmosphere. Very long range predictions require a more accurate prediction of the aerodynamics than is now available. The effect of drag and lift on the satellite orbit are well known but accurate prediction of these forces for a given satellite has not been possible because of the lack of information of the type that can be gained in the proposed experiment. The NASA Skylab orbit decay is a clear example of a need for more accurate aerodynamic information than has been used in the past. With better knowledge of the aerodynamic drag and lift properties, the orbit decay of Skylab could likely be delayed considerably.

Upper atmospheric density determination has been largely performed from the reduction of orbit decay data. Thus, errors in aerodynamic information is also transferred to the density values obtained. These errors are also found in the determination of upper atmospheric wind and wave motion as deduced from the orbit perturbation of a satellite. The experiments proposed here would enable the accurate determination of density and winds by reducing the uncertainty in the aerodynamic properties.

The contribution that these experiments would have to the field of rarefied gas dynamics is considerable since very little accurate data now exists. Laboratories have been unable to simulate the low density, high velocity flows characteristic of satellite motion in the upper atmosphere. Considerable work has been done in computer simulation but further advances need experimental verification and test. The experiments proposed here would provide the required information which could then open the way for such advances as satellite orbit control using aerodynamic lift and drag.

001-11  
P103

LETTER

May 1-2, 1978  
Huntsville, Alabama

R. E. Smith  
NASA/Marshall Space Flight Center



If you need any more data, please give me a call at 205-453-3101.

Sincerely,

  
Robert E. Smith  
Atmospheric Sciences Division  
Space Sciences Laboratory

### III. ELECTRODYNAMICS AND PLASMA STUDIES

#### SUMMARY

David L. Reasoner  
NASA/Marshall Space Flight Center

This session was devoted to discussions of uses of a Tethered Satellite System for studies of electrodynamic and plasma processes in the ionosphere and lower thermosphere. Professor Peter M. Banks and Dr. Roger Williamson of Utah State University addressed the topics of electrodynamic studies using an insulated, conducting tether and some initial experiments. Dr. Mario Grossi of the Smithsonian Astrophysical Observatory discussed the interactions of a conducting tether satellite system with the ionosphere and magnetic field. Noble Stone of NASA/MSFC spoke on the uses of a tether system to study plasma flow interactions and wake and sheath structures of large bodies in the ionosphere. Dr. David S. Evans of NOAA/SEL discussed using the tether for chemical releases at low altitudes. Additionally, valuable comments were contributed by members of the audience, and Dr. L. H. Brace of NASA/GSFC contributed a summary on using a tether satellite for measurements of the dynamic behavior of the lower thermosphere and ionosphere. The following is a brief summary of the topics discussed, and for a more complete discussion, the reader is referred to the contributions of the individual authors and speakers which are attached to this report.

It should be emphasized that for most of these experiments a tethered satellite is not simply an alternate method of performing an experiment; rather it is the only method within reasonable technological bounds.

Conducting Tether Electrodynamics Studies - The deployment of an insulating, conducting tether with lengths of 10-100 km would represent a large-scale system which would react strongly with the magneto-ionic medium of the ionosphere and make it possible to conduct a variety of exciting scientific experiments. The motion of the conducting tether through the magnetic field will produce a  $\vec{V} \times \vec{B}$  potential of up to 20 kilovolts (for a 100 km tether). This dynamo, in conjunction with a voltage monitor and current controller on the Shuttle provides a means of performing a large number of experiments. A fundamental experiment would be to determine the current-voltage characteristics of a body

in the ionospheric plasma, particularly that of a large body at high potentials. The large dynamo potentials generated may lead to plasma wave generation, non-linear current voltage characteristics, and local particle acceleration especially if the tether is aligned along a magnetic field line. The dynamo potentials can also be used to furnish power to the Shuttle for battery charging or the E.M.F. can be used directly to power a particle accelerator with high efficiency.

The tether system can be used to drive currents along magnetic field lines and investigate current-driven instabilities which are thought to be important in the auroral ionosphere. Furthermore, the tether dynamo and associated current system can also be used as a simulation of certain planetary electrodynamic phenomena, particularly the interaction of Io and Almathea with the Jovian magnetosphere.

A conducting tether can also serve as an antenna, both for the generation and reception of electromagnetic waves. Long tethers up to 100 km can be used for the generation of waves especially at the lower ULF frequencies ( $\sim 1$  Hz) where shorter conventional boom-type antennas would not be suitable. The antenna current could be produced either by conventional circuitry or by modulation of the  $\vec{V} \times \vec{B}$  dynamo driven current in the tether. In this latter scheme the orbiter kinetic energy can be converted directly to wave energy. As a passive antenna, the long conducting tether would offer an extremely sensitive detector for ionospheric electric fields, especially low-latitude weak electric fields such as those associated with the  $S_q$  current system dynamo which so far have eluded direct measurement.

Plasma Flow Interactions - A large class of problems of ionospheric and astrophysical interest involve the interactions of a body with a flowing plasma. Many of these are large body problems, that is the dimension of the body is large compared to the Debye length and particle gyroradii in the plasma. These problems cannot be studied effectively in laboratory plasma chambers and are difficult to attack theoretically. The tether system can offer an excellent opportunity to accomplish these sorts of studies in the ionosphere, wherein the test body (typically a balloon  $\sim 100$  meters in diameter) can be tethered to the Shuttle and thus avoid the station-keeping problem due to the high differential drag. A free-flying test body would

require a prohibitive amount of fuel for station-keeping. With such a large tethered body in place, the plasma flow interactions can be studied with a diagnostics package on a free-flyer. Furthermore, with the test body attached to the orbiter, it would be possible to control its electric potential in a straight forward manner, and thus modify the body-plasma interactions. The tether line can also carry at an intermediate point a small diagnostics package to monitor the ambient medium well-removed from the perturbing effects of both the Shuttle and the test body.

Chemical Releases - The orbiter kinetic energy is about  $2 \times 10^{19}$  ergs which is an amount of energy sufficient to supply the global aurora for  $\sim 1000$  sec. The tether system can be used to release a fraction of the orbiter kinetic energy into the lower ionosphere in a controlled manner and produce significant perturbations. For example, 100 kg of argon released at 140 km altitude represents a power level of  $3 \times 10^6$  watts which must be absorbed by the surrounding medium. The released energy density is 2-10 times the ambient energy density, and it is not known how this energy would be absorbed and/or converted in the ionosphere. The ionospheric conductivity can be modified by the release of appropriate gases, and in fact the conductivity can be either reduced or increased by choice of released material. The study of auroral dynamics and current systems can be greatly facilitated by such an ionospheric modification technique. The use of a tethered satellite system for chemical releases offers a unique opportunity to deliver gas releases at altitudes less than 200 km with large horizontal dispersions and at precisely controlled times. Furthermore, the orbiter kinetic energy can be delivered directly to the ionosphere. Only a tethered satellite system can accomplish all of these objectives simultaneously.

Lower Thermosphere and Ionosphere Dynamics - A tethered satellite permits resolution of the global dynamic behavior of the ionosphere and thermosphere between  $\sim 110$  and 200 km. Free-flying satellites cannot be maintained in circular orbits in this region. This region is important because it is the site of absorption and dissipation of tidal waves propagating upward from the lower atmosphere. Therefore, measurements permit the dynamic processes

occurring below to be examined, and their effect upon the lower ionosphere to be studied. This region is also the site of absorption of the solar ultraviolet radiation, the prime source of heating of the thermosphere and ionosphere. Also, in the auroral regions it is the altitude range where most of the energy of auroral primaries is deposited and the energy of acoustic gravity waves generated in the aurora is dissipated. Initial experiments would involve a single instrumented tethered satellite, and advanced experiments measuring horizontal and vertical gradients can be done with multiple packages on a single tether.

## The Electrodynamic Tether

by

F. Roger Williamson, P.M. Banks and K. Oyama  
Center for Research in Aeronomy  
Utah State University  
Logan, UT 84322

In our first report, "The Tethered Balloon Current Generator - A Space Shuttle-Tethered Subsatellite for Plasma Studies and Power Generation" [Williamson and Banks, 1976] (hereinafter called the TBCG report), we discussed the feasibility of deploying an insulated, conducting tether with a large diameter, conducting surface balloon attached. At the time this study was undertaken, it was not obvious that a tether system was technically feasible nor was it apparent that substantial current flow could be produced with a large conducting balloon. In the TBCG report we found that both of these technical problems were solvable, and we have since studied in somewhat more detail the scientific and technological results which can be expected from a Shuttle Electrodynamic Tether System (SETS).

The scientific problems to which the Electrodynamic Tether can be applied were partially treated in the TBCG report. We have since considered several more areas of scientific investigation which are suitable for study with an Electrodynamic Tether and have formulated recommendations for an evolutionary development program which ties together many of the studies.

The essential component of an Electrodynamic Tether System is an insulated, conducting tether. A voltage monitor and a current controller then provide a means of performing the majority of the measurements and experiments involved in the scientific investigations. The scientific areas of study which have been identified include the following:

- active experiments with SETS/TBCG produced field-aligned currents
- potential difference measurements between widely spaced (10-100 km) regions in the ionosphere
- plasma disturbance generation and propagation
- wave injection studies in the VLF to ULF (micropulsation) region
- current-voltage characteristic of a spherical satellite
- simulation of the phenomena produced by Io, one of the moons of Jupiter
- chemical release perturbations of ionospheric conductivity

Technological features of the Electrodynamics Tether which are of interest and which may contribute to the capacity for conducting scientific studies from the Shuttle Orbiter include:

- electrical power generation using the  $\vec{V} \times \vec{B}$  generated emf in the conducting tether
- self-powered sub-LF transmitters by modulating the tether current
- self-powered electron or ion accelerators with electrical power supplied directly from the tether
- charge neutralization of the Orbiter during electron accelerator operations

The scientific advances to be expected from the use of an Electrodynamic Tether are attributable to several features of the system. First of all, the size of the system (the long tether) is larger by one or two orders of magnitude than any previous space probe and relatively larger yet than laboratory based systems. Secondly, the large amounts of electrical power which may be generated with the system may provide the practical means to carry out some experiments. Finally, it will be possible to do controlled, active experiments with field-aligned currents over relatively large regions of the ionosphere. The large dimensions of the SETS, the support systems required and the coordinated measurements carried out with other

instruments can only be performed using a Space Transportation System such as the Space Shuttle.

Both scientifically and technologically, a SETS is feasible. Two phase B studies supported by MSFC will be completed in February of 1979. These studies and the work on tether dynamics previously performed at MSFC and at SAO all indicate that a Tethered Subsatellite System can be built and operated from a Shuttle Orbiter. The scientific and techno-

ical benefits from operating an Electrodynamic Tether system are also clearly established. Because the SETS is so greatly different from any other system which has previously flown, it should not be surprising if many of the areas of investigation are not yet well defined nor if some of the most interesting problems must await flight experience. On the other hand, all of the early SETS missions can easily be devoted to studying well-defined problems with certain valuable scientific results.

#### Potential difference/electric field measurements

The simplest measurement which can be made with a SETS is the potential difference between two widely spaced regions in the ionosphere. One of the outstanding problems in space physics is the nature of ionospheric electric fields. Our knowledge at present is limited largely to measurements of electric fields with satellite probes of a few tens of meters in size and to measurements over larger regions using chemical releases but with limitations in ionospheric conditions and location and which themselves produce substantial perturbations in the ionosphere. With an Electrodynamic Tether we can directly measure potential differences in the ionosphere over distances of 10-100 km (or possibly greater distances) instead of measuring the electric field in a small region and then inferring potential drops. A large amount of data exists on the electric field

morphology of the ionosphere and many of the problems and questions which have arisen as a result of electric field studies could be answered with potential difference measurements as obtained with an Electrodynamic Tether.

The very large separation between the ends of the Electrodynamic Tether should permit measurements with a much greater sensitivity than previously attained for observing average electric fields. The physical size of the Orbiter is relatively small compared to the probe separation and induces relatively little uncertainty in the measurement. The disturbance produced by the presence of the probe is also relatively small since it depends only slightly on the size of the probe and not at all on the separation between the ends of the tether. For the majority of the time during a mission, the two ends of the tether will be on widely spaced field lines. Depending upon the particular orbit and the position of the end of the tether with respect to the Orbiter, the two ends of the tether will occasionally be on the same field line and the potential drop parallel to  $\vec{B}$  over distances of 10-100 km can be measured. The electric field parallel to  $\vec{B}$  is a problem of fundamental importance in space physics, and considerable theoretical and experimental effort is applied to this problem.

Ordinarily, the voltage observed between the two ends of the tether will be produced by the  $\vec{V} \times \vec{B}$  generated emf and may be as large as 200 mV/m in an equatorial orbit. The  $\vec{V} \times \vec{B}$  emf produces a voltage given by  $\Delta V_B = \vec{V}_S \times \vec{B} \cdot \vec{L}$  where  $\vec{V}_S$  is the spacecraft velocity,  $\vec{B}$  is the magnetic field and  $\vec{L}$  is the tether vector (between the two electrical ends of the tether). The values of  $\vec{V}_S$ ,  $\vec{B}$  and  $\vec{L}$  will be well known during a mission, and within the error limits in these quantities, we can predict the contribution to  $\Delta V$ . The difference between the calculated  $\Delta V_B$  and the

measured  $\Delta V$  is attributable to ionospheric electric fields which contribute an additional term to the potential difference  $\Delta V_E = \vec{E} \cdot \vec{L}$ , where  $\vec{E}$  is the ionospheric electric field.

The contribution from  $\vec{V} \times \vec{B}$  for the idealized case of a circular orbit and a centered dipole magnetic field is shown in Figure 1. Although a more realistic calculation will show larger variations throughout an orbit, the  $V \times B$  emf is not very rapidly changing and small scale changes in the ionospheric electric field should be easily observable as is known from satellite electric field measurements.

For a 10 km conducting tether the  $\vec{V} \times \vec{B}$  generated potential may be 2000 volts. Very large ionospheric electric fields may, on occasion, increase this potential substantially ( $\sim 5000$  volts). A 100 km tether increases the potential proportionately to 20,000 volts.

#### I-V Characteristic of a spherical satellite

The early Electrodynamic Tether missions will most likely not have a large balloon on the far end but rather a small sphere one meter in diameter with a conducting surface. If a means of controlling the current flow in the tether is available, several interesting studies can be performed including the determination of the current-voltage or I-V characteristic of a small, spherical satellite. Linson (1969) has reviewed the literature on the subject and also proposed a theory for the I-V characteristic. The various theories as compared by Linson are shown in Figure 2.

On a 10 km tether with 1000-2000 volts available for measuring the I-V characteristic of a small, spherical satellite attached to the tether, it is possible to perform a remarkably ideal measurement of the characteristic for comparison with the various theories. The ionospheric plasma conditions available for investigating the I-V characteristic vary over several orders

of magnitude in electron density and perhaps a factor of two in temperature. It would be a bit surprising if the I-V measurements simply pointed to one of the theories. It is more likely that the characteristic will be less regular than the theories suggest.

Beyond the simple determination of an I-V characteristic, several important problems exist which depend on the results of this measurement. The uncertainties in the nature of the I-V characteristic are related in part to the cross-field mobility of electrons. The generation of plasma instabilities and plasma turbulence in the neighborhood of the satellite will undoubtedly be dependent on the current; very little is known about the disturbances likely to be produced by the current and their relationship to the collection of electrons.

If currents at least as large as the thermal electron flux,  $j_e = ne \left[ \frac{kT}{2m_e} \right]^{1/2}$  can be collected by the tethered subsatellite, substantial amounts of electrical power can be generated with an Electrodynamic Tether where the potential available is determined by  $\vec{V} \times \vec{B} \cdot \vec{L}$ . If the current can be increased an order of magnitude above the thermal electron limit as shown in Figure 2, obvious benefits from increased electrical power would result.

By modulating the current in the tether, it may be possible to utilize the Electrodynamic Tether as a self-powered transmitter and antenna at frequencies in the sub-LF range. The I-V characteristic may be highly time dependent which would affect the capability for self-excited wave injection studies.

If the Orbiter end of the tether is attached directly to the cathode of an electron accelerator, no Orbiter power would be required for operation of the electron accelerator other than for control purposes. The amount of beam current available depends in part on the I-V characteristic of the tethered sub-satellite. The long, conducting tether behaves like a long

transmission line, however, and for times up to the millisecond range may supply substantially larger currents than indicated by the I-V characteristic. The tether is highly charged when the current is small and large current pulses may be available for short times with a consequent impact on the very serious problem of charge neutralization of electron accelerators operated from the Space Shuttle Orbiter.

The early SETS missions will establish the capabilities of the system for performing potential difference measurements and driving currents in the ionosphere. Most of the scientific and applications features of the Electrodynamic Tether, which we have discussed here and in the TBCG report, can be developed in future missions with a high degree of confidence once the basic capabilities are determined in the early missions.

In another report, "An Electrodynamic Tether Experiment Program" (Oyama, et. al, 1978), we have described in somewhat more detail several specific studies which can be performed during later missions once the capabilities of the SETS as described above are known. In most of the areas of scientific or applications interest we can define in relatively great detail geophysical measurements programs and active, controlled experiments which can be performed with a SETS. There already exists a large number of individual studies with well-defined objectives which are suitable for the SETS.

#### Technical Concerns

For those not directly involved with the Tethered Satellite System (TSS) studies, the feasibility of deploying such a long tether is a difficult one to accept. Nonetheless, after many years of study, it is quite apparent that the tether is practical and plans for implementing the TSS are progressing very favorably. A major effort has been devoted to establishing the dynamics of a TSS and attention is now turning to

less serious problems but ones which must be resolved before a SETS is deployed.

### Electrodynamic Drag

In 1975 we sent to MSFC a request for them to run the tether dynamics program with an additional force on the tether produced by electrodynamic drag when the tether carried a current of 1 amp and also of 10 amps. The analysis by MSFC showed that only very small changes in the tether dynamics are produced at the 1 amp level. At 10 amps the displacement of the tether from equilibrium is larger but still not unstable. In any case the electrodynamic force depends directly on the magnitude of the current flowing in the tether and is zero when the current is turned off. In some advanced experiments it may be possible to drive tether currents as large as 10 amperes. In the early missions the upper limit on tether current is closer to 1 ampere. The first SETS mission will probably carry a conducting sphere of 1 meter diameter which can collect a thermal electron current at 400 km altitude of approximately 1 mA. An order of magnitude enhancement in the current is still only 0.01 ampere which would be difficult to detect in tether dynamic effects.

The tension in a 10 km tether with a mass of 295 kg and a subsatellite mass of 200 kg is about 14 newtons maximum. The tether forces produced by electrodynamic drag,  $\vec{F} = i\vec{L} \times \vec{B}$ , can be simply calculated if the electrical power produced by the tether is equated to the power derived from the electrodynamic drag on the tether  $P = \vec{F} \cdot \vec{V}_s$ , where the spacecraft speed  $V_s$  is known to be about 7.7 km/sec at 400 km altitude. In the early missions, the maximum electrical power which can be extracted is about 2000 volts X 0.01 ampere or  $P \sim 20$  watts. The electrodynamic drag in this case is  $F = P/V_s \sim 0.003$  newtons or 0.02% of the tension in the tether produced by the gravity gradient.

At some future time we expect to increase the electrical power generating capability of the system into the 1-10 kw range by increasing the size of the collector to perhaps 100 meter diameter and/or increasing the length of the tether beyond 10 km to some 100 km. At the 1 kw power level the drag is 0.13 newtons, and at 10 kw it is 1.3 newtons-- still less than the 14 newton tether tension. Since the tether tension is proportional to both the mass of the system and the length of the tether, if a greater tether tension is needed to offset the electrodynamic force at higher power levels, then the size of the system can be increased accordingly. In any case, the electrodynamic force only exists when the SETS is producing electrical power and the power can always be turned off if necessary. For any manner in which the electrical power is utilized, it will be necessary to emit an electron current from the Orbiter which is equal to the current in the tether. A one ampere tether current requires a one ampere electron beam. Turning off the electron beam turns off the tether current and turns off the electrodynamic drag.

Another reference point for comparison with the electrodynamic drag force is the amount of atmospheric drag on a 30 meter diameter balloon at 400 km altitude. In the TBCG report we find atmospheric drag is on the order of 0.5 newtons. Atmospheric drag on a 10 km tether is less than this value and both values are much less than the tether tension which produces a restoring force if the tether is displaced from the equilibrium established by the gravity gradient.

#### Dielectric Requirements

If the tether current is to be controlled, as required by all of the investigations we have discussed, the tether must be covered with a high quality insulating material which has an electrical breakdown point greater than the potential difference expected between the two ends of

the tether, and the insulation must also limit the leakage current to the conductor to less than some level which permits the investigation to be performed. We have described the current collected by a bare wire in Morrison, et. al, 1978.

The dielectric leakage per unit length at position  $\ell$  along the tether is given by  $\frac{dI}{d\ell} = \frac{\pi \ell D}{\rho t} E$ , where  $D$  is the conductor diameter,  $\rho$  is the dielectric resistivity,  $t$  is the dielectric thickness and  $E$  is the  $\vec{V} \times \vec{B}$  generated emf. Integrating the current along the tether gives the current at position  $\ell$  which is  $I = \frac{\pi E \ell^2}{2} \cdot \frac{D}{\rho t}$ .  $E$  has a maximum value of about 0.2 v/m. Assuming that  $t$  is determined by the electrical breakdown requirement, then  $t$  for a 10 km tether coated with teflon is about 0.1 millimeter, and  $I$  is less than  $10^{-9}$  A when  $D$  is 1 mm.

The insulation requirement is much more severe for a 100 km tether where the dielectric must not breakdown at potentials exceeding 20,000 volts. Since the leakage current is proportioned to  $\ell^2$ , the dielectric resistivity must also be very good if controlled current experiments are to be successful at the same current levels as for a 10 km tether.

The tether will possibly encounter micrometeorites which penetrate the insulation. In addition, pinholes in the insulation are very likely to occur during fabrication and handling. So long as the total leakage current through the insulation remains at a sufficiently low level, the SETS studies will not be affected. In the early SETS missions the maximum tolerable leakage current is about  $10^{-9}$  A.

#### SETS Development

The first TSS mission will probably be a 100 km tether deployed below the Orbiter with a subsatellite containing a magnetometer for mapping the earth's geomagnetic field. Following this demonstration flight, a first SETS mission could be performed using a conducting tether insulated with teflon and deployed above the Orbiter with a small conducting

sphere attached to the end. The primary instrumentation in the spherical subsatellite would be a current controller and a voltage monitor. Support instrumentation in the Orbiter bay would be required for emitting electrons from the Orbiter end of the tether and for observing the electrical potential of the Orbiter relative to the local plasma. Instrumentation of this type will be flown on the OFT-4 mission. Many other instruments, located either in the Orbiter bay or in the tethered sphere, would be useful during the first mission and could be coordinated with the prime experiment depending upon the available resources.

In later missions, additional instrumentation could be added to the basic SETS including transmitters, receivers, electrical power storage systems, a large diameter conductor (balloon), plasma diagnostics, particle measurements and a maneuverable subsatellite for observing phenomena far from the end of the tether but on the same magnetic field line.

The first phase of a SETS development is relatively straightforward given the existence of the TSS and the anticipated results from the Vehicle Charging and Potential (VCAP) experiment on the OFT-4 mission.

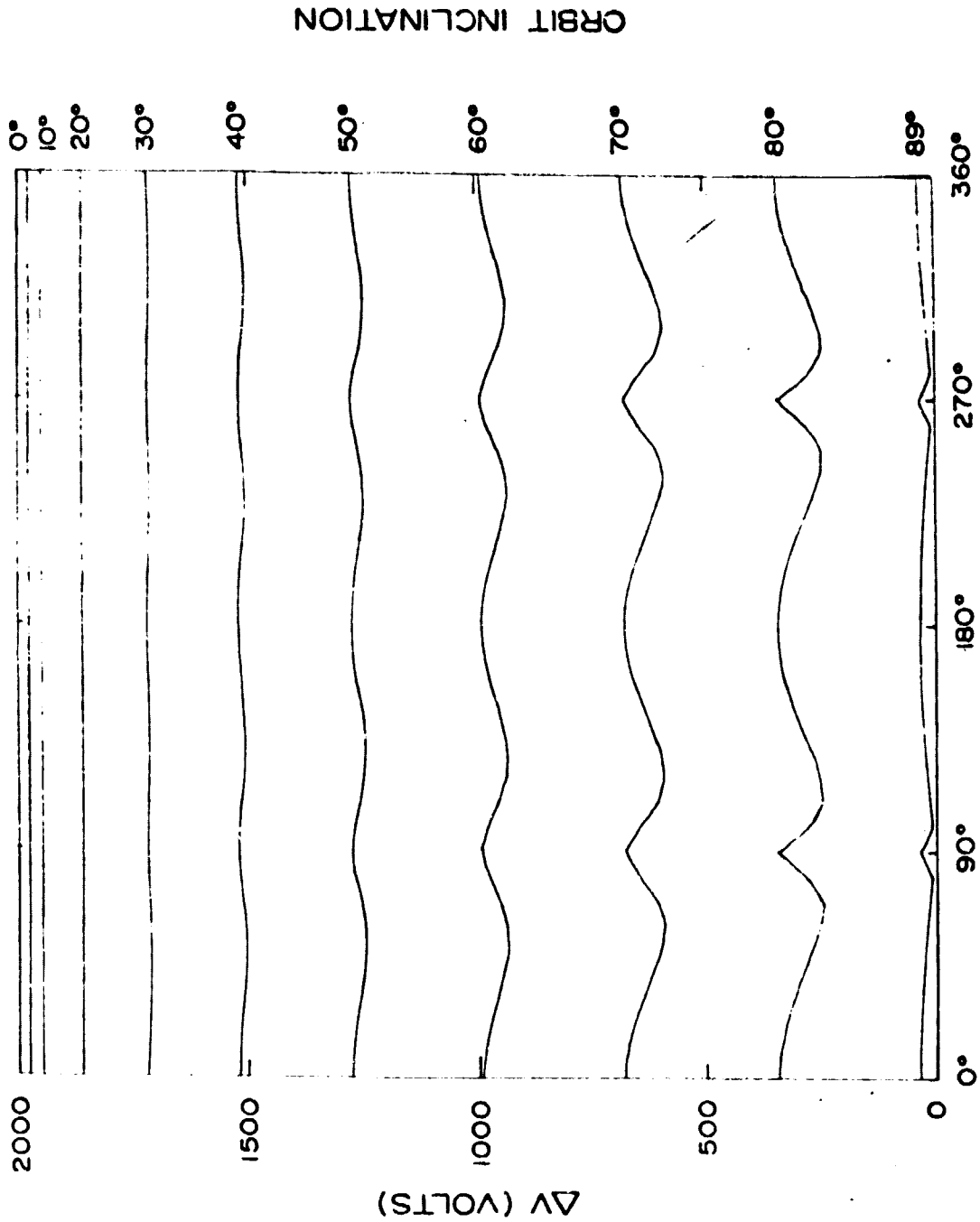
#### REFERENCES

1. Linson, Lewis M., Current-Voltage Characteristics of an Electron-Emitting Satellite in the Ionosphere, *J. Geophys. Res.*, 74, 2368-2375, 1969.
2. Morrison, Phillip, W.B. Thompson and P. Roger Williamson, Current Collection by a Long Wire in Near-Earth Orbit, submitted to IEEE transactions.
3. Oyama, K., P. Roger Williamson, and P.M. Banks, An Electrodynamic Tether Experiment Program, Internal Report, CRA-1978.
4. Williamson, P. Roger and P.M. Banks, The Tethered Balloon Current Generator -- A Space Shuttle-Tethered Subsattellite for Plasma Studies and Power Generation, Final Report to NOAA for Contract USDC-NOAA 03-5-022-60, January 16, 1976

# BALLOON - SHUTTLE POTENTIAL DIFFERENCE

$$\Delta V = \vec{V}_0 \times \vec{B} \cdot \vec{D} \quad V_0 = 7.7 \text{ KM/S}$$
$$D = 10 \text{ KM}$$

ALTITUDE = 400 KM



ORBIT LONGITUDE  
Figure 1

ORIGINAL PAGE IS  
OF POOR QUALITY

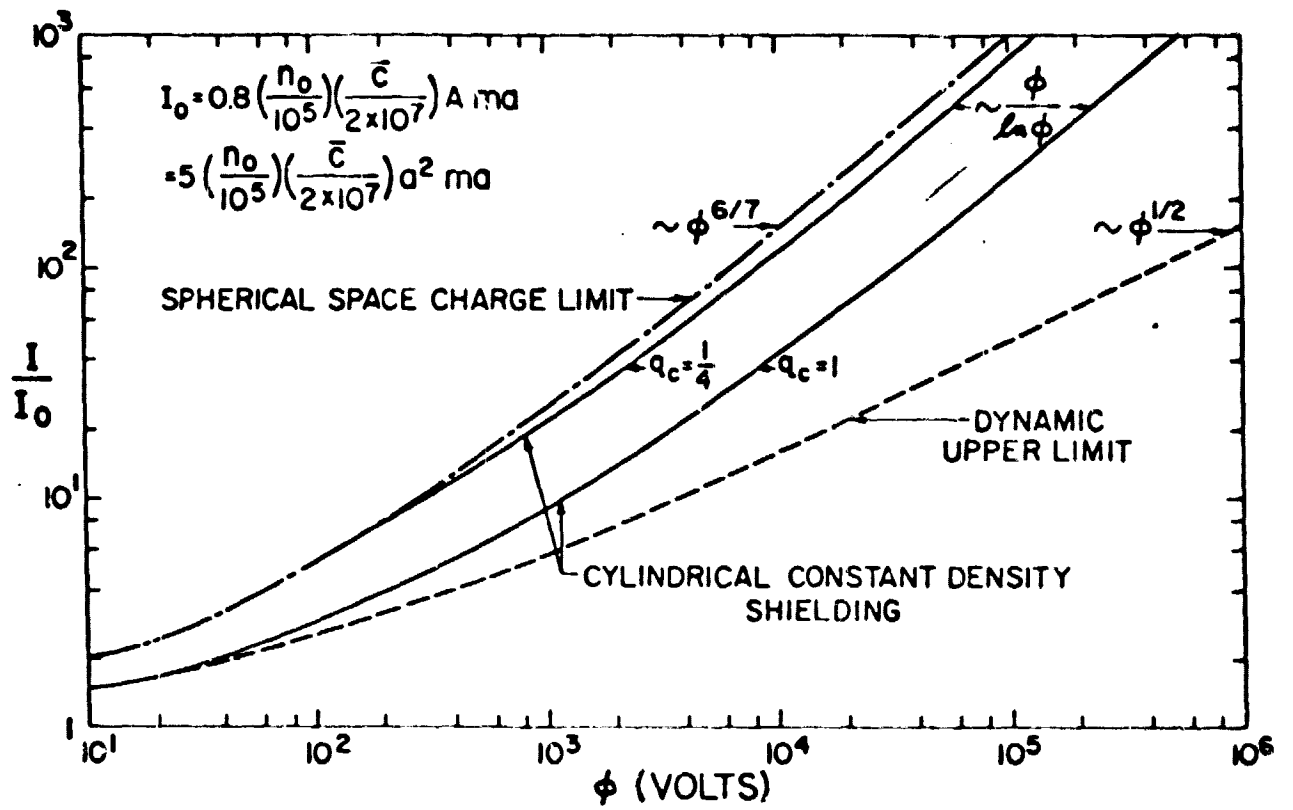


Figure 2

INTERACTIONS OF A TETHERED SATELLITE SYSTEM WITH THE IONOSPHERE  
(SUMMARY)

Mario D. Grossi and Giuseppe Colombo

Harvard-Smithsonian Center for Astrophysics  
Cambridge, Massachusetts 02138

Paper Presented At  
NASA-MSFC Workshop on the Uses of a Tethered Satellite System  
May 2-3, 1978  
Huntsville, Alabama 35801

## INTERACTIONS OF A TETHERED SATELLITE SYSTEM WITH THE IONOSPHERE

Mario D. Grossi and Giuseppe Colombo

Harvard-Smithsonian Center for Astrophysics  
Cambridge, Massachusetts 021381. Introduction

The Tethered Satellite System (TSS) will be the first large structure deployed in space. Even if its length is limited to 20 km (and we strongly urge that a length of 100 km be adopted), it will be at least fifty times longer than anything that has been orbited thus far.

When constructed of metal (either coated or uncoated with dielectrics), this large space structure will react strongly with the magneto-ionic medium of the Earth's ionosphere and will allow unprecedented scientific experiments to be conducted.

Because of the  $\vec{V} \times \vec{B}$  effect, a voltage as high as 35 to 50 KV can develop between the two end terminations of the tether, which will act as a kind of "unipolar inductor" or self-powered generator capable of exciting with its electromotive force a large variety of wave phenomena in the ionosphere. We used the words "unipolar inductor" because of the direct analogy that we see between the conducting tether and "Io, a Jovian Unipolar Inductor" (Goldreich and Lynden-Bell, 1969). As a matter of fact, we see this analogy with Io (and, in general, the ability of the tether to perform in the Earth's ionosphere as a source of electrodynamic effects of planetological significance) as a clear indication of the great scientific value of the TSS project.

When excited by a Shuttle-borne transmitter, the tether can then be used as an antenna in the ELF and ULF bands, which will make it possible to

C - }

generate artificial micropulsations and also to experiment with the radiative properties of long thin wires embedded in an unbound magnetoionic plasma — a not inconsequential issue in radio physics and radio engineering.

## 2. Status of the Interaction Theory

The theory of interaction must treat first the area of current and potential distribution along the tether. Then it must extend to the types of wave excitation expected to take place in the ionosphere because of the presence of the orbiting tether.

In a bare-metal tether, 100 km in length and a millimeter in diameter, the resistance of the tether is essential in determining current and potential profiles (Dobrowolny, Colombo, and Grossi, 1976). The typical current profile appears to be characterized by two current spikes, each a fraction of an Ampere, localized at the two ends of the tether, for a length of about 10 km. Much smaller values characterize the rest of the tether. Similarly, most of the potential drop corresponding to the  $\bar{V} \times \bar{B}$  effect appears to be localized near the two ends of the tether.

In an insulated metallic tether with terminating electrodes, the interactions with the ionosphere are strongly dependent on the dimensions of the electrodes. With electrodes of very large dimensions (spheres with diameter of 15 to 20 m, or equivalent), the current in the tether is limited by the wire resistance, and values of approximately 2 Ampere are to be expected. An accurate computation of the voltage with respect to the plasma of a complex termination such as in the case of the Shuttle is yet to be performed.

The theory indicated above for the tether's electromotive force generation and current/voltage profiles along the wire is reasonably well developed. An important addition would be a detailed study of the tether wake.

In regard to the type of wave that the tether as a self-powered generator will excite in the ionosphere, it is of interest to recall the

debate on the "Alfven Wings" of the late 1960's (Drell et al., 1965; Chu and Gross, 1966). This mechanism would be active in the ULF band. Another mechanism is expected to be active at much higher frequencies, more precisely at the electron gyrofrequency at the foot of the geomagnetic field line that passes through the tether. We think that this area deserves careful study and detailed planning.

Although a theory specifically devoted to this wave excitation by the tether has not yet been worked out, the analogy with Io that we have already mentioned provides important elements. Earlier work by Goldreich and Lynden-Bell (1969), Gurnett (1972), and Oya (1974) on the Jovian decametric wave emission attributes to the electromotive force of an orbiting conducting body the ability of accelerating ionospheric electrons and ultimately producing the decametric bursts through a coherent cyclotron radiation mechanism.

We plan to develop this theory in time to provide guidance for an observational program to be carried out on the first Shuttle flight with a metal tether onboard. We hope to include in this observational program the "listening" to the radio noise produced by the tether in a wide spectrum of frequencies from ULF to HF and an attempt to detect possible UV emissions at the foot of the line of force passing through the tether itself.

### 3. Advisable Interaction Experiments

Listening in the frequency bands mentioned above can be performed with magnetometers and radioreceivers, arranged in ground networks and installed in subsatellites. Their position with respect to the geometry of the wave emission will be carefully chosen because of the sharp directionality expected, at least for the emissions near the gyrofrequency.

Subsidiary studies on the tether include measurement of the current and voltage with respect to the terminating electrodes, impedance measurements, probing of the plasma sheath, radiation patterns, etc.

If theoretical calculations will confirm feasibility, the foot of the line of force involved in the search for UV emissions will be observed. It is known that the Copernicus Telescope in orbit has successfully detected UV emissions from the foot of the Io line of force. We are taking steps to have the IUE Explorer (a joint NASA/ESA initiative) look in 1979 for UV emissions at the foot of the Io and of the Amalthea lines of force. Similar observations will be performed, at our suggestion, from Voyager.

The values of the Table show that the comparison between TSS and Amalthea is not unreasonable. The distances involved in our observations of TSS would be in fact in our favor.

Table 1. Analogy between TSS and Jovian Satellites Io and Amalthea.

	Size (km)	Magnetic field (Gauss)	Relative velocity (km/sec)	Tip-to-Tip Voltage (KV)
Io	3000	0.05	60	900
Amalthea	300	0.75	7.5	150
TSS	20 100	0.5 0.5	8 8	8 40

#### 4. Conclusions

The versatility of the TSS project makes this system suitable for use in a variety of disciplines (Colombo et al., 1974) and the Workshop has been truly an interdisciplinary event.

However, its electrodynamic and electromagnetic uses, which motivated early efforts (Grossi, 1973) to make it a reality, are perhaps among the most appealing features of this system. They are, in fact, the only ones in which the tether itself is the instrument and in which the experiments that can be conducted are truly novel, qualitatively different from the ones that could be performed with satellites and even with Skylab.

## References

- Chu, C. K., and R. A. Gross (1966), Alfvén waves and induction drag on long cylindrical satellites, AIAA Journ., vol. 4 (no. 12), pp. 2209-2214, December.
- Colombo, G., E. M. Gaposchkin, M. D. Grossi, and G. C. Weiffenbach (1974), Shuttle-borne Skyhook: A new tool for low-orbital-altitude research, SAO Reports in Geoastronomy No. 1, September.
- Dobrowolny, M., G. Colombo, and M. D. Grossi (1976), Electrodynamics of long tethers in the near-earth environment, SAO Reports in Geoastronomy No. 3, October.
- Drell, S. D., H. M. Foley, and M. A. Ruderman (1965), Drag and propulsion of large satellites in the ionosphere: An Alfvén propulsion engine in space, Journ. Geophys. Res., vol. 70 (no. 13), pp. 3131-3145, July 1.
- Goldreich, P., and D. Lynden-Bell (1969), Io, a Jovian unipolar inductor, Astrophys. Journ., vol. 156, pp. 59-78.
- Grossi, M. D. (1973), A ULF dipole antenna on a spaceborne platform of the PPEPL class, Letter Report to NASA/MSFC, Contract NAS 8-28203, May 11.
- Gurnett, D. A. (1972), Sheath effects and related charged-particle acceleration by Jupiter Satellite Io, Astrophys. Journ., vol. 175, pp. 525-533, July 15.
- Oya, H. (1974), Origin of Jovian decameter wave emissions - Conversion from the electron cyclotron plasma wave to the ordinary mode electromagnetic wave, Planet. Space Sci., vol. 22, pp. 687-708.

THE TETHERED SUBSATELLITE AS A TOOL FOR LARGE BODY PLASMA FLOW  
INTERACTION STUDIES

by:

Nobie H. Stone  
Space Sciences Laboratory  
Marshall Space Flight Center  
MSFC, Alabama 35812

and

Uri Samir  
Dept. of Geophysics and Planetary Sciences  
Tel Aviv University  
Tel Aviv, ISREAL  
and  
University of Michigan  
Ann Arbor, Michigan 48109

## I. The Rational for Large Body Plasma Flow Interaction Studies:

The interaction of a flowing plasma with a body is of interest because of the large number of examples of this type phenomena found in nature. Many of these examples, such as the earth's magnetosphere and comets are well known to us. The investigation of plasma flow interactions (PFI) in the earth's ionosphere is of interest because it is yet another extension of the same general class of phenomena and because of the impact of the interaction on in situ measurements of the ambient plasma medium.

In the past, ionospheric PFI studies have been fragmentary (incomplete in the parameters measured and/or spatial mapping) and have dealt only with diagnostic probes or the satellites themselves (small to medium size bodies with respect to the Debye length). With the aid of the Space Shuttle and the Tethered Satellite System (TSS) these investigations can be extended to a larger range of body size (large compared to the Debye length and the ion Larmor radii), which will probably involve different physical mechanisms. Such an extension will help develop a better understanding of the basic interaction mechanisms involved and how they are effected by changes in the parameters of the plasma. The large body problem is especially important since it can not be performed effectively in the laboratory and is difficult to attack theoretically.

In some cases, the large body PFI experiments can be made to qualitatively simulate some aspects of natural phenomena. As an example, we will consider the interaction of the Moon with the solar wind. It is evident that a strict Vlasov scaling is out of the question. However, in recent years a concept known as qualitative scaling has been developed which allows a considerable relaxation of the rigid Vlasov laws (Falthammer, 1974). Under qualitative scaling, parameters much greater/smaller than unity are required to remain so but are not required to maintain the same order of magnitude, while parameters of order unity are scaled as closely as possible. In qualitative scaling, the

emphasis is on reproducing the correct physical process for study, rather than the exact interaction morphology.

Table 1 gives some important dimensionless parameters for the Moon in the solar wind and a large balloon in the earth's ionosphere at an altitude of 400 km. Note that with the exception of  $S$  and  $(R_o/L+)$ , all ratios are much greater than unity (where  $S = (M_e V_o^2/2kTe)^{1/2}$ ,  $R_o$  = Balloon radius,  $L+$  = ion cyclotron radius, and  $V_o$  = orbital velocity).  $S$  and  $(R_o/L+)$  values are very close for both cases so that the qualitative scaling conditions appear to be met.

Perhaps the most important ratio for simulating a body the size of the Moon is  $(R_o/L+)$  which is analogous to the Knudsen number in fluid mechanics. According to Dryer (1970), this parameter can be used to determine whether a continuum or a kinetic approach must be used in theoretical treatments ( $R_o/L+ \gg 1 \rightarrow$  continuum approach,  $R_o/L+ \ll 1 \rightarrow$  kinetic approach). Note that the value of  $(R_o/L+)$  for the Moon does not provide a decisive answer and falls into a "transition" region (Wu and Dryer, 1973). It therefore appears that, for bodies the size of the Moon or smaller, it is questionable if a continuum approach deals with the correct physical mechanisms, while a kinetic approach is impractical. It is possible that large body PFI studies in the ionosphere may help answer this question and better define the limits of the two approaches.

Finally, the plasma wake is being considered as a source of ultra high vacuum for growing high purity crystals in space. The conceptual device, called the plasma wake shield, could benefit greatly from timely large body PFI studies.

## II. Experimental Requirements:

The variables that need to be measured as a function of space and time for the large body PFI experiments are: the ion and electron temperatures and densities, the ion flow direction, flow velocity and mass, the space potential and electric fields. For the most part, standard diagnostic instruments, or instruments now under development, can provide these measurements. In addition, some of these variables may be provided by remote techniques. All measurements should be made by a mapping instrument package in the disturbed zone concurrent with a complete set made in the ambient medium. This is necessary to separate temporal and spatial fluctuations generated by the body from those naturally occurring in the ambient medium.

From the scaling parameters given in Table 1, we find that the body should consist of a spherical balloon and range in size up to 300 m in diameter in order to provide the correct  $(R_n/L^+)$  value. The surface characteristics should be varied for different experiments (conducting or insulating). For conducting bodies, provisions should be made to control the body potential. For large insulating bodies provisions should be made to measure differential charging of the surface.

The spatial volume of interest consist of a small frontal region where a bow shock may exist under certain circumstances, and the downstream wake. The extent of these regions is not accurately known for large bodies and the definition of the limits of the disturbed zone should be the object of early experiments. Since, for such large bodies, the sheath fields are not expected to have an important influence, the ion void swept out by the moving body may be expected to fill by thermal or other processes such as ambipolar diffusion. The disturbance can therefore be expected to be confined to a "Mach" angle defined in terms of the ion acoustic speed. This is typically less than  $20^\circ$  in the lower ionosphere. Figure 1 shows a conceptual arrangement of the balloon and the mapping and ambient monitoring instrument packages using the TSS.

Figure 2 shows an example mapping maneuver for investigating the frontal and near wake regions. In order to maintain consistent conditions, it is desirable that such a maneuver be completed within one orbit in a region where ionospheric conditions are relatively constant (i.e., avoiding the polar regions and the terminators). This would require that the mapping be completed in approximately 15 minutes.

### III. Utilization of the Tethered Satellite System:

The primary purpose of the TSS in large body PFI studies is to deploy the test body and maintain its position with respect to the orbiter. As indicated in Figure 1, it may also be used to deploy an ambient monitor.

The fact that a tether is, in deed, required to maintain such large bodies as indicated in Table 1, is graphically demonstrated in Figure 3. This shows the separation distance, produced by differential drag between the Shuttle and large balloon type bodies, as a function of time and body radius at 400 km altitude. The maximum time shown is 15 minutes which is the desired length of the mapping maneuvers. After this time, the 20 m body is still within a few km of the orbiter, which is permissible if only one mapping is required. However, reuse would require repositioning, possibly by a maneuverable subsatellite.

For the larger bodies of 100 m to 200 m in radius, the separations grow to the order of  $10^2$  km, which is not practical, even for a single mapping maneuver. The acceleration of two bodies can be matched by equating their ballistic coefficients (Mullins, 1975), however, for balloons with  $R_0 > 50$  m, this would require a ballast mass in excess of  $10^6$  kg and is therefore not practical. Therefore, for bodies of this size the tether becomes essential for station keeping.

Having shown the tether to be necessary for the large body experiments, we must now determine if tethered balloons of this size are practical--Is the drag on the balloon excessively great?--Is the system stable?--What magnitude of current must be handled by the tether to implement the voltage control discussed in Section II?

Figure 4 shows the drag force  $F_D$  on balloons of several different radii,  $R_0$ , as a function of altitude. From the report by Rupp and Laue (1978), we take a tether tension of 100 N. to be the current design criteria. As expected, the figure shows that the drag becomes large rapidly with decreasing altitude and, certainly, below 200 km large body experiments are not practical. It is therefore immediately obvious that only an upward deployment can be used.

The exact range of permissible balloon radii and altitudes depends on the maximum allowable angle the TSS can make to the vertical. This was not given in the reports on the TSS although angles of  $50^\circ$  are shown (Rupp and Loue, 1978). We assume  $45^\circ$  to be a reasonable design criteria and take the satellite mass to be 175 kg (the design value given by Rupp and Laue). Then a balloon with  $R_0 = 150$  m can be deployed as low as 400 km. Therefore, from these initial drag considerations, the size of bodies in the  $R_0 \sim 10^2$  m range is not a problem.

The stability of the system must be considered in two contexts. From the above drag considerations, the configuration appears to be stable. However, a second concern is steady-state stabilization; how stationary is the balloon once deployed? To perform the experiment illustrated by Figure 2, three axis position coordinates of the mapping package relative to the balloon are required. These coordinates should be known to an accuracy of at least  $0.1 R_0$ . Long period (order of hours) drifts of the balloon should not present any problem. However, short period oscillations must be damped or otherwise accounted for.

The primary concern in biasing the balloon is handling the current collected, either by conduction to the orbiter through the tether or by charged particle emission at the balloon. Most PFI experiments will probably involve negative biasing, and hence, the collection of a net positive ion current. According to Williamson and Banks (1976), the body potential is not a major factor in the collection of electrons (only  $\sim 14\%$  enhancement for a 2 kV bias). It is therefore reasonable to expect the positive ion current to be essentially independent of body bias. The positive current collected by the balloon will therefore consist primarily of the ion flux swept out by the balloon's movement. The resulting current is shown in Figure 5 as a function of altitude for several balloon sizes. There does not appear to be any difficulty with negative biasing with the possible exception of the 150 m and 200 m radii balloons at 400 km altitude. However, the current drops off rapidly on either side of 400 km and this region could be avoided.

Positive biasing is expected to be more difficult to achieve. The actual current collected is more difficult to estimate, but if the thermal electron current can be taken as an indication, even at 300 km altitude, a balloon with  $R_0 = 100$  m would collect  $\sim 50$  amps. This value grows rapidly with increased balloon radius and altitude.

The deployment rate of the TSS is in the range of 10 to 50 m/s. This is sufficient to provide a large part of the required maneuvering capability represented by Figure 2. Since the trajectory lengths across the disturbed zone are on the order of 0.5 to 1.5 km, a single traverse could be carried out typically in one or two minutes. The critical question is what kind of undesirable gyrations of the balloon, if any, would be initiated by such maneuvers.

#### IV. Conclusions:

1. It has been shown that the qualitative scaling laws can be satisfied for some aspects of certain astrophysical plasma flow interactions by utilizing the TSS to deploy and maintain bodies ranging from 50 to 150 m in radius.
2. Questions about this application of the TSS requiring further consideration include:

a. Are there other, or more detailed, considerations which impact the stability of the TSS for such large bodies? What is the practical limit on size?

b. How can balloons of this size be inflated? Considerations would include dynamic and electrodynamic forces on the balloon's surface and leak rates, which may effect the experiment.

c. Steadiness of the TSS after deployment.

d. The extent to which the TSS can be made to perform or supplant mapping maneuvers.

#### V. References:

Dryer, Murray, Cosmic Electrodynamics 1, 115, 1970.

Fahleson, U., Planet. Space Sci. 15, 1489, 1967.

Falthammer, C. G., Space Sci. Rev. 15, 803, 1974.

Mullins, L. D., NASA TMX-64948, 1975.

Rupp, C. C., NASA TMS-64963, 1975.

Rupp, C. C. and Laue, S. H., Proc. of the 1978 Goddard Mem. Symp., No. 78-048, Washington, D.C., 1978.

Williamson, P. R. and Banks, P. M., "The Tethered Balloon Current Generator-A Space Shuttle-Tethered Subsatellite for Plasma Studies and Power Generation", NOAA Contract Report 03-5-022-60, 1976.

Wu, S. T. and Dryer, M., "Kinetic Theory Analysis of Solar Wind Interaction with Planetary Objects," in Photon and Particle Interactions with Surface in Space, D. Reidel Pub. Co., Holland, 1973.

BODY	$\frac{R_0}{(m)}$	S	$\frac{R_0}{\lambda_D}$	$\frac{R_0}{L_{\dagger}}$	$\frac{R_0}{L}$	$R_M$
MOON	$1.74 \times 10^6$	15	$3 \times 10^5$	29	$1 \times 10^3$	$1 \times 10^{10}$
BALLOON IN IONOSPHERE	150	5	$4 \times 10^4$	30	$5 \times 10^3$	$3.5 \times 10^2$

$$S = (M_+ V_0^2 / 2kT_e)^{1/2}$$

$\lambda_0 \equiv$  DEBYE LENGTH

$L \equiv$  LARMOR RADIUS

$$R_M \approx 10 \frac{(\epsilon_0 R_0 V_0 (kT_e))^{3/2}}{C^2 M_e^{1/2} e^2}$$

TABLE 1. SCALING PARAMETERS

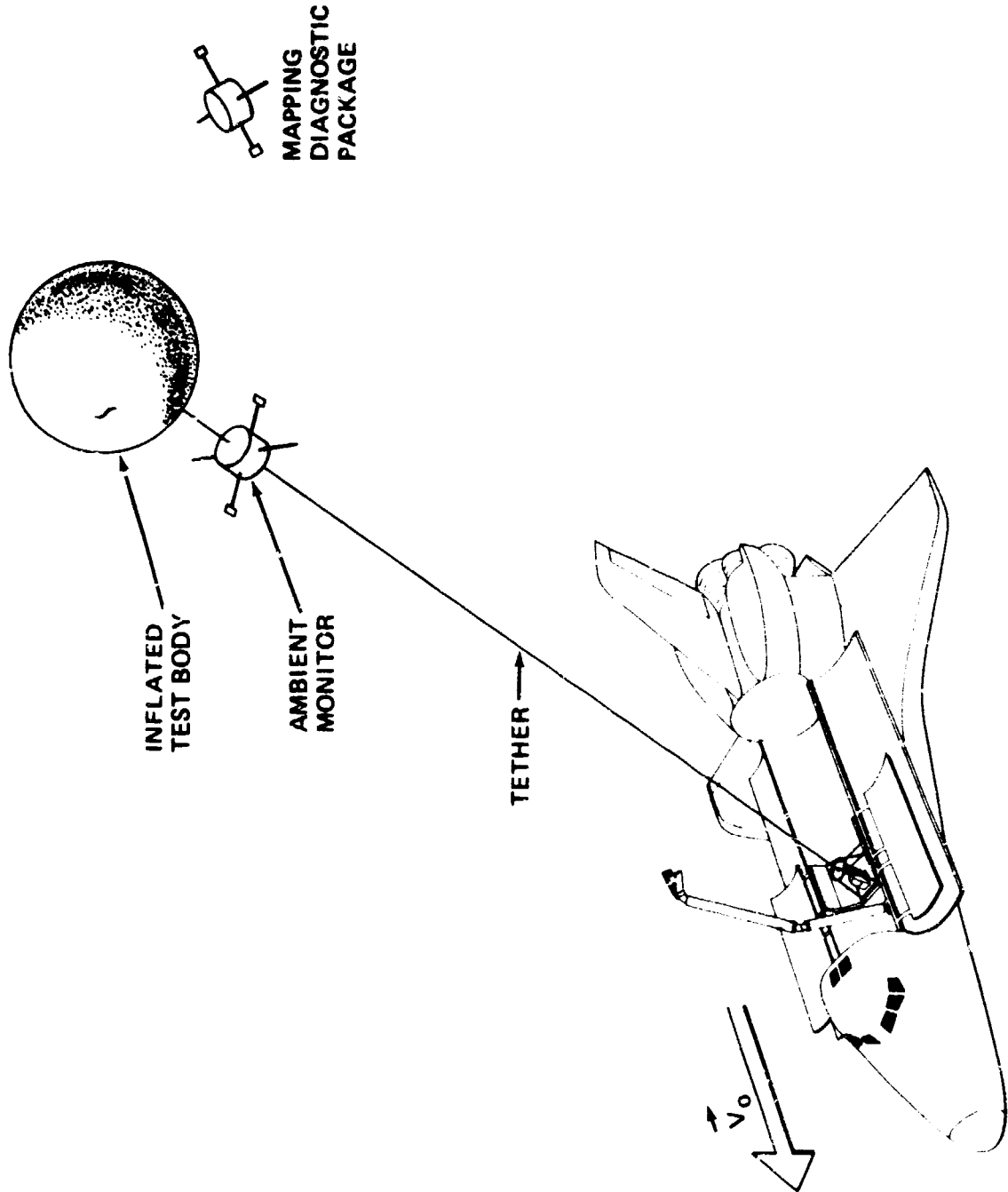


Figure 1

$R_0 = 100 \text{ m}$   
TOTAL DISTANCE:  $\sim 5 \text{ km}$   
 $\Delta t \sim 15 \text{ min}$   
 $\Delta v \sim 150 \text{ m/sec}$   
SUBSAT: MASS 658 kg  
THRUST:  $\sim 160 \text{ N (35 lb)}$

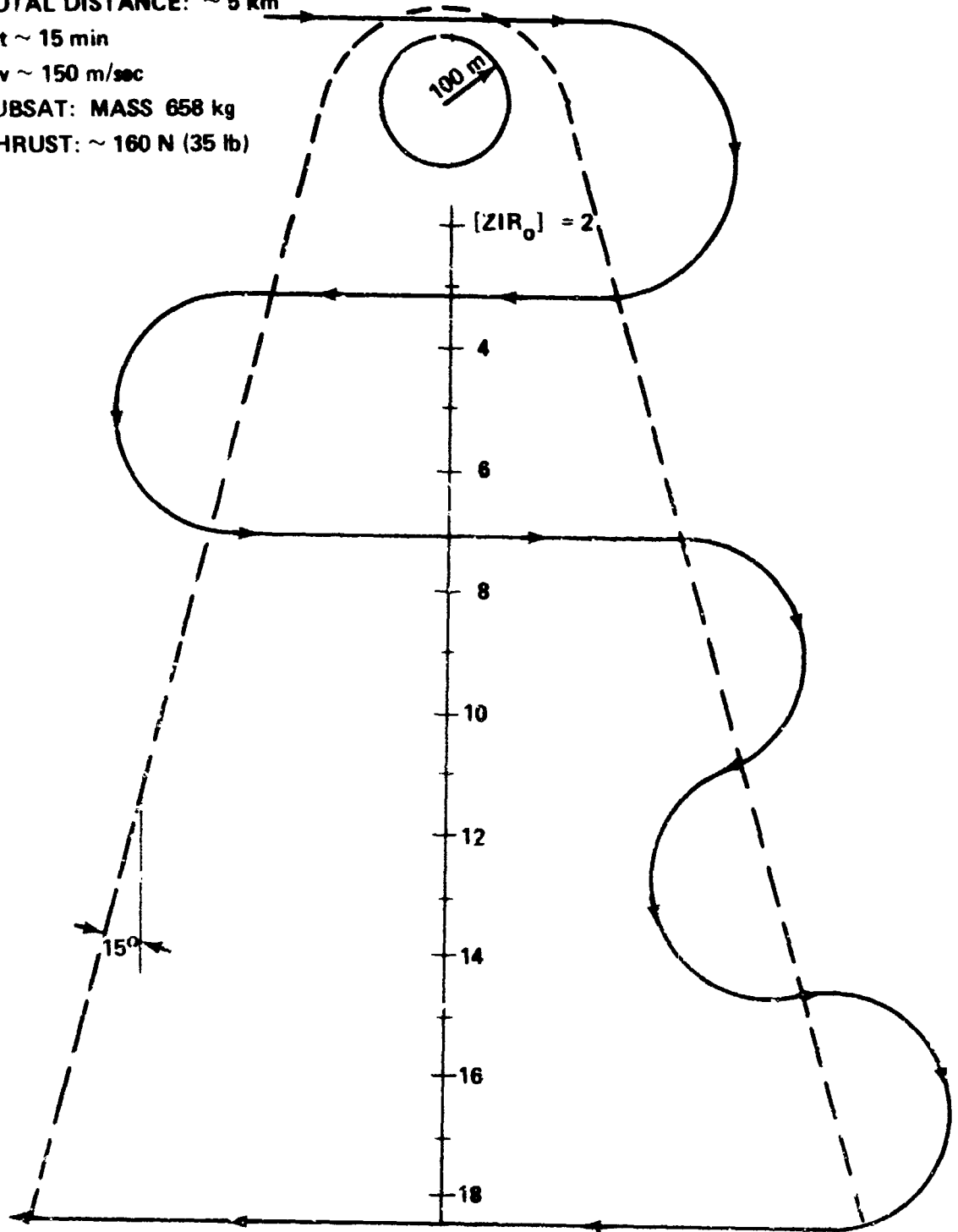


Figure 2

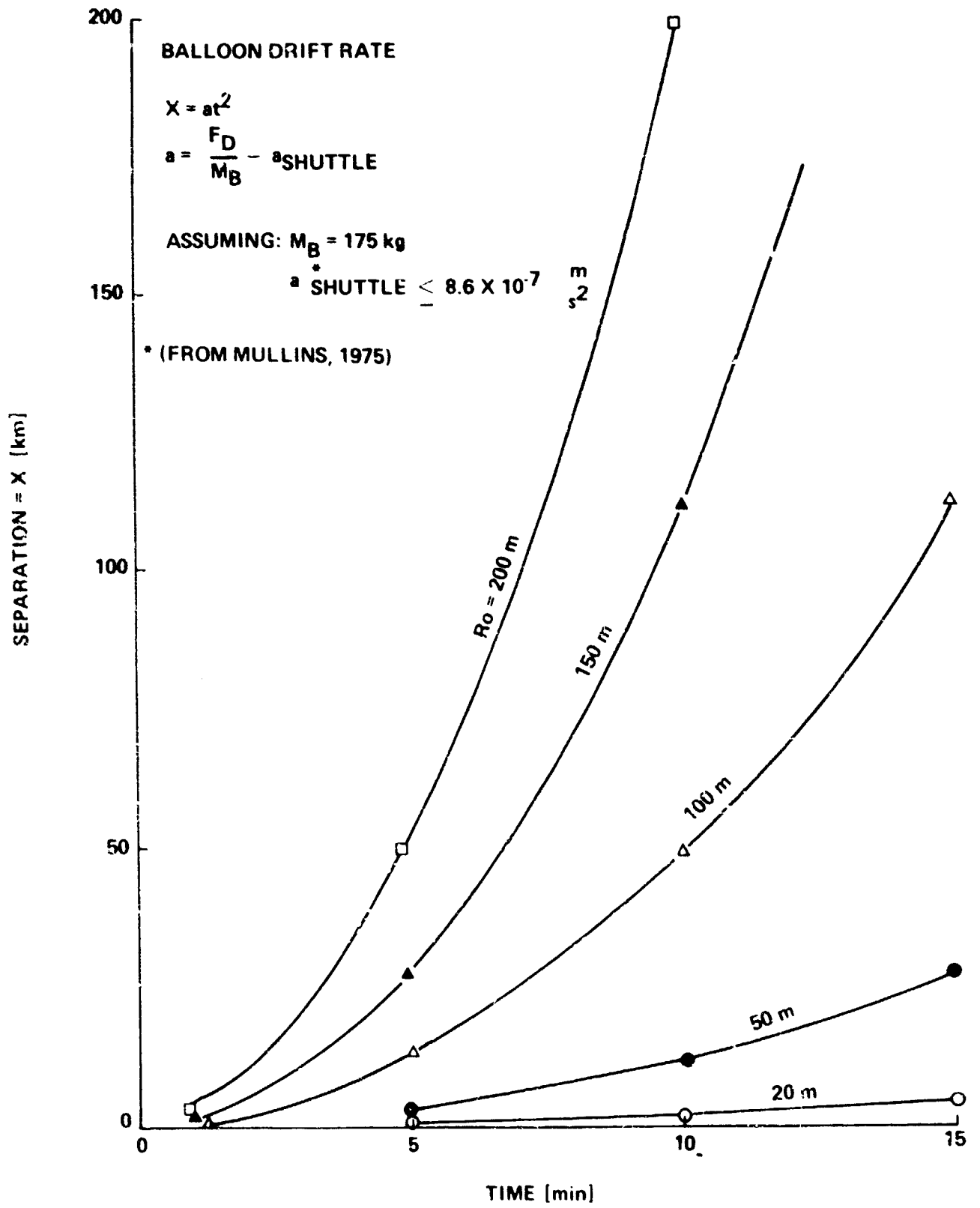


Figure 3

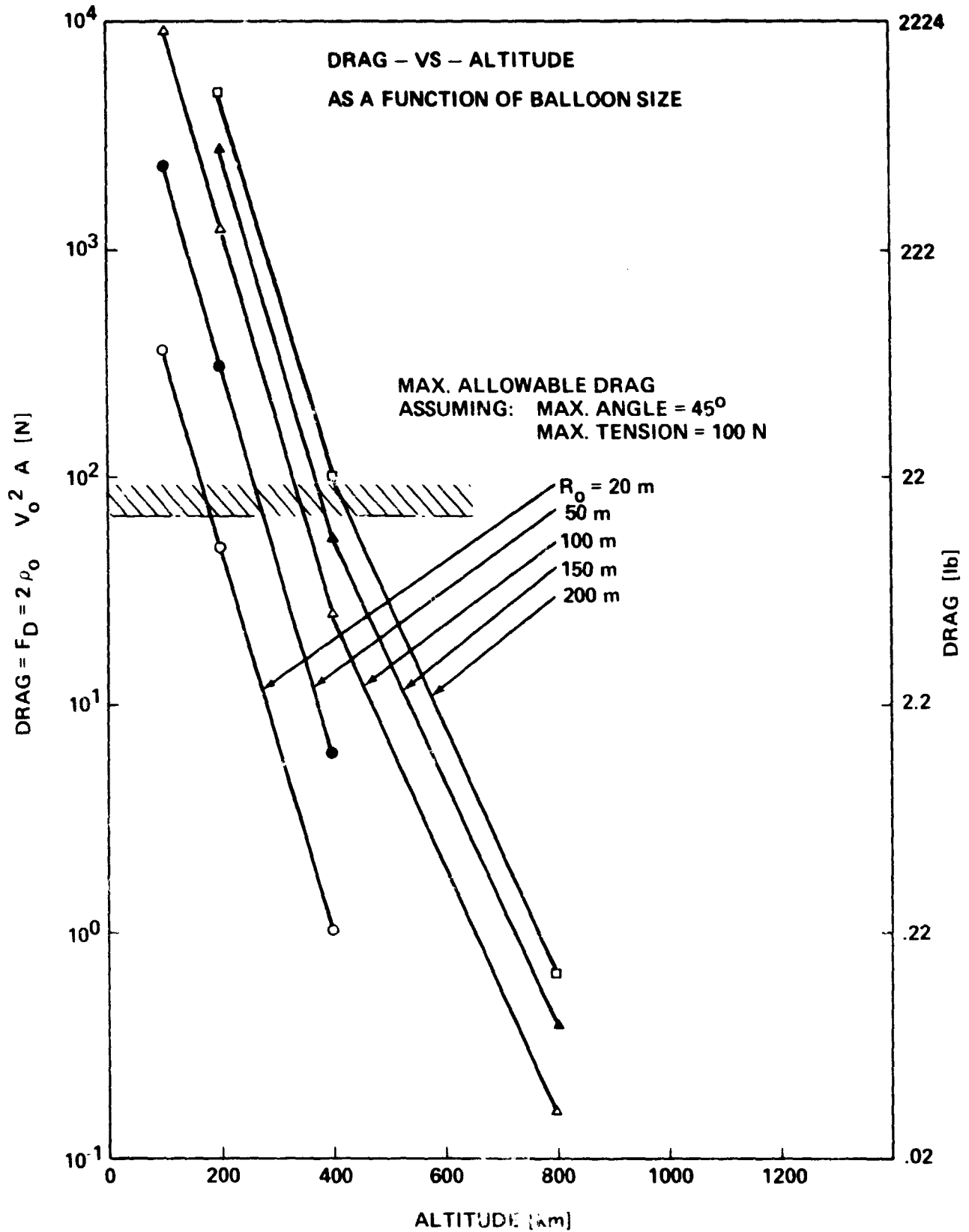


Figure 4

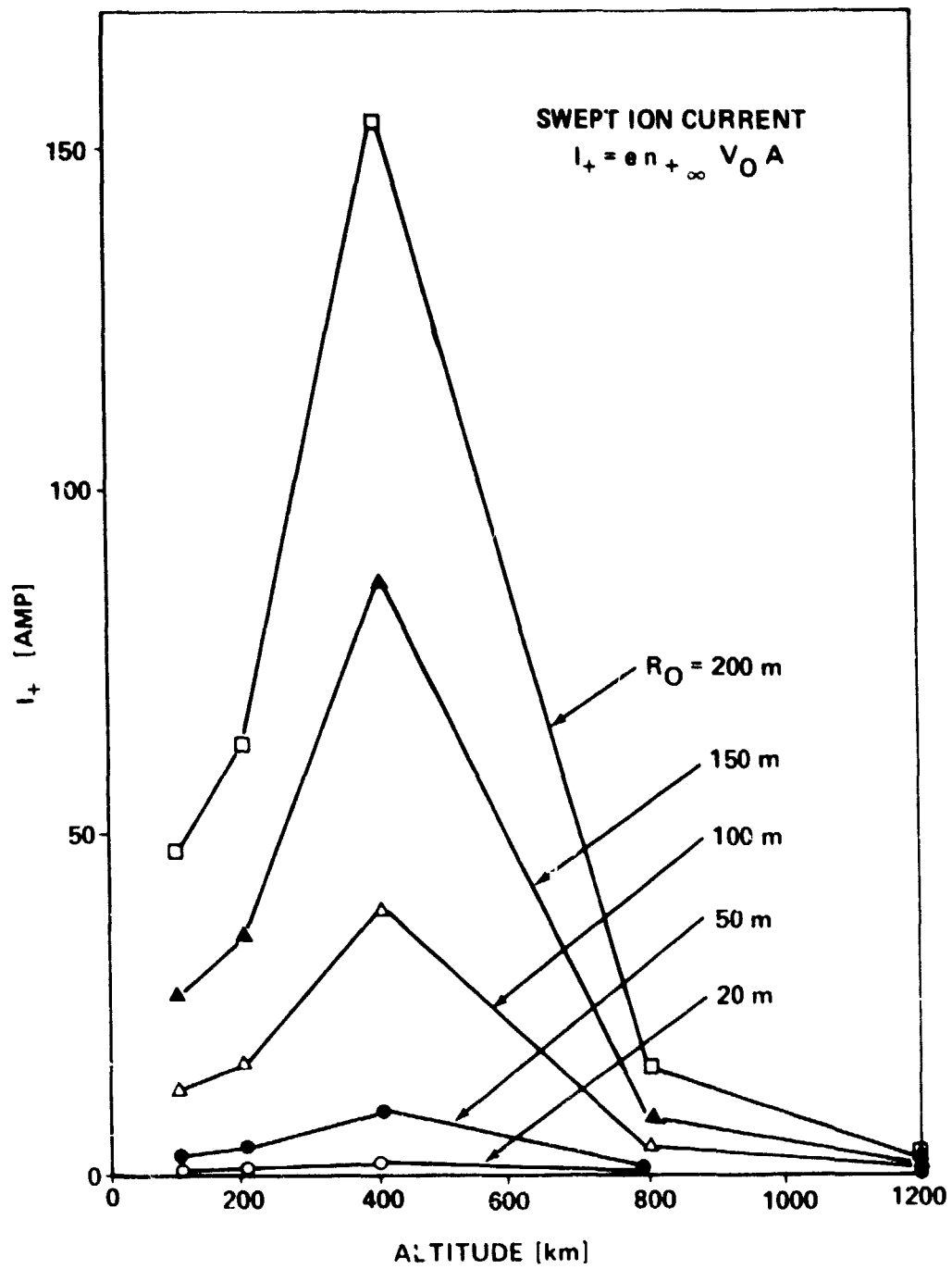


Figure 5

011  
12  
1A

## IV. ENGINEERING AND OPERATIONAL APPLICATIONS

### SUMMARY

M. P. L. Siebel  
NASA/Marshall Space Flight Center

The Tethered Satellite System (TSS) provides for a general extension of the Shuttle capabilities. It further adds a great deal of flexibility to the operations in orbit. From the examples given below, it will be seen that Shuttle operational capabilities are enhanced for three main reasons:

- o Reduction of propellant consumption for many missions
- o Greater availability of electrical energy
- o Greater safety to crew and vehicle

#### 1. Station Keeping

A satellite, another Shuttle or other device may be held by the Shuttle/tether system in a station-keeping mode without expenditure of propellants. Such station keeping is useful in various situations when the tethered satellite needs to be in a "clean" environment, that is removed from the electrical and magnetic fields generated by the Shuttle, or when the outgassing of the Shuttle is detrimental to some experiments. Conversely, the satellite itself may be best placed remotely from the Shuttle; e. g., if it contains a hazardous process/experiment or a radio active power supply.

#### 2. Power Transfer

When a power generating module or satellite is left in orbit for revisits by the Shuttle, the tether which permits station keeping can also readily be used as a power transfer line. The power of the module can be generated by solar cells, nuclear means or by fuel cells. The power generated when it is not needed by the Shuttle can be stored in batteries or as kinetic energy by electrically reboosting the power supply satellite.

### 3. Satellite Capture

The use by the Shuttle of a permanently orbiting power module implies the repeated capture of the module by the Shuttle, either by docking or by using the tether suitably deployed to "hook" into the power module. This latter mode of "capture" can of course be used also to capture other satellites for retrieval (e. g., Teleoperator). Retrieval may be desired for repair, refurbishment or return to the ground.

### 4. Power Generation

A means of generating power is to use a conducting tether. The tether will have an electrical potential difference between its ends proportional to its length and to the value of  $\bar{v} \times \bar{B}$  where  $\bar{v}$  is the effective velocity of the Shuttle and  $\bar{B}$  the magnetic field of the Earth. When a current is drawn from this system; i. e., when power is used, the Shuttle orbit will decay. Reboost is then possible and this represents a relatively efficient conversion of, say, chemical energy into electrical energy. Energy storage is in the form of kinetic energy which can be used as required.

### 5. Assembly of Large Structures in Space

Large structures are planned for assembly in space. The elements of the structures will be transported to space by the Shuttle. When complete, the structures will be autonomous and will be oriented by a control system. During erection, however, the elements will have to be controlled by other means. Rigid remote manipulator systems are presently envisaged. These systems have a number of shortcomings, for example, they are relatively short, and a large structure in the vicinity of the Shuttle may present potential hazards. The use of a single or multiple tether system would permit the deployment of elements of structures to a safe distance and assembly of the total structure there while still providing adequate control of position and attitude of the elements. Construction cranes provide earthbound examples of the techniques envisaged.

### 6. Cargo Transfer

When a tether line is used between two vehicles, say two Shuttles, or a Shuttle and a structure being assembled in space, then the line can be used as a guide for moving cargo from one vehicle to the other. This is, of course, important in moving structural elements from the Shuttle

cargo bay to the structure. It may also be used for resupply of satellites kept in orbit permanently, or for the retrieval of products processed on such satellites.

#### 7. Stabilization of Structures and Antennas

The tether line is in tension owing to gravity gradient effects. The force can be used to stabilize structures in space with the local vertical gravity gradient as the reference force. Rotations around the tether must be accomplished by other means. The tether, of course, permits the erection of antennas for transmission and reception at ultra-low frequencies (ULF) and higher frequencies.

#### 8. Vehicles Permitting Adjustable Low 'G'

When two bodies orbit with a tether line joining them, then the C. G. of the system is in the true zero 'g' (free fall) orbit. The off-orbit bodies will be subject to accelerations of a magnitude depending on their distance from the system's C. G. For certain scientific processes, true zero acceleration will be needed and can be attained by attaching a sub-satellite at the appropriate point along the tether. For other applications, values of acceleration lying between the value of 'g' at the Earth's surface and 0 may be needed; these values are obtainable at other locations along the tether line. These low values of acceleration are not obtainable on Earth, at least not for any significant duration and make possible processes depending on partial 'g'.

#### 9. Gradient Measurement and Interferometry

A great deal of information about physical phenomena can be obtained by performing simultaneous measurements at various altitudes above the Earth. A knowledge of the magnetic and gravitational field gradients for example will enhance the interpretation of the crustal and other data and give statistical verification of the results. Similarly, gradient measurements of ionic and neutral densities in the upper atmosphere will help in the interpretation of the phenomena. A single tether system can thus provide data obtainable only by several propelled autonomous vehicles---an enterprise too costly and complex to envisage. Similarly, interferometry to detect wave phenomena usually requires the use of two satellites. These can now be joined by the tether and will present new opportunities for incident wave measurement.

#### 10. Controlled Reentry and Orbit Adjust

By lowering certain payloads to, say, 120 km they will reenter at a known rate and land within a predictable footprint. Excess or other payloads may well be returned in this manner. As an extension of this idea, the drag generated by a tethered satellite could be used to cause the Shuttle itself to change orbits or even to return in the event of de-orbit thruster failures.

In conclusion, it may be said that the Tethered Satellite System presents to the Shuttle new operational modes and a significant extension of orbital capabilities as well as the possible extension of stay-times and cargo handling.

May 4, 1978  
ES01

## APPENDIX A

Sponsored by

THE UNIVERSITY OF ALABAMA  
IN HUNTSVILLE

### AGENDA

Workshop on the Uses of a Tethered Satellite System

May 2-3, 1978

Hilton Inn

Huntsville, Alabama

#### Tuesday, May 2, 1978

- 08:45 Coffee and Doughnuts
- 09:00 Welcome and Discussion of Agenda
- S. T. Wu, The University of Alabama in Huntsville  
Workshop Coordinator
- J. Hoomani, Dean, School of Science and Engineering,  
The University of Alabama in Huntsville
- C. A. Lundquist, NASA/MSFC
- Remarks from NASA Headquarters
- J. W. Haughey - Office of Space Transportation Systems
- 09:30 Tethered Satellite System
- J. Laue, NASA/MSFC
1. Background and Status  
J. Laue, NASA/MSFC
  2. System Description  
Chris Rupp, NASA/MSFC
  3. System Dynamics  
Chris Rupp, NASA/MSFC
- 10:50 Coffee Break
- 11:00 Discussion
- 12:00 Lunch
- 13:30 Geological Measurements
- C. Lundquist, NASA/MSFC

1. Application of TSS for Mapping the Earth's Magnetic Field  
P. Coleman and Malcom G. McLeod, University of California,  
Los Angeles
  2. Gravity Gradient Measurements  
P. M. Kalagon, Smithsonian Astrophysical Observatory
  3. Satellite Magnetometry for Geological Applications  
Robert Regan, Earth Sciences Division, Phoenix Corp.
- 14:30 Discussion
- 15:00 Coffee
- 15:15 Atmospheric Measurements
- G. Carignan, University of Michigan
  1. Neutral Atmosphere  
G. Carignan, University of Michigan
  2. The Need for Measurements in the Lower Atmosphere  
C. A. Reber, NASA/GSFC
  3. The Interaction of a Tethered Satellite With the  
Atmosphere and the Resultant Environment  
J. H. deLeeuw, Inst. for Aerospace Studies, University of  
Toronto
  4. Measurements of Reactive Species  
J. G. Anderson, University of Michigan
  5. Mass Spectrometric Measurements  
A. O. C. Nier, University of Minnesota
  6. Atmospheric Electrification  
Heinz W. Kaseimer, NOAA/ERL
  7. Chemical Release  
J. P. Heppner, NASA/GSFC  
D. S. Evans, NOAA/SEL
- 18:30 Beer and Barbecue at Burritt Museum

Wednesday, May 3, 1978

- 08:30 Coffee and Doughnuts
- 08:45 Ionospheric Measurements and Applications  
David L. Reasoner, NASA/MSFC
1. Electrodynamics: Studies with a Tethered Subsatellite  
Peter M. Banks, Utah State University
  2. Tethered Subsatellite Characteristics and Initial Experiments  
P. Roger Williamson, Utah State University
  3. Interaction of a Tethered Subsatellite with the Ionosphere  
M. D. Grossi, Smithsonian Astrophysical Observatory
  4. The Tethered Subsatellite as a Tool for Large Body Plasma  
Flow Interaction Studies  
Nobie H. Stone, NASA/MSFC

5. Chemical Release Experiments Using the TSS  
J. P. Heppner, NASA/MSFC  
D. S. Evans, NOAA/ERL

10:45 Discussion

11:15 Technology Applications

M. P. Siebel, NASA/MSFC

1. Tethered Satellite: Potential Technology Applications

M. P. Siebel, NASA/MSFC

2. Satellite Elongation into a True "Sky-Hook"

Allyn C. Vine, Woods Hole Oceanographic Institute

12:00 Lunch

13:00 User Group Meetings

14:30 User Group Reports and Concluding Remarks

15:30 Adjourn

## APPENDIX B

ISS Workshop Participants  
(Sponsored by The University of Alabama in Huntsville)  
May 2 and 3, 1978

ARTHUR, C. W.

ES53

NASA

MSFC, Alabama 35812

(205) 453-0028

COMFORT, RICHARD H.

The University of Alabama in Huntsville

P. O. Box 1247

Huntsville, Alabama 35807

(205) 895-6404

BANKS, PETER

Department of Physics-Aeronomy Center

Utah State University

Logan, Utah 84322

(801) 752-4100

CROUCH, DONALD S.

Martin Marietta Aerospace

Denver Division

Denver, Colorado 80201

(303) 973-4837

BRACE, LARRY H.

621

Goddard Space Flight Center

Greenbelt, Maryland 20771

(301) 982-4575

DeNOYER, JOHN M.

Director, EROS Program

USGS

1925 Newton Square

Reston, Virginia 22092

(703) 860-7881

BURSNALL, W. J.

Program Manager

Ball Aerospace Systems Division

P. O. Box 1062

Boulder, Colorado 80306

(303) 441-4236

EVANS, DAVE

Space Environmental Laboratories

NOAA

Boulder, Colorado 80302

(303) 499-1000

CARIGNAN, GEORGE R.

Laboratory of Space Physics

Department of Atmospheric Sciences

and Oceanic Engineering

University of Michigan

Ann Arbor, Michigan 48105

(313) 764-9462

FONTHEIM, ERNEST

Space Physics Research Lab

University of Michigan

Ann Arbor, Michigan 75080

(313) 764-7220

COLEMAN, PAUL

Space Sciences Center

Institute of Geophysics and Planetary Physics

University of California at Los Angeles

Los Angeles, California 90024

(213) 825-1776

GROSSI, M. D.

Center for Astrophysics

Smithsonian Astrophysical Observatory

60 Garden Street

Cambridge, Massachusetts 02138

(617) 495-7433

HAUGHEY, J. W.  
MTG-3  
NASA  
Washington, D. C. 20546  
(202) 755-3024

LAUE, JAY H.  
PS01  
NASA  
MSFC, Alabama 35812  
(205) 453-0163

HEELIS, ROD  
The University of Texas at Dallas  
P. O. Box 688  
Richardson, Texas 75080  
(214) 690-2851

LINSON, LEWIS  
Science Application, Inc.  
1200 Prospect Street  
P. O. Box 2351  
LaJolla, California 92037  
(714) 459-0211, Ext. 349

HUGHES, PETER  
University of Toronto  
18 Cherry Blossom Lane  
Thornhill, Canada L3T3B9  
(416) 667-7719

LUNDQUIST, C. A.  
ES01  
NASA  
MSFC, Alabama 35812  
(205) 453-3105

HUNG, R. J.  
The University of Alabama in Huntsville  
P. O. Box 1247  
Huntsville, Alabama 35807  
(205) 895-6077

MARTIN, JOE  
Martin Marietta Aerospace  
Denver Division  
Denver, Colorado 80201  
(303) 973-4837

KALAGHAN, P. M.  
Center for Astrophysics  
Smithsonian Astrophysical Observatory  
60 Garden Street  
Cambridge, Massachusetts 02138  
(617) 495-7281

McLEOD, MALCOLM  
Space Sciences Center  
Institute of Geophysics and Planetary  
Physics  
University of California at Los Angeles  
Los Angeles, California 90024  
(213) 825-1044

KARR, G. R.  
The University of Alabama in Huntsville  
P. O. Box 1247  
Huntsville, Alabama 35807  
(205) 895-6330

NIER, A. O. C.  
University of Minnesota  
Institute of Technology  
School of Physics and Astronomy  
Minneapolis, Minnesota 55455  
(612) 373-3325

KASEMIR, HEINZ W.  
NOAA/APCL  
Boulder, Colorado 80302  
(303) 499-1000, ext. 6249

OYAMA, KOH-ICHIRO  
Utah State University/University of Tokyo  
Logan, Utah 84322  
(801) 752-4100

KLEIN, DON  
Ball Aerospace Systems Division  
3322 Memorial Parkway, S.W.  
Huntsville, Alabama 35801  
(205) 883-7231

REASONER, DAVID L.  
ES53  
NASA  
MSFC, Alabama 35812  
(205) 453-3037

REBER, C. A.  
624  
Building 21, Room 252  
Goddard Space Flight Center  
Greenbelt, Maryland 20771  
(301) 982-6534

RECAN, ROBERT  
Phoenix Corporation  
1600 Anderson Road  
McLean, Virginia 22101  
(703) 790-1450

RHEINFURTH, M. H.  
ED01  
NASA  
MSFC, Alabama 35812  
(205) 453-3153

RICHMOND, ART  
R43  
Space Environment Lab/ERL  
NSAA  
Boulder, Colorado 80302  
(303) 499-1000

ROBERTS, BILL  
PS02  
NASA  
MSFC, Alabama 35807  
(205) 453-3431

RUPP, CHARLES C.  
PD12  
NASA  
MSFC, Alabama 35812  
(205) 453-5730

SIEBEL, M. P. L.  
ES01  
NASA  
MSFC, Alabama 35812  
(205) 453-3031

SIMPSON, JOHN  
Ball Aerospace Systems Division  
Boulder, Colorado  
(303) 441-4005

SMITH, DONALD  
AFGL/OP  
Hanscom Air Force Base, Massachusetts 01731  
(617) 861-2336

SMITH, ROBERT E.  
ES81  
NASA  
MSFC, Alabama 35812  
(205) 453-3101

SNOEDY, W. C.  
ES51  
NASA  
MSFC, Alabama 35812  
(205) 453-2573

SWENSON, GARY  
ES44  
NASA  
MSFC, Alabama 35812  
(205) 453-3040

TAEUSCH, D. R.  
Space Physics Research Laboratory  
University of Michigan  
2455 Hayward Street  
Ann Arbor, Michigan 48109  
(313) 764-6578

THOMPSON, W. B.  
University of California in San Diego  
LaJolla, California 92093  
(714) 452-4173

VINE, ALLYN C.  
Woods Hole Oceanographic  
Woods Hole, Massachusetts  
(617) 548-1400

WILLIAMSON, P. ROGER  
Utah State University  
Logan, Utah 84322  
(801) 752-4100, Ext. 7878

WILLIS, SAM  
PSDC  
NASA/GSFC  
Greenbelt, Maryland 20771  
(301) 982-4560

WINNINGHAM, DAVID  
The University of Texas at Dallas  
P. O. Box 688  
Richardson, Texas 75080  
(214) 690-2835

WOLFE, JERRY A.  
General Electric  
122 Blue Ridge Road  
Plymouth Meeting, Pennsylvania 19462  
(215) 828-4593

WU, S. T.  
The University of Alabama in Huntsville  
P. O. Box 1247  
Huntsville, Alabama 35812  
(205) 895-6413

## APPENDIX C

TETHERED SATELLITE SYSTEM

by

Charles C. Rupp and Jay H. Laue

Summary of a Presentation for the  
Proceedings of the 1978 Goddard Memorial Symposium  
Washington, D. C. 20009  
March 8-10, 1978

N81-29493

214

NO. 78-048

SHUTTLE/TETHERED SATELLITE SYSTEM

Charles C. Rupp and Jay H. Laue

Summary of a Presentation for the  
Proceedings of the  
1978 Goddard Memorial Symposium  
Washington, DC 20009

March 8, 9, 10, 1978

National Aeronautics and Space Administration  
George C. Marshall Space Flight Center  
Marshall Space Flight Center, Alabama 35812

## SHUTTLE/ TETHERED SATELLITE SYSTEM

Charles C. Rupp<sup>+</sup>

Jay H. Laue<sup>+</sup>

A tethered satellite system has been conceived as a device to extend the capability of the Space Shuttle to perform scientific/ applications investigations and operational activities. The concept envisions a multiple-use tethered system with closed-loop control, capable of supporting a payload or satellite suspended from the Shuttle cargo bay, toward or away from the Earth, at distances up to 100 kilometers from the Shuttle. This paper discusses the background and results of early analyses and feasibility studies, and presents a design and operational description of the system. Also presented are a discussion of potential applications of the Tethered Satellite System, and plans for an operational verification flight in 1982.

### INTRODUCTION

The Shuttle/ Tethered Satellite System (TSS) is a unique system currently being defined which will utilize the Earth-orbiting Shuttle as a base for its operation, and will be capable of deploying numerous types of payloads to orbits significantly different from that of the Shuttle (Figure 1). These "satellite" payloads,

---

<sup>+</sup> Mr. Charles C. Rupp and Mr. Jay H. Laue, Program Development, NASA/ Marshall Space Flight Center, Alabama.

although tethered to the Shuttle, can be permanently placed in their new orbits, retrieved, refurbished, and reconfigured for subsequent missions.

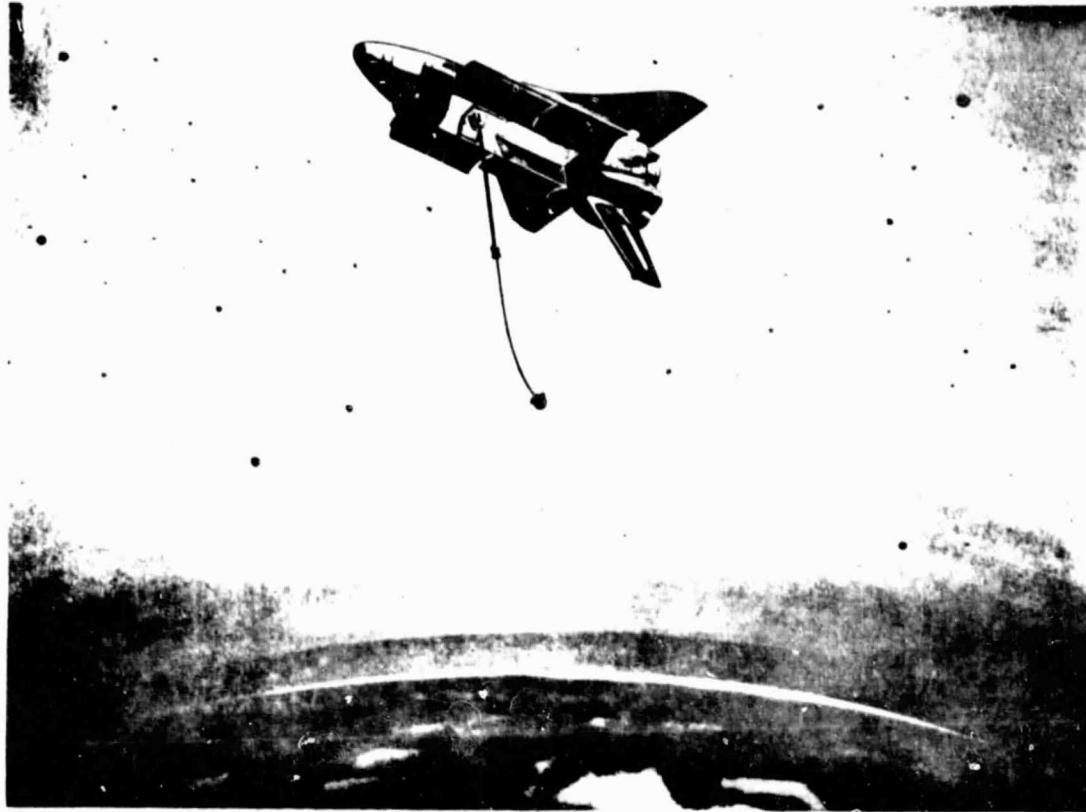


Fig. 1 Shuttle/Tethered Satellite System

Most applications currently envisioned for the tethered satellite system involve deployment of the payload to a low Earth orbit (100-120 km) from the Shuttle which is orbiting at its minimum practical altitude capability of approximately 200 km. However, the satellite payload can also be deployed upward to a higher altitude.

Key elements of the system include an extendible boom and tether which are essential to the deployment and retrieval of the satellite (or payload). The payload, initially restrained by the extendable boom, is positioned to a safe distance (20-50 meters) from the Shuttle. At this point it is released and a combination

ORIGINAL PAGE IS  
OF POOR QUALITY

of initial velocity, gravity gradient, and atmospheric drag cause the satellite to deploy to the new orbit. After completion of the experiment, the tether is retracted until the satellite is recaptured by the extended boom, and the satellite/boom combination is restowed in the Shuttle. Deployment and retrieval of the satellite is computer-operated by controlling the tether tension and velocity.

## BACKGROUND

A variety of space applications involving tethered objects have been proposed in recent years. Retrieval of stranded astronauts by "throwing a buoy on a tether" from a rescue vehicle to an astronaut and then reeling the tether back was such a consideration. The equations of motion for this maneuver were investigated by Eades and Wolfe<sup>1</sup> and by the Marquardt Corporation<sup>2</sup> using an open loop control law which applied precalculated tension to the tether for deployment and retrieval. The scheme was never developed for an actual rescue mission because of several unsolved problems and because other rescue techniques were subsequently pursued.

Another early tether application was studied involving a tethered (rather than hard-docked) interface between the Apollo Telescope Mount (ATM) and the Orbital Workshop (OWS)<sup>3</sup>. Conceived as a means of station keeping between the two bodies, this approach was found unattractive because of the difficulties in precisely determining and controlling the tugging forces to be applied and in providing the constant manned supervision which would be required to ensure flight safety.

Two successful orbital space flights, Gemini XI and Gemini XII, involved tether experiments in which the manned Gemini space vehicle was tethered to an unmanned Agena vehicle<sup>4</sup>. The Gemini XI flight demonstrated a rotating configuration in which the Gemini spacecraft was tethered to the Agena by 30.48 m (100 ft) of polyester webbing. Centrifugal force maintained tension in the tether following

spin-up of the configuration using the Gemini thruster reaction control system. The Gemini XII flight demonstrated a gravity gradient stabilized configuration.

The idea of a tethered satellite approach for attaining low Earth orbits was put forth in 1974 by the Smithsonian Astrophysical Observatory<sup>5</sup>. In their proposal to the Atmospheric, Magnetospheric, and Plasmas in Space (AMPS) Science Working Group, Columbo et al. of Smithsonian described the use of a long tether system, called "Skyhook," for low altitude research. To deploy the tethered satellite, it was suggested that a large balloon be attached to the satellite. It was expected that atmospheric drag would pull the balloon behind the main satellite and downward, thereby deploying the tether. Several additional reports were subsequently prepared by Smithsonian which addressed various aspects of the tethered satellite approach. Subsequent to Smithsonian's "Skyhook" proposal, studies initiated at the Marshall Space Flight Center (MSFC) showed the feasibility of deploying, stabilizing, and retrieving long tethered satellites with an active control system utilizing gravity gradient forces instead of atmospheric drag. The mathematical formulation of the control laws which enable the tether control system to function and a brief statement of system hardware requirements, as described by Rupp<sup>6</sup>, resulted from this study. Further work at MSFC<sup>7</sup> investigated several aspects concerning the feasibility of tethered satellites. These studies addressed dynamics, control, thermal, aerodynamics, and communication aspects with the general conclusion that there was no evidence to indicate that the concept was not feasible.

Recently, there have been a number of analytical studies of tethered systems by various groups within the government and industry. One of these was a study of tethered system dynamics and control by Kulla<sup>8</sup>. This study was in general agreement with the findings of earlier references. The simulation results showed the shape of the tether during deployment and also investigated deployment and retrieval to a distance of 1 km. A conceptual design study addressing the areas

of requirements, system interfaces, design, layout, and cost was performed by the Marshall Space Flight Center<sup>9</sup>. This study is being used as an initial reference in system definition studies currently under contract by NASA.

### TETHERED SATELLITE APPLICATIONS

It is anticipated that the tethered satellite system will greatly extend the capabilities of the Shuttle Orbiter. Several preliminary proposals have been submitted to the NASA by interested investigators, and significant "informal" interest has been expressed. The potential applications described below and illustrated in Figure 2 provide a representative sampling of investigative interest.

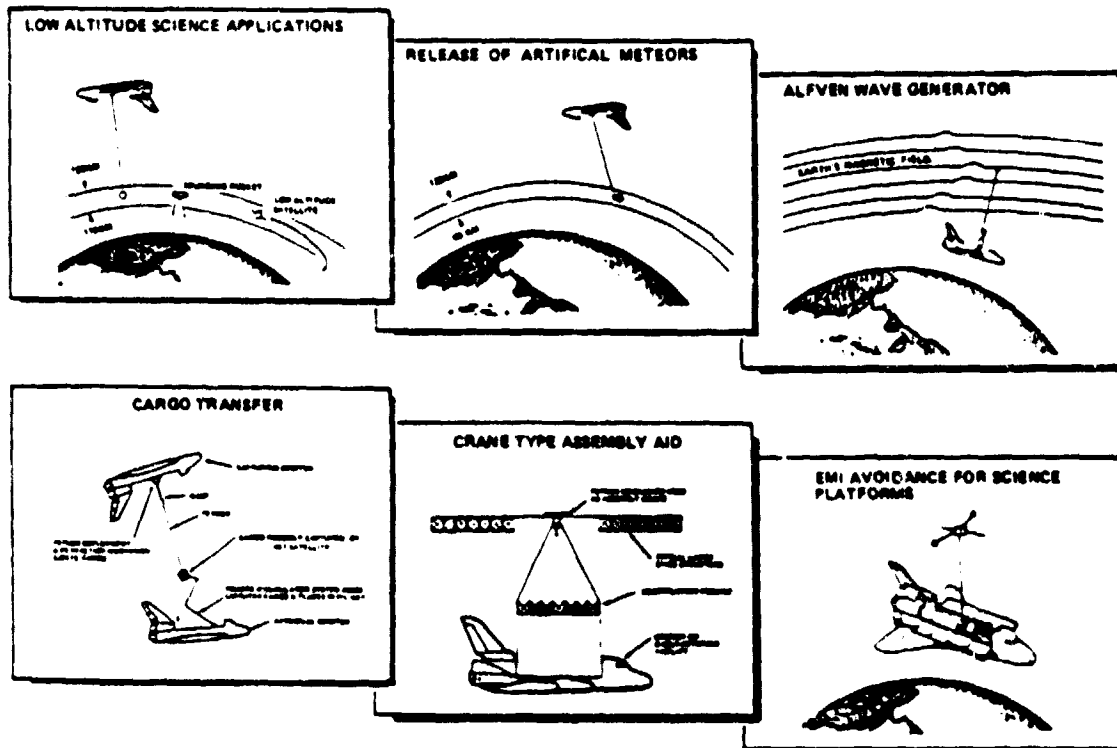


Fig. 2 Potential Tethered System Applications

#### Low Altitude Science/ Applications

Typical science/ applications involve payloads deployed by the tether or using the tetherline itself as part of the science instrument. Low altitude science applications include gravity and magnetic field mapping, reentry research, Earth

surveillance, plasma physics, pollutant measurements, and in situ calibration and evaluation of free flying satellite instruments such as microwave, infrared, and ultraviolet sensors.

#### Release of Artificial Meteors

The tether system can be used to deploy packages for the release of various chemicals to stimulate various phenomena. For example, barium can be released for ionization studies. Deploying a package into the upper atmosphere would allow chemicals to be released by ablation over a long path to study effects of meteors.

#### Alfven Wave Generator

The Earth's magnetic field can be studied by forcing current to flow in the tetherline. Propagation of the resulting field perturbation, called Alfven waves, can lead to a more thorough understanding of the dynamics of the Earth's magnetic field.

#### Cargo Transfer

A tetherline can be used as a crane to maneuver structural elements into place. The tetherline "crane" can be on either the supply vehicle or on the receiving platform. Cargo transfer can also be accommodated either using the tetherline as a crane or as a highline.

#### Assembly Aid

A large space structure such as an antenna can be gravity-gradient stabilized using a tetherline to suspend a counterweight. Temporary stabilization of pieces of structure during assembly can be accomplished, thus simplifying the tasks of teleoperators.

#### Disturbance Avoidance

A tetherline can also be used to deploy science payloads away from the Orbiter to avoid Orbiter-induced environmental disturbances. Deployment can be along

local vertical either toward the Earth or away from the Earth. The distance payloads can be deployed is limited by practical considerations such as available mission time and aerodynamic heating.

### TETHERED SATELLITE SYSTEM DESCRIPTION

The Tethered Satellite System is composed of the basic elements shown in Figure 3. The system can be deployed either up away from the Earth, as implied by the drawing, or down toward the Earth.

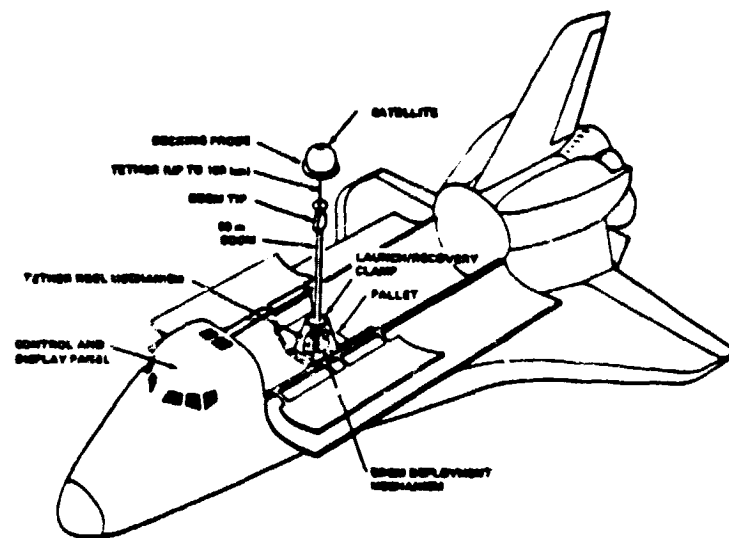


Fig. 3 Tethered Satellite System

The first element is a satellite which can have a wide variety of shapes and masses but the aerodynamic and mass characteristics must be known. The satellite is fitted with a docking adapter which mates with a capture mechanism at the boom tip. The tether is a very flexible metallic or synthetic line approximately 1 mm in diameter up to 100 km or more in length. A 50-meter boom is used for initial satellite deployment: to ensure against snagging the Orbiter and to capture the satellite during retrieval.

The launch/ recovery clamp cradles the satellite while it is stowed in the payload bay.

The heart of the system is the reel mechanism containing the tether supply reel; tether tension, length, and rate sensors; and a servo drive motor. A digital control computer uses the sensor information and a closed loop control algorithm to calculate drive commands for the reel motor. A control and display panel mounted at the Orbiter aft flight deck is provided for crew operation of the system.

Overall tethered satellite system characteristics are shown in Table 1.

Table 1

SYSTEM CHARACTERISTICS

Overall Size (LWH)	2.9 × 1.8 × 3.6 meters
Total Mass	705 kilograms
Satellite Mass	175 kilograms
Power (Peak/Average)	1128/121 watts
Tether Length	100 kilometers

The Tethered Satellite System will be pallet-mounted and stowed onboard the Orbiter as shown in Figure 4. The relatively small volume and light weight of the system permit sharing a Shuttle mission with other payloads.

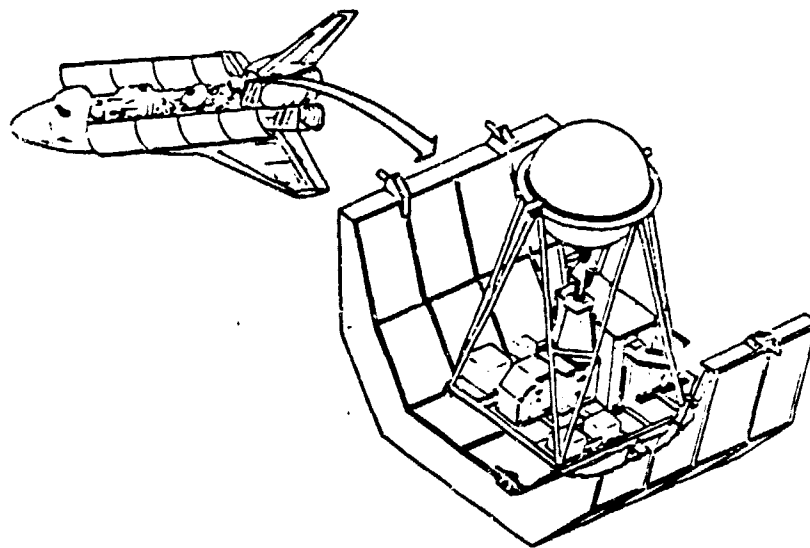


Fig. 4 System Layout in Payload Bay

## TETHERED SATELLITE SYSTEM OPERATION

Stabilization of the tethered satellite can be explained using the spring-mass pendulum analogy shown in Figure 5. If the spring-mass parameters are tuned so that the stretch frequency is the same as the swing frequency, swing energy will be rapidly transferred to the stretch motion and vice-versa. A viscous damper can be added to damp the stretch motion directly thereby indirectly damping the swing motion.

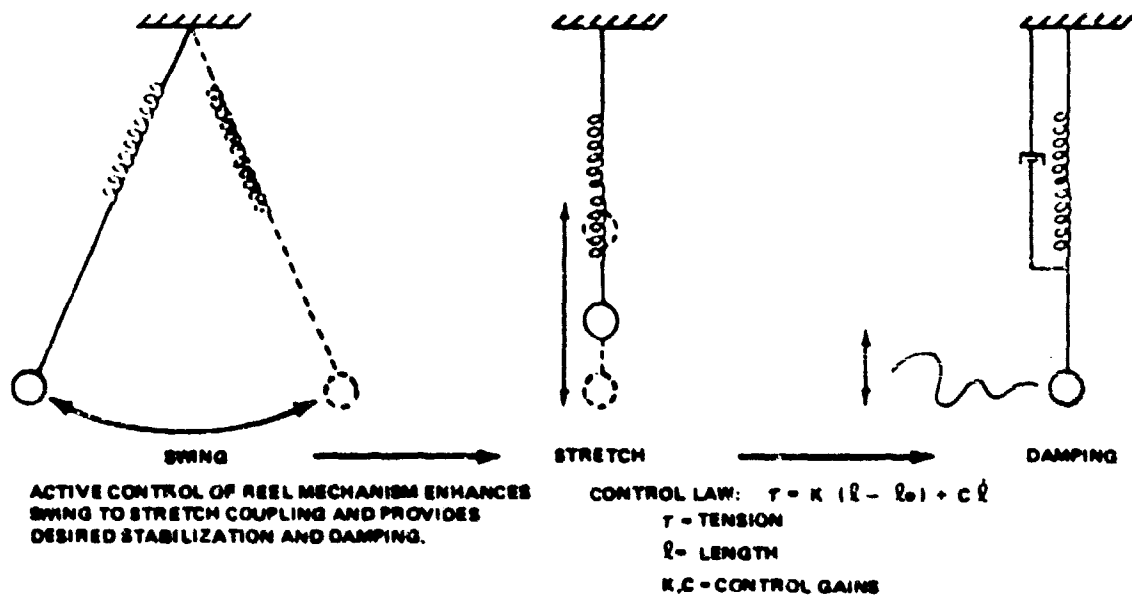


Fig. 5 Stabilization

The tethered satellite reel mechanism reels the tether in and out producing satellite motion similar to motion of the spring mass pendulum. The control algorithm is a tension command as a function of tether length and length rate. Adjustment of the gains in the control algorithm tunes the reeling frequency to the swinging frequency. On Earth, the swing frequency of a pendulum is a function of the gravitational acceleration and pendulum length. In orbit, the pendulum is centered at a point of zero gravity and has only gravity gradient acting on it. The frequency of the orbital pendulous libration is <sup>1/2</sup>two times the orbital rate for librations in the orbital plane and <sup>3/2</sup>three times orbital rate for librations out of the orbital

plane. Coriolis forces cause the two frequencies to be different. This difference prevents the existence of a steady state coning motion which could not be sensed and controlled by the reel mechanism. Reference 6 presents the equations of motion for the tethered satellite and discusses the control system design. The control algorithm can be used to deploy the tethered satellite as shown in Figure 6.

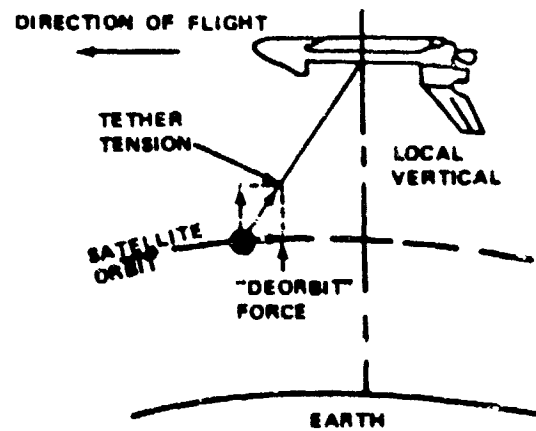


Fig. 6 Deployment

Deployment of a tethered satellite is initiated by placing the satellite a short distance away from the Orbiter with the extendible and retractable boom. Alternatively, the satellite can be given an initial velocity along local vertical with a catapult or other launcher. Either method, or a combination of the two, causes the satellite trajectory to move ahead of and down from the Orbiter for deployment toward the Earth. If the satellite is desired to be deployed upward, away from the Earth, the initial velocity or position should be in an upward direction and the resulting trajectory moves upward and behind the Orbiter.

As the satellite moves away from the Orbiter, the tether is unwound from the reel. The reel drive motor operates as a brake applied against the gravity gradient force which is acting on the satellite mass. This braking action provides a tension on the tether which causes the satellite to move further downward (or upward as the case may be). This action can be explained by observing that the

tetherline tension can be thought of as having a vertical and a horizontal component. The horizontal component is of the proper direction to further deorbit the satellite (or boost the satellite for upward deployment) thus causing the satellite trajectory to move further downward (or upward).

The tension required to accomplish the deployment is computed by the control computer as was done for stabilization. For the deployment case, the tension which is commanded is slightly lower than the gravity gradient force which would be applied to the satellite mass if the satellite were in equilibrium at any given distance. A tension greater than this amount will cause retrieval which will be discussed later. The control law has a deployment rate limit which limits the speed of the reel and motor to a safe value.

Retrieval of the tethered satellite is similar to deployment except that the control law commands a tension greater than the equilibrium tension at a given satellite distance. This causes the motor and reel to retrieve the tetherline. As shown in Figure 7, the retrieval trajectory lies slightly behind local vertical for the downward deployed system or slightly ahead of local vertical for the upward deployed system. Another difference between retrieval and deployment is that

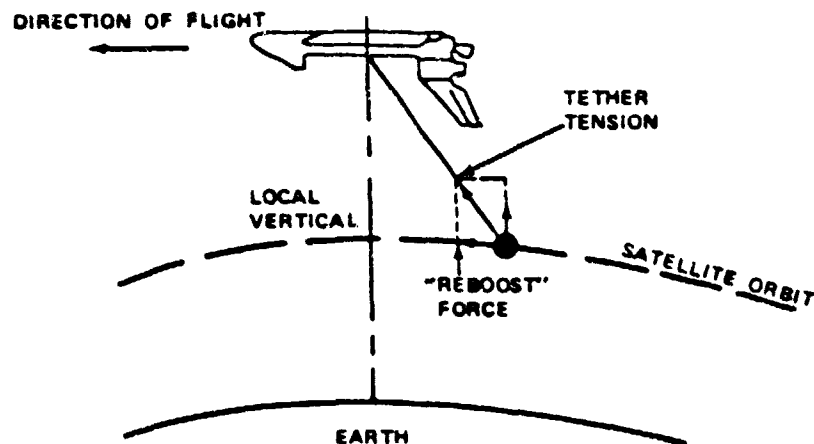


Fig. 7 Retrieval

deviations from the desired trajectory are more difficult to damp during retrieval and therefore more time is required to effect the retrieval. The terminal phase of the retrieval occurs very slowly and capture of the satellite is accomplished using the deployment boom capture mechanism. In this terminal phase, the satellite is slowly drawn into the boom tip and then the boom is retracted, drawing the satellite back into the launch/recovery clamp in the Orbiter payload bay.

Figure 8 is an operational sequence for a typical mission.

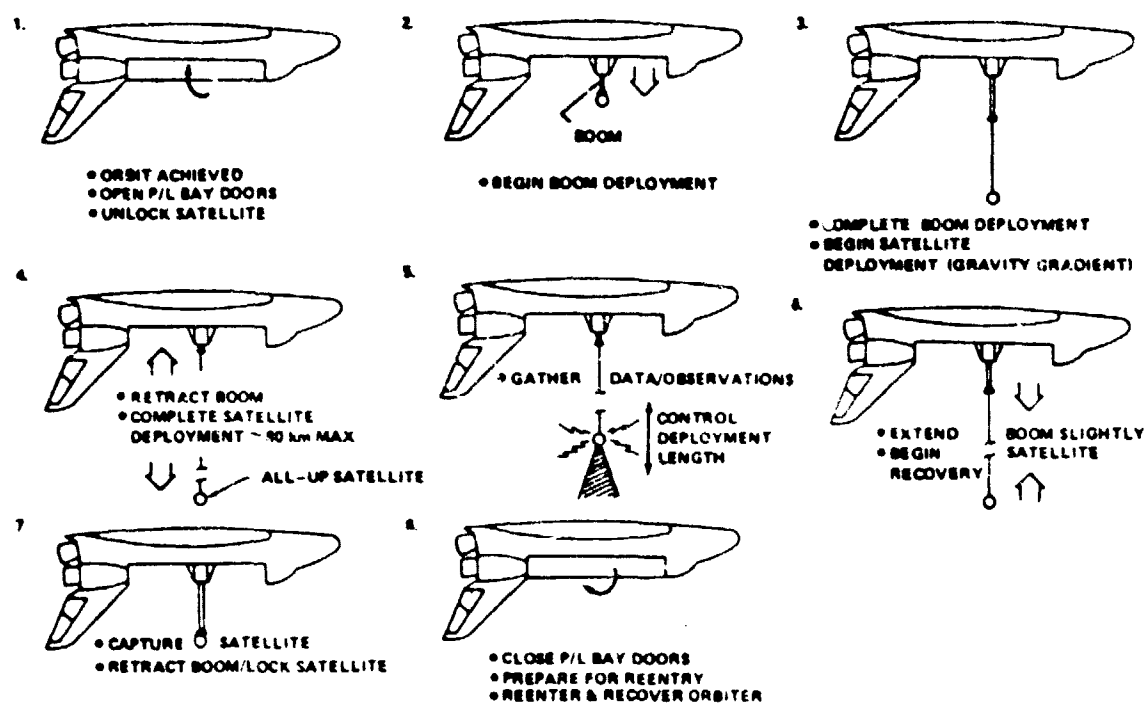


Fig. 8 Operational Sequence

### ENGINEERING STUDIES

The following engineering studies are discussed to show some of the important characteristics and limitations of the Tethered Satellite System. Figure 9 shows a plot of the gravity gradient force which is the vertical component of the tether tension. As shown, the gravity gradient force is a function of tether length and satellite mass. Typical science satellites on the order of 200 kilograms produce a tether tension of about 100 Newtons (22 lb) at a length of 100 km. The same tether system can support very large payloads at shorter distances.

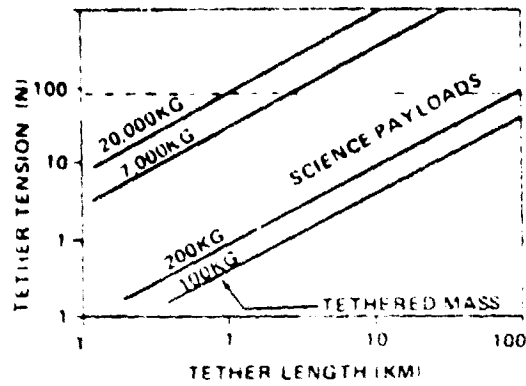


Fig. 9 Gravity Gradient Force

Atmospheric drag produces a horizontal component of tether tension which is a function of altitude, tether length and diameter. Figure 10 shows a drag force of about 18 Newtons (4 lb) which is produced by a 1.0 mm diameter tether deployed 80 km from an Orbiter at 200 km altitude. It is interesting that the tether frontal area to the relative wind is much larger than typical satellite areas. A one square meter area satellite has the same area as a 1 km length of 1 mm tether.

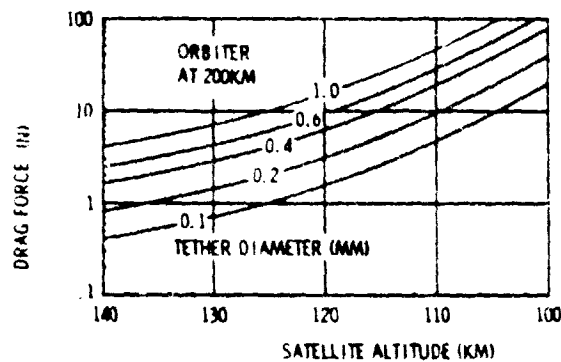


Fig. 10 Drag Force Due to Tether

The horizontal and vertical components of tether tension are combined vectorially to produce the total tension. The atmospheric drag also causes the tethered satellite to lag behind local vertical (see Figure 11). The angle of the lag is shown for two typical satellite masses. Heavier satellites allow deeper penetration of the satellite for a given tether length.

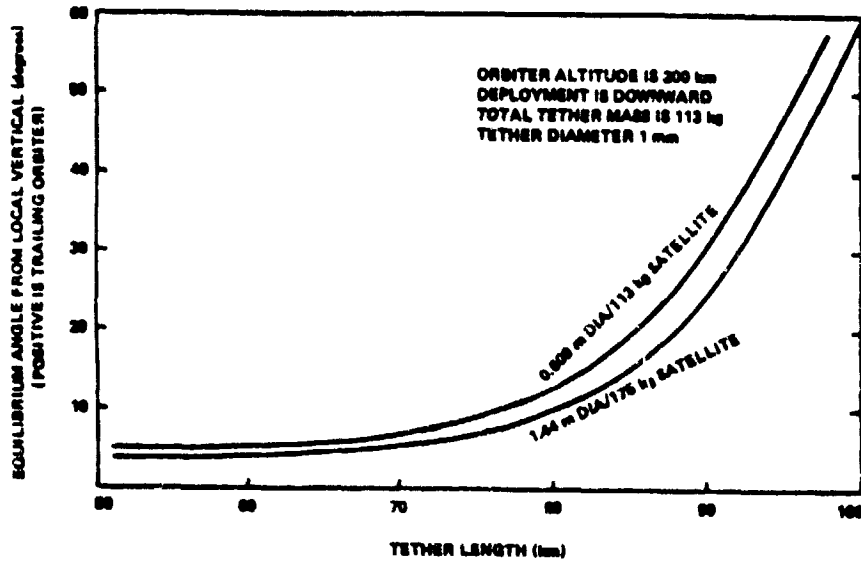


Fig. 11 Angle Satellite Lags Local Vertical

Atmospheric drag also has a predominant effect in determining the temperature the satellite must withstand. Figure 12 shows a plot of the satellite temperature versus altitude. The temperature of the tether rises in a similar fashion as the altitude drops. Satellites can be designed with active temperature control systems to handle high temperatures. However, there are very few ways the tether can be protected from high temperatures.

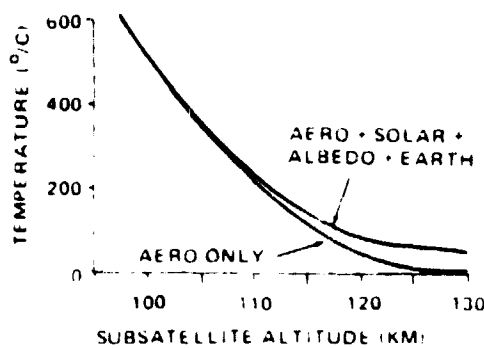


Fig. 12 Spherical Satellite External Temperature

A satellite deployment and retrieval trajectory is shown in Figure 13. Atmospheric drag is neglected in the simulation. A 100 km round trip takes about 19 hours when peak tether rates are limited to less than 10 meters per second.

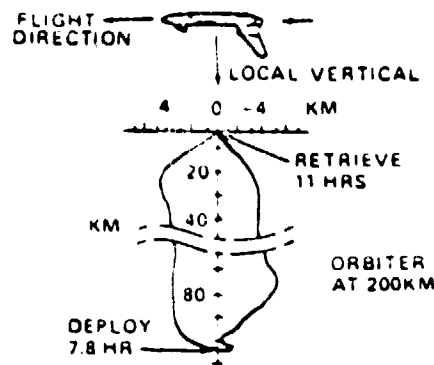


Fig. 13 Deployment/Retrieval Trajectory

When atmospheric drag is added to the trajectory simulation in Figure 14, the pulsating effect of the diurnal variations of atmospheric density cause the swing angle to vary in addition to lagging behind the local vertical. The excitation of the swing angle librations gets more pronounced as the satellite gets lower into the atmosphere. This effect along with the high temperature at low altitude limit the lowest altitude attainable by a given system design.

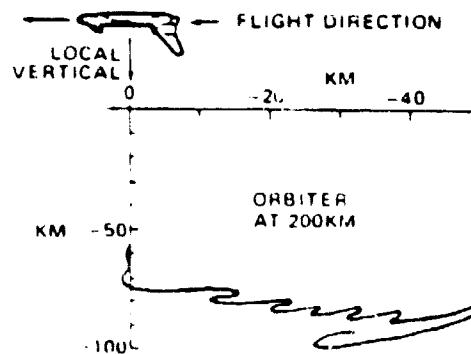


Fig. 14 Deployment Trajectory with Atmospheric Drag

The satellite trajectory simulations shown above do not model the shape or vibrations of the tether. Simulations of tether dynamics are very involved and time consuming and are not usually used as design tools but are used for verification. The first simulation depicting tether shape is a planar model derived by Kulla<sup>3</sup> (see Figure 15). This particular result was chosen to illustrate the capabilities of the simulation and do not represent flight expectations since the tether system

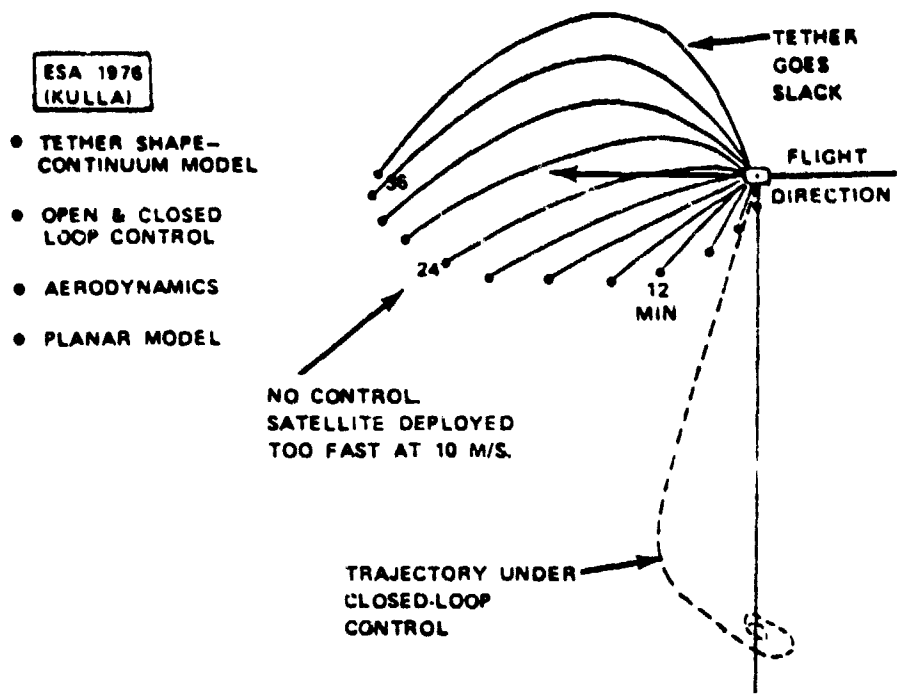


Fig. 15 Tether Shape Using a Planar Continuum Model

did not use closed loop control and initially the satellite was purposely deployed too fast. Here the shape of the tether is shown every three minutes. Contrasted with the uncontrolled trajectory is a satellite trajectory under closed loop control.

A more recent tether shape simulation by Kalagan<sup>10</sup> is shown in Figure 16. Up to 20 mass elements are used to model the tether system. The shape of the tether is shown every 100 seconds with increasing time moving from left to right. Again, the flight conditions are not too realistic because the simulation is begun with the tether along local vertical and then released with no control. One interesting aspect of the simulation is the wave motion that travels from the satellite to the Orbiter is reflected by the Orbiter and then travels back to the satellite.

The engineering studies represent efforts to study questions concerning tether system feasibility. Future work is centering on system optimization and design to meet specific scientific payload requirements.

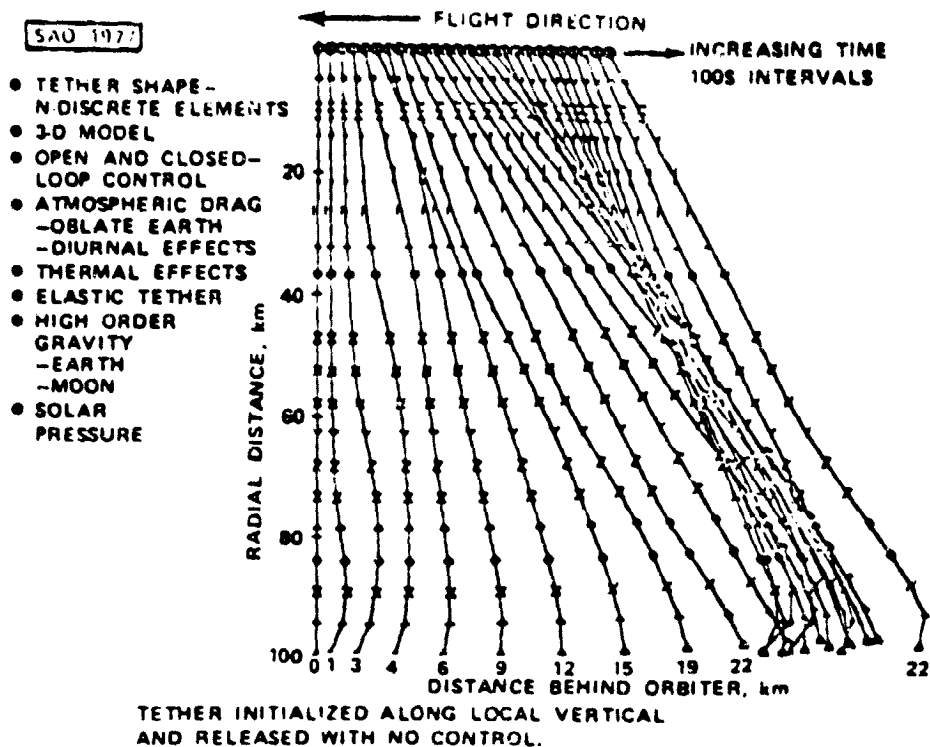


Fig. 16 Tether Shape Using a Discrete Element Model

#### DEFINITION AND DEVELOPMENT

Based on the potential of the tethered satellite concept for extending the Space Shuttle's capability to support scientific investigations and operational activities in space, NASA has established the Shuttle/Tethered Satellite System (TSS) as a project for further definition.

Following competitive procurement procedures, NASA awarded contracts, in late 1977, to the Ball Brothers Research Corporation and the Martin Marietta Corporation for preliminary design studies of the Shuttle/Tethered Satellite System. In concert with the overall objectives of the project, the contracts called for the preliminary design, specifications, program plans, and cost estimates for an Operational Verification Flight in 1982. It was specified that the satellite flying on this mission would carry engineering instrumentation required for the operational verification and for measuring the various parameters of the environment

to which the satellite would be exposed. These parameters will be used to influence the design of future generations of tethered satellites.

In addition to engineering and environmental instrumentation, the definition studies call for accommodation of additional payload instrumentation on the verification flight. The particular payload, or "passenger experiment," that has been identified by NASA for initial consideration in this context is an Earth magnetic field mapping experiment. The instrumentation requirements and operational objectives for this experiment are the subject of a parallel, NASA-sponsored study by the University of California, Los Angeles.

The overall schedule for the Shuttle/Tethered Satellite System projects a fully operational system by February 1983.

#### CONCLUSIONS

Based on the analyses and design studies performed to date, deployment, stabilization, and retrieval of a tethered satellite system are feasible from the dynamics and systems design aspects. Definition studies are currently underway and are expected to provide preliminary designs and data necessary to proceed into a development phase leading to an operational capability in 1983.

Accommodation of a wide range of science, applications, and technology payloads is the subject of current investigation through various contracted studies. Within NASA, a Tethered Satellite System Working Group has been established to provide an internal liaison mechanism between user and development organizations. Present planning anticipates operational missions using the Shuttle/Tethered Satellite System in the early 1983 time frame.

#### REFERENCES

1. Eades, J. B. and Wolf, Henry, Tethered Body Problems and Relative Motion Orbit Determination, Final Report. Contract NAS5-21453, Analytical Mechanics Associates, Inc., August 1972.

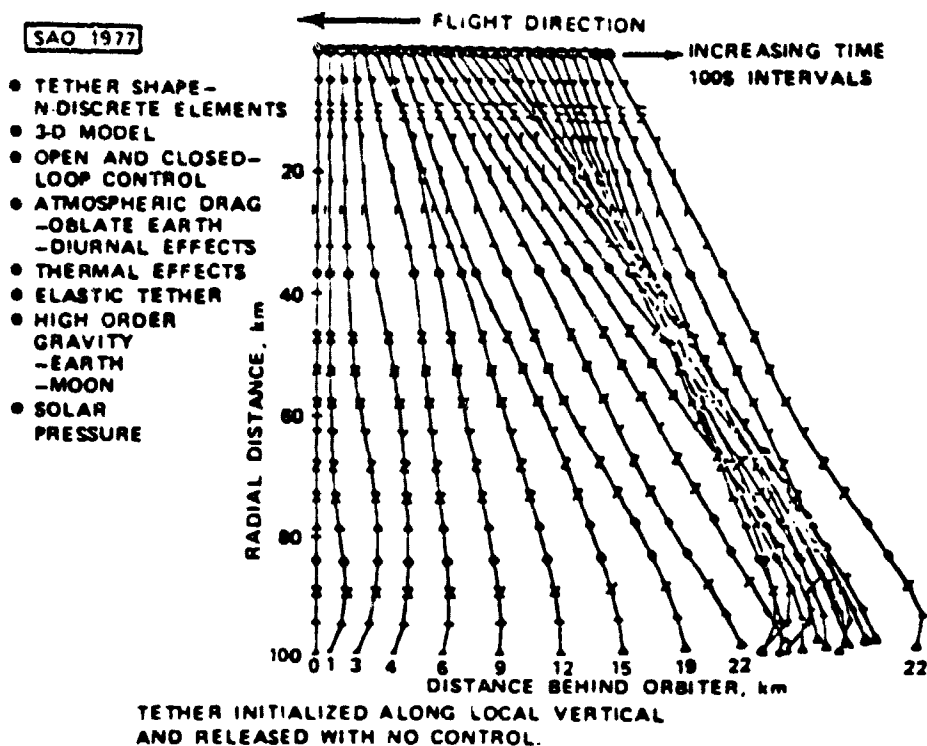


Fig. 16 Tether Shape Using a Discrete Element Model

#### DEFINITION AND DEVELOPMENT

Based on the potential of the tethered satellite concept for extending the Space Shuttle's capability to support scientific investigations and operational activities in space, NASA has established the Shuttle/Tethered Satellite System (TSS) as a project for further definition.

Following competitive procurement procedures, NASA awarded contracts, in late 1977, to the Ball Brothers Research Corporation and the Martin Marietta Corporation for preliminary design studies of the Shuttle/Tethered Satellite System. In concert with the overall objectives of the project, the contracts called for the preliminary design, specifications, program plans, and cost estimates for an Operational Verification Flight in 1982. It was specified that the satellite flying on this mission would carry engineering instrumentation required for the operational verification and for measuring the various parameters of the environment

to which the satellite would be exposed. These parameters will be used to influence the design of future generations of tethered satellites.

In addition to engineering and environmental instrumentation, the definition studies call for accommodation of additional payload instrumentation on the verification flight. The particular payload, or "passenger experiment," that has been identified by NASA for initial consideration in this context is an Earth magnetic field mapping experiment. The instrumentation requirements and operational objectives for this experiment are the subject of a parallel, NASA-sponsored study by the University of California, Los Angeles.

The overall schedule for the Shuttle/Tethered Satellite System projects a fully operational system by February 1983.

#### CONCLUSIONS

Based on the analyses and design studies performed to date, deployment, stabilization, and retrieval of a tethered satellite system are feasible from the dynamics and systems design aspects. Definition studies are currently underway and are expected to provide preliminary designs and data necessary to proceed into a development phase leading to an operational capability in 1983.

Accommodation of a wide range of science, applications, and technology payloads is the subject of current investigation through various contracted studies. Within NASA, a Tethered Satellite System Working Group has been established to provide an internal liaison mechanism between user and development organizations. Present planning anticipates operational missions using the Shuttle/Tethered Satellite System in the early 1983 time frame.

#### REFERENCES

1. Eades, J. B. and Wolf, Henry, Tethered Body Problems and Relative Motion Orbit Determination, Final Report. Contract NAS5-21453, Analytical Mechanics Associates, Inc., August 1972.

2. Straly, W. H. and Adlhoch, R. W., Study of the Retrieval of an Astronaut from an Extra-Vehicular Assignment. The Marquardt Corporation, Van Nuys, California, TMC Report No. S-356, November 1, 1963.
3. Perrine, B. S., A Method for Soft Tethered Stationkeeping. NASA TM X-53643, Marshall Space Flight Center, July 31, 1967.
4. Lang, D. L. and Nolting, R. K., Operations with Tethered Space Vehicles. NASA SP-138, Gemini Summary Conference, 1967.
5. Colombo, G., et al., Shuttle-Borne "Skyhook": A New Tool for Low-Orbital-Altitude Research. Proposal by Smithsonian Institution Astrophysical Observatory, September 1974.
6. Rupp, C. C., A Tether Tension Control Law for Tethered Subsattellites Deployed Along Local Vertical. NASA TM X-64963, Marshall Space Flight Center, September 1, 1975.
7. Baker, W. P., et al., Tethered Subsattelite Study. NASA TM X-73314, Marshall Space Flight Center, March 1976.
8. Kulla, P., Dynamics of Tethered Satellites. TMM/76-119/PK/AVS, European Space Agency, April 1976.
9. Preliminary Design Office, Shuttle Tethered Satellite System Design Study, NASA TM X-73365, Marshall Space Flight Center, December 1976.
10. Kalaghan, P., et al., Study of the Dynamics of a Tethered Satellite System (Skyhook), Final Report (Draft), December 1977.